

**IONIC EXCHANGES BETWEEN GLASS IONOMERS
AND DEMINERALISED DENTINE**

by

Hien Ngo BDS, MDS

**A thesis submitted in fulfilment of the requirements for
the degree of
Doctor of Philosophy**

**School of Dentistry
The University of Adelaide**

TABLE OF CONTENTS

Abstract		xx
Declaration		xxii
Acknowledgements		xxiii
Chapter 1	Introduction & Literature Review	1
1.1	Introduction	1
1.2	Literature review	2
1.2.1	The nature of enamel and dentine	3
1.2.1.1	Composition	4
1.2.1.1.1	<i>Organic</i>	4
1.2.1.1.2	<i>Inorganic</i>	5
1.2.1.2	Permeability of enamel and dentine	8
1.2.1.3	Mineralisation	9
1.2.1.4	The interaction of teeth with the oral environment	12
1.2.1.5	Changes with caries	13
1.2.1.5.1	<i>Structure and biological changes</i>	14
1.2.1.5.2	<i>Discolouration</i>	15
1.2.1.6	Current clinical approaches to repair or replace carious dentine	17
1.2.1.6.1	<i>Classical approach</i>	18
1.2.1.6.2	<i>Stepwise excavation</i>	18
1.2.1.6.3	<i>Indirect pulp capping</i>	19
1.2.1.7	Potential for remineralisation	20
1.2.2	Glass-ionomer cement	24
1.2.2.1	Chemical composition and microstructure	24
1.2.2.2	Setting reaction	26
1.2.2.3	Release of fluoride and other ions	29

1.2.2.4	Remineralisation of adjacent enamel and dentine	34
1.2.3	Methods for evaluation of remineralisation	35
1.2.3.1	Quantitative methods	37
1.2.3.1.1	<i>Microradiography</i>	37
1.2.3.1.1.1	<i>Transverse microradiography (TMR)</i>	38
1.2.3.1.1.2	<i>Longitudinal microradiography (LMR)</i>	40
1.2.3.1.1.3	<i>Wavelength independent microradiography (WIM)</i>	40
1.2.3.1.2	<i>Electron beam microanalysis</i>	41
1.2.3.1.3	<i>Wet chemical analysis</i>	43
1.2.3.2	Semi-quantitative methods	43
1.2.3.2.1	<i>Polarised light</i>	43
1.2.3.2.2	<i>Hardness</i>	45
1.2.3.2.2.1	<i>Surface microhardness (SMH)</i>	45
1.2.3.2.2.2	<i>Cross section microhardness (CSMH)</i>	46
1.2.3.2.3	<i>Permeability</i>	48
1.2.3.2.3.1	<i>Iodine absorptiometry</i>	48
1.2.3.2.3.2	<i>Iodine permeability</i>	48
1.2.4	Considerations in regards to assessment methods	49
1.2.4.1	Specimen preparation procedures	49
1.2.4.2	Magnitude of change	51
1.2.4.3	Protocols of specimen analysis	52
Chapter 2	Overview of this study	54
2.1	Hypothesis of the study	54
2.2	Overall approach to achieving the objectives of the study	54

Chapter 3	Selection & validation of method of mineral profile analysis	57
3.1	Introduction	57
3.2	Materials and methods	58
3.2.1	Preparation procedure for enamel specimens	58
3.2.1.1	Lesion preparation: pH cycling protocol	58
3.2.2	Preparation procedure for dentine specimens	60
3.2.3	TMR analysis for enamel and dentine lesions	61
3.2.4	EPMA analysis for enamel and dentine lesions	62
3.3	Results	63
3.4	Interpretation	67
Chapter 4	Preliminary analysis of ionic release from glass-ionomers when exposed to simulated oral conditions	69
4.1	Introduction	69
4.2	Materials and methods	69
4.2.1	Selection and preparation of glass ionomer specimens	69
4.2.2	Preparation of eluting solutions	70
4.2.3	Experimental method	70
4.2.4	Determination of concentrations of ions present in eluting solutions	72
4.2.5	Analysis of diffusion characteristics of cumulative data	73
4.3	Results	73
4.3.1	Cumulative release for luting and lining materials	74
4.3.2	Cumulative release for restorative materials	75
4.3.3	Cumulative release for resin modified materials	77
4.3.4	Cumulative release for high strength restorative materials	77
4.3.5	Comparative Ca/Sr, F, Al release in eight materials	78
4.3.5.1	Calcium	79

4.3.5.2	Strontium	79
4.3.5.3	Fluoride	80
4.3.5.4	Aluminium	82
4.3.6	Diffusion based characteristics of each material	84
4.3.6.1	Calcium/Strontium	84
4.3.6.2	Fluoride	86
4.3.6.3	Aluminium	88
4.4	Interpretation	90
4.4.1	General observations	90
4.4.2	Significance of the elements selected for analysis	91
4.4.3	Comparison of profiles of ions released between product categories	91
4.4.4	Comparison between release profiles at different pH levels	91
4.4.5	Consideration of the mechanism of release	92
4.4.6	A preliminary analysis for evidence of diffusion	93
4.4.7	Significance of the results	93
Chapter 5	Initial studies to investigate the ionic transfer from Fuji IXGP into demineralised dentine in vivo and in vitro and into sound dentine	95
5.1	Fuji IXGP and demineralised dentine in vivo	95
5.1.1	Introduction	95
5.1.2	Materials and methods	96
5.1.2.1	General organisation of the in vivo study	96
5.1.2.2	Collection of the ART restored teeth	97
5.1.2.3	Preparation of the teeth for EPMA	97
5.1.2.4	EPMA method	98
5.1.2.5	SEM analysis	99
5.1.3	Results	100

5.1.4	Interpretation	104
5.2	Development & validation of an in vitro model	106
5.2.1	Introduction	106
5.2.2	Materials and methods	107
5.2.2.1	General descriptions	107
5.2.2.1.1	<i>Preparation of artificial carious dentine lesions</i>	107
5.2.2.1.2	<i>Placement of the restorations</i>	109
5.2.2.1.3	<i>Preparation of samples for EPMA analysis</i>	109
5.2.2.1.4	<i>EPMA</i>	112
5.2.2.2	Experimental design	114
5.2.3	Results	114
5.2.3.1	Experiment A: Consistency of mineral profiles across the artificially produced carious lesions	114
5.2.3.1.1	<i>Group 1: 7 days of exposure to demineralising solution</i>	115
5.2.3.1.2	<i>Group 2: 14 days of exposure to demineralising solution</i>	117
5.2.3.1.3	<i>Group 3: 21 days of exposure to demineralising solution</i>	118
5.2.3.1.4	<i>Statistical analysis</i>	120
5.2.3.2	Experiment B: Similarity of the profiles of strontium and fluorine found in the in vitro and in vivo lesions	125
5.2.4	Interpretation	126
5.2.4.1	Which mineral, how much and where?	127
5.2.4.2	How reproducible is the model?	128
5.2.4.3	Is the pattern of penetration of strontium and fluorine in the in vitro model consistent with that found in the in vivo study?	128
5.3	Baseline analysis of strontium and fluorine penetration from Fuji IXGP into sound dentine	128
5.3.1	Background	128
5.3.2	Materials and methods	128

5.3.3	Results	130
5.3.4	Interpretation	131
Chapter 6	A comprehensive analysis of the ionic exchange behaviour from different types of glass-ionomer and demineralised dentine	133
6.1	Introduction	133
6.2	High strength glass-ionomers: Fuji IXGP	134
6.2.1	Background	134
6.2.2	Materials and methods	134
6.2.2.1	Study design	134
6.2.2.2	Placement of the restorations	134
6.2.2.3	EPMA and Statistical analysis	135
6.2.3	Results	136
6.2.3.1	Representative EPMA profiles (Fuji IXGP)	136
6.2.3.1.1	<i>7 day artificial lesion</i>	136
6.2.3.1.2	<i>14 day artificial lesion</i>	136
6.2.3.1.3	<i>21 day artificial lesion</i>	137
6.2.3.2	EPMA elemental maps	137
6.2.3.2.1	<i>7 day artificial lesion treated for 21 days</i>	138
6.2.3.2.2	<i>7 day artificial lesion treated for 42 days</i>	140
6.2.3.2.3	<i>14 day artificial lesion treated for 21 days</i>	141
6.2.3.2.4	<i>14 day artificial lesion treated for 42 days</i>	142
6.2.3.2.5	<i>21 day artificial lesion treated for 21 days</i>	143
6.2.3.2.6	<i>21 day artificial lesion treated for 42 days</i>	144
6.2.3.3	Statistical analysis	145
6.2.3.3.1	<i>7 day lesion treated with Fuji IXGP</i>	145
6.2.3.3.2	<i>14 day lesion treated with Fuji IXGP</i>	145

6.2.3.3.3	<i>21 day lesion treated with Fuji IXGP</i>	146
6.3	High fluoride releasing GIC: Fuji VI	146
6.3.1	Background	146
6.3.2	Materials and methods	146
6.3.3	Results	146
6.3.3.1	Representative EPMA profiles (Fuji VI)	147
6.3.3.1.1	<i>7 day artificial lesion</i>	147
6.3.3.1.2	<i>14 day artificial lesion</i>	147
6.3.3.1.3	<i>21 day artificial lesion</i>	148
6.3.3.2	EPMA elemental maps	148
6.3.3.2.1	<i>7 day artificial lesion treated for 21 days</i>	149
6.3.3.2.2	<i>7 day artificial lesion treated for 42 days</i>	150
6.3.3.2.3	<i>14 day artificial lesion treated for 21 days</i>	151
6.3.3.2.4	<i>14 day artificial lesion treated for 42 days</i>	152
6.3.3.2.5	<i>21 day artificial lesion treated for 21 days</i>	153
6.3.3.2.6	<i>21 day artificial lesion treated for 42 days</i>	154
6.3.3.3	Statistical analysis	155
6.3.3.3.1	<i>7 day lesion treated with Fuji VI</i>	155
6.3.3.3.2	<i>14 day lesion treated with Fuji VI</i>	155
6.3.3.3.3	<i>21 day lesion treated with Fuji VI</i>	156
6.4	RMGIC dentine adhesive FujiBond LL	156
6.4.1	Background	156
6.4.2	Materials and methods	156
6.4.3	Results	157
6.4.3.1	Representative EPMA profiles (Fuji Bond LL)	157
6.4.3.1.1	<i>7 day artificial lesion</i>	157

6.4.3.1.2	<i>14 day artificial lesion</i>	158
6.4.3.1.3	<i>21 day artificial lesion</i>	158
6.4.3.2	Statistical analysis	159
6.4.3.2.1	<i>7 day lesion treated with Fuji Bond LL</i>	159
6.4.3.2.2	<i>14 day lesion treated with Fuji Bond LL</i>	160
6.4.3.2.3	<i>21 day lesion treated with Fuji Bond LL</i>	160
6.5	Statistical analysis of combined results for 21 day exposure	160
6.6	Statistical analysis of combined results for 42 day exposure	161
6.7	Interpretation	162
6.7.1	General observations	162
6.7.2	Elemental distribution map	164
Chapter 7	Discussion	165
7.1	Restatement of objectives and overall design of the study	165
7.2	EPMA as a measurement method	166
7.3	Selection of glass-ionomer to be tested	168
7.4	<i>In vivo</i> study	170
7.5	Design and validation of the <i>in vitro</i> model	170
7.6	Ionic exchange behaviour of the three glass-ionomers and demineralised dentine	172
7.7	Overall summary and conclusion	173
Bibliography		175
Appendix A	Additional results for Chapter 4	Appendix A1
	Ketac Cem: Incremental Release	A1
	Ketac Bond: Incremental Release	A1

Fuji II: Incremental Release	A2
Fuji II F: Incremental Release	A2
Fuji II LC Improved: Incremental Release	A3
Ketac Fil Plus: Incremental Release	A3
Ketac Molar: Incremental Release	A4
Fuji IXGP: Incremental Release	A4

Appendix B Additional results for Chapter 5.1	Appendix B1
--	-------------

Sample 1: Coded as FG46	B2
Sample 2: Coded as FG95	B3
Sample 3: Coded as FG22	B4
Sample 4: Coded as FG32	B5
Sample 5: Coded as FG54	B6
Sample 6: Coded as FG61	B7
Sample 7: Coded as FG72	B8
Sample 8: Coded as FG1001	B9
Sample 9: Coded as FG1203	B10
Sample 10: Coded as FG135	B11
Sample 11: Coded as FG1502	B12
Sample 12: Coded as FG1103	B13
Sample 13: Coded as FG1402	B14

Appendix C Additional results for Chapter 5.2	Appendix C1
--	-------------

Correlation between left and right sides of 7 day lesions	C1
Correlation between left and right sides of 14 day lesions	C2
Correlation between left and right sides of 21 day lesions	C3

Appendix D Additional results for Chapter 6.2

Appendix D1

High strength glass-ionomer Fuji IXGP: 7 day artificial lesion treated for 21 days	D1
High strength glass-ionomer Fuji IXGP: 7 day artificial lesion treated for 42 days	D2
High strength glass-ionomer Fuji IXGP: 14 day artificial lesion treated for 21 days	D3
High strength glass-ionomer Fuji IXGP: 14 day artificial lesion treated for 42 days	D4
High strength glass-ionomer Fuji IXGP: 21 day artificial lesion treated for 21 days	D5
High strength glass-ionomer Fuji IXGP: 21 day artificial lesion treated for 42 days	D6
High fluoride releasing glass-ionomer Fuji VI: 7 day artificial lesion treated for 21 days	D7
High fluoride releasing glass-ionomer Fuji VI: 7 day artificial lesion treated for 42 days	D8
High fluoride releasing glass-ionomer Fuji VI: 14 day artificial lesion treated for 21 days	D9
High fluoride releasing glass-ionomer Fuji VI: 14 day artificial lesion treated for 42 days	D10
High fluoride releasing glass-ionomer Fuji VI: 21 day artificial lesion treated for 21 days	D11
High fluoride releasing glass-ionomer Fuji VI: 21 day artificial lesion treated for 42 days	D12
Resin Modified Glass Ionomer adhesive FujiBondLL: 7 day artificial lesion treated for 21 days	D13
Resin Modified Glass Ionomer adhesive FujiBondLL: 7 day artificial lesion treated for 42 days	D14
Resin Modified Glass Ionomer adhesive FujiBondLL 14 day artificial lesion treated for 21 days	D15

Resin Modified Glass Ionomer adhesive: FujiBondLL: 14 day artificial lesion treated for 42 days	D16
Resin Modified Glass Ionomer adhesive FujiBondLL: 21 day artificial lesion treated for 21 days	D17
Resin Modified Glass Ionomer adhesive FujiBondLL: 21 day artificial lesion treated for 42 days	D18

List of figures

Figure 1	Composition of enamel by weight% and volume%	4
Figure 2	Composition of dentine by weight% and volume%	5
Figure 3	Diagram of an individual calcium hydroxy apatite crystal	6
Figure 4	Scanning electron microscope micrographs of enamel prisms	6
Figure 5	Transmission electron microscope micrographs of dentine showing its major components and the porous nature of dentine	7
Figure 6	Dentine infused with resin then dissolved to reveal the dense tubular system	9
Figure 7	Strontium concentration as analysed in synthetic carbonated apatite vs. Sr concentration in the precipitating media	12
Figure 8	Schematic drawing to illustrate the relationship between the hardness curve corresponding to the infected and affected zones found in carious dentine	20
Figure 9	The four phases in the setting reaction of glass-ionomer cement	28
Figure 10	TMR profile showing: lesion depth and mineral loss value	39
Figure 11	The zone of interaction between the electron beam and the solid specimen	41
Figure 12	Overall approach to achieving the objectives of the study	56
Figure 13	EPMA mineral content profiles of enamel specimen treated with 1450ppm NaF	63
Figure 14	TMR mineral content profiles of enamel specimen treated with 1450ppm NaF	64
Figure 15	Ca:P ratio is maintained right through demineralised and sound enamel	64
Figure 16	EPMA mineral content profiles of enamel specimen treated with 0ppm NaF	65

Figure 17	TMR mineral content profiles of enamel specimen treated with 0ppm NaF	65
Figure 18	Correlation between the EPMA and TMR depths of lesions	66
Figure 19	EPMA mineral content profiles of three two week dentine artificial lesions	66
Figure 20	Ca:P ratio in demineralised and sound dentine	67
Figure 21	Set of six samples exposed to the storage media	71
Figure 22	Stand for samples allowing free flow of the solution around each sample	71
Figure 23	Ketac Cem, relative cumulative release of Ca, F and Al at different pH	74
Figure 24	Ketac Bond, relative cumulative release of Ca, F and Al at different pH	75
Figure 25	Fuji II, relative cumulative release of Sr, F and Al at different pH	75
Figure 26	Fuji IIF, relative cumulative release of Ca, F and Al at different pH	76
Figure 27	Ketac Fil Plus, relative cumulative release of Sr, F and Al at different pH	76
Figure 28	Fuji II LC Improved, relative cumulative release of Sr, F and Al at different pH	77
Figure 29	Ketac Molar, relative cumulative release of Ca, F and Al at different pH	77
Figure 30	Fuji IXGP, relative cumulative release of Sr, F and Al at different pH	78
Figure 31	Comparative calcium release at different pH	79
Figure 32	Comparative strontium release at different pH	79
Figure 33	Comparative fluoride release at different pH	80/81
Figure 34	Comparative aluminum release at different pH	82/83
Figure 35	Comparative diffusion characteristics for Ca/Sr release at different pH	84/85/86

Figure 36	Comparative diffusion characteristics for F release at different pH	86/87/88
Figure 37	Comparative diffusion characteristics for Al release at different pH	88/89/90
Figure 38	Sample immediately after sectioning	98
Figure 39	Sample ready for coating with carbon before EPMA and SEM	98
Figure 40	EPMA was carried out in four separate regions	100
Figure 41	Typical mineral profiles found in carious dentine, in a large lesion, adjacent to the glass-ionomer restoration.	101
Figure 42	Typical mineral profiles found in a small carious lesion in dentine, adjacent to a glass-ionomer restoration.	101
Figure 43	Depth of lesion and depth of penetration of Sr and F found in the thirteen samples.	103
Figure 44	The first two steps in the preparation of the <i>in vitro</i> model	108
Figure 45	Molars with prepared cavity, ready for the placement of glass-ionomer	109
Figure 46	Isomet Slow Speed Saw	110
Figure 47	The five steps involved in preparing the sample for EPMA	110
Figure 48	Samples in a special holder to ensure plano-parallelism	111
Figure 49	Abramin polishing machine	111
Figure 50	Example of a sample ready for EPMA	112
Figure 51	EPMA machine, model SX51	113
Figure 52	Loss of CA from dentine	115
Figure 53	Mineral profile of a sample in the 7 day group	116
Figure 54	Mineral profile of a sample in the 14 day group	117
Figure 55	Mineral profile of a sample in the 21 day group	119
Figure 56	Mineral profiles found in the control region	126
Figure 57	Mineral profiles found in the test region	126

Figure 58	Parameters used to express the depth of the lesion, amount of calcium loss and amount of strontium gained	128
Figure 59	Ionic exchange pattern between Fuji IXGP and sound dentine	131
Figure 60	Overview of experimental design for each material.	134
Figure 61	7 day lesion treated with Fuji IXGP for 21 days	136
Figure 62	7 day lesion treated with Fuji IXGP for 42 days	136
Figure 63	14 day lesion treated with Fuji IXGP for 21 days	136
Figure 64	14 day lesion treated with Fuji IXGP for 42 days	137
Figure 65	21 day lesion treated with Fuji IXGP for 21 days	137
Figure 66	21 day lesion treated with Fuji IXGP for 42 days	137
Figure 67	7 day lesion exposed to Fuji IXGP for 21 days.	139
Figure 68	7 day lesion exposed to Fuji IXGP for 42 days.	140
Figure 69	14 day lesion exposed to Fuji IXGP for 21 days	141
Figure 70	14 day lesion exposed to Fuji IXGP for 42 days	142
Figure 71	21 day lesion exposed to Fuji IXGP for 21 days	143
Figure 72	21 day lesion exposed to Fuji IXGP for 42 days	144
Figure 73	7 day lesion treated with Fuji VI for 21 days	147
Figure 74	7 day lesion treated with Fuji VI for 42 days	147
Figure 75	14 day lesion treated with Fuji VI for 21 days.	147
Figure 76	14 day lesion treated with Fuji VI for 42 days	147
Figure 77	21 day lesion treated with Fuji VI for 21 days	148
Figure 78	21 day lesion treated with Fuji VI for 42 days	148
Figure 79	7 day lesion exposed to Fuji VI for 21 days	149
Figure 80	7 day lesion exposed to Fuji VI for 42 days.	150
Figure 81	14 day lesion exposed to Fuji VI for 21 days	151
Figure 82	14 day lesion exposed to Fuji VI for 42 days	152

Figure 83	21 day lesion exposed to Fuji VI for 21 days	153
Figure 84	21 day lesion exposed to Fuji VI for 42 days	154
Figure 85	7 day lesion exposed to Fuji Bond LL for 21 days.	157
Figure 86	7 day lesion exposed to Fuji Bond LL for 42 days	157
Figure 87	14 day lesion exposed to Fuji Bond LL for 21 days	158
Figure 88	14 day lesion exposed to Fuji Bond LL for 42 days	158
Figure 89	21 day lesion exposed to Fuji Bond LL for 21 days	158
Figure 90	21 day lesion exposed to Fuji Bond LL for 42 days	159
Figure 91	Ketac Cem, relative incremental release of Ca, F and Al at different pH	A1
Figure 92	Ketac Bond, relative incremental release of Ca, F and Al at different pH	A1
Figure 93	Fuji II, relative incremental release of Ca, F and Al at different pH	A2
Figure 94	Fuji II F, relative incremental release of Ca, F and Al at different pH	A2
Figure 95	FujiIII LCImproved, incremental release of Ca, F and Al at different pH	A3
Figure 96	Ketac Fil Plus, incremental release of Ca, F and Al at different pH	A3
Figure 97	Ketac Molar, incremental release of Ca, F and Al at different pH	A4
Figure 98	Fuji IXGP, incremental release of Ca, F and Al at different pH	A4
Figure 99	Mineral profiles of four regions in sample FG46	B2
Figure 100	Mineral profiles of two regions in sample FG95	B3
Figure 101	Mineral profiles in two regions of FG22	B4
Figure 102	Mineral profiles of four regions in sample FG32	B5
Figure 103	Mineral profiles in two regions of FG54	B6
Figure 104	Mineral profiles in two regions of FG61	B7
Figure 105	Mineral profiles in three regions of FG72	B8
Figure 106	Mineral profiles in three regions of FG72	B9
Figure 107	Mineral profiles in three regions of FG54	B10

Figure 108	Mineral profiles in two regions of FG135	B11
Figure 109	Sample FG1502	B12
Figure 110	Sample FG1103	B13
Figure 111	Sample FG1402	B14

LIST OF TABLES

Table 1	Electrolyte composition of plasma	11
Table 2	Minimum detection limits based on beam settings of 15kV and 20mA	62
Table 3	Glass-ionomer cements to be tested	70
Table 4	Concentrations found in the standard used for calibration and Minimum Detection Limits for the elements of interest	99
Table 5	Average depth of carious dentine and average depth of penetration of Sr and F	102
Table 6	Correlation coefficient for the levels of strontium and fluorine in the three zones	103
Table 7	Concentrations found in the standard used for calibration and Minimum Detection Limits for the elements of interest	113
Table 8	L _{Ca} and ΔZ_{Ca+P} for all samples in the 7 day group.	116
Table 9	L _{Ca} and ΔZ_{Ca+P} for all samples in the 14 day group	118
Table 10	L _{Ca} and ΔZ_{Ca+P} for all samples in the 21 day group	119
Table 11	Correlation between left and right sides of 7 day lesions	121
Table 12	Correlation between left and right sides of 14 day lesions	122
Table 13	Correlation between left and right sides of 21 day lesions	123
Table 14	Comparison between left and right sides of 7 day lesions	124
Table 15	Comparison between left and right sides of 14 day lesions	124
Table 16	Comparison between left and right sides of 21 day lesions	125
Table 17	Mean ΔZ_{Ca+P} and intra group consistency of ΔZ_{Ca+P} for the different groups	145
Table 18	7 day lesion, comparison between treatment times with Fuji IXGP	145
Table 19	14 day lesion, comparison between treatment times with Fuji IXGP	145
Table 20	21 day lesion, comparison between treatment times with Fuji IXGP	146

Table 21	Intra group consistency between control and test of $\Delta ZCa+P$ for the different groups.	155
Table 22	7 day lesion, comparison between treatment times with Fuji VI	155
Table 23	14 day lesion, comparison between treatment times with Fuji VI	155
Table 24	21 day lesion, comparison between treatment times with Fuji VI	156
Table 25	Intra group consistency between control and test of $\Delta ZCa+P$ for the different groups	159
Table 26	7 day lesion, comparison between treatment times with Fuji Bond LL	159
Table 27	14 day lesion, comparison between treatment times with Fuji Bond LL	160
Table 28	21 day lesion, comparison between treatment times with Fuji Bond LL	160
Table 29	The uptake of fluorine and strontium in 7 day group	161
Table 30	The uptake of fluorine and strontium in 14 day group	161
Table 31	The uptake of fluorine and strontium in 21 day group	161
Table 32	The uptake of fluorine and strontium in 7 day group	162
Table 33	The uptake of fluorine and strontium in 14 day group	162
Table 34	The uptake of fluorine and strontium in 21 day group	162

ABSTRACT

Glass-ionomer cement has been used in the Atraumatic Restorative Technique (ART) for stabilisation of carious lesions. The infected layer or fully demineralised dentine is removed by dental hand instruments only and glass-ionomer cement is placed to restore the lesion leaving the affected layer or partly demineralised dentine underneath. There are many anecdotal and some published reports of the ability of these materials to remineralise partly demineralised dentine.

The major objectives of this investigation are:

1. To scientifically demonstrate the ability of glass-ionomers to remineralise partly demineralised dentine *in vivo* and *in vitro*.
2. To determine the nature of the remineralisation process.
3. To determine those factors having greatest impact on the remineralisation process.

Those objectives are partly met with the use of EPMA and an *in vitro* model, specially designed to simulate clinical conditions as closely as possible.

With EPMA, it is possible to identify, quantify and trace the migration of different elements, found in glass-ionomer, into the partly demineralised dentine. The results lead to a better understanding of the possible mechanisms involved.

There have been anecdotal and clinical reports on the remineralisation of carious dentine left at the base of glass-ionomer restorations. This was confirmed in a human *in vivo* study.

The information derived from it was utilised in the design of an *in vitro* model to allow in depth study of the effects, on the remineralisation process, of the following two variables:

- The level of remaining minerals in dentine
- The length of contact with the glass-ionomer

The results support the hypothesis that the close adaptation of glass-ionomer cement to demineralised dentine will lead to the uptake of apatite forming ions into dentine and lead to its remineralisation. The process involved first the diffusion then the precipitation of

both strontium and fluorine from the glass ionomer into the partly demineralised dentine. This process is dependent on the glass-ionomer, the level of demineralisation of dentine and the time that it stays in contact with the glass-ionomer.

The combination of Fuji VI with a treatment time of 42 days has the best potential for remineralisation. However, further study is required before the mechanism involved can be fully understood.

DECLARATION

This work contains no material which has been accepted for the award of any other degree or diploma in any university or other tertiary institution to the best of my knowledge and belief, contains no material previously published or written by another person except where due reference has been made in the text.

I give consent to this copy of my thesis, when deposited in the University Library, being available for loan and photocopying.

Signed:

Date:

Hien Chi Ngo

ACKNOWLEDGMENTS

The work leading to this thesis cannot be achieved without the guidance, assistance and encouragement from a number of people.

I begin by thanking Miss Celia Baker, Dr Michelle Fraser and Dr Do Giang Loc for their technical support in the laboratory and statistical analysis of the results. Also, it would be impossible to carry out this study without the guidance from the staff of the Adelaide Microscopy Centre of the University of Adelaide. In particular, I received important guidance from Dr Hugh Rosser and Mr John Terlet, while developing the protocols for EPMA analysis.

The assistance I received from GC Corporation, Japan and 3M ESPE, USA was invaluable. Their willingness to support this study both in advice, materials and funding played an essential part in the completion of the experimental phase of this study.

My greatest source of inspiration for this work has been Dr Graham Mount and Dr John McIntyre. Both have dedicated their career to the betterment of dentistry and they have been my supervisors and mentors. They have guided me right from the beginning of this project and contributed a great deal to this manuscript with their discerning and constructive remarks.

My appreciation also goes to Mr Michael Williams, Dr John Abbott, Professor Lindsay Richards and Professor Rory Hume for their support and encouragement over the course of this study.

Finally, a special mention goes to my wife and two children. In the early stage of this project, my wife, while pregnant with our first child, volunteered her labour and assisted me in performing the experiments described in Chapter 4. Their love, sacrifice and understanding have allowed me to finish this piece of work. To them I owe the biggest debt of gratitude.

Chapter 1: Introduction & Literature Review

1.1 Introduction

One of the major quests in conservative dentistry has been to find a material to replace lost and damaged tooth structures which has a close affinity, physically and chemically, to tooth tissue and at the same time will minimise the risk of further damage. The development of the glass-ionomers has been a significant step in this search, even though they still fall short of an ideal replacement.

Up to this time, almost all the restorative materials used in dentistry have been biologically inert. However, it was shown previously that silicate cement released fluoride ions, and these were taken up into surrounding tooth structure. Recently glass ionomer cements were shown to have similar properties and the sustained release of fluoride was identified as a reason for its anti-cariogenicity (Mount 1988; Forsten 1998; Francci, Deaton et al. 1999).

One of the more interesting uses of glass ionomer cement has been in the Atraumatic Restorative Technique (ART) for stabilisation of carious lesions in developing countries. This “Low Tech-Low Cost” approach allows the delivery of restorative care without the need for electricity and high-tech equipment. The infected layer or fully demineralised dentine is removed by dental hand instruments only and glass-ionomer cement is placed to restore the lesion leaving the affected layer or partly demineralised dentine underneath.

This technique is now used in developed countries for indirect pulp capping but has not been investigated scientifically up to the present time. There are many anecdotal and some published reports of the ability of these materials to remineralise partly demineralised dentine. If this is so, it has very significant implications for current restorative methodology. It is essential to gain a more thorough understanding of the ways in which glass-ionomer interacts with partially demineralised dentine, in order to ensure, not only that it is used to greatest advantage, but also to permit further material developments to be

investigated. The purpose of this investigation is to scrutinise the ways in which glass-ionomer and demineralised dentine interact at both the chemical and physical level.

The major impetus of this investigation is:

1. To scientifically demonstrate the ability of glass-ionomers to remineralise partly demineralised dentine *in vivo* and *in vitro*.
2. To determine the nature of the remineralisation process.
3. To determine those factors having greatest impact on the remineralisation process.

1.2 Literature review

As an introduction to this investigation it is necessary to review the nature of healthy enamel and dentine and the alterations that can take place as a result of caries. The composition of these materials both organic and inorganic will have a bearing on the changes in the levels of mineralisation over time as a result of wear and tear, age and disease. If the changes are significant then both materials must be permeable. Current concepts on permeability in both newly erupted as well as mature tooth structure will be discussed and the significance of permeability as this relates to the possibility of demineralisation and subsequent remineralisation. In other words the significance of the interaction between the tooth and its surroundings, primarily saliva which of course is saturated with mineral at all times.

The structural and biological changes that take place within tooth structure as a result of the caries process, including colour change, is highly significant in terms of this research. The potential for remineralisation has been deeply investigated over recent years and the current attitude to this will be investigated because this is the basis of the present presentation.

Having investigated current thinking on tooth structure, there will be a review of glass ionomer materials because it is suggested that these have the greatest potential of all

restorative materials to assist in the healing and repair of a carious lesion. It has already been clearly demonstrated that these materials contain many of the ions that are contained in hydroxyapatite and that there is a degree of porosity in their microstructure. The setting reaction needs to be reviewed and the present knowledge of the release of fluoride and other ions will be discussed and this will lead to consideration of ion uptake into adjacent tooth structure.

It is suggested that current methods used for the study of remineralisation fail to take into account a number of significant factors. A number of technologies are available that provide a higher level of accuracy and repeatability. Three X-ray microradiographic methods will be discussed as well as electron beam microanalysis. There will be some discussion of semi-quantitative methods such as polarised light and micro-hardness; all of these will be compared for their value in research in this significant area.

The results of this review will lead to the rationale for the selection of the materials and methods utilised in this study and details of the study will then be presented.

1.2.1 The nature of enamel and dentine

The body of a tooth is composed of three mineralised tissues: enamel, dentine and cementum as well as the non-mineralised tissue, the pulp. For the purpose of this review, the discussion will concentrate on the first two as they are the major components of a tooth and dentine is the major focus of this investigation.

Dental caries is a chronic bacterial disease that can affect enamel, dentine and cementum through a localised destruction of tooth structure by the end products of bacterial metabolism. Carious lesions usually start in enamel and as this tissue is acellular, the living reparative events generally triggered by an infectious process in soft tissues cannot occur. Furthermore, the stability of enamel is entirely dependent on the chemical balance of its immediate surrounding environment. The breaking down of enamel is gradual and will

eventually expose the pulpo-dentinal organ to bacterial metabolic products long before any bacteria can be detected at the dentino-enamel junction (Thylstrup and Qvist 1987).

In order to understand the mechanism by which bacterial end products initiate demineralisation in enamel and dentine and the subsequent reparative response from the pulpo-dentinal organ through the remineralisation process, it is necessary to first consider the physical and chemical nature of both the enamel and dentine.

1.2.1.1 Composition

1.2.1.1.1 Organic

The organic matrix is negligible in enamel but in dentine both the aqueous organic gel and collagen matrix play an important role in maintaining its integrity. The average composition of enamel and dentine in terms of weight % and volume % is illustrated in **Figure 1** and **Figure 2** (Brudevold, Steadman et al. 1960).

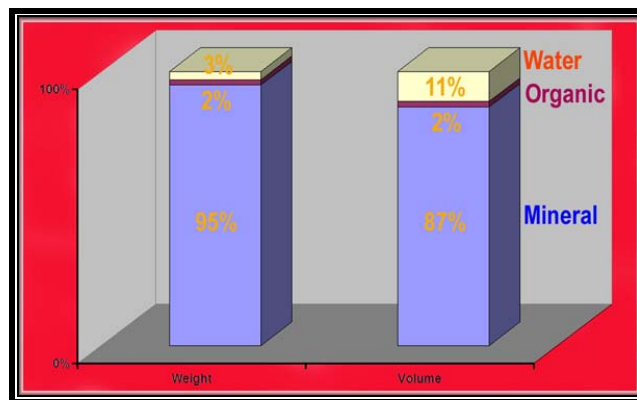


Figure 1: Composition of enamel by weight% and volume%. (Brudevold, Steadman et al. 1960)

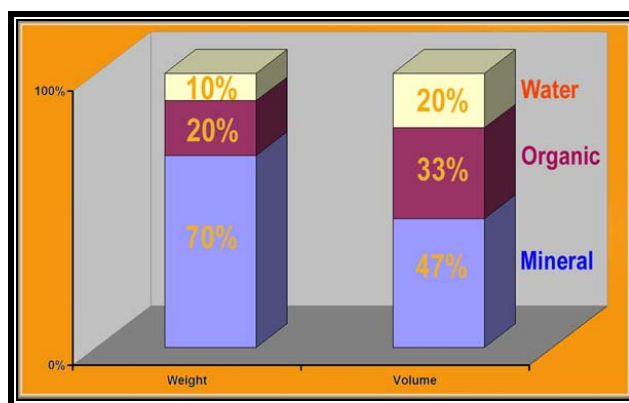


Figure 2: Composition of dentine by weight% and volume %. (Brudevold, Steadman et al. 1960)

Due to the difference in density of the three major components, weight % does not illustrate well the spatial proportion occupied by each part. The permeable nature of these two tissues is best appreciated through their composition in term of volume %, **Figure 1** and **Figure 2** (Brudevold, Steadman et al. 1960). When considered in terms of volume%, water becomes a major component of both enamel and dentine; it contributes up to 11% in enamel and 20% in dentine.

Histologic and microstructural studies of developing teeth show that the aqueous organic gel forms a contiguous three dimensional matrix in both enamel and dentine and the mineral crystals are dispersed in it. For this reason it is to be expected that tooth enamel, and more so dentine, is highly permeable for diffusion of small ions and molecules. The aqueous organic gel forms the transport channel to allow both de- and remineralisation to occur.

1.2.1.1.2 Inorganic

The mineral phase of enamel and dentine is composed entirely of hydroxyapatite (HAP) which can be described, as a hydrated form of calcium phosphate, with the formula $\text{Ca}_{10}(\text{PO}_4)_6(\text{OH})_2$. In both enamel and dentine, HAP exists in the form of tiny mineral

crystals, surrounded by a hydration shell and embedded in an aqueous organic matrix, **Figure 3**. The hydration shell also contributes to the amount of water found in enamel and dentine as shown in **Figure 1** and **Figure 2**.



Figure 3: Diagram of an individual calcium hydroxy apatite crystal showing its components: C: crystal core, A: ionic adsorption layer, H: hydration shell, S: aqueous organic material. (Nikiforuk 1985)

Nature produces many types of calcium phosphate and these differ in their calcium to phosphorus ratio and their solubility is dependent upon the pH of the environment (Driessens 1982). The crystals are bathed in the aqueous organic gel occupying the intercrystalline space as seen in **Figure 4**.

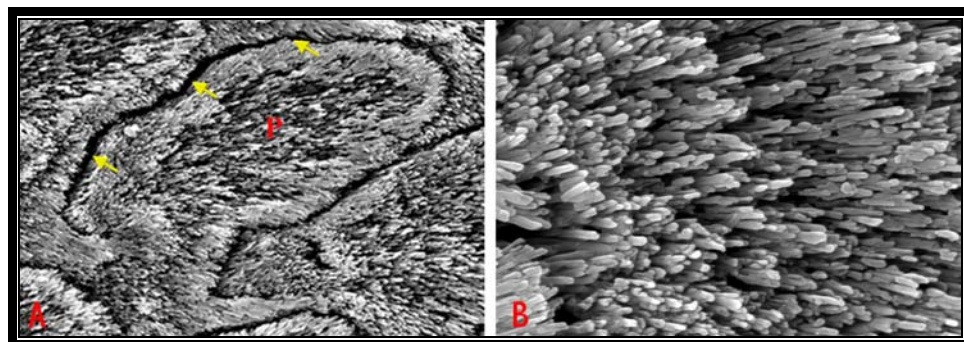


Figure 4:

A: Scanning electron microscope (SEM) micrographs of enamel prisms showing the interprismatic space (yellow arrows) with a periphery of densely packed crystals. P is the centre of the prism with less densely packed crystals.

B: Higher magnification of crystals showing space occupied by an aqueous organic gel matrix. (Personal Data)

1.2.1.1.3 Water

The presence of the hydration shell means that the crystal is electrically charged and can therefore attract ions that are able to play a part in de- and remineralisation. The remaining water forms the aqueous organic gel that fills the spaces between the rods and this forms the main diffusion pathway into and through the enamel.

Dentine contains 20% water by volume and some of this water is in the form of the hydration shell and the aqueous organic matrix occupies the intercrystallar space. As in enamel, this forms a diffusion pathway for water and organic molecules to diffuse through dentine. The contribution of this diffusion pathway is relatively minor when compared with the flow allowed by the dentinal tubules and the associated complex network of lateral microtubules **Figure 5**.

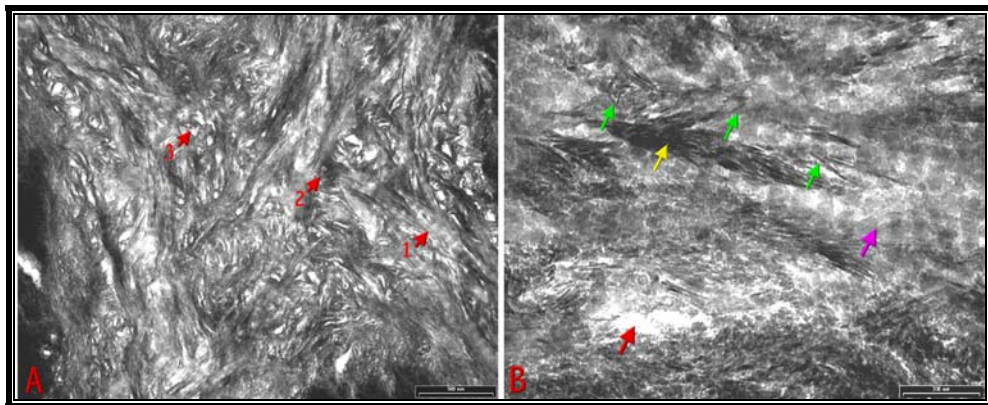


Figure 5: Transmission electron microscope (TEM) micrographs of dentine showing its major components and the porous nature of dentine.

A: Overview of dentine microstructure 1: Collagen with typical cross banding, 2: Crystals of hydroxyapatite, 3: Micro tubules.

B: High magnification of A showing a micro tubule (red), crystal bundle (yellow arrow), individual needle shape crystals (green arrow) and collagen cross banding (purple) (Personal Data).

1.2.1.2 Permeability of enamel and dentine

Enamel is a secretory product of cells derived from the stratified epithelium of the oral cavity. The permeability of enamel is not so obvious because of its dense appearance. Several investigators have demonstrated the permeability of tooth enamel by qualitative experiments using, for example, radioactive tracers (Sognaes, Shaw et al. 1955; Yen, Bogoroch et al. 1958) or polarised light microscopy (Darling, Mortimer et al. 1961). It has been shown that organic molecules can penetrate into tooth enamel and replace part of the water molecules. As the penetration depends on the size of the organic molecules, these authors have proposed a molecular sieve behaviour for enamel.

Flow of water through tooth enamel has been demonstrated with microscopes (Bergman 1963) and with manometers (Poole, Tailby et al. 1963). Proton NMR studies showed that most of the water found in enamel is free water and the remainder is probably present as the hydration shell around the crystals (White, Bowman et al. 1988). The nature of the diffusion channels through enamel will be discussed later.

Dentine, on the other hand, is mesodermal in origin and possesses characteristics similar to bone. It is hollow with a complex network of tubules and microtubules designed to house and protect a living organ, the dental pulp. This intricate network is illustrated in **Figure 6**. The SEM micrographs reveal that, apart from the major dentinal tubules with diameter ranging between 2 to 5 μ m, the network is also composed of microtubules with diameter as small as a few nanometres. These can also be seen in TEM micrographs **Figure 5**. It is apparent that this network contributes greatly to the permeability of this tissue and therefore plays an important role in governing the ion transfer process.

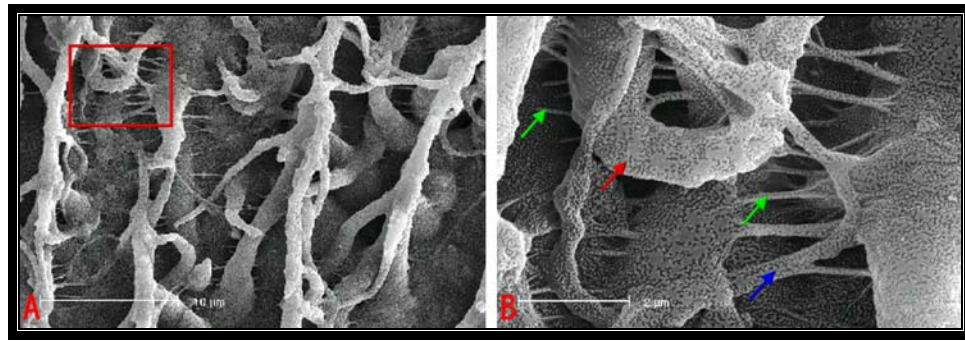


Figure 6: Dentine was infused with resin then dissolved to reveal the dense tubular system.

A: SEM micrograph showing the primary dentine tubules as well as the lateral tubule network.

B: Higher magnification of the selected area in A, showing the lateral branches (red arrow) extending from the major tubules. This network was further divided into sub micron (blue arrow) and finally finer division at the nanometre level (green arrow) (Personal Data).

1.2.1.3 Mineralisation

When any tissue undergoes calcification, an organic matrix is laid down first and subsequently mineralised. There have been various mechanisms proposed for the infusion of the organic matrix of dentine and enamel with apatite mineral and they fall into three general areas:

1. Raising the concentrations of calcium and phosphate in the local environment to supersaturation levels would cause spontaneous precipitation of HAP crystals.
2. Providing substances which create nucleating sites for HAP crystals or remove barriers to such sites
3. Removing or neutralizing mineral inhibitors

All these mechanisms may occur in either an intracellular and or extracellular manner.

It has been proposed (Robinson, 1923) that alkaline phosphatase hydrolysed phosphate esters may produce an excess of free inorganic phosphate at calcification sites and

therefore increase the local calcium phosphate supersaturation level of body fluids. The following macromolecules, present in various calcifying systems, are examples of materials which at some time have been suggested as heterogeneous nucleation substrates for hydroxyapatites: γ -carboxyglutamate-(Gla) containing proteins (Hauschka 1979), phosphoproteins (Dimuzio and Veis 1978), glycoproteins (Van Dyke, Levine et al. 1979), calcium-acidic phospholipids-phosphate complexes (Boskey 1978), proteolipids (Boyan-Salyers 1980), and collagen (Glimcher 1976). It is now believed that collagen itself is not an apatite nucleator but just a framework in and on which mineral in bone and dentine may be deposited (Hohling, Neubauer et al. 1971) (Glimcher 1976).

Other substances closely associated with collagen, such as phosphoproteins, appear to serve as nucleators of mineral. The steric arrangement of the phosphate groups in these phosphoproteins is optimal for the binding of calcium and for the subsequent formation of apatite crystals. It has been shown that phosphoproteins will induce direct hydroxyapatite formation in highly supersaturated calcium phosphate solutions from which amorphous calcium phosphate would have formed in the absence of these phosphoproteins (Nawrot, Campbell et al. 1976).

Calcium phosphates precipitate by a simple physico-chemical process from a solution which is supersaturated with calcium, phosphate and other apatite forming ions. However, the presence of nucleators may lower the critical supersaturation at which the first nuclei forms and therefore facilitates the precipitation process. In the mineralisation of biological tissues, organic molecules serve as nuclei for the precipitation of calcium phosphates.

In theory, calcium phosphates found in bone and dental hard tissues are present in the form of HAP [$\text{Ca}_{10}(\text{PO}_4)_6(\text{OH})_2$], as this is, thermodynamically, the most stable form at neutral and slightly acidic pH.

However, there are various ions present in the surrounding body fluid and those that can fit into the crystallite structure of HAP are often incorporated, during the mineralisation phase of the development of a tooth, as impurities (**Table 1**).

pH	7.0
Calcium	2.5 mmol/l
Phosphate	1 mmol/l
Carbonate	27 mmol/l
Other ions: Na, K, Cl	249 mmol/l

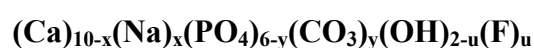
Table 1: Electrolyte composition of plasma (Driessens 1982)

In nature, there is often isomorphous substitution in mineral and biological HAP. Calcium has many possible substitutions such as sodium, magnesium, strontium, zinc and many other cations. Phosphate can be replaced by carbonate in up to 24% of the available sites in the apatite structure. Hydroxyl is normally replaced by fluoride (Trautz 1967). The type and concentration of these ions depends on their availability during the formation of the tissues, which in turn depends on their environmental levels and whether the body allows the passage of the respective ions to the site of precipitation (Weatherell and Robinson 1973).

Two of these impurities, carbonate and fluoride deserve special attention because they affect the reactivity and solubility of the HAP and are present in large enough concentrations in pre-eruptive enamel and dentine.

The third impurity that is of special interest in this study is strontium, as it will be used, together with fluoride, in investigations to trace the ionic exchange patterns between glass ionomer and carious dentine.

The apatite of dental hard tissue has been described by the following formula (Arends and Davidson 1975; Featherstone and Nelson 1980; LeGeros 1991):



Featherstone demonstrated that when carbonated apatite is precipitated in the presence of sodium, strontium and/or fluoride, sodium is taken up proportionally to carbonate and all available strontium and fluoride are incorporated at the concentrations tested (**Figure 7**). It was also concluded that the acid solubility of the carbonated apatites increased markedly in proportion to carbonate inclusion. This reactivity is reduced by 50% when strontium and fluoride are incorporated together into the apatites (Featherstone, Shields et al. 1983).

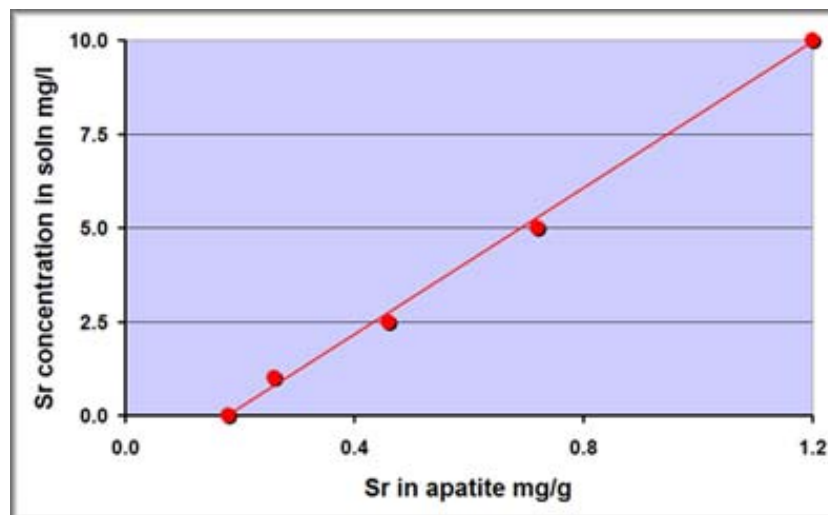


Figure 7: Strontium concentration as analysed in synthetic carbonated apatite vs. Sr concentration in the precipitating media (Featherstone, Shields et al. 1983).

1.2.1.4 The interaction of teeth with the oral environment

As the tooth is located in an environment subject to many chemical interactions, its microstructure and chemical composition are continually subject to change. Following eruption, the immature exposed enamel begins a process of maturation, increasing its resistance to external physical and chemical forces. The erupted tooth lives entirely in the presence of saliva and is subjected frequently to chemical de- and remineralisation processes.

For example, after the intake of fermentable carbohydrates, acids accumulate in the dental plaque and the pH at the pellicle to tooth interface falls. However, saliva contains calcium

and phosphate ions at concentrations which are supersaturated with respect to HAP and can provide a certain level of protection and repair.

The solubility of the HAP is pH dependent and at low pH more calcium and phosphate are needed in the surrounding fluids to maintain a condition of supersaturation and therefore prevent its dissolution. Up to a certain level this is possible because healthy saliva maintains a saturated level of calcium and phosphate at neutral pH. Below a pH of around 5.5, however, normal saliva becomes undersaturated with regard to those minerals and HAP starts to dissolve (Larsen and Bruun 1996).

In comparison to HAP, the carbonated apatite form of dental mineral is more soluble to acids produced by bacterial metabolism but during the remineralisation process a less soluble material, with a composition somewhere between HAP and fluorapatite, reprecipitated on the surface of partially demineralised crystals (ten Cate and Featherstone 1991).

1.2.1.5 Changes with caries

Enamel and dentine differ markedly from each other in terms of developmental origin as well as structure. Enamel is derived from the ectodermal component of the tooth germ while the dentine-pulp complex is derived from the mesenchymal component.

The enamel is avascular and acellular and cannot respond to injuries whereas the dentine and the dentinal cells, the odontoblasts, are integral parts of the dentine-pulp complex. As such, they need to be considered a vital tissue possessing specific defence reactions to external insults (Grayson, Marshall et al. 1997; Dung and Liu 1999). The nature and magnitude of the response will reflect both the extent of the injury and the tissue conditions in the dentine-pulp complex. The pathogenesis of caries is such that the degree of tissue injury and consequent tissue responses may represent quite a broad spectrum. The nature of these responses will reflect the stage of the tooth's life in terms of the cellular

activity and general tissue conditions. It is therefore clear that there is no single response to caries but rather a range of responses reflecting both the disease process and host tissue activity.

Whilst the bacterial aetiology of caries is well established, there is a limited understanding of the dynamic nature of the tissue changes within the dentine-pulp complex in response to lesions that vary in their rate of progression. Lesions may be slowly or rapidly progressing, or even arrested. Furthermore, the dynamics of lesion progression may change during the course of the disease process, depending on the microbial metabolic activity. This presents particular problems to the investigator in terms of attempting to correlate a particular degree of caries challenge with the tissue responses.

1.2.1.5.1 Structural and biological changes

The early white-spot caries lesion in enamel represents the earliest sign of demineralisation. Before it has completely penetrated the full depth of the enamel, it can stimulate a reaction from the dentine-pulp complex in the form of tubular sclerosis in the dentine. As the lesion further progresses at approximal surfaces it develops into a conical shape, in the direction of the amelodentinal junction and underlying dentine. A hyper mineralised zone may develop in the dentine prior to histological evidence of the lesion reaching the amelodentinal junction (Johnson, Taylor et al. 1969; Bjorndal and Thylstrup 1995). This zone of dentinal sclerosis represents a cellular and/or physicochemical reaction and the mechanisms responsible for the formation of this material will be further considered below. Another early sign of dentine demineralisation is a brownish discoloration and this will be discussed in a separate section.

Tubular sclerosis is the most common defence reaction by the dentine-pulp complex (Stanley, Pemeira et al. 1983; Silverstone and Hicks 1985) It is a gradual mineralisation of the peritubular dentin which can lead to complete obturation of the tubules, particularly the

smaller lateral branches of the tubules. It can result from stimulus to the odontoblastic process within the dentinal tubule, as a result of age changes, attrition of teeth even at an early age and, most commonly, caries.

Caries will accelerate tubular sclerosis provided it progresses slowly enough. However, very rapid caries may not give dentine enough time to fully sclerose. In the presence of vital odontoblasts even mild stimuli through demineralised but still intact enamel may lead to sclerosis.

The tubular sclerosis observed in the presence of caries may be the result of either initial mineralisation of the peritubular space followed by calcification of the odontoblast process, or an initial intracytoplasmic calcification followed by a secondary peri-odontoblastic mineralisation (Frank and Voegel 1980). In addition to the presence of intratubular hydroxyapatite crystals, large rhombohedral crystals have been observed and identified as whitlockite crystals (Frank and Voegel 1980; Daculsi, LeGeros et al. 1987). At the light microscope level it is not possible to distinguish between the different forms of sclerosis, and in prepared sections the obturated dentinal tubules appear translucent because the mineral in the tubules makes the tissue more homogeneous, reducing the scattering of light passing through the affected tissue. Sclerotic dentin is therefore often referred to as translucent (transparent) dentine or a translucent zone.

Bacterial acids can dissolve the minerals so that the collagen framework becomes exposed to acids and enzymes.

1.2.1.5.2 Discolouration

Discolouration is an important factor used by clinicians in determining the status of a caries lesion. In the past it was regarded as desirable to remove all discoloured enamel and dentine in preparation for the placement of a restoration but it is now recognised that colour is unrelated to demineralisation. The possible causes of discolouration of dentine

and the relationship between colour change and the remineralisable status of carious dentine at the base of a cavity will be reviewed.

The initial research which dealt specifically with the discolouration of dentine found in caries lesions was carried out in the 1950s and 1960s (van Reenen 1955; Armstrong 1964). Reiss showed that isolated cariogenic bacteria induced browning of protein in the presence of the phenolic amino acid tyrosine in a manner similar to melanin formation. Melanins are pigments that occur in hair and skin and are formed by the oxidation of tyrosine (Reiss 1938). Dreizen, Armstrong and co-workers focused their study on the Maillard reaction, this is the reaction between sugar and either proteins or amino acids. They simulated browning reactions on dental tissues or pure biochemical compounds *in vitro*. The resemblance between *in vitro* and *in vivo* gross features, such as elemental composition, colour, and collagen degradability, was inferred as proof that the same reaction would occur under clinical conditions (Dreizen, Spirakis et al. 1964; Armstrong 1968).

Another approach was the purification and analysis of the brown pigment formed in carious dentine. Engel isolated a pigment from caries lesions and the infrared spectrum of the isolate resembled that of a Maillard pigment. It showed one absorption band that was absent in sound dentine, characteristic of carbonyl groups, and marked bands for aromatic double bonds (Engel 1971). In support of the above finding was the isolation of two additional chemicals from carious dentine, a glycosylated peptide (Armstrong 1968) and hexitollysine (Kuboki, Ohgushi et al. 1977).

External pigments may represent another source of lesion stain. Kidd and co-workers demonstrated that caries lesions do take up food dyes *in vitro* (Kidd, Joyston-Bechal et al. 1990).

Contamination of mineral by metal ions during remineralisation may be another cause of discoloration. Different metals were found in higher amounts in caries lesions than in sound tissue: iron (Torell 1957; Torell 1957), zinc and copper (Little and Steadman 1966),

and manganese (Bao, Vernois et al. 1990). Malone observed only trace amounts of metals in carious and sound dentine (Malone, Bell et al. 1966). The presence of metal ions is rather circumstantial, perhaps depending on the diet.

Some bacteria identified in carious material are known to form pigments. For example, propionic-acid bacteria (Lee, Shalita et al. 1978) and black-pigmented *Porphyromonas gingivalis* (Shah, Bonnett et al. 1979) produce haem pigments. Boue and co-workers found no correlation between lesion discolouration and the presence of *Porphyromonas gingivalis* (Boue, Armau et al. 1987). Neither did Bjorndal find black-pigmented bacteria in every black lesion (Bjorndal, Larsen et al. 1997).

It was also suggested that the discolouration precedes the bacteria that penetrate the demineralised dentine (Fusayama, Okuse et al. 1966). It is likely that this colour change is brought about by compounds diffusing ahead of the bacteria. Recently, the Maillard reaction in carious dentine was investigated in more detail. The content of Maillard products increases as does the Maillard related fluorescence (370 & 440nm) (Kleter 1998). In the anaerobic and acidic environment at the lesion front, the Maillard reaction seems therefore most likely to occur with small aldehydes derived from bacterial metabolism. The matrix would darken while the lesion front progresses with time. The outer layers, which have been subjected to the Maillard reaction longer than the lesion front, would therefore appear darker, in accordance with clinical observations.

1.2.1.6 Current clinical approaches to repair or replace carious dentine

The clinical approaches to deal with carious dentine during cavity preparation can be classified into the following three approaches (Kidd 2004):

- Classical approach
- Stepwise excavation
- Indirect pulp capping

1.2.1.6.1 Classical approach

Complete removal of all softened and discoloured dentine is designed to eliminate all infected tissue and create a hard foundation to support a restoration. Aggressive hand instrumentation and a round steel bur is used in a non selective manner, often resulting in removal of healthy tissue and accidental exposure of the pulp. In young patients, the rate of pulp exposure after excavation of large caries lesions in permanent molars has been reported to be as high as 40% (Leskell, Ridell et al. 1996). The technique has been designed to ensure the elimination of all micro-organisms. However, it has been shown that this is not always possible and some micro-organisms will remain even when all soft dentine is removed and the cavity treated with a solution of sodium hypochlorite, CarisolvTM (Lager, Thornqvist et al. 2003).

1.2.1.6.2 Stepwise excavation

This technique was first described by Bodecker (Bodecker 1938). He suggested that only part of the soft dentine should be removed and the cavity restored using a temporary material such as zinc oxide eugenol. This is removed after a period of time and cavities were re-entered and further excavation carried out before the placement of the permanent restoration. This approach is designed to minimise the risk of direct pulp exposure by arresting the lesion progression and allowing time for the formation of tertiary dentine within the pulp chamber during the interim period.

This technique was tested in a controlled randomised clinical study comparing it with the classical approach. It was found that the incidence of direct pulp exposure was 17.5% for the stepwise excavation method compared with 40% for the classical method (Leskell, Ridell et al. 1996). These findings were echoed by a similar study carried out on deciduous teeth which reported 15% percent of pulps exposed with the classical approach compared

with 53% in the stepwise excavation group (Magnusson and Sundell 1977). A practice based study found a much lower rate of pulp exposure, 5.3%, with the stepwise excavation method (Bjorndal and Thylstrup 1998).

1.2.1.6.3 Indirect pulp capping

As described above, the second stage final excavation allows removal of the remaining infected dentine. It was thought that this was necessary because the carious process would continue in the presence of infected tissue. However, as described by Hilton (Hilton and Summit 2000), in the indirect pulp capping technique the lower layer of softened demineralised dentine is allowed to remain and therefore there is no need to re-enter. In two clinical trials, this soft and wet dentine was left on the floor of the cavity and it was concluded that the clinical performance of these restorations was not adversely affected (Mertz Fairhurst, Curtis et al. 1998; Ribeiro, Baratieri et al. 1999). Mertz-Fairhurst et al. found that after 10 years, the lesion progression was arrested and the clinical result was acceptable.

Massler and Fusayama suggested that there are two parts to a carious lesion. The outer layer is infected by micro-organisms and is not remineralisable while the inner layer is composed of remineralisable and slightly infected dentine (**Figure 8**) (Fusayama, Okuse et al. 1966; Massler 1967). It was suggested that only the infected layer should be removed during cavity preparation and the affected layer can then be lined with calcium hydroxide or glass-ionomer. In 1965, the affected layer was first shown to harden as a result of remineralisation (Eidelman, Finn et al. 1965).

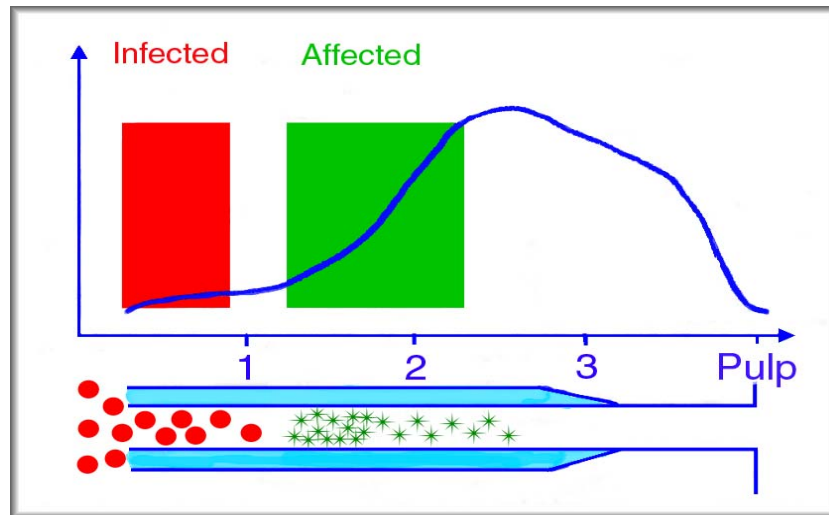


Figure 8: Schematic drawing to illustrate the relationship between the hardness curve corresponding to the infected and affected zones found in carious dentine. The diagram below the chart shows the relationship between the bacterial invasion front and the mineralisation of the dentinal tubule (Fusayama 1993).

The differentiation between the infected and affected layer poses considerable difficulties for the clinician. Fusayama developed a caries dye detector (Fusayama and Terashima 1972) to differentiate these two layers and it was suggested that the dye staining front corresponds to the junction between the infected and affected layers. However, this finding was not supported by later studies (Anderson, Loesch et al. 1985; Kidd, Joyston-Bechal et al. 1993).

1.2.1.7 Potential for remineralisation

Dentine is very sensitive to wear and chemical dissolution but is also capable of adapting to the oral environment. ten Cate placed specimens of previously unexposed dentine in the mouth and subsequently subjected them, along with aged and non treated control samples, to cariogenic challenges (ten Cate, Damen et al. 1998). The study showed that an adaptation period increased the caries resistance substantially. Many recent studies have reported on the potential of fluoride treatments to assist in remineralising previously

demineralised dentine, suggesting that the dentine substrate is quite reactive, both in demineralisation and remineralisation. Laboratory studies showed a dose response between fluoride levels in solution and the remineralisation of dentine.

In-situ studies demonstrated that fluoride dentifrice treatments could shift the environment in favour of remineralisation, not only for enamel but also dentine (Sullivan, Charig et al. 1997).

Kashani reported that dentinal lesions, at interproximal sites, remineralised even better than enamel ones when fluoride was applied with fluoridated toothpicks (Kashani, Birkhed et al. 1998). Inaba and co worker reported that dentine can be hypermineralised when placed in contact with a mineralising fluid (Inaba, Ruben et al. 1996). This implied that mineral content now exceeded that of sound dentine, suggesting that some of the collagen and water phase may have been replaced with mineral.

Using an *in situ* model, Zuidgesst showed that hypermineralisation of dentine is a real phenomenon in the mouth when dentine is in close contact with a fluoride releasing restorative material. This is probably one of the mechanisms behind the reported lower secondary caries levels associated with this type of restoration (Zuidgeest, Herkstroter et al. 1990).

Convincing evidence for the mineralisation properties of the dentinal tissue is the formation of secondary and tertiary dentine. These are processes of mineralisation driven by the odontoblast cells which lay down the organic matrix and this is then filled in with apatite crystallites.

As discussed in 1.2.1.5.1, in developing sclerotic dentine, a purely physicochemical crystallisation takes place. In the advancing front of dentine caries the deposition of calcium phosphate crystals in the tubules has been reported. This leads to the underlying tissue becoming less accessible for invading bacteria, acids, and other metabolites. Thus,

although the initial dentinal tissue is porous due to the tubular structure, the character is changed at a time when porosity is detrimental rather than advantageous.

One of the research questions most recently addressed is whether there is still scope for a non-invasive approach when coronal caries has passed the enamel-dentine junction and entered into dentine. Available data suggests that demineralised dentine can still be partially remineralised (Arends and Christoffersen 1990; Zuidgeest, Herkstroter et al. 1990; ten Cate, Damen et al. 1998).

It is known that fluoride inhibits demineralisation and enhances remineralisation of both enamel and dentine and it could be assumed that its effect on these two tissues would be similar. However, there are some important differences between the two materials. Firstly, in dentine, there is a large proportion (about 33 vol%) of organic matrix, which is composed mainly of collagen, type I. Secondly, dentine contains about 5% by weight of carbonate, which is double the amount for enamel and carbonate is highly soluble (Featherstone 1994). The solubility is also influenced by the size of the crystallites, which are considerably smaller in dentine than in enamel. Smaller crystallites dissolve faster when placed in an acidic and undersaturated solution.

Featherstone reported a graduated dose response between the fluoride concentration in a dentifrice and demineralisation (Featherstone, McIntyre et al. 1987; Featherstone 1994). ten Cate did a comparative pH-cycling study of enamel and dentine, where treatments included; no treatment (negative control); the presence of low-concentration fluoride during demineralisation and remineralisation and the simulation of a non-fluoride dentifrice treatment once a day. A fluoride concentration of 0.06 ppm was chosen, because this corresponds to fluoride levels in saliva when using fluoride products. The results of this series suggested that there is a difference in demineralisation susceptibility between enamel and dentine. They also concluded that, unlike enamel, in dentine there is a difference between the effects of low constant fluoride levels and the dentifrice treatment.

For dentine, the dentifrice treatment was much more effective. This is consistent with the view that the smaller crystallites in dentine, with a larger surface area, need higher amounts or concentrations of fluoride for the processes at the crystallite surfaces to be affected.

Featherstone concluded that the mechanisms that govern the de- and remineralisation process in enamel also play an important role in controlling root caries (Featherstone 1994). He found that fluoride also plays an important role in inhibiting demineralisation, and at the same time, enhances remineralisation.

Collagen is the matrix onto which the apatite crystallites were precipitated during dentineogenesis. During demineralisation, the apatite is the first to be dissolved; thus exposing the collagen. The remaining collagen then serves as a diffusion barrier slowing down demineralisation, but it remains subject to denaturation, enzymatic degradation, and solubilisation (Klont and ten Cate 1990; Klont and ten Cate 1991; Klont and ten Cate 1991; Kleter, Damen et al. 1994). Once the matrix is removed it can no longer nucleate new apatitic crystals.

At double the demineralisation rate and half the mineral content of sound enamel, not only can caries spread much faster in dentine than in enamel but this also leads to a condition of irreparable damage because no remineralisation is possible once the tissue is completely depleted of mineral. However, various experiments have shown that dentine demineralisation is partly inhibited by fluoride whether it is available from either short-term treatments or continually present.

As the pH rises and crosses the saturation level for apatite, mineral starts to reprecipitate onto the remaining apatite crystallites. The chemical composition of the resulting mineral phase depends on the supply of calcium, phosphate and other ions that could be incorporated into the crystalline lattice. This is often referred to as remineralisation and the changing pH cycle is referred to as the “de- and remineralisation cycle”.

This process can then be further divided into two distinct categories, “external” and “internal remineralisation”. The term external remineralisation should be used when it occurs at the saliva tooth interface. In this situation the saliva supplies the elements required such as calcium, phosphate, other apatite forming ions at an appropriate pH level. The external de- and remineralisation cycle is an essential element in the maturation process of enamel after eruption. The difference in chemical composition between surface and sub-surface enamel reflects the posteruptive history of the tooth, with fluoride being the highest at the enamel surface. At the same time it explains the phenomenon of subsurface demineralisation during caries (LeGeros, Ming et al. 1983) and why unerrupted enamel is more soluble (Koulourides, Keller et al. 1980).

The term “internal remineralisation” should be reserved for situations where the process occurs inside a tooth, for example at the restoration/tooth interface. Here the restorative material used and any pulpal fluid that can reach the interface will provide the required elements and conditions.

1.2.2 Glass ionomer cement

1.2.2.1 Chemical composition and microstructure

The composition of glass-ionomer cements is complex to the extent that no two commercial products are chemically identical. In the following section, glass-ionomer cement in general and the chemical features common to all member of this class of material will be discussed.

Glass-ionomer cement was first described by Wilson as the product of an acid-base reaction between a glass powder and a polyalkenoic acid (Wilson 1978). The product of the reaction is a hydrogel salt acting as a binding matrix, holding the glass particles together as a solid mass.

The basic component of contemporary glass-ionomer cement is a calcium or strontium based alumino-silicate glass containing fluoride. The acid is a polyelectrolyte, which is a copolymer of unsaturated carboxylic acids known as alkenoic acids. The most common form utilised in the current generation of glass-ionomer cement is poly acrylic acid.

The composition of the glass can be varied greatly, although those based on ion-leachable calcium, or strontium, alumino-silicates are the only ones to have found practical applications (Wilson and Kent 1972; Wilson 1978; Wilson, Groffman et al. 1985). The glass can be prepared by melting alumina (Al_2O_3), silica (SiO_2), other metal oxides, metal fluorides and metal phosphates at temperatures ranging from $1,100^\circ\text{C}$ to $1,500^\circ\text{C}$ then pouring the melt onto a metal plate or into water to quench the glass. The metal ions are usually selected from the following group, aluminium (Al), calcium (Ca), strontium (Sr), zinc (Zn), sodium (Na), potassium (K) and lanthanum (La). The glass is ground to a fine powder then surface treated to control the setting time of the final mix. The finer the particle size the more rapid the setting and the stronger the cement will be.

In the original formulation (Wilson, Crisp et al. 1980), calcium fluoride (CaF_2), alumina (Al_2O_3) and silica (SiO_2) were combined to form a glass suitable for cement formation. Minor components, such as cryolite (Na_3AlF_6) and aluminium phosphate (Al_3PO_4), are added to modify the properties of the final cement.

The formulations of the original glass are listed below in increasing order of complexity (Wilson 1978):

1. $\text{SiO}_2\text{-Al}_2\text{O}_3\text{-CaF}_2$
2. $\text{SiO}_2\text{-Al}_2\text{O}_3\text{-CaF}_2\text{- Al}_3\text{PO}_4$
3. $\text{SiO}_2\text{-Al}_2\text{O}_3\text{-CaF}_2\text{- Al}_3\text{PO}_4\text{-Na}_3\text{AlF}_6$

As will be discussed later, calcium can be substituted by strontium in the glass. Also, it is interesting to note that the last two formulations contain three of the components essential for remineralisation of tooth structure: calcium, phosphate and fluoride.

Calcium may be replaced wholly by strontium and partly by barium or lanthanum to give a radio-opaque glass. Strontium has a similar ionic radius and valence to that of calcium ($\text{Sr}^{2+} = 1.13\text{\AA}$, $\text{Ca}^{2+} = 0.99\text{\AA}$), so it can replace calcium without disrupting the glass structure. This does not apply to barium or lanthanum because the ionic radius of these two elements is much larger than calcium ($\text{La}^{3+} = 1.35\text{\AA}$, $\text{Ba}^{2+} = 1.35\text{\AA}$) so the replacement can only be partial (Wilson and Mc Lean 1988).

Fluoride and phosphate are essential components because they decrease the melting temperature in the manufacturing process and improve the working characteristics of the mixed paste. Fluorine is first introduced as calcium fluoride and is used as a flux during the melting phase. The inclusion of these two will contribute to an increase in the strength of the set cement and enhance translucency. The release of fluoride ions over a prolonged period will contribute to the therapeutic value of the cement. (Wilson, Groffman et al. 1985; Forsten 1998).

The fluoroaluminosilicate glass possesses a unique mechanism of fluorine release. Originally, the main source of fluoride release was thought to be from the cement matrix but it was recently suggested by Saito and co-workers that some of the fluorine originates from the glass core and is released via the matrix (Saito, Tosaki et al. 1999). Significantly, the release of fluorine does not affect the physical properties of glass-ionomer.

The ionomer glasses are decomposed by acids. All the glasses contain aluminium and this can enter the silica network, displacing silicon to give the network an overall negative charge. This makes the glass basic and therefore susceptible to attack by hydrogen ions from the acid and this is an essential property for cement formation.

1.2.2.2 Setting reaction

A silica glass is a highly crosslinked network of connected silicon and oxygen atoms. It is resistant to acid attack because it does not carry an electric charge. By contrast, the

ionomer glass has a similar network to that of silica, but it contains negative sites because aluminium has partly replaced silicon in the glass network. These negative sites are vulnerable to attack by the positively charged hydrogen ions (H^+) of the acid.

It follows then that the Al_2O_3/SiO_2 ratio of the glass is crucial, and is required to be 1:2 or more by mass for cement formation (Kent, Lewis et al. 1979; Wilson, Crisp et al. 1980). Only then is there sufficient replacement of silicon by aluminium to render the network susceptible to acid attack. This ratio determines whether the glass network will break down at all when exposed to acids, and the rate at which the breakdown occurs.

Glasses used in practice are generally more complex than the simple three component systems described above and the fluxing action of calcium fluoride is generally supplemented by the addition of cryolite (Na_3AlF_6). The flux reduces the temperature at which the glass will fuse and increases the translucency of the set cement. Aluminium phosphate (Al_3PO_4) is also often included in the glass fusion mixtures because it too improves translucency.

When the cement powder and aqueous liquid are brought together to form a paste, the glass powder reacts with the polyalkenoic acid to form a salt hydrogel which becomes the binding matrix. The glass-ionomer cement sets and hardens by a transfer of metal ions from the glass to the polyacrylic acid, which causes gelation in the aqueous phase.

The metal ions calcium, strontium, and aluminium will combine with the carboxylic acid groups of the polyacid to form the polyacid salts matrix, and the glass surface is changed to a silica hydrogel.

In 1988, it was suggested that the setting reaction can be divided into four distinct phases: initial contact between powder and liquid, acid attack on the glass particle, gelation of the matrix and hardening of the matrix (Wilson and Mc Lean 1988). The course of the cement forming reaction is depicted in **Figure 9**.

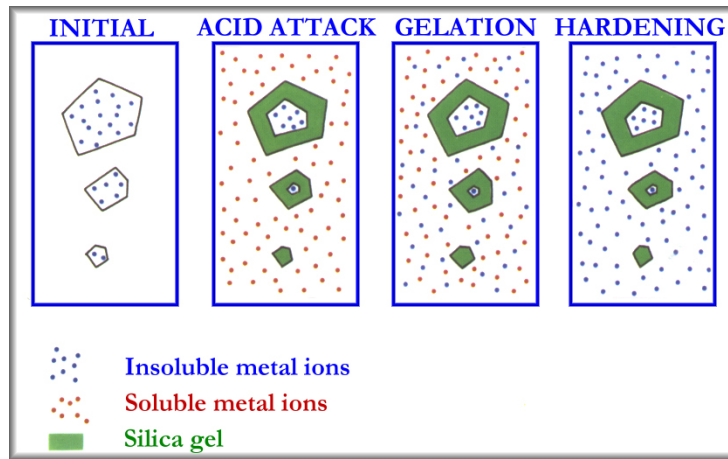


Figure 9: The four phases in the setting reaction of glass-ionomer cement (Wilson and Mc Lean 1988).

During the initial phase, the freshly mixed and unattached glass particles are dispersed in the polyacid liquid.

The acid attack phase starts with the decomposition of the glass at the surface and the release of cement forming metal ions, such as Al^{3+} , Ca^{2+} , Sr^{2+} and F^- . These metal ions migrate into the aqueous phase of the cement. As the surface layer of the glass is depleted of these ions, it degrades into a silica rich layer. A silica gel layer is then formed at the interface between the cement matrix and the glass particles. As the reaction proceeds, the concentration of the ions in the matrix increases with the preferential build up of calcium and strontium over aluminium (Crisp and Wilson 1974). The pH rises as the polyacrylic acid is converted into polyacrylates and the viscosity of the paste increases.

The silica rich gel phase on the surface of the glass needs a period of weeks or even months to harden fully and the compressive strength of a glass-ionomer cement increases over one year (Suzuki, Tosaki et al. 1995). At any time during the early reaction and setting process, these materials are sensitive to both hydration and dehydration.

1.2.2.3 Release of fluoride and other ions

Fluoride-releasing restorative materials have been used for many decades with a well-known example being silicate cements, which were known anecdotally for their low secondary caries rates. Recently, the fluoride release has been a more intentional part of the development of products such as fluoride-releasing amalgams, glass-ionomers and composites. Fluoride released from glass-ionomers and composites has been studied extensively. Initial studies reported that fluoride is released primarily during the first weeks after placing the restoration, although a sustained release has been measured for years (Swartz, Phillips et al. 1984; Wilson, Groffman et al. 1985; Forsten 1995; Forsten 1998).

Of the total amount of fluoride in the set cement, only a small fraction is available for release. Walls pointed out that unless the ions are important to the matrix structure then their loss need not be harmful to the physical properties of the cement (Walls 1986). The high fluoride content ensures that a substantial amount of fluoride can be released in the early life of the restoration, but this will gradually decrease over time. The pattern and total amount released is not dependent on the total fluoride content of the cement but it is partly controlled by the amount of sodium that is available to re-establish electron neutrality in the cement (Meryon and Smith 1984; Wilson, Groffman et al. 1985).

Even when fully set, glass ionomer cements release ions and absorb water in an aqueous environment. The ions released include sodium, fluoride, silica and traces of calcium (Wilson, Groffman et al. 1985; Povich, Pioneer et al. 1988). Wilson studied this over a period of twenty months and found that these species were still being released at the end of the experimental period, albeit at a diminished rate. A similar release was later confirmed for resin modified glass-ionomers (Tam, McComb et al. 1991).

Although many studies have reported a sustained release of fluoride from set glass-ionomer stored in distilled water over a long period of time (Swartz, Phillips et al. 1984; Wilson, Groffman et al. 1985; Forsten 1990), the mechanism of fluoride release is still not

completely understood. It is generally accepted that there may be two reactions involved. First a short-term reaction of high fluoride release corresponding to initial elution due to the maturation process, during which fluoride ions are released from the surface as well as from within the bulk of material. The surface process activity declines after a while leaving the bulk diffusion process to continue over a long period in an apparently inexhaustible fashion. The second reaction is a long-term low release of fluoride, that can be attributed to the equilibrium diffusion processes (Meryon and Smith 1984; De Moor, Verbeek et al. 1996).

De Moor and co-workers investigated fluoride release from a series of conventional and metal-reinforced glass-ionomers. They suggested that the cumulative amount of fluoride released (F_c) in distilled water at 37°C as a function of time (t) can be described by the following equation:

$$F_c = (Fl * t) / (t + t') + (b * \sqrt{t})$$

Equation 1: F_c : cumulative amount of fluoride release

Fl : maximum value of fluoride released during the short term reaction.

t : time

t' : half life of the short term reaction process

b : constant that expresses the measure of the driving force during the slow release period (De Moor, Verbeek et al. 1996)

When glass-ionomers are immersed in water at neutral pH, the total fluoride release is affected by the following two factors, in addition to those discussed earlier:

- **Microporosity:** Amalgam alloy admixed cements were found to release higher amounts of fluoride than those of conventional glass-ionomers due to increased microporosity, which increases the effective surface area for release (Thorton, Retief et al. 1986; Forsten 1990; Horsted Bindslev and Larsen 1990; De Moor, Verbeek et al. 1996).

- Contact area between the glass particles and the polyalkenoic acid. For silver cermet cements, in which silver particles are sintered to glass particles, the effective contact area between the glass particles and polyalkenoic acid is reduced, leading to a reduction in fluoride release, especially during the initial elution period (Thorton, Retief et al. 1986; Horsted Bindslev and Larsen 1990; De Moor, Verbeek et al. 1996).

At low pH, there is a significant increase in fluoride release, suggesting that an erosive mechanism is activated under these conditions through possibly, a preferential dissolution of the glass particles (Cranfield, Kuhn et al. 1982; Forss 1993).

Many studies have suggested that glass-ionomer has the ability to recharge fluoride. There is *in vitro* evidence supporting the theory that recharging is feasible through an ion exchange process (Forsten 1991). In the presence of an inverse fluoride concentration gradient, glass-ionomers absorb fluoride from its surroundings into its matrix. The reservoir of fluoride will then be released when the level of fluoride in the environment drops (Forsten 1991; Takahashi, Emilson et al. 1993; Diaz-Arnold, Holmes et al. 1995).

Other reports have demonstrated that a recharging of the restoration occurs during topical application and brushing with a fluoride dentifrice. This lengthens the period over which a sizeable release, and consequently effects on the mineralisation process, could be expected. Locally, in particular in the immediate vicinity of the restoration, high fluoride levels prevail, which could help to strengthen the surrounding tooth structure against demineralisation.

Most of the data on the fluoride releasing capacity of glass-ionomers has been in relation to aqueous solutions. Some researchers have felt this to be not clinically relevant so investigations have been undertaken to determine the fluoride release processes under conditions simulating the oral environment or *in vivo*.

One approach was to use artificial saliva. Comparative data on the fluoride release from the same brands of glass-ionomers stored in distilled water or in artificial saliva revealed a

reduction in the release when using the latter (De Schepper, Berry et al. 1990; El-Mallakh and Sarkar 1990).

Rezk-Lega and co-workers used non-stimulated human saliva as an immersion medium. A significant reduction in fluoride release occurred which was mainly attributed to the adsorption of HPO_4^{2-} and the formation of the pellicle from the protein component of saliva (Rezk Lega, Ogaard et al. 1991).

In the early 1990s, several studies addressed the important question of whether the fluoride released from glass-ionomer is sufficient to increase the fluoride concentration in saliva. These studies provided evidence of elevated fluoride concentration in saliva for weeks after a glass-ionomer restoration was placed. Therefore it was suggested that these materials are effective short-term intra-oral fluoride releasing devices (Hallgren, Oliveby et al. 1990; Koch and Hatibovic-Kofman 1990; Hatibovic-Kofman and Koch 1991; Hattab, el Mowafy et al. 1991).

The following conclusion can be drawn from the results of the fluoride release experiments:

- Data derived from experiments performed in distilled water or in any other artificial medium should not be directly extrapolated into the clinical situation
- As the actual amount of fluoride required to exert a cariostatic effect has not yet been determined, the levels of fluoride release should not be used as primary criteria for material selection
- Fluoride release is an ion exchange process, and ionic species can only be exchanged with the environment to maintain diffusion equilibrium
- *In vivo* the fluoride levels in saliva may be increased after glass-ionomer application, but within a few weeks are reduced to baseline levels

It is difficult to make a direct comparison of fluoride release data from different studies because there is no common way of presenting it.

Cumulative fluoride values are variously given as a function of time in mg F⁻, ppm F⁻, mg F⁻ per unit volume of the cement, or mg F⁻ per surface area unit of the cement. Because elution is a surface phenomenon, the results should be expressed as mass per unit of total specimen surface area (Wilson, Groffman et al. 1985) to allow for direct comparisons among materials and studies. The rationale for expressing the results in cumulative mode is weak because the experimental procedure for measuring fluoride release involves an open system, in which partial or complete replacement of the immersion liquid is conducted at different time intervals.

It should also be noted that when using the fluoride-selective electrode there is a total ionic strength adjustment buffer solution added. This means that measurements represent the maximum amount of ionizable fluoride available in the solution and not the actual ionised fraction.

A high level of fluoride can also affect the microflora. Bibby et al first demonstrated in 1940 that carbohydrate metabolism in pure cultures of oral streptococci and lactobacilli was inhibited by fluoride (Bibby and van Kesteren 1940). Since then, many reports have been published on direct and indirect effects of fluoride on the energy and biosynthesis metabolism of oral bacteria and on dental plaque ecology (Bibby and Fu 1986; Bowden 1990; Hamilton 1990; Marquis 1995). There is still debate, however, as to whether the antimicrobial effects of fluoride do contribute to caries prevention, at the concentration usually reached and maintained intra-orally.

An important argument in this debate is that it seems that the fluoride concentrations needed for antimicrobial effects surpass significantly the concentration needed to reduce the solubility of apatite. In clinical situations, the pellicle and plaque complexes form a physical barrier to fluoride elution from glass-ionomers and acts as a fluoride reservoir. This situation has been the subject of many studies and *in situ* experiments have shown

high levels of fluoride in plaque growing adjacent to glass-ionomer restorations (Forss, Jokinen et al. 1991; Benelli, Serra et al. 1993).

Although the antibacterial activity of glass-ionomers has been extensively studied, data in the literature are not conclusive in establishing whether this biological activity is solely due to fluoride release (Seppa, Torppa-Saarinen et al. 1992; Yap, Khor et al. 1999). There are other elements that are simultaneously released from glass-ionomers, such as aluminium which is one of the major constituents (Forss 1993; Nakajima, Sano et al. 1995) and the antibacterial activity of aluminium salt solutions against cariogenic micro-organisms has been reported (Oppermann and Rolla 1980). Hayacibara and co-workers suggested that the simultaneous release of both aluminium and fluoride from glass-ionomers contributes to the observed antibacterial properties of this class of material (Hayacibara, Rosa et al. 2003).

1.2.2.4 Remineralisation of adjacent enamel and dentine

One of the desirable properties of a restorative material would be that it should protect the adjacent tooth structures from further acid attacks. It is suggested that glass-ionomers can impart a certain degree of protection and both laboratory and clinical studies have shown, an absence of cavity wall lesions, as well as a reduction in lesions on the enamel surface adjacent to the glass ionomer cement when compared with control cavities (Dezand and Johansson 1984; Retief, Bradley et al. 1984; Hicks, Flaitz et al. 1986; Swift 1989; Forss and Seppa 1990; Erickson 1992; ten Cate and van Duinen 1995; Tam, Chan et al. 1997).

In vitro studies have demonstrated an increased fluoride concentration at the interface (Wesenberg and Hals 1980; Retief, Bradley et al. 1984; Skartveit, Tveit et al. 1990; Tsanidis and Koulourides 1992; Momoi and Mc Cabe 1993). However, the status of this fluoride has not been determined (Seppa, Salmenkivi et al. 1992). In the case of topically applied fluoride and dentifrice, it is known that the fluoride can be present in the form of

fluorapatite, calcium fluoride or non specifically absorbed fluoride. (White, 1995). This is not the case with glass-ionomers as it is reasonable to expect that the initial low pH of glass-ionomers may induce dissolution of the adjacent apatite and redeposition of calcium salts incorporating fluoride, which is initially released at high rates. Evidence to support such an interaction has been presented in only one *in vitro* study, where fluoridated apatite was identified at the interface between a conventional glass-ionomer restorative and cavity walls (Geiger and Weiner 1993).

With the established properties of adhesion and fluoride release glass-ionomer is most apposite in the treatment of the early carious lesion, whether in fissures or smooth surfaces, in adults or children. It has made possible several minimal and microcavity designs.

1.2.3 Methods for Evaluation of Remineralisation

The disease of caries represents demineralisation of tooth structure, both enamel and dentine. This phenomenon has been deeply researched in the past and has generally been considered to be irreversible. However, it is apparent that this is not so and given the correct circumstances beginning with the elimination of the bacterial cause of the disease, it is now known that remineralisation can take place.

The problems of studying the speed and depth of penetration of demineralisation has always posed problems because of the nature of the materials being studied. Enamel is a heavily mineralised material with limited porosity while dentine has approximately half the mineral content and is highly porous with a relatively soft collagen matrix. Also the fact that it is an intra-oral problem and is hard to simulate *in vitro* adds to the complexities.

Both materials need to be studied not only together but also separately and great care should be taken in interpreting the results. The following questions will always be significant.

Three questions are normally asked:

1. How much mineral was lost or gained
2. Where was the mineral lost or gained
3. Which mineral was lost or gained

To assay the changes in mineral content, a number of techniques are currently in use, some more quantitative than others. These techniques are discussed below, with an emphasis on the advantages and disadvantages offered by each. Sample preparation, the importance of protein penetration, nominal mineral loss threshold and the applicability to dentine are also considered.

Methods used for the analysis of tooth de- and remineralisation include techniques with various degrees of sophistication and quantitative capabilities. They can be roughly classified into those providing quantitative and semi-quantitative measures of change in mineral content.

The quantitative methods for direct analysis reviewed in this chapter include:

1. Three X-ray microradiographic methods:
 - Transverse (TMR)
 - Longitudinal (LMR)
 - Wavelength independent (WIM)
2. An electron beam microanalysis method:
 - Electron probe micro analysis (EPMA)

3. Wet chemistry

The semi-quantitative methods include:

1. Polarised light
 - Polarised light photomicroscopy (PL)
2. Microhardness
 - Surface microhardness (SMH)
 - Cross-section microhardness (CSMH)

3. Iodine permeability

- Iodine absorptiometry
- Iodide permeability (Ip)

These provide indirect measures of mineral movement in the tissue with various degrees of precision. They may measure changes in real physical parameters, for example polarised light will measure the general porosity of the dental tissues, while surface microhardness will measure the change in surface structural strength. In other words, indirect methods measure properties which change with mineral content variations and are indirect measure of mineral gain or loss (White 1987; White 1988)

The accuracy of all the above test methods is dependent on three factors:

1. Specimen preparation
2. Magnitude of change in mineral contents in relation to the detection limits of the analysis technique
3. Analysis protocol and associated artefacts

Planning a research project includes selection of one or more methods of measurement and will be based on the aim of the project, therefore the quantities to be measured. The design of the study dictates the level of sensitivity required. For example if the study design calls for comparison between two groups of independent individuals or samples, then the repeatability of the method need not be much better than the biological variations of the individuals or samples.

1.2.3.1 Quantitative methods

1.2.3.1.1 Microradiography

The technique of mineral quantification by means of x-ray absorption has, in principle, been known since the 1940s (Thewlis 1940). Microradiography has been developed slowly as a suitable method for mineral quantification in dental tissues. Three different

microradiographical techniques will be described: transverse, longitudinal, and wavelength independent.

1.2.3.1.1.1 Transverse microradiography (TMR)

The best known type of microradiography is TMR (transverse microradiography), also known as contact microradiography. In TMR, the sample is cut into thin slices, from 90 to 200 μm for enamel or for dentine, prepared planoparallel and oriented perpendicularly to the anatomical tooth surface.

The slices are placed on a piece of radiographic film together with a calibration aluminium step wedge and irradiated by monochromatic x-rays. The optical density of the developed film is dependent on the mineral content of the specimen. Densitometry can be used to calculate the mineral content by means of a formula proposed by Angmar, which is expressed in vol% or in $\text{kg}\cdot\text{m}^{-3}$ (Angmar Mansson, Carlstrom et al. 1963; Groeneveld and Arends 1975; Arends and Ten Bosch 1985; de Josselin de Jong, ten Bosch et al. 1987).

From a TMR experiment, the researcher can measure two main parameters: the lesion depth L_d , in μm , and the mineral loss value ΔZ , in $\text{vol}\% \cdot \mu\text{m}$ or $\text{kg}\cdot\text{m}^{-2}$.

L_d values are determined from the mineral distribution (**Figure 10**) in the microradiogram as the distance from the outer surface of the specimen to the position where the mineral content is 95% of that of the sound tissue.

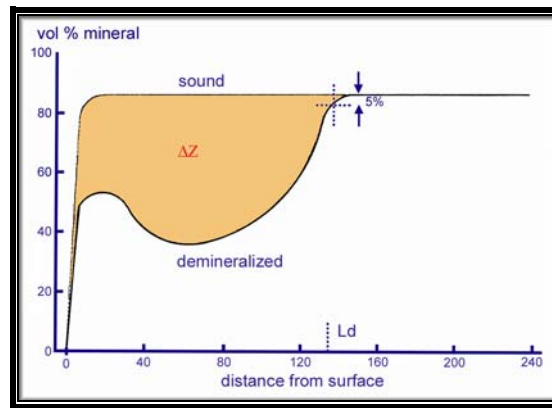


Figure 10: TMR profile showing: lesion depth (L_d) and mineral loss value (ΔZ) (Arends and ten Bosch 1992).

ΔZ is the integrated difference between the microradiogram of the sample with mineral loss and that of the sound sample (Gelhard and Arends 1983; Dijkman, Schuthof et al. 1986; Arends, Christoffersen et al. 1989).

As a lesion is further demineralised, both L_d and ΔZ increase in magnitude. The accuracy of TMR for enamel in lesion depth L_d , is about 5 μm and in ΔZ about 200 vol%. μm . For dentine, these two values are about 5 μm and 140 vol%. μm (Arends, Christoffersen et al. 1989).

The advantages of the TMR are:

1. Mineral loss, or gain, is measured quantitatively with reasonable accuracy
2. Mineral distribution can be determined

The disadvantages of TMR are:

1. The technique requires the destruction of the sample
2. Phenomena less than 10 μm from the anatomical surface are not measured due to the resolution of the densitometer slit width and specimen curvature
3. The presence of ions with a very high absorption coefficient for x-rays can lead to misinterpretation of TMR data
4. Does not tell investigators the nature of mineral present

For example, tin ions (Sn) can be adsorbed onto the outer enamel surface after SnF₂ application and produce an artefact. Alternatively, strontium (Sr) and aluminium (Al) can migrate from glass-ionomers into demineralised dentine, causing X-ray absorption that can be interpreted as an increase in mineral content.

1.2.3.1.1.2 Longitudinal microradiography (LMR)

In LMR, longitudinal tooth samples are prepared, cut parallel to the anatomical tooth surface with a thickness of 0.5 mm. X-ray projections on photographic film are made of these planoparallel samples, together with an aluminium step-wedge. The resulting microradiographic images are then scanned automatically under a densitometer.

The absolute amount of mineral per unit area can be calculated (de Josselin de Jong, van der Linden et al. 1987; de Josselin de Jong, van der Linden et al. 1988). The major advantage of LMR is that the amount of mineral in enamel and dentine can be determined repeatedly, which allows mineral changes to be determined serially (Zuidegeest, Herkstroter et al. 1990). It allows a high level of accuracy but the main disadvantage is that it is not widely available.

1.2.3.1.1.3 Wavelength independent microradiography (WIM)

WIM uses polychromatic high-energy X-rays ($\leq 60\text{kV}$) for non-destructive determination of the mineral content in whole teeth. The technique uses a reference step-wedge made from an alloy with a mass attenuation coefficient that has a wavelength independent ratio to the mass attenuation coefficients of enamel and dentine.

The technique is capable of measuring the amount of mineral per unit area in enamel and dentine with a thickness between 0.3 to 6 mm, even with natural curved surface. The detection limit is about $0.01 \text{ kg}\cdot\text{m}^{-2}$ or $310 \text{ vol}\% \cdot \mu\text{m}$. When a whole tooth is used, this

deteriorates to 0.05 kg.m^{-2} or $1500 \text{ vol\%}.\mu\text{m}$ (Herkstroter, Noordmans et al. 1990). This is a useful research tool, in particular with respect to mechanism studies.

1.2.3.1.2 *Electron beam microanalysis*

Since its introduction by Moseley in 1913, EPMA has become one of the most powerful instruments for the microanalysis of inorganic and organic materials. In the electron-probe microanalyzer (EPMA), a preselected small area of a solid specimen is bombarded with electrons in a high vacuum. The resulting emission includes: backscattered primary electrons, low energy photo-electrons and Auger electrons, together with characteristic x-ray emission superimposed on a background of continuous x-radiation. The X-ray spectrum from the specimen is recorded by means of a type of crystal detector known as wavelength dispersive spectrometers (WDS). The use of a highly focused electron beam enables a very small selected area to be analysed. In the case of a solid specimen, the x-ray spectrum originates from a volume of a few cubic micrometers, as illustrated in **Figure 11**.

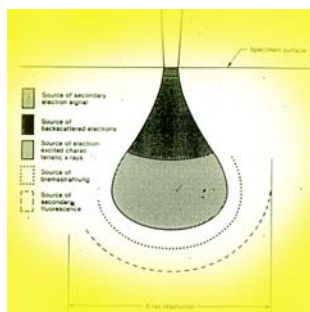


Figure 11: The zone of interaction between the electron beam and the solid specimen.

The measurement can be done at a quantitative and qualitative level. In quantitative mode, the intensities of the X-ray lines from the specimen are compared with those from standards of known composition. The measured intensities require certain instrumental corrections, including the subtraction of background X-ray level from the continuous X-ray spectrum. The correction is normally carried out automatically by using a computer

method known as “ZAF corrections” which takes into consideration factors such as the atomic number (*Z*) of selected elements, the absorption (*A*) and fluorescent (*F*) factors of the sample. The increased use of the computers in conjunction with the EPMA has greatly improved the quality of the data obtained. From the corrected wavelength and the intensity of the lines in the X-ray spectrum, the elements present may be identified and their concentrations calculated.

In a recent development, a quantitative compositional map can provide useful information on the distribution of different elements in a sample. In this mode, a complete semi-quantitative analysis is carried out under computer control at every discrete analysis point in a scanned field. The concentration values are assembled into images with a computer digital image processor by encoding the concentration axes with an appropriate colour scale. Every pixel is supported by the complete numerical concentration values of the relevant elements.

There is ample evidence arising from the use of these techniques to demonstrate that fluoride and other ions released from different glass-ionomers are taken up by the adjacent enamel and dentine. Tveit and co-workers, used EPMA to study the fluoride uptake by enamel and dentine. They only reported semi quantitative values because the technology available at that time, only allowed line scanning (Tveit 1980; Tveit, Totdal et al. 1985).

The advantages of an EPMA over other mineral profile analysis techniques are:

1. High spatial resolution: compositional information can be gathered with a spatial resolution on the order of 1 μ m
2. Quantitative analysis can be carried out accurately of the order less than 1% of the amount present for a given element
3. Minimal sample preparation and it is possible to work with bulk samples
4. Automated and computer controlled operation

5. Semi-quantitative compositional mapping provides an excellent method of studying the distribution of various elements within a sample
6. Ability to detect fluorine and other lower molecular weight elements which play a significant role in tooth tissue integrity

The disadvantages are:

1. The samples have to be dehydrated
2. Required equipment is expensive

1.2.3.1.3 Wet chemical analysis

The determination of calcium and phosphate in solutions in which a hard tissue is dissolved by means of an acid is in principle, a good method to quantify de- and remineralisation of the tooth tissue and the method has been used in *in vitro* studies.

However, the analysis is destructive, and only flat samples can be used. The samples are cut into two parts, that is, an experimental and a control part. The experimental part can then be subjected to intra-oral de- or remineralisation and compared with the control by dissolving the samples or parts of the samples in acid then determining the calcium and phosphate content of the solution.

The method has the following disadvantages:

1. Only a very large mineral gain or loss is measurable
2. Mineral distributions are not measurable
3. Curved whole samples cannot be used

1.2.3.2 Semi-quantitative methods

1.2.3.2.1 Polarised light

Polarised light microscopy analysis is a very sensitive technique for showing changes in hard tissues and permitting the measurement of porosity change. With respect to de- and

remineralisation, birefringence experiments can qualitatively show mineral loss and mineral gain. Thin sections of about 80 μ m are prepared and studied under a polarised light microscope.

Readings of the total path difference are recorded at various intervals along a transverse running from the outer surface through the lesion into sound enamel. The birefringence is calculated from the path difference and is, in general, denoted by $(n_e - n_o) \times 10^4$, where n_e and n_o represent the extra ordinary and ordinary refractive index respectively.

Surveys along the same transverse can be carried out after imbibition with various liquid media (eg. water, quinoline, and Thoulet's medium). However polarised light experiments are difficult to interpret quantitatively.

The total birefringence is the sum of the negative intrinsic birefringence and the positive birefringence. In enamel, the intrinsic birefringence is influenced by the volume of the crystallites, their arrangement and inclination with respect to the light beam, as well as by the birefringence of the mineral itself. The form birefringence is determined mainly by index of refraction differences between the crystallite and surrounding medium and also by the relative crystallite volume and orientation. Furthermore, prism shape and orientation, as well as carbonate content, water content, and organic material content, have noticeable influences on the total birefringence.

The polarised light technique is qualitatively useful in the estimation of mineral loss and gain. A correlation between birefringence and mineral content data from microradiography with adequate correlation coefficients has not been established. Polarised light measurements can provide quantitative information on the pore volume (porosity) in de- and remineralised enamel, and on lesion characteristics.

It can be used as a measure of lesion depth and size of the zones within the lesion. It is a very good adjunct to show the characteristics of lesions, small surface zones and root caries lesions (Featherstone 1992).

1.2.3.2.2 *Hardness*

Microhardness indentation measurements have been used to determine de- and remineralisation effects since the first *in situ* studies of Koulourides (Koulourides 1966). In this method, a Knoop or Vickers diamond is positioned on the sample with a given load for a given time. The indentation length left by the diamond is determined microscopically in μm .

Microhardness tests can provide indirect evidence of mineral loss or gain as a result of de- or remineralisation. If indentation length values increase the tissue has lost mineral and if the indentation length values decrease, the tissue has gained mineral.

The relation between microhardness indentation values and mineral content is however, empirical. Quantitative mineral contents can be obtained only when calibrated against a quantitative technique like TMR.

Two different types of hardness measurements must be distinguished:

1. Surface microhardness (SMH)
2. Cross-section microhardness (CSMH)

1.2.3.2.2.1 *Surface microhardness (SMH)*

Most important in hardness determinations is the fact that reliable measurements can be made only on flat surfaces. The outer tooth surface is generally too curved to allow for reliable hardness indentations on the anatomical surface (Arends, Schuthof et al. 1980). However, providing the indenter load is perpendicular to the flat surface, a linear relation between the Knoop indentation length and lesion depth can be found with a good correlation coefficient ($r = 0.95$). A similar empirical relation has been found by White for Vickers hardness indentations (White 1987).

By use of the relation:

$$\Delta D = \left[\sqrt{VHN_i} - \sqrt{VHN_f} \right] \times 100$$

VHN_i=initial Vicker hardness measure

VHN_f=final Vicker hardness measure

it can be shown that ΔD is directly proportional to the microradiographically determined ΔZ ($r = 0.94$). The difference between Knoop and Vickers hardness measurements is mainly the penetration depth of the indenter. For an indentation length of 100 μm , the Knoop indenter penetrates about 3.5 μm , whereas the Vickers diamond reaches a depth of about 14 μm .

Although this method is attractive because of its simplicity, it is not generally used because of the disadvantages listed below. It is an excellent method for screening lesions prior to use in an intra-oral model study.

The disadvantages of SMH measurements in the assessment of de- and remineralisation are:

1. Flat surfaces are needed
2. The information is qualitative only
3. Phenomena such as lesion shape, mineral redistribution, as well as protein uptake in situ, might influence the indentation length values
4. A linear relationship between indentation length and lesion depth is valid only in a limited range of lesion depth values (Arends, Schuthof et al. 1980; Zero, Rahbek et al. 1990)

1.2.3.2.2 Cross section microhardness (CSMH)

In CSMH the specimens must be cut perpendicular to the tooth surface, Knoop indentations are then made from the outer enamel surface inward in 25 μm steps up to several hundred μm depth with the long axis of the diamond indenter being parallel to the

outer surface. In a study carried out by Featherstone and co-workers. (Featherstone, ten Cate et al. 1983), it was shown that the Vol% of mineral as determined from microradiography was directly proportional to $(I)^{-1}$, with a good correlation coefficient ($r = 0.92$); I is the Knoop indentation length in μm . For human enamel, the following relationship has been established:

$$V\%(MINERAL) = 11.3 + 4.3 \times \sqrt{(14230K)} / I$$

K =indenter load in grams, I =Knoop indentation length in μm

Using the above equation, I values can be directly converted to volume percentages of mineral.

The CSMH method has the following advantages:

1. The mineral content can be calculated quantitatively so mineral loss and mineral gain values can be estimated
2. The mineral profile (volume% of mineral as a function of the distance from the outer surface) can be obtained.

A disadvantage is that the outermost $25\mu\text{m}$ of a sample cannot be included in the measurements.

A summary of microhardness as it relates to de- and remineralisation quantification can be set out as follows:

- Microhardness indentation measurements (SMH) with the indenter perpendicular to the surface give qualitative information on mineral changes
- Microhardness indentation experiments with the indenter parallel to the surface (CSMH) provide indirect information on the mineral content and can be used for quantitative assessment of de- and remineralisation. It can be used as a substitute for TMR for enamel studies.
- Microhardness experiments have been carried out mainly on enamel.

Their use for dentine presents numerous problems due to relaxation of the dentine indentation with time and the shrinkage effects due to drying (Herkstroter, Noordmans et al. 1990).

1.2.3.2.3 Permeability

1.2.3.2.3.1 Iodine absorptiometry

In this method, photons with energy of 27.4 keV resulting from the decay of a ^{125}I source are used to irradiate longitudinal tooth sections. The geometry of sample and beam are analogous to the one used in LMR. The incident and the transmitted radiation flux are measured with a scintillation counter. The amount of absorbed photon radiation is a measure of the amount of mineral per unit area ($\text{kg}\cdot\text{m}^{-2}$).

It has been shown (Almqvist, Wefel et al. 1988) that the change in photon radiation due to a dentine sample placed in the beam is linearly correlated ($r=0.83$) with the amount of Ca lost *in vitro* as determined by chemical analysis. This method provides quantitative mineral loss and gain data with sensitivity, comparable to that of TMR.

1.2.3.2.3.2 Iodine permeability

Bakhos and co-workers (Bakhos, Brudevold et al. 1977) introduced a method of measuring changes in the permeability of tooth surfaces, the Ip test. Such measurements are related to the pore volume of enamel and can give, in principle, sensitive estimates of the initial stages of de- and remineralisation. Samples are completely covered with 2M KI solution for 3 min and wiped off; the window on the enamel sample is covered with water for 40s to permit back-diffusion of iodide. The water is quantitatively recovered by an absorbent disk. The iodide content of the disk is determined by an iodide-specific electrode and is a measure of Ip.

Several papers by Brudevold and co-workers have shown that the method is a sensitive tool for the measurement of permeability changes in the tooth surface. However, the relation between I_p changes and the amount of mineral lost or gained is not yet clear. Ten Bosch and Angmar (ten Bosch and Angmar Mansson 1991) showed that the relation between ΔI_p and the amount of Ca lost had a moderate correlation coefficient ($r = 0.55$).

The iodide permeability test has been combined with the SMH microhardness test (Zero, Rahbek et al. 1990) and the correlation between these two experimental techniques was moderate. This is not very surprising, because surface porosity and deformation by indentation are two quite different physico-chemical phenomena. The iodide permeability test is most likely very sensitive to several surface changes.

At present, the indications that this test can be reliably used to assess de- and remineralisation are weak (Zero, Rahbek et al. 1990).

1.2.4 Considerations in regards to assessment methods

1.2.4.1 Specimen preparation procedures

In practice, a major limitation to the accuracy of information provided by techniques for the evaluation of de- and remineralisation lies not in fundamental limits of techniques but in practical application of *in vitro* or *in vivo* testing. Among potential limits, specimen handling procedures are extremely important.

In the case of TMR, the most common direct measure of mineral change, successful application requires that planoparallel cross-sections of roughly 80-100 μ m in thickness be prepared in enamel and dentine (Groeneveld and Arends 1975). Typically, this is accomplished through cross-sectioning of relatively thick slabs (> 150 μ m) followed by reduction to the required thickness through various polishing procedures (ten Cate and Exterkate 1986; White 1987). A review of the available literature shows that, despite widespread practice, only a handful of authors have demonstrated that it is possible to

prepare planoparallel cross-sections in a reproducible fashion using polishing techniques. White reported a 10-20% variations in thickness affecting radiographic precision (White and Nancollas 1990).

The proper assessment of dentine in studies of root surface caries is difficult. The problems of expansion and shrinkage in dentine, owing to hydration or dehydration of its collagen framework, are well documented. For TMR, shrinkage occurs during sample preparation (Ogaard, ten Bosch et al. 1989). In PL, shrinkage even happens during the immersion of the sample in various media (Wefel, Clarkson et al. 1985). This shrinkage does not affect total determination of mineral loss or mineral gain (ΔZ) for TMR, LMR, or WIM but does result in loss of depth profile (L_d) measurement of the sample in TMR.

In practice, dentine shrinkage during preparation for TMR can be reduced by fixing the collagen, using high speed films and maintaining humidity during x-ray exposure periods. However, none of these will eliminate shrinkage totally.

Although TMR, LMR and WIM can be used on dentine samples, the potential for shrinkage means that PL and microhardness evaluation of dentine are both useful. Since PL measures porosity, shrinkage of specimens in various imbibition media can produce artefacts. In addition, reactivity of collagen matrix with PL immersion media could theoretically influence subsequent porosity evaluations (although this has not been studied). Last, the more porous nature of dentine makes it likely there will be less oriented mineral growth within tubules thus confounding measures of form birefringence for different refractive index imbibing media. As an important exception to these criticisms, the lesion depth in dentine stored in water measured with polarised light microscopy probably represents an excellent measure of degree of acid penetration when compared to TMR where shrinkage invariably occurs.

For microhardness, the elastic properties of dentine make measurements suspect both on the surface and in cross-section. Despite this problem, authors have reported an empirical

quantitative association between cross-sectional hardness on dentine and TMR (Featherstone, ten Cate et al. 1983), suggesting that with careful control, these methods can provide comparable results. For best results it was suggested that samples be allowed sufficient time to stabilize between actual indentation and measurement.

Improvements and innovations in model designs have been numerous in *in-situ* research, and include the use of single-section and multiple-section sandwich techniques (Melberg, Castrovince et al. 1986; Wefel, Maharry et al. 1987). This and improvements in methods such as the use of WIM and LMR have enabled researchers to consider studies of intra-oral remineralisation and demineralisation phenomena longitudinally with time. This can be achieved by removing specimens part way through the test, analysing them, and returning them to the mouth. However there is concern about the effects of extra-oral time and analytical procedures on subsequent reactivity of the lesion substrates. Polarised light analysis, for example, involves the immersion of lesions in media such as quinoline or acetone, and these may be retained within lesions, thus affecting subsequent reactivity. Other techniques, such as TMR and hardness, may result in significant drying of specimens. This could influence subsequent remineralisation and demineralisation processes.

1.2.4.2 Magnitude of change

Another important factor in the choice of appropriate methods for the assessment of demineralisation and remineralisation processes is the magnitude of change anticipated following treatment. The remineralisation rate *in vivo* is relatively slow, with a dependency upon both the saliva and substrate (Arends and Ten Bosch 1985; Dijkman, Schuthof et al. 1986; Strang, Damato et al. 1988). While remineralisation rates of from 100 to 500 ΔZ units/month are quite typical in demineralising conditions, under high cariogenic stress, mineral loss can average up to four times this amount (Wefel, Clarkson et al. 1985).

Some perspective or estimate of the magnitude of these changes anticipated during testing must be important to the researcher using intra-oral models, since it determines, among other things, the types of techniques best suited for analysis, both statistically and from a sensitivity aspect. For example, protocols where the mineral content changes over 4000 ΔZ units require fewer sample replicates or can tolerate less precise analytical techniques. This means that PL would be a sufficient analysis methodology if MR were unavailable as compared with those protocols where total ΔZ changes are 1/10th as large. As the amount of total change becomes less pronounced, the more critical is the precision of the analytical techniques in order to record sensitive discriminative data between treatment groups.

1.2.4.3 Protocols of specimen analysis

In addition to variations in protocols for specimen analysis with individual techniques, there is also considerable variation among researchers in the combination of parameters analysed and reported in studies. For example, although TMR can provide information on total mineral content changes, lesion depth, and maximum and minimum mineral content, the combination of these reported parameters varies from study to study, making the relative comparison of results difficult.

Summary of current methodology for determining mineral profile in tooth structure:

1. The evaluation of ΔZ is the primary measure of mineral loss or gain. This is best accomplished with TMR, WIM, or LMR but can be substituted with CSMH, if appropriate protocols for evaluation are standardised.
2. The second measure of primary value is lesion depth (L_d) since this defines the magnitude of penetration and damage from acid. Depth measurements are also desirable, because their relation to ΔZ changes gives information on the nature of acid destruction (e.g., softening versus subsurface). Depth can be measured directly with

CSMH, TMR, or PL. Depth measurement in dentine is difficult if dehydration is involved in the sample preparation.

3. Lesion porosity is a valuable secondary measure which complements other techniques. This can be measured directly with PL or with iodide permeability.
4. Surface microhardness is suited as a complementary measure to direct techniques. It is particularly valuable as a calibration measure for lesion preparation (White 1987)

Chapter 2: Overview of this study

2.1 Hypothesis of the study

This study was designed to test the following hypothesis:

Close adaptation of glass-ionomer cement to demineralised dentine will lead to the uptake of apatite forming ions into dentine and lead to the potential for remineralisation.

2.2 Overall approach to achieving the objectives of the study

As stated in the introduction to Chapter 1, the major impetus for this study was to investigate how glass-ionomers interact with partially demineralised dentine. In particular do they contribute to the remineralisation of this structure and if so, how? The focus is intended to be mainly at the molecular and ultra-structural level.

This is a huge task, and as often happens, it was possible only to analyse a number of aspects of this process, through choosing tests intended to provide that information which might contribute the most valuable answers towards the objective.

The tests chosen were as follows:

1. Mineral Profile Analysis: The initial requirement was to choose the method of mineral profile analysis which gave the most important information on background patterns and changes in mineral and structural profiles. The Electron Probe Micro-Analysis (EPMA) method was chosen following the review of a variety of methods. As most previous analyses of density profile of tooth structure had been through Micro-radiography (MR), it was initially necessary to compare the information gathered for each method to validate the choice of that method (Chapter 3).
2. Background information on ionic release in a simulated *intra-oral* environment: The second series of tests was carried out to provide background information on the types of minerals which might be leached from the glass-ionomers in a fluid situation. This was

intended to pinpoint those elements which could be transported into partly demineralised dentine, which would have an increased water component, and which should therefore be followed in mineral profile analysis of the dentine after contact with glass-ionomer.

The test chosen was to place a wide variety of glass-ionomers into saliva simulated fluids, at a range of pH levels often experienced in the oral environment (Chapter 4).

3. Ionic exchange between glass-ionomer and demineralised dentine:

a. Initial Pilot Studies: The major focus of the study was to investigate the type of ionic exchanges which occur at a molecular level between glass-ionomer and demineralised dentine and to determine the observed and potential contribution these make to the structural integrity of each material.

The ultimate example of this interaction is that which occurs *in vivo*. It was realised that it would be difficult both ethically and experimentally to use this method to study the ionic exchange processes as extensively as needed. A small pilot study was carried out to establish an example of the types of ionic interaction which may occur between glass-ionomer and demineralised dentine *in vivo* (Chapter 5.1). Any *in vitro* model of the interaction would need to have some resemblance in ionic transfer pattern to be a reliable alternative.

b. Development and validation of an *in vitro* model: An *in vitro* model was developed, simulating the type of interaction between glass-ionomer and demineralised dentine which occurs in the ART method of restoration placement. This was tested for validity in distinguishing between control and test sections (Chapter 5.2).

On validation, it was used for a number of investigations into the precise nature of the ionic exchanges between different types of glass-ionomer and demineralised dentine (Chapter 6).

Each of these aspects of the research project will be dealt with individually, with the combined nature of the results being discussed in Chapter 7.

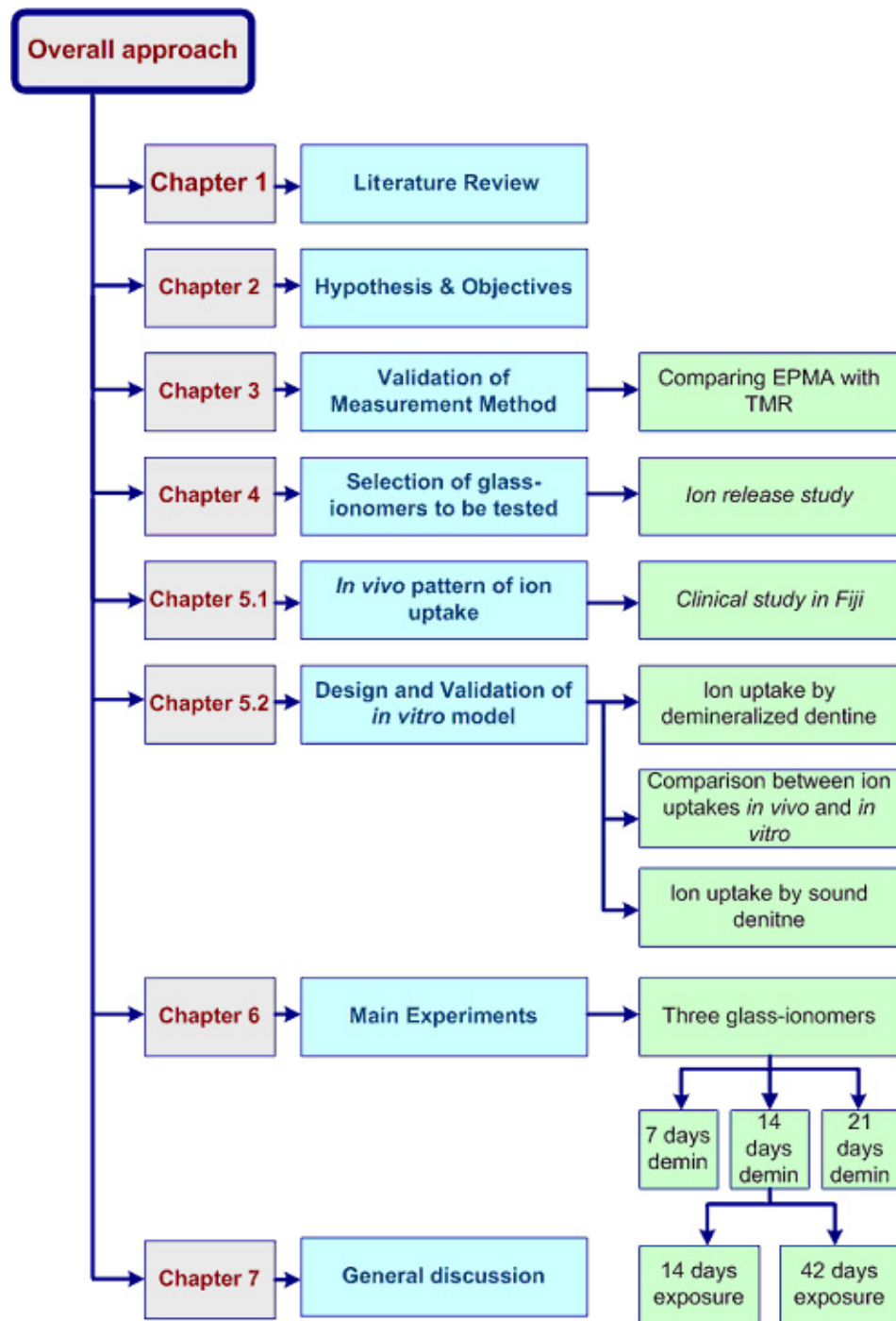


Figure 12: Overall approach to achieving the objectives of the study.

Chapter 3: Selection & validation of method of mineral profile analysis

3.1 Introduction

As stated in Chapter 2, the major objective of this thesis involves the study of possible interactions between restorative materials and dental hard tissues. Thus it is important to utilise an analysis method that can accurately measure small changes in mineral content of tooth structure, both enamel and dentine. Currently, transverse microradiography (TMR) is the accepted tool for this purpose. However, electron probe microanalysis (EPMA) can yield both qualitative identification of elements and quantitative compositional information so it was decided to initially compare the two methods. To validate its choice, it was decided to compare the results achieved in profiling mineral content in teeth and associated structure using this method, with those obtained using transverse micro-radiography (TMR) analysis.

The question to be answered by this experiment was:

- Is EPMA a suitable method to analyse the mineral and chemical content of enamel and dentine?

To meet the above objective, the experiment was designed to compare:

- The lesion depth levels (l_d) of artificial incipient caries in enamel and dentine as determined by EPMA and TMR
- The mineral profiles from the same samples, using EPMA and TMR
- The relative concentrations of calcium and phosphate in enamel and dentine as measured by EPMA compared with existing chemical analysis data

A good correlation between the results from TMR and EPMA would validate the selection of EPMA as the main investigative tool and it has the following advantages over TMR:

- It can measure quantitatively

- a. Major elements: Ca and P
- b. Minor elements: Sr and F
- It can measure in small volume: μm^3
- Sample preparation is relatively simple

3.2 Materials and methods

3.2.1 Preparation procedure for enamel specimens

Enamel specimens used for comparative analysis between EPMA and TMR were obtained from a pH cycling remineralisation study. These specimens provided areas of de- and remineralisation, prepared under controlled conditions. For the present comparisons, specimens were selected from two treatment groups of pH cycling, those treated with a 1450 ppm NaF dentifrice and those treated with a placebo dentifrice, free of fluoride.

3.2.1.1 Lesion preparation: pH cycling protocol

Eight enamel samples were prepared by cutting 4 mm diameter by 5 mm thick cores from extracted human teeth using a diamond core drill. The teeth were stored in 1% thymol in de-ionised distilled water (DDW) and maintained at room temperature. Enamel cores were mounted in ¼ inch diameter leucite rods with dental acrylic (Dura Base, Reliance Mfg. Co., USA) covering all sides except the prepared surface. Abrasion with 600-grit silicon carbide (Linde No.3, AB Gamma Polishing Alumina, PSI, USA) water slurry was used to remove approximately 50 μm of the outer enamel, and the sample was finally polished for 90 minutes with gamma alumina to a high finish. Enamel specimens found to have a surface imperfection were rejected.

The demineralisation of specimens was carried out by immersion in 25 mL of a solution containing 0.5M/L lactic acid and 0.2% Carbopol 907 (B.F. Goodrich Co., UK) 50% saturated with respect to hydroxyapatite (HAP), pH 5.0, for 96 hrs at 37°C (White 1987).

Lesions formed following this procedure are generally 60-80 μm in depth (White 1988). After demineralisation, specimens were rinsed with DDW and analysed for surface microhardness with a Leitz miniload tester (Leitz, Wetzlar, Germany) at a constant load of 200 g. Hardness numbers based on the Vickers Hardness Scale ($\text{VHN}_{\text{initial}}$) were recorded three times on each specimen, then averaged. Specimens were placed in groups of four in such a way that the average hardness of each group of specimens was not significantly different ($p < 0.05$, ANOVA).

Approximately 1/3 of the surface of each specimen was covered with an acid-resistant nail polish. This area remained covered throughout the experiment to serve as a reference for later microradiographic analyses. Each group was placed in 20 mL of fresh, pooled human saliva for a period of one hour to form an initial layer of pellicle on the demineralised enamel surfaces.

Dentifrice slurries were prepared by mixing 5 g of dentifrice (Procter & Gamble, USA) with 15 g of fresh, pooled human saliva for four to five minutes prior to use. Fresh slurry was prepared for each treatment. Treatments were made four times per day for a total of six days. After each dentifrice slurry treatment, which lasted for one minute, specimens were rinsed with DDW, then placed in approximately 20 mL of fresh, pooled saliva until the time of the next treatment. The saliva bath was freshened three times daily.

Between the second and third treatments each day, specimens were exposed to a further three hours of treatment at room temperature (unstirred) with 25 mL of fresh demineralisation solution of the same composition used to form the initial lesions. At any time specimens which were not being treated with dentifrice slurries or in demineralisation solution were left soaking in pooled human saliva (stirred).

After six days of treatment, specimens were analysed for fluoride content by means of a microdrill biopsy technique (Sakkab, Cilley et al. 1984). After being analysed for fluoride uptake, specimens were exposed to an acid challenge assessment. For this, one half of the

“remineralised” surface area of each of the specimens was covered with additional nail polish. The portion of the surface that remained uncovered was then exposed to 8 mL of freshly prepared demineralisation solution for a period of seventy-two hours at 37⁰C (unstirred).

Following the completion of the lesion preparation, pH cycling, and post-treatment “acid challenge” assessments, each specimen included three areas representing:

1. C, control ninety six hours demineralised lesion
2. T, treatment for six days of pH cycling remineralisation
3. A, acid challenge post treatment.

There were eight specimens with a total of twenty-four areas. Four of the specimens received treatment with 659 ppm F ion dentifrice, and the remaining four were treated with fluoride free dentifrice (Procter & Gamble, USA). After being sectioned, these areas could be compared by both TMR and EPMA analysis.

3.2.2 Preparation procedure for dentine specimens

Three premolars, extracted for orthodontic reasons, were stored in DDW containing 0.1% thymol until required. All teeth were clinically sound and had no apparent physical damage.

The outer layer of cementum and dentine was removed from an interproximal area of the root, using 220 grit silicon carbide abrasive paper (Siawat WA, Zurich, Switzerland) under water. Blocks of dentine (6 x 7 x 1.5 mm) were then prepared using a water-cooled diamond saw. All samples were embedded in cold curing polymethylmethacrylate (PMMA; DeTrey, Weybridge, United Kingdom) with the abraded surface exposed. Before being subjected to demineralisation, the exposed surface was abraded again on wet silicon carbide abrasive paper, grit 800 (Siawat WA, Zurich, Switzerland).

Artificial caries lesions were developed by the use of a 0.1M sodium lactate gel containing 6wt% carboxymethylcellulose (CMC, AKZO, Arnhem, The Netherlands) at pH 5 and incubated at 37⁰C for two weeks. The standard gel volume was always 100 mL per six samples.

After demineralisation and careful washing, the dentine blocks were sectioned and microradiographed as described below.

3.2.3 TMR analysis for enamel and dentine lesions

Thin sections of specimens for comparative analysis were prepared using a hard-tissue sectioning saw (Gillings-Hamco Hard Tissue Sectioning Machine, NY, USA). This technique requires a 100 µm thick, plano-parallel section to be removed from each of the specimens for microradiographic analysis. The specimen was placed flat on a photographic plate of Kodak S0953 film (Eastman Kodak, Rochester, NY, USA) and radiographed along with an aluminium stepwedge for calibration (steps ranged from 25 to 200 µm in thickness). Using microdensitometry, it was possible to calculate the mineral content in volume percentage using Angmar's formula (Angmar Mansson, Carlstrom et al. 1963). The radiographs were analysed by a computer based image analysis system (Inspektor Research, The Netherlands).

The density reading for sound enamel beneath each lesion was normalised to a value of 87 vol% mineral. Mineral profile scans were made from the three areas of interest (C, T and A). The use of TMR to measure the mineral content of enamel and dentine has been described by Arends, (Arends and ten Bosch 1992) and de Josselin de Jong (de Josselin de Jong, ten Bosch et al. 1987).

3.2.4 EPMA analysis for enamel and dentine lesions

After being microradiographed, the enamel and dentine slices were mounted in Araldite (Giga Cyber, Victoria, Australia), in preparation for EPMA analysis by wavelength dispersive spectrometry (WDS). Since a smooth surface is essential for microanalysis, the samples were polished progressively down to 0.3 μm grit with an aluminium oxide micro-abrasive system (Micro-finishing, 3M, Minneapolis, MN, USA) and then dehydrated under vacuum for 48 hours for removal of any unbound water. To minimise charging during analysis, the samples were coated in a vacuum evaporator with a thin layer of carbon.

Using an electron probe microanalyzer Cameca SX51 (Cameca, Corbevoie, France), the same operating conditions for both enamel and dentine were used. The excitation voltage was kept at 15 kV and the current at 20 mA. The diameter of the electron beam was 2 μm , and counting time was ten seconds at each point.

Wilberforce fluorapatite was used as a standard, and the PAP modified version of the ZAF software package (Cameca, Corbevoie, France) was used for correction. Two diffracting spectrometers were assigned to collect information for calcium and phosphorus simultaneously. Spot analysis was performed at 2 μm intervals along a transverse line perpendicular to the outer surface. A set of 5 lines was performed for each enamel sample and 7 lines for each dentine sample. Based on the above beam conditions, the calculated minimum detection limits are listed in **Table 2**.

Element	Collection Time	Weight %
Ca	10 sec	0.05%
P	10 sec	0.12%
F	10 sec	0.05%

Table 2: Minimum detection limits based on beam settings of 15 kV and 20 mA

To average out local anomalies at individual analysis points, the average concentrations of calcium and phosphorus were calculated for the points lying at the same depth from the edge of the sample surface. The average values were then plotted against distance from the surface to give the mineral content profile of each lesion.

3.3 Results

Figure 13 shows a typical EPMA profile of wt% mineral, combined Ca and P, as a function of depth for the three areas C, T, and A of a sample treated with 1450 ppm NaF. The effects of the treatment with a six day remineralisation protocol using 145 ppm F (area T) and the post-treatment acid challenge (area A) were apparent, with the smaller depth of lesion (l_d) and the apparently smaller ΔZ in comparison with the control area (area C).

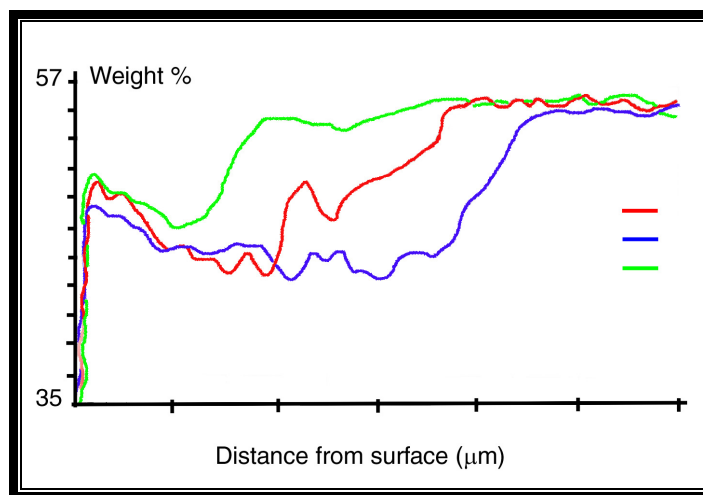


Figure 13: EPMA mineral, combined Ca and P, content profiles of the three zones C,T and A on an enamel specimen treated with 659 ppm F ion dentifrice

The three profiles of mineral content in vol% mineral as measured by TMR (**Figure 14**) showed similar relationships among the three curves. The TMR profile of areas T and A showed the presence of a distinct peak between 40 and 60 μm from the surface. These peaks were also present at the corresponding positions in the EPMA profiles.

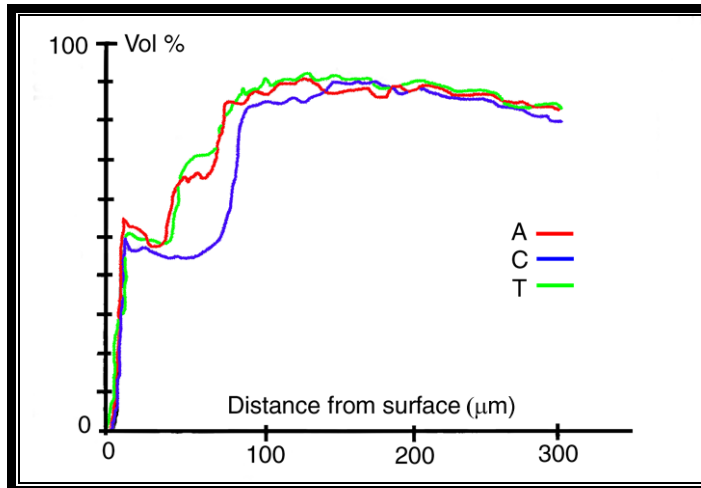


Figure 14: TMR mineral content profiles of the same enamel specimen as in **Figure 13**

During the demineralisation of dental hard tissues, the dissolution of hydroxyapatite meant that both calcium and phosphate were lost at the same rate. This is confirmed by **Figure 15**, which shows that the calcium to phosphorus ratio stayed virtually constant right through the sample, in sound as well as in demineralised enamel.

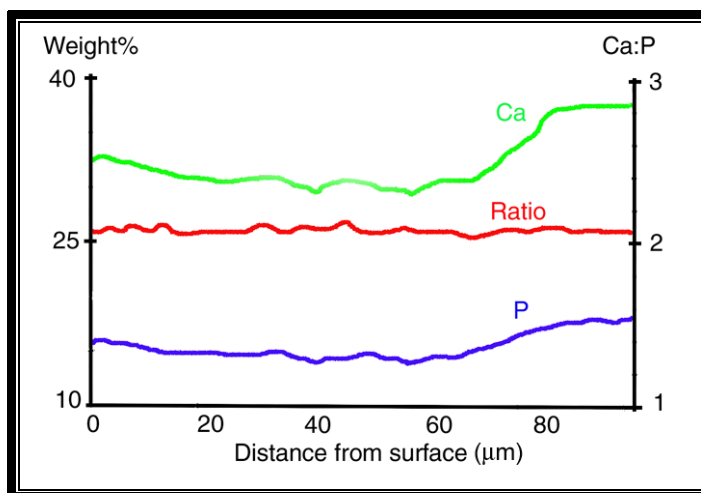


Figure 15: Ca:P ratio is maintained right through demineralised and sound enamel.

Figure 16 gives typical EPMA mineral content profiles for the three zones, C, T, and A, on a sample treated with placebo fluoride-free dentifrice. The depths of lesions (l_d) in zones C and T were similar, while the area exposed to post-treatment acid challenge (zone A) had a

larger depth of lesion. The timing for the introduction of the second acid challenge was marked by a peak at approximately 70 μm . This corresponded well with the TMR profiles in **Figure 17**.

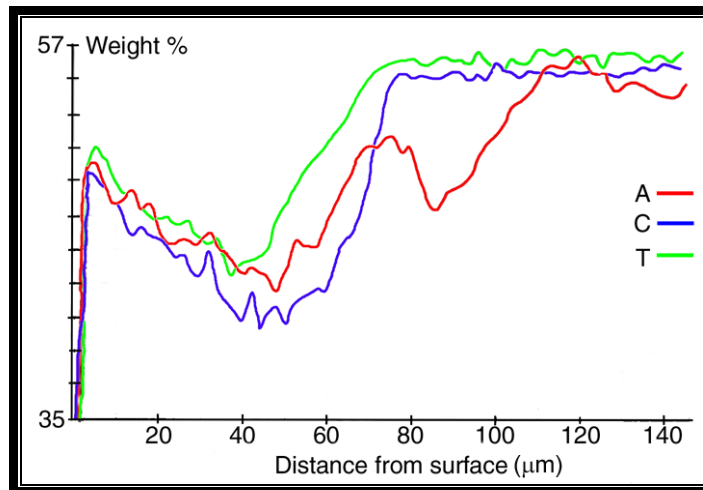


Figure 16: EPMA mineral content profiles of the three zones C, T and A on an enamel specimen treated with 0 ppm NaF.

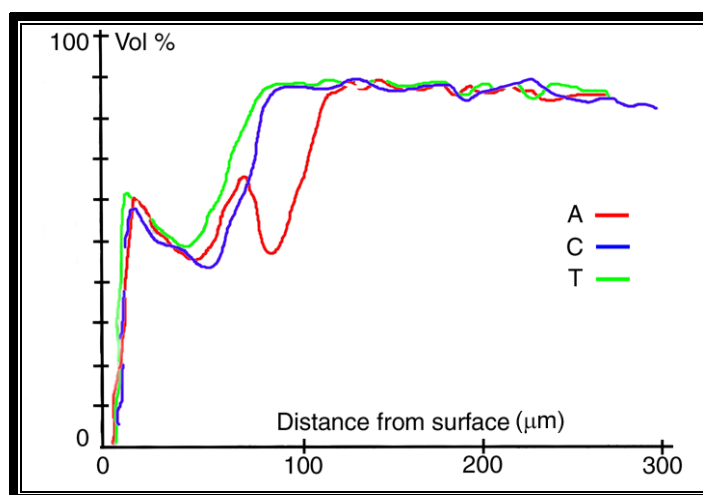


Figure 17: TMR mineral content profiles of the same enamel specimen as in **Figure 16**.

The depth of lesion for each zone, as measured by EPMA and TMR, was plotted (**Figure 18**), and a paired t-test showed that the difference between the two sets of data was not significant.

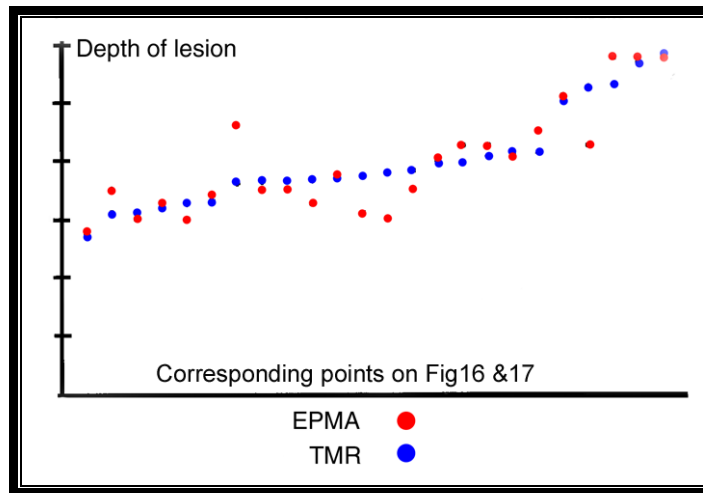


Figure 18: Good correlation between the EPMA and TMR depths of lesions. Paired t test: NS ($p < 0.05$)

The EPMA results for the three dentine samples are shown in **Figure 19**. The depth of lesion was 88 μm for one lesion and approximately 62 μm for the remaining two. The Ca:P ratios for the three samples were plotted against distance from the surface in **Figure 20** and remained constant in the demineralised zone as well as through the zone of sound dentine.

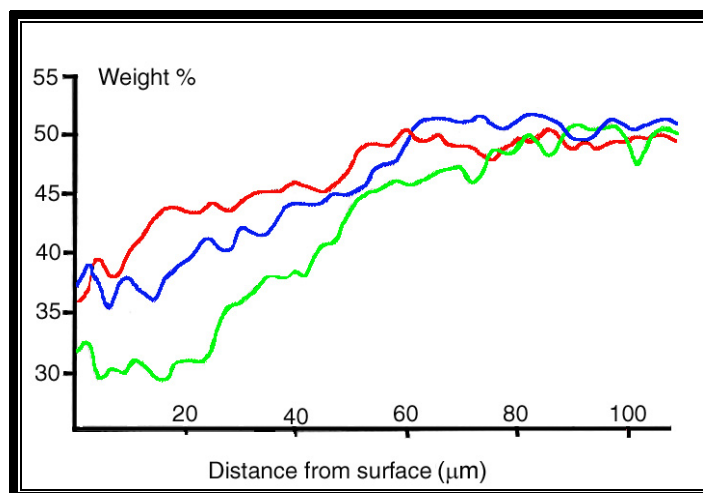


Figure 19: EPMA mineral content profiles of three two week dentine artificial lesions

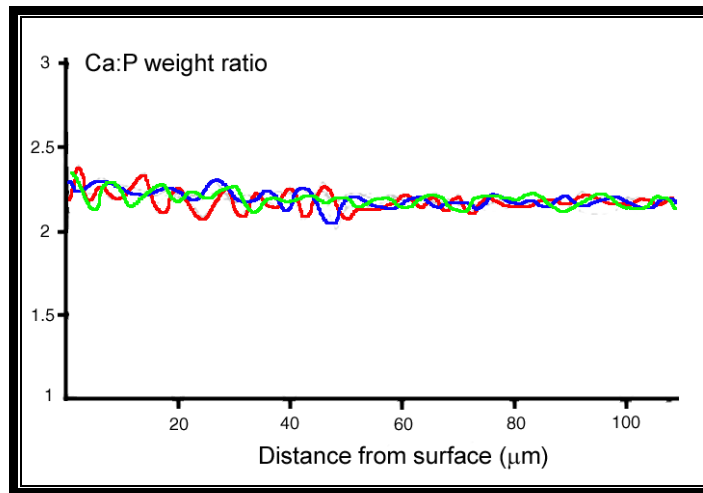


Figure 20: Ca:P ratio in demineralised and sound dentine

3.4 Interpretation

The results from this study show a close agreement between the mineral content profiles derived from EPMA and TMR analyses of enamel and dentine. In enamel, there is no significant difference in the depth of lesions determined by the two methods. Furthermore, the concentrations of calcium and phosphorus in sound enamel and dentine, as determined by EPMA, also agree with data derived from chemical analysis (Brudevold, Steadman et al. 1960). The Ca:P weight ratio of 2.1 for enamel and 2.18 for dentine compare well with the ratio 2.15 of pure stoichiometric hydroxyapatite.

The data from TMR analysis are expressed as vol% mineral, while EPMA gives results in terms of wt% mineral. The conversion between the two sets of data is complicated by the fact that, under EPMA, the specimens are exposed to high vacuum, and local density is unknown.

TMR is also a projection technique, and the information is the sum of total mineral over the thickness of the section. Elemental compositional information cannot be derived from this technique. EPMA identifies the elements present and their relative concentrations in a small volume of material. From a small mass, 3×10^{-12} g of enamel or dentine, an EPMA with WDS (see 3.2.4) will give the concentrations of calcium, phosphorus and fluorine

present with the minimum detection limits listed in **Table 2**. The accuracy of EPMA is dependent on the following factors:

- There must be a suitable standard of known composition, and it should be homogeneous at a microscopic level. Accurate analysis can be performed with simple standards consisting of a pure element. In studying enamel and dentine, fluorapatite was selected as a standard
- The specimen must have a flat, highly polished surface placed at a known angle to the incident beam and the spectrometers
- The specimen must be homogeneous on the micro scale
- The specimen must be stable under electron bombardment

The results from this study suggest that EPMA offers a simple and accurate way to determine the depths of lesions in artificial caries lesions created in both enamel and dentine. The major advantage that EPMA has over TMR is that it provides the researchers with quantitative data on the elements present at a microstructural level and allows for the study of extra parameters not available with TRM, for example, the pattern of distribution and penetration of elements which are radio-opaque, for example Sn, Sr, Al etc., from external sources into carious lesions.

Chapter 4: Preliminary analysis of ionic release from glass-ionomers when exposed to simulated oral conditions

4.1 Introduction

Fluoride ion release from glass-ionomer has been intensely studied (Forsten 1990; Forsten 1991; Forsten 1995). Not only can it be released in significant concentration, as described in the literature review, it can also be taken back up into the glass-ionomer (Forsten 1998). However it is likely that a number of other elemental components of glass-ionomer, such as Al, Sr and Na also might be leached, especially where acidic conditions prevail in the oral environment.

Even though the investigation is focused on the ionic transfers between glass-ionomer and demineralised dentine, it was considered important to determine the range and concentration of ionic species released from a range of glass-ionomers into a simulated saliva at a range of pH levels representing those often experienced in the mouth.

The purpose of this test was to determine those elements which might be most likely leached into demineralised dentine and the likely quantities from each of the glass-ionomers tested.

4.2 Materials and methods

4.2.1 Selection and preparation of glass ionomer specimens

The following glass-ionomers were selected for analysis (**Table 3**). These represent the categories most frequently used worldwide at the present time. The glass ionomers were mixed according to the manufacturers' instructions, and syringed into stainless steel washers (1 mm thick and 8 mm in diameter) then placed against Mylar strips (Hawe Neos Dental, Bioggio, Switzerland) both above and below. The specimens were allowed to set under a load of 100 g. The Mylar strips were left in place to allow the material to mature for thirty minutes. Excess material was removed, using a scalpel blade, and the exposed

surface area mathematically determined before later immersion into test leaching solutions. The total surface area of glass ionomer exposed to the solution, from all six samples (**Figure 21**), was approximately 132 mm².

Name of GIC	Glass	Type	Use	P:L (w/w)	Manufacturer
Fuji II	Sr	Chemical cure	Rest.	2.7/1.0	GC
Fuji IILC Improved	Sr	Res. modified	Rest.	3.2/1.0	GC
Fuji IX	Sr	Chemical cure	Rest.	3.5/1.0	GC
Fuji IIF	Ca	Chemical cure	Rest.	1.8/1.0	GC
Ketac Molar	Ca	Chemical cure	Rest.	3.4/1.0	3M ESPE
Ketac Fil Plus	Sr	Chemical cure	Rest.	3.2/1.0	3M ESPE
Ketac Cem	Ca	Chemical cure	Luting	2.0/1.0	3M ESPE
Ketac Bond	Ca	Chemical cure	Lining	3.0/1.0	3M ESPE

Table 3: Glass-ionomer cements to be tested

4.2.2 Preparation of eluting solutions

The solutions used in this study contained calcium and phosphate ions, supersaturated to the concentration present normally in saliva, together with acetate buffers. They consisted of a base 0.5M acetic acid, 2.2 mM CaHPO₄ and DDW. The stock solution was based on the artificial demineralizing solution developed by ten Cate and Duijsters (ten Cate and Duijsters 1982). The pH was adjusted, using 0.5M NaOH solution, to 3.5, 4.5, 5.5 or 6.5. These were intended to represent the various pH levels of saliva to which glass ionomer may be subjected when exposed to the oral environment.

4.2.3 Experimental method

The following method was used for this study:

1. Controls: Six unfilled stainless steel dies were placed, using a stand to allow free flow of the storage media (**Figure 21**), in the four categories of eluting media. These were incubated at 37°C and agitated continuously for seventy days.
2. Test specimens: Six specimens of each glass-ionomer material were held in a stand and were placed in 250 ml plastic containers and immersed in 40 ml of the four different eluting media (**Figure 22**). The specimens were incubated at 37°C and agitated continuously for varying periods as described in item four.
3. There were three repetitions of each test condition and the results presented on the charts in the results section were the average of the set of three repeats.
4. The samples of elution media were collected and stored, and new media replaced on day 1, 2, 3, 7, 14, 21, 28, 35, 42 and 56 from the beginning of the experiment. The eluting solutions were finally removed at day 70 and the samples stored at 4°C until analysed.

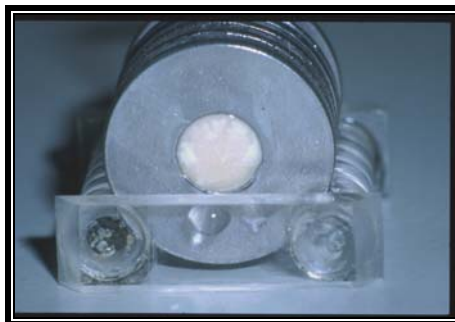


Figure 21: A set of six samples with a total surface area of 132 mm² exposed to the storage media.

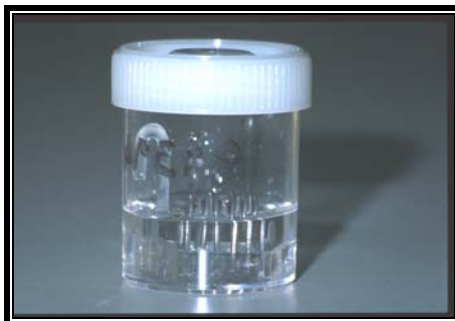


Figure 22: The stand kept the samples separated to allow free flow of the solution around each sample.

4.2.4 Determination of concentrations of ions present in eluting solutions

Ca, Sr and Al ion concentrations were determined from Inductively Coupled Plasma Optical Emission Spectrometer (IPC-OES) (ARL 3580B, ARL, Switzerland) analysis of each solution. The instrument was set up to analyse all the above elements simultaneously, using an array of photo-multipliers which were set in fixed positions to detect the wavelengths required.

As the concentrations, of the above elements, in the samples were well below the theoretical maximum detection limit (MDL) the samples did not have to undergo dilution before testing. The equipment was calibrated against standards solutions containing 1 ppm Sr, 10 ppm Al, and Ca after every twelve measurements

Fluoride ion determination for each solution was carried out with a Combination Fluoride Specific Electrode (Orion Research, Beverley, USA) used in combination with Total Ionic Strength Adjustment Buffer IV (TISAB IV) (Orion Research, Beverley, USA) to bind any calcium and aluminium ions present and maintain a more equitable ionic content between samples. TISAB IV was added to eluant samples on a 1:1 concentration basis. Fluoride standard solutions were also adjusted with equivalent volumes of TISAB IV.

The procedure is described below:

1. A standard fluoride curve of fluoride concentration against mV readings was prepared from each 1 ppm and 10 ppm fluoride standard/TISAB IV solution. A new fluoride standard curve was determined each day of reading
2. The mV reading was determined for each unknown sample/TISAB IV solution
3. The concentration of fluoride ion in each unknown sample was determined from the standard curve in ppm concentrations
4. These ppm concentrations of fluoride ion were converted initially to $\mu\text{g}/\text{mm}^2$ and finally to mmol/mm^2

The temperature of the samples, standards and TISAB IV were kept constant during the measurement. Data from these analyses were recorded initially as incremental amounts of elements released at the collection and replacement times listed above. These were then collated to show the cumulative amounts of each material released.

All data was assembled to provide graphs of concentrations of all ions tested, collated at progressive incremental levels, against time periods of collection. In most cases, the highest release was recorded on the first day; the cumulative data was charted from day two of collection so the reader can gain an idea on the level of this initial release. The incremental data for every collection period can be found in Appendix A.

4.2.5 Analysis of diffusion characteristics of cumulative data

The cumulative data were analysed against square root of time, in order to determine the degree to which the rate of release followed the characteristics of a diffusion based mechanism.

4.3 Results

The concentrations of the elements leached from the various glass-ionomers at the incremental collection times were converted to cumulative concentration data. The results for each glass-ionomer at each pH level are presented below in cumulative form as the main interest lies in the total release over seventy days as well as comparison with previously published data. In addition, the incremental release results are listed in Appendix A. Three sets of data are presented only for each glass-ionomer. Calcium data were recorded only where the glass-ionomer was calcium based. Strontium was recorded for the strontium based glass-ionomers.

The results were grouped according to the clinical usage characteristics and chemical properties of each material, as described below:

- Luting and lining: Ketac Cem and Ketac Bond
- Restorative: Fuji II, Fuji IIF, Ketac Fil Plus
- High Strength Restorative: Fuji IX, Ketac Molar
- Resin Modified: Fuji IILC Improved

The cumulative release in mmol/mm^2 by time in days is presented for each of the eight materials tested. The first data point on the horizontal axis starts from day two so its intercept with the vertical axis represents the cumulative release during the first forty-eight hours. The charts were prepared in this way to facilitate the study of the effect of pH on this initial burst release.

4.3.1 Cumulative release for luting and lining materials

Cumulative release of Ca, F and Al in mmol/mm^2 with time, for luting and lining materials

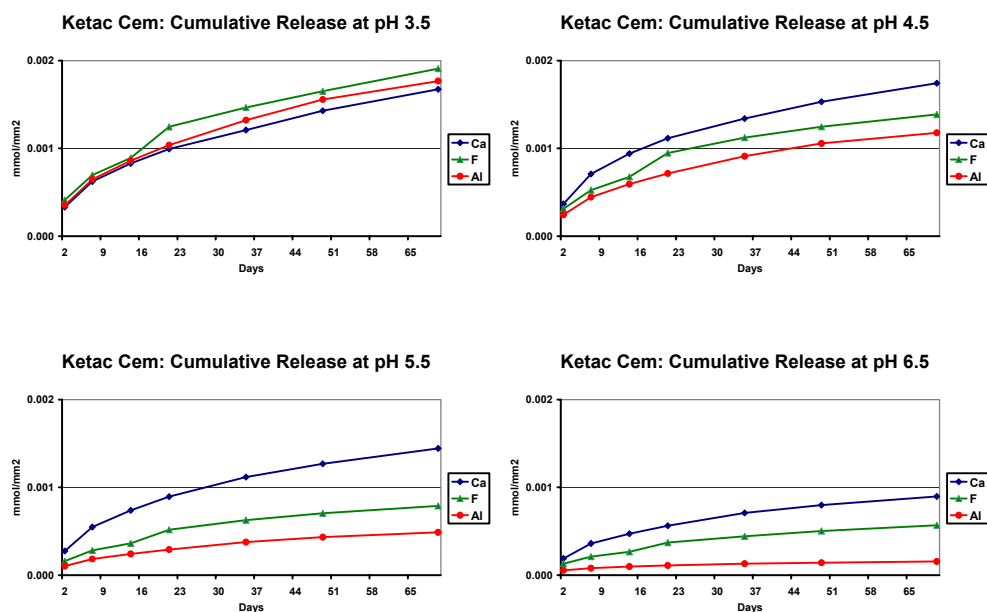


Figure 23: Ketac Cem, relative cumulative release of Ca, F and Al at different pH

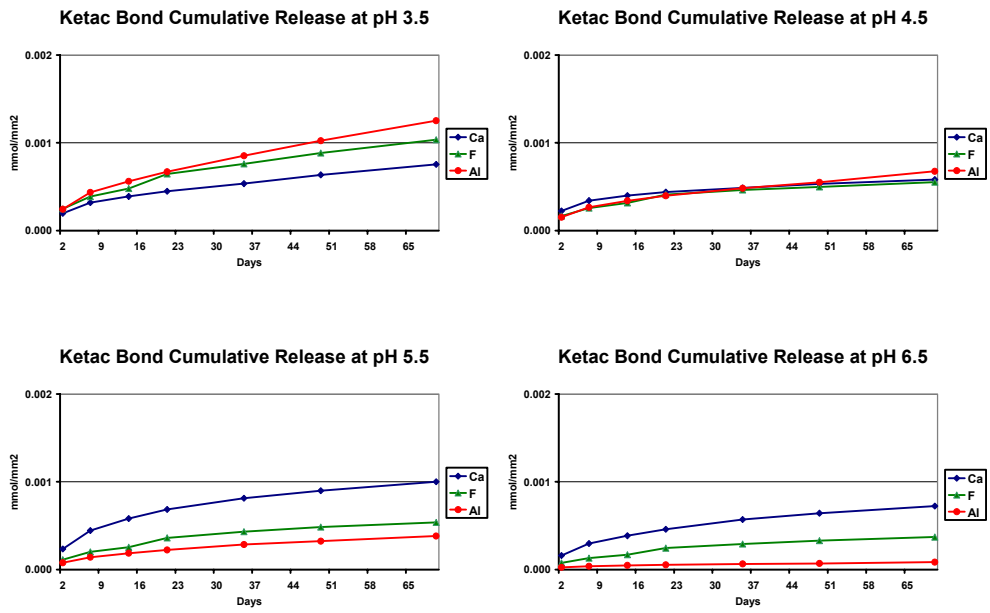


Figure 24: Ketac Bond, relative cumulative release of Ca, F and Al at different pH

4.3.2 Cumulative release for restorative materials

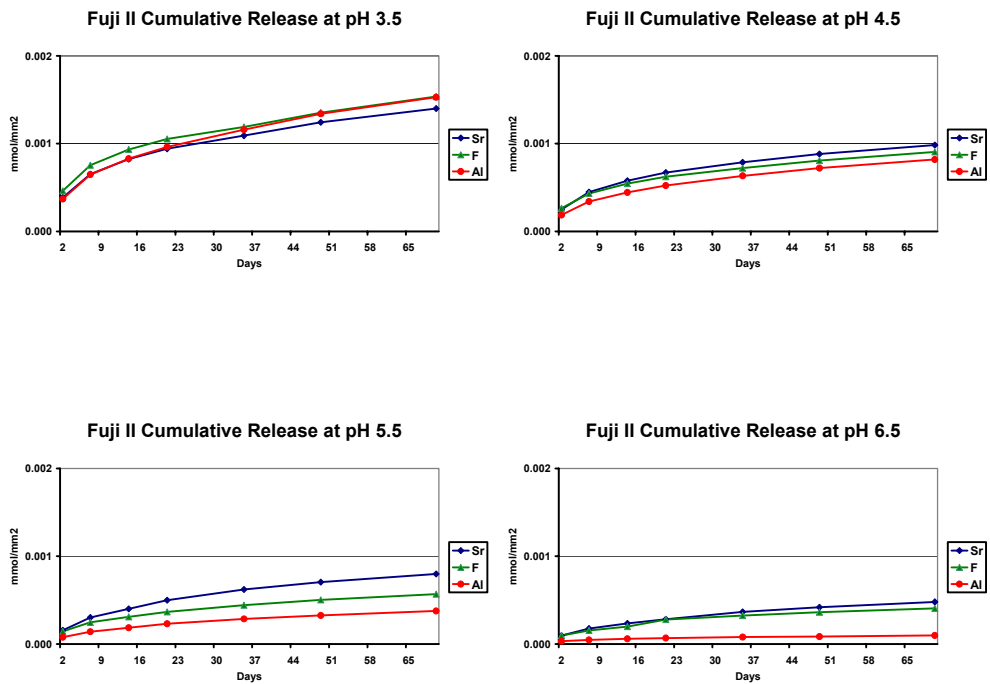


Figure 25: Fuji II, relative cumulative release of Sr, F and Al at different pH

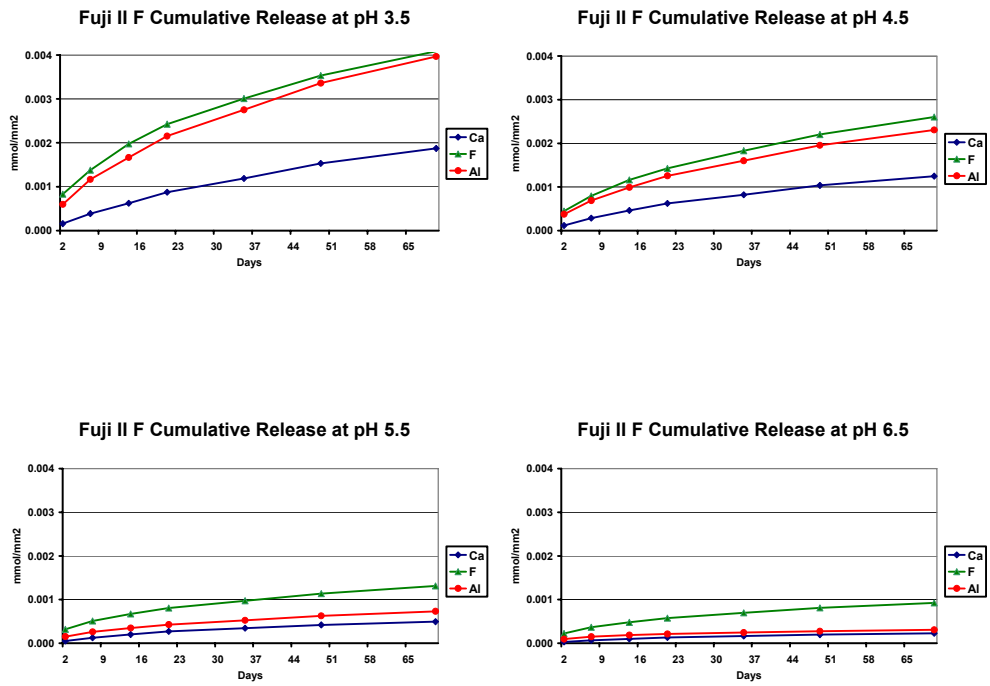


Figure 26: Fuji IIF, relative cumulative release of Ca, F and Al at different pH
(NB: different y axis scales because of high release)

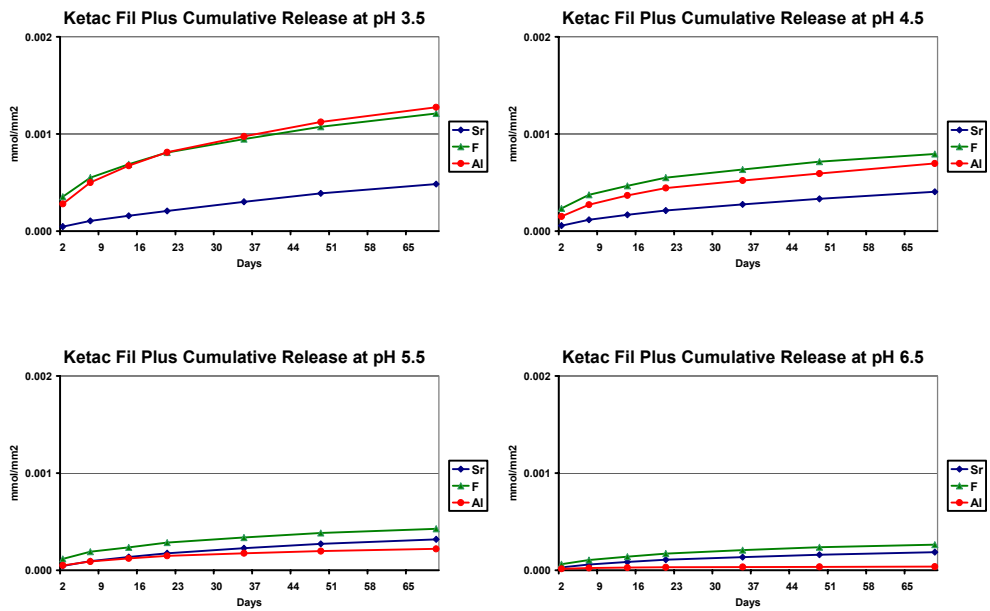


Figure 27: Ketac Fil Plus, relative cumulative release of Sr, F and Al at different pH

4.3.3 Cumulative release for resin modified materials

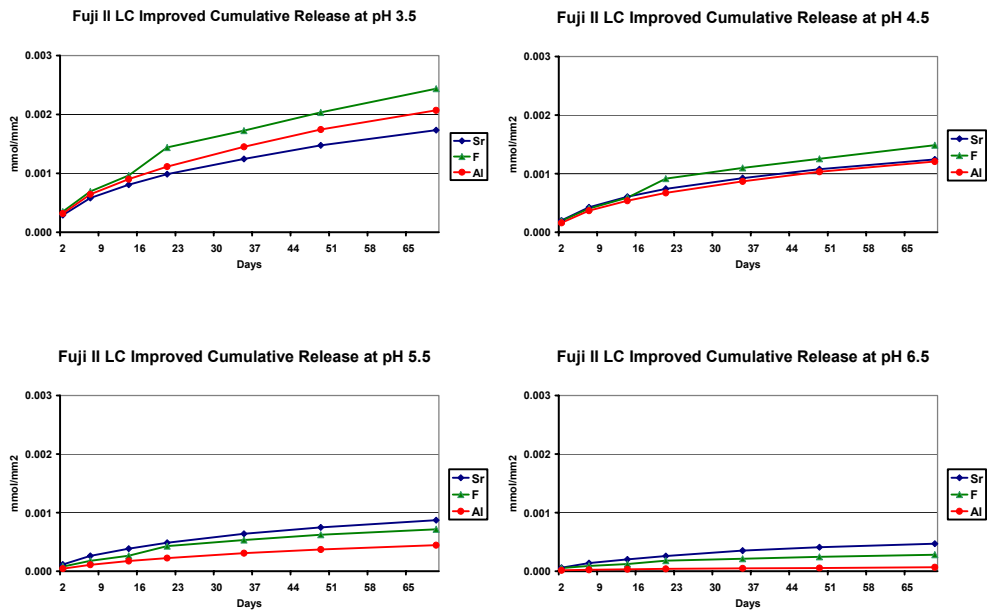


Figure 28: Fuji II LC Improved, relative cumulative release of Sr, F and Al at different pH

4.3.4 Cumulative release for high strength restorative materials

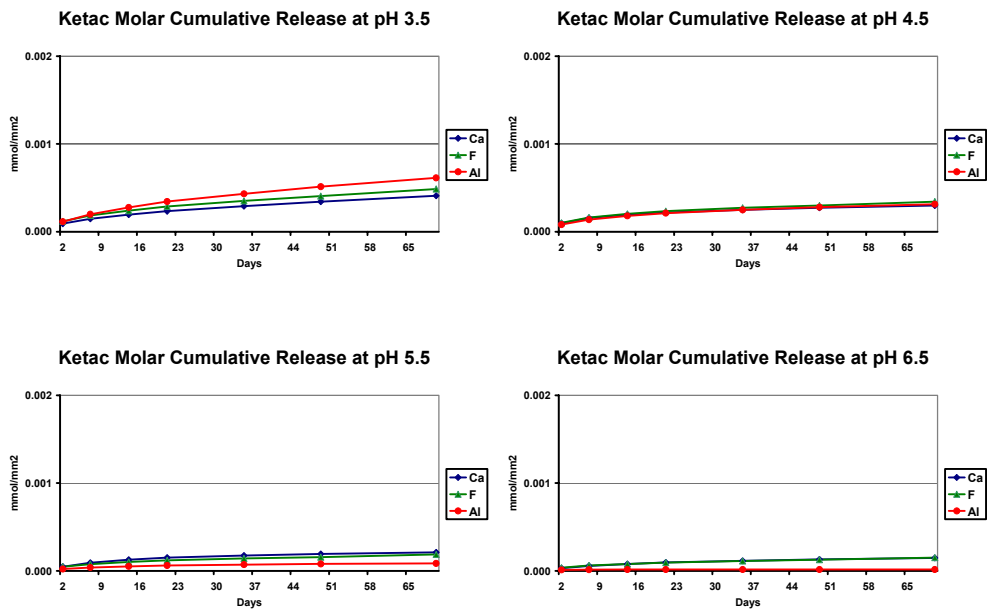


Figure 29: Ketac Molar, relative cumulative release of Ca, F and Al at different pH

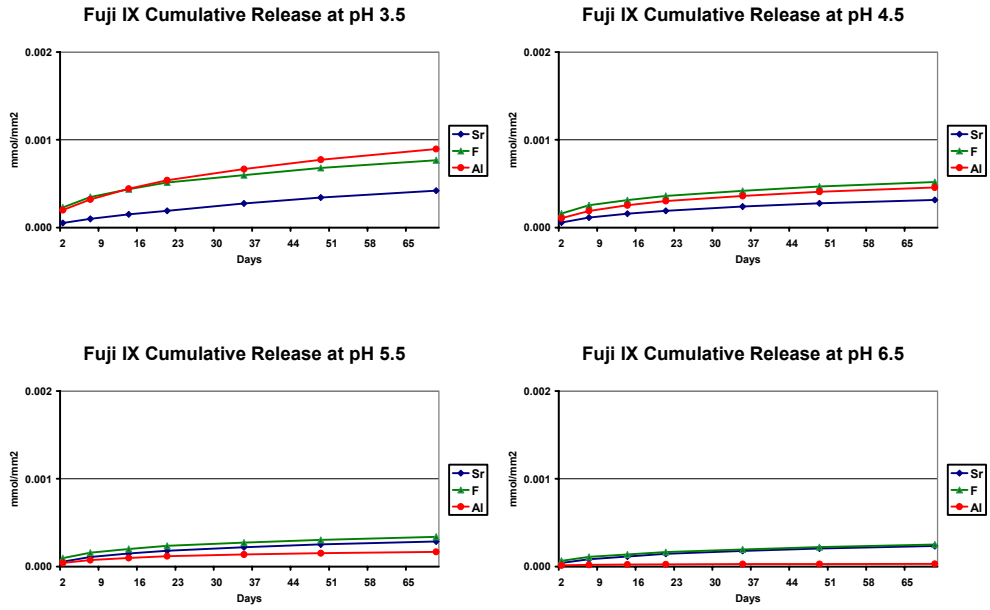


Figure 30: Fuji IXGP, relative cumulative release of Sr, F and Al at different pH

4.3.5 Comparative Ca/Sr, F, Al release in eight materials

As discussed in the introduction, Fuji IXGP, Fuji II, Fuji IILC Improved and Ketac Fil Plus contain Sr based glasses whereas Fuji IIF, Ketac Molar, Ketac Bond and Ketac Cem contain Ca based glasses. In the following section, the results will be presented as a comparison for the different elements at the four levels of pH tested.

4.3.5.1 Calcium

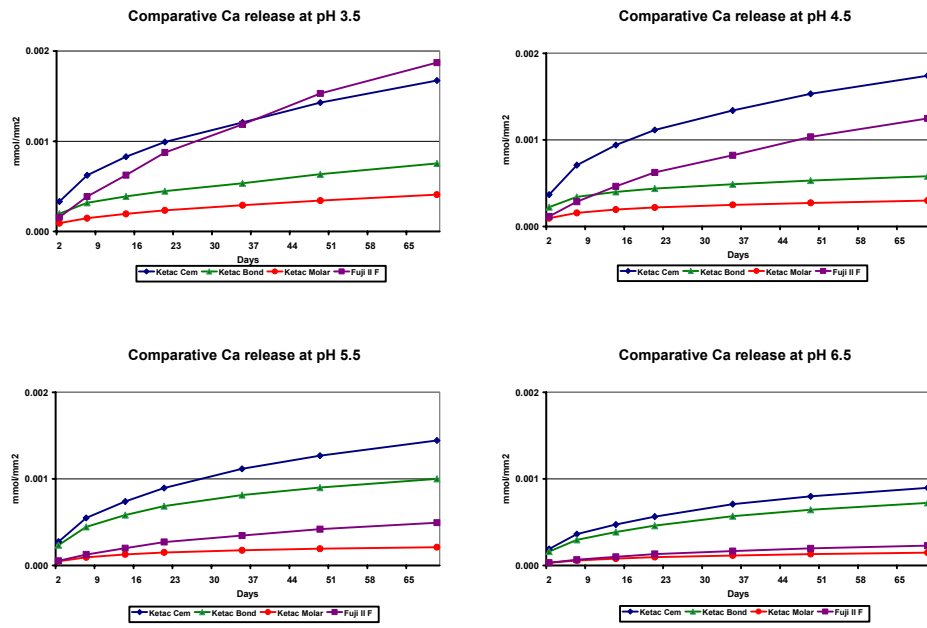


Figure 31: Comparative calcium release at different pH

4.3.5.2 Strontium

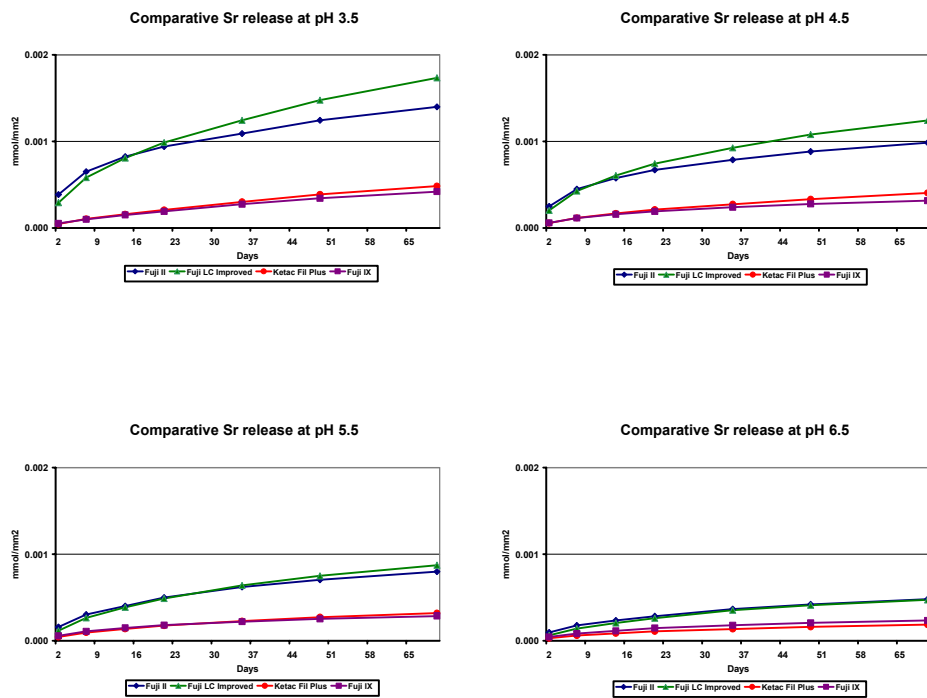
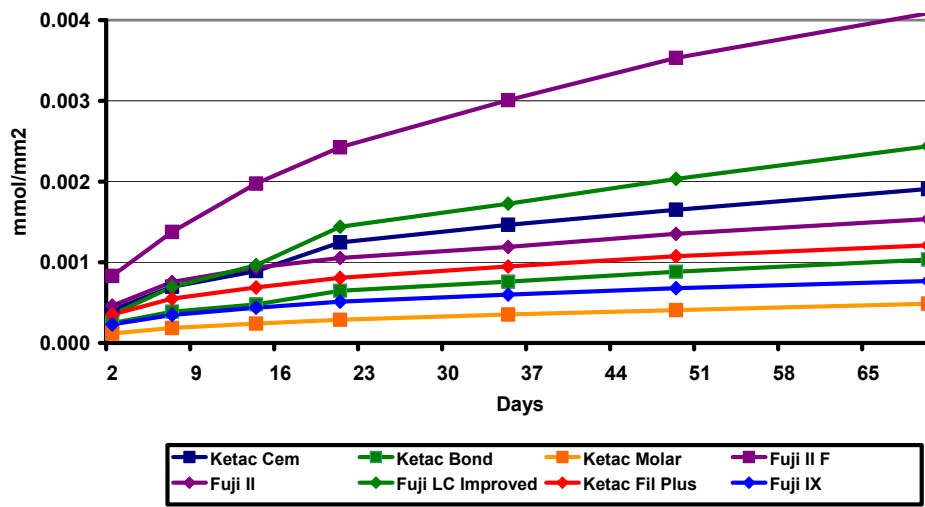


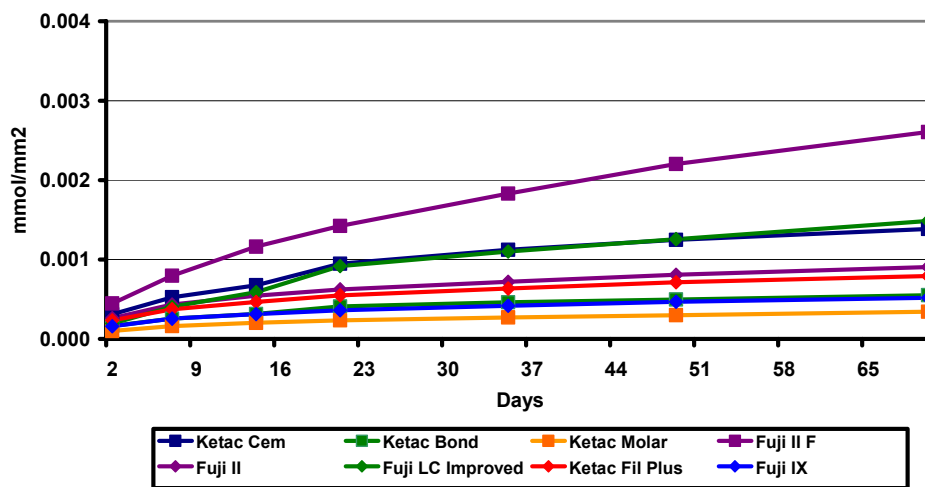
Figure 32: Comparative strontium release at different pH

4.3.5.3 Fluoride

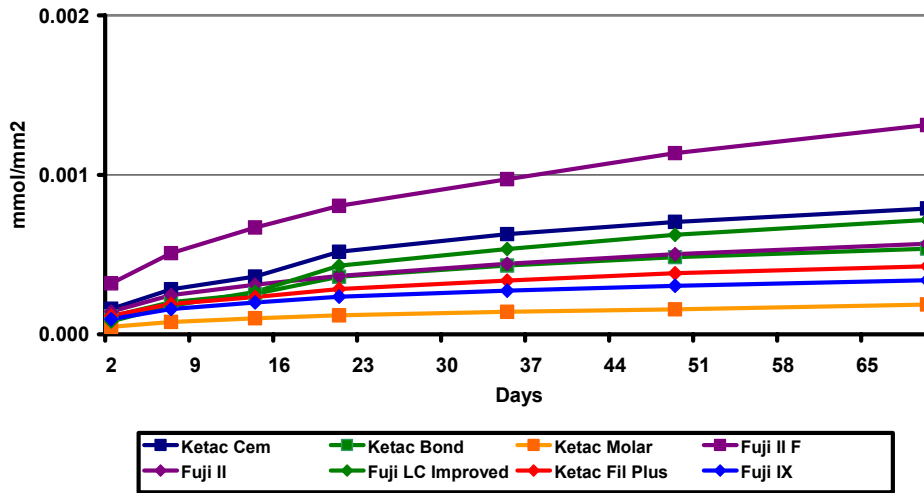
Comparative F release at pH 3.5



Comparative F release at pH 4.5



Comparative F release at pH 5.5



Comparative F release at pH 6.5

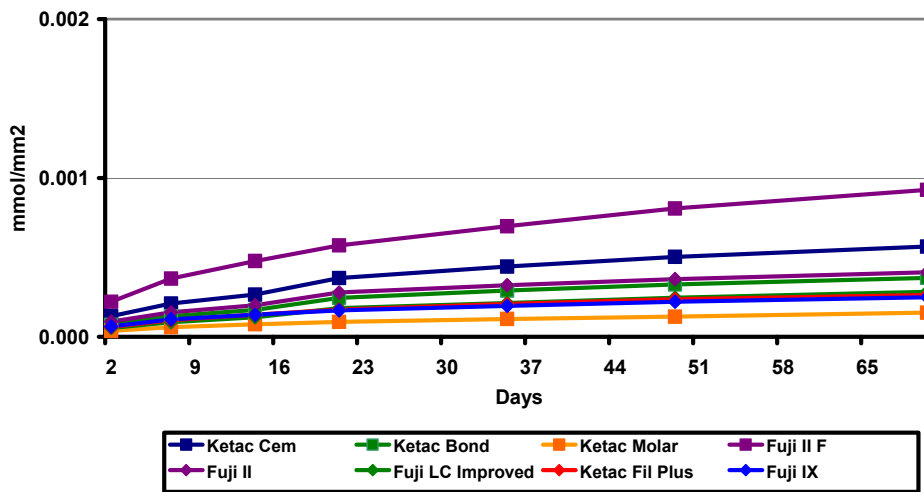
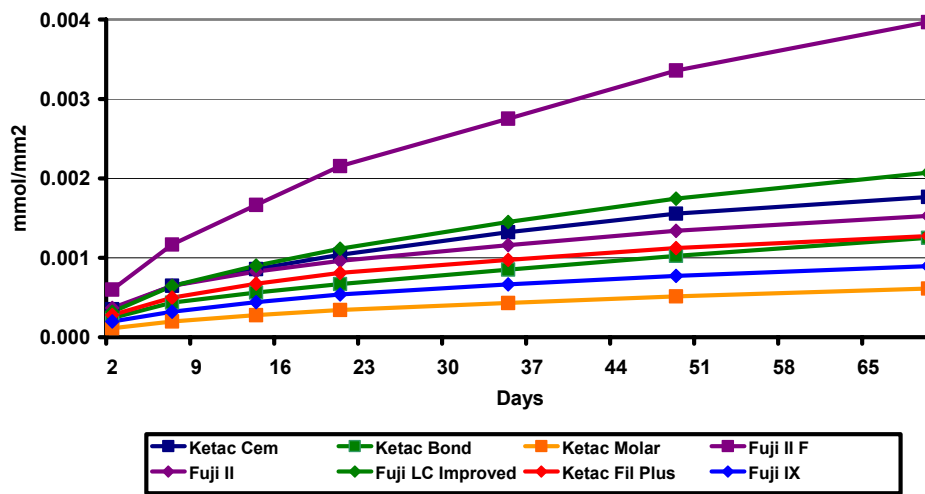


Figure 33: Comparative fluoride release at different pH

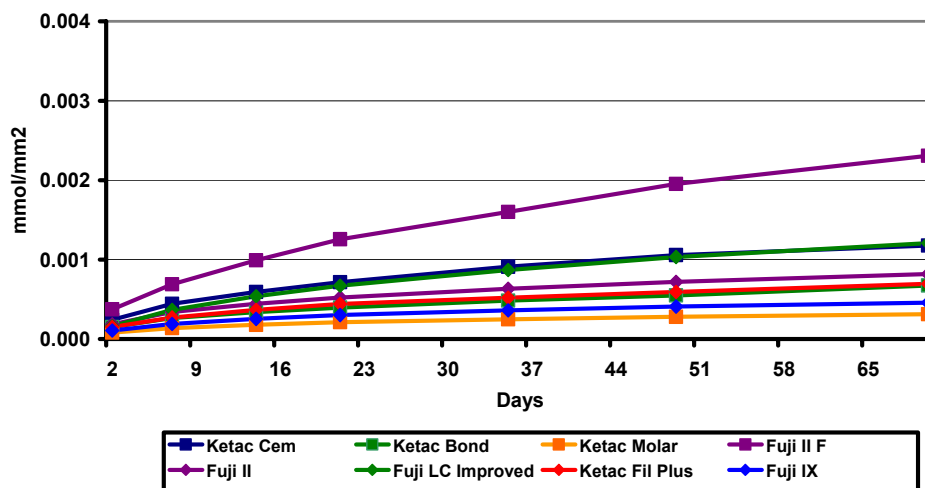
(NB: different y axis scales at pH 3.5 and 4.5 because of high release)

4.3.5.4 Aluminium

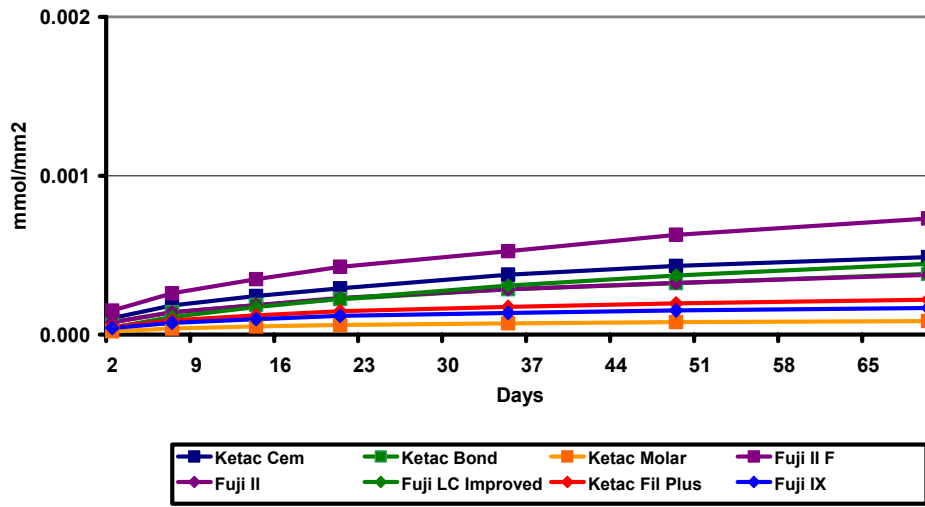
Comparative Al release at pH 3.5



Comparative Al release at pH 4.5



Comparative Al release at pH 5.5



Comparative Al release at pH 6.5

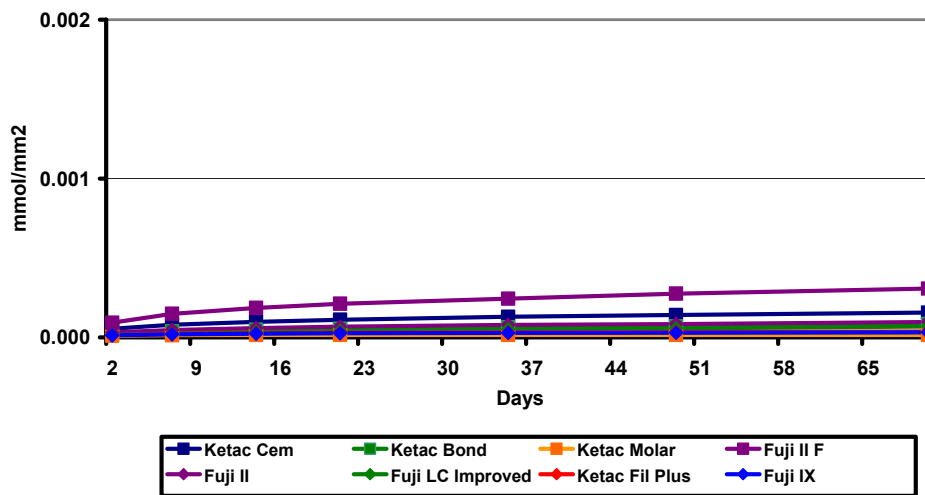
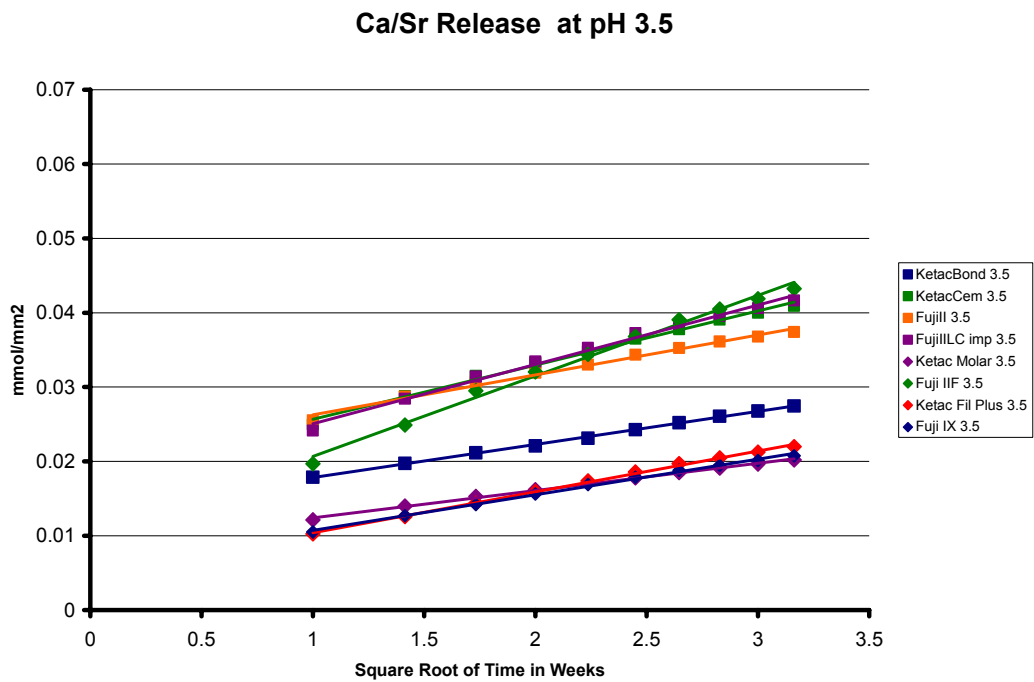


Figure 34: Comparative aluminium release at different pH
 (NB: different y axis scales at pH 3.5 and 4.5 because of high release)

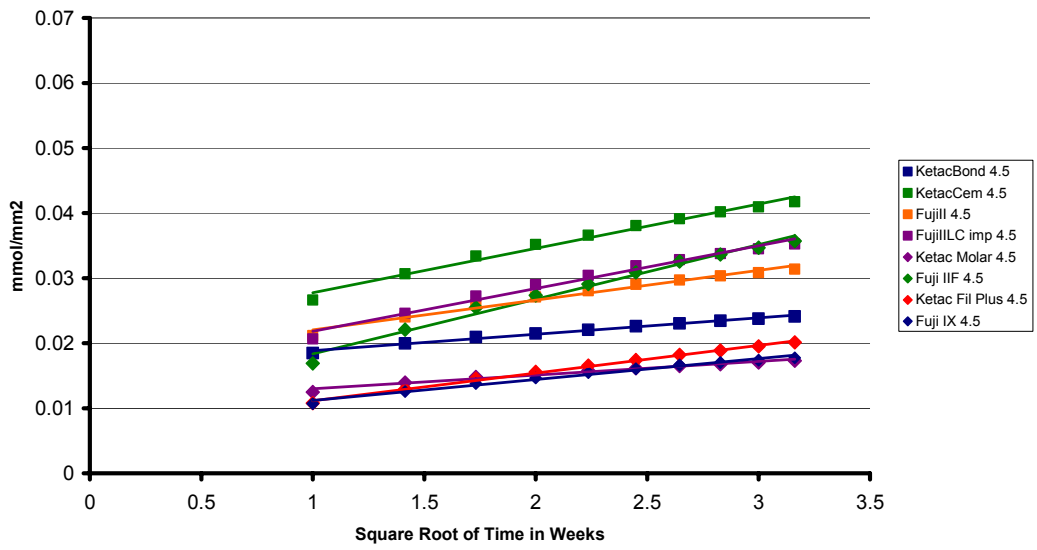
4.3.6 Diffusion based characteristics of each material

In order to analyse the diffusion based characteristics of the three elements in each glass-ionomer, the cumulative concentrations released need to be charted against the square root of time. By charting concentrations of elements released as mM/mm^2 against the square root of time in weeks, a direct comparison of the release level of the different elements can be compared between glass-ionomers. The release of calcium or strontium are presented below.

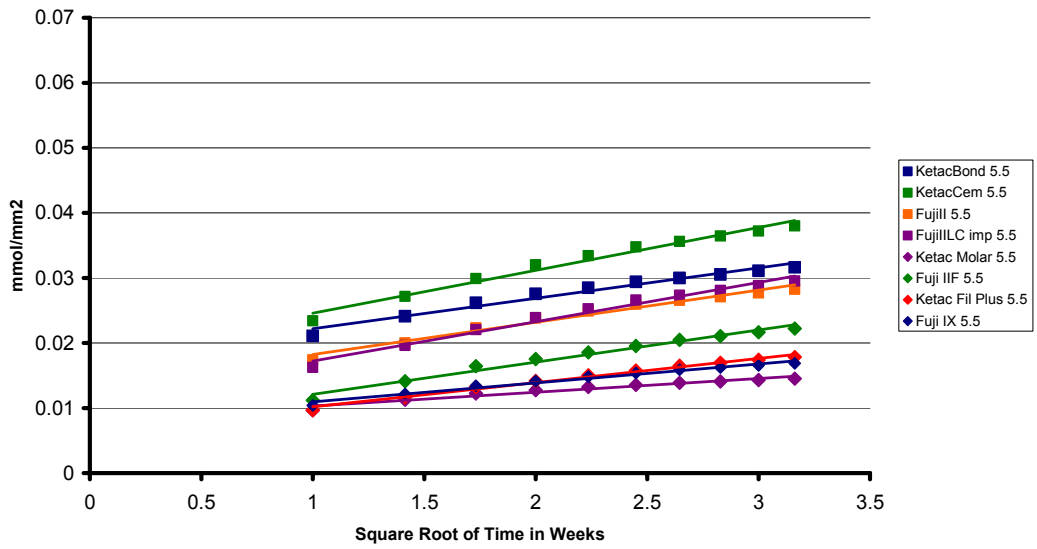
4.3.6.1 Calcium/Strontium



Ca/Sr Release at pH 4.5



Ca/Sr Release at pH 5.5



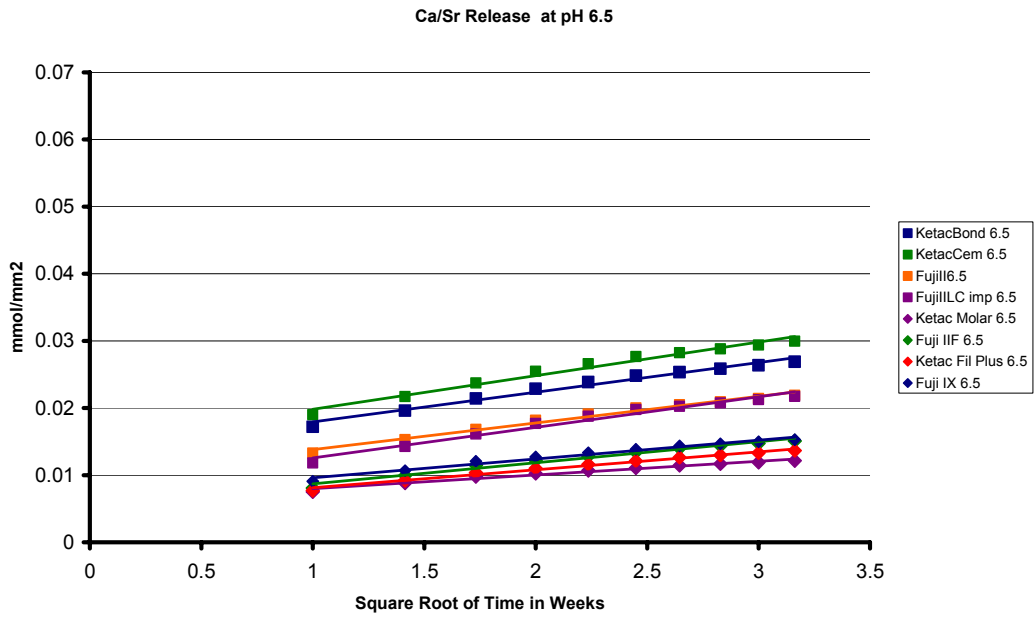
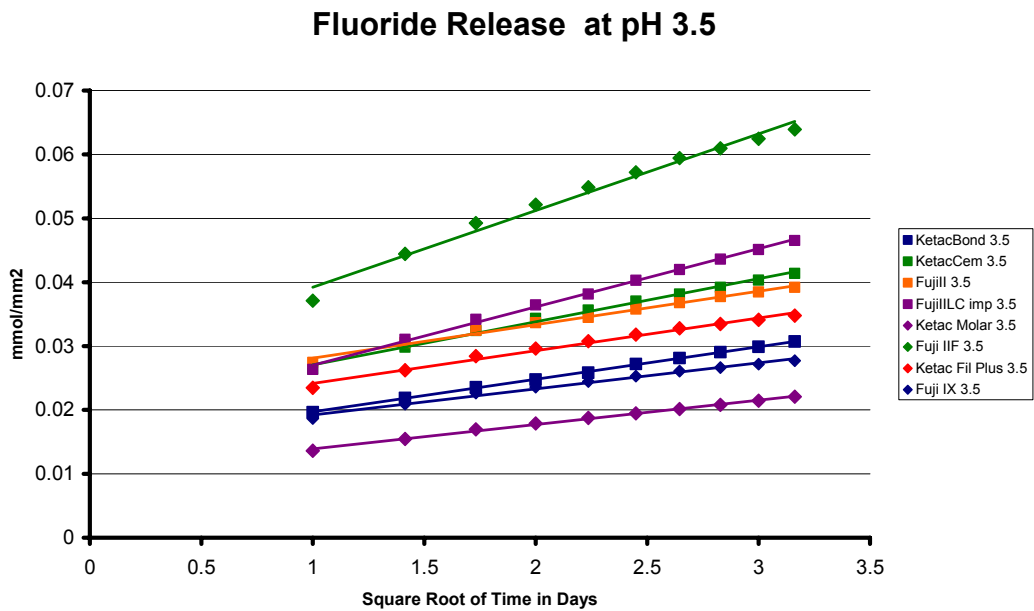
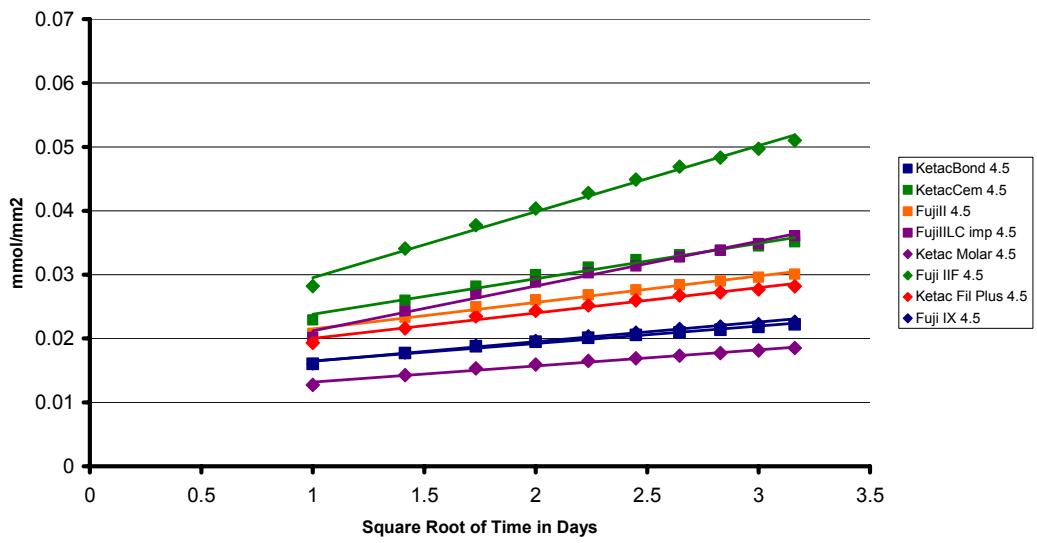


Figure 35: Comparative diffusion characteristics for Ca/Sr release at different pH

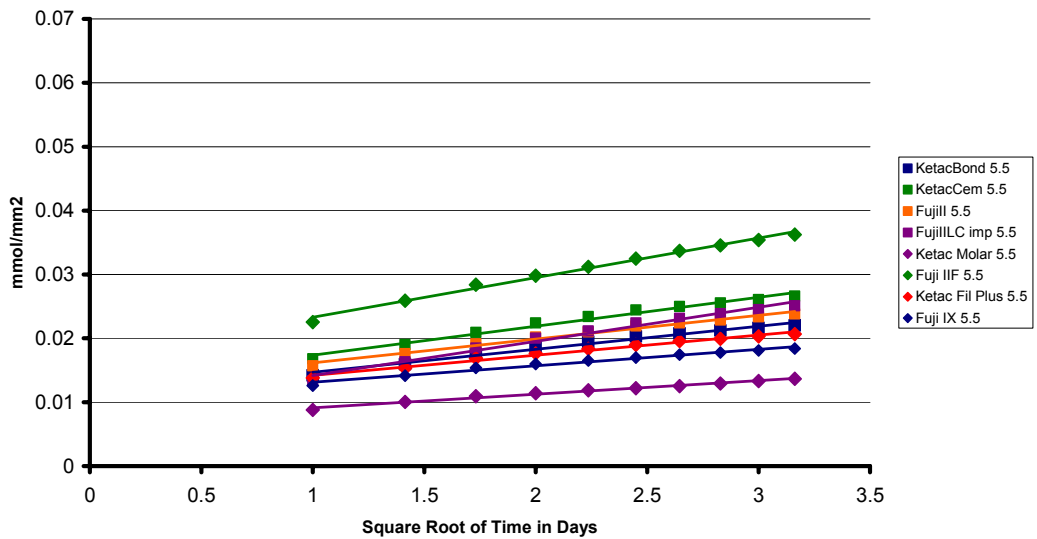
4.3.6.2 Fluoride



Fluoride Release at pH 4.5



Fluoride Release at pH 5.5



Fluoride Release at pH 6.5

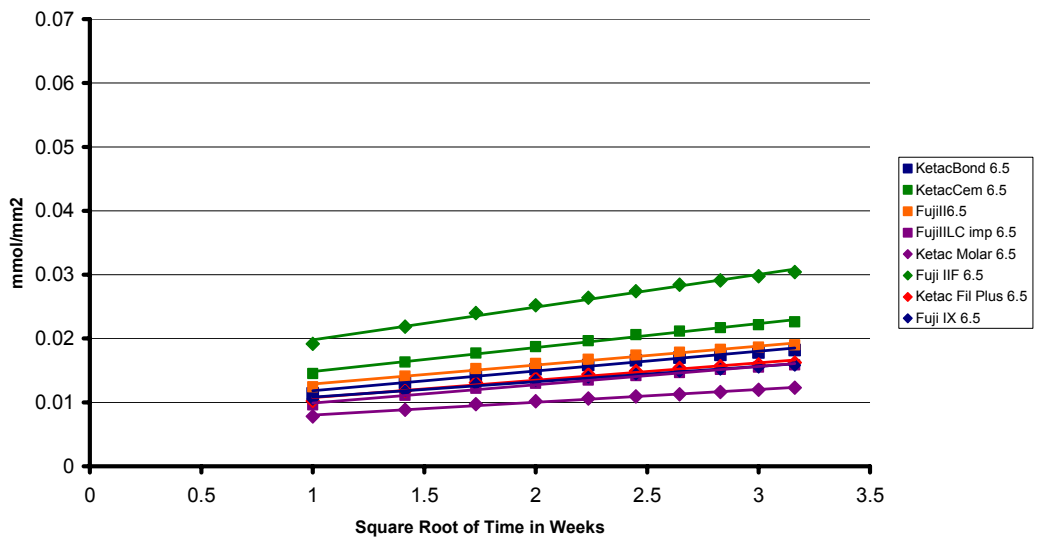
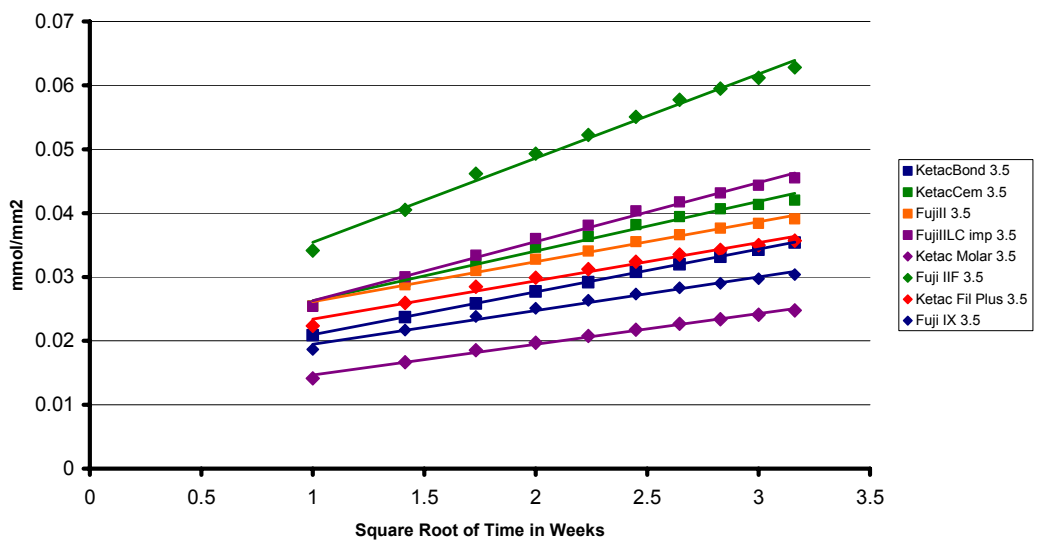


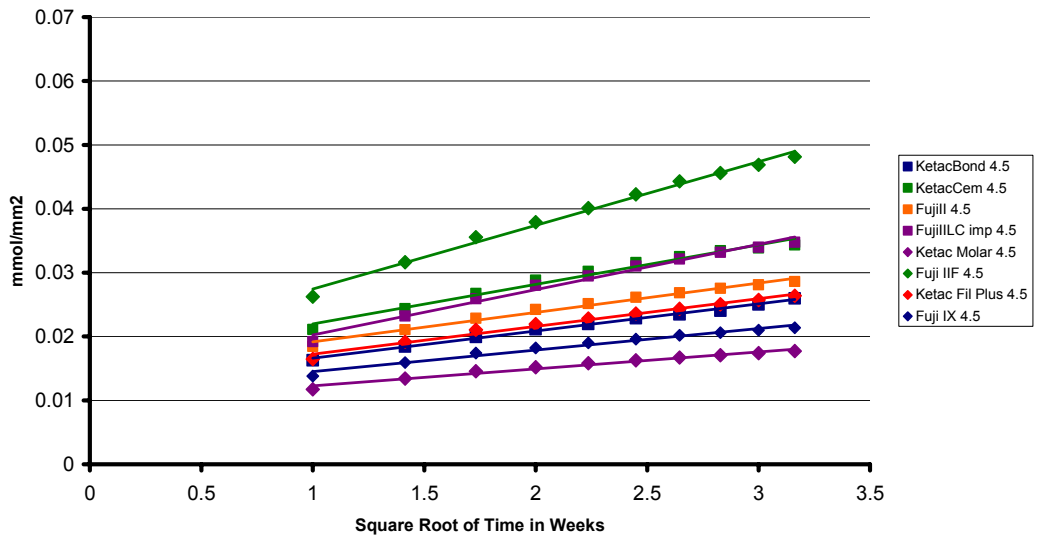
Figure 36: Comparative diffusion characteristics for F release at different pH

4.3.6.3 Aluminium

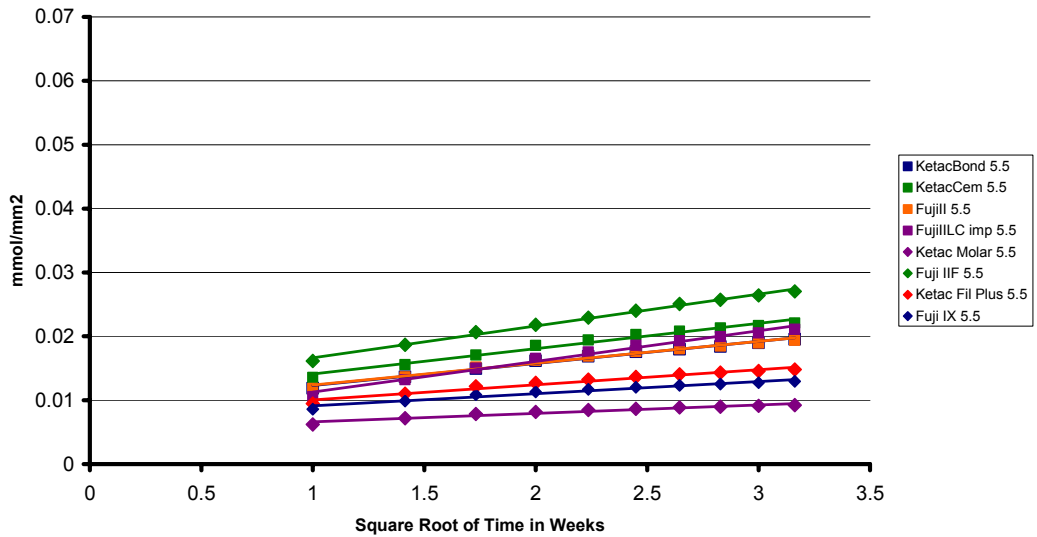
Aluminum Release at pH 3.5



Aluminum Release at pH 4.5



Aluminum Release at pH 5.5



Aluminum Release at pH 6.5

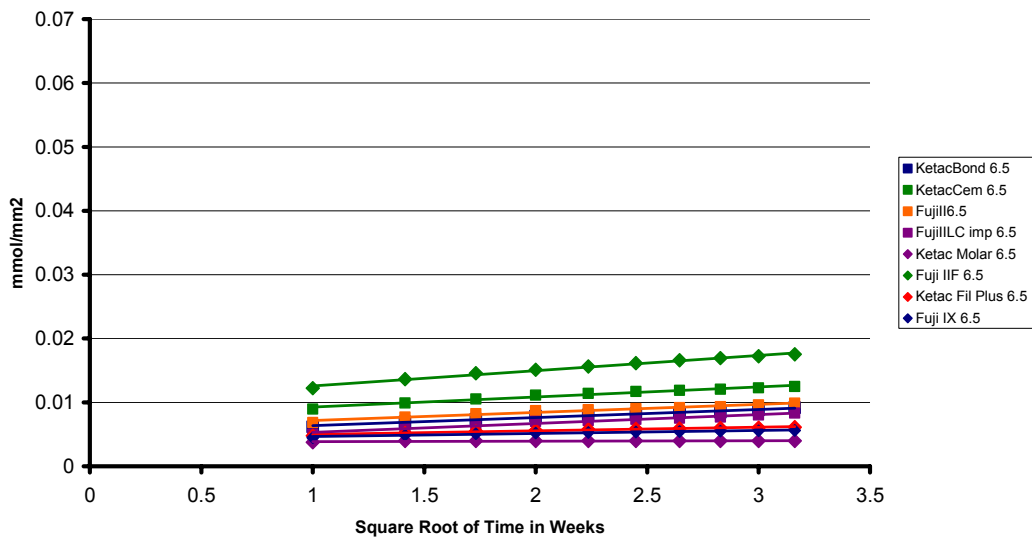


Figure 37: Comparative diffusion characteristics for Al release at different pH

4.4 Interpretation

4.4.1 General observations

At the time of testing, the materials selected represent a wide range of currently available glass-ionomer products. They can be broadly divided into two groups based on the composition of the glass; one group is based on calcium, while the other, on strontium. One material, Fuji IIF (GC Corporation, Tokyo, Japan) was a high fluoride releasing restorative glass-ionomer. Even though it is not available anymore, Forsten showed that after an initial burst effect of fluoride release the flow gradually decreased and after some months, settled to a constant level (Forsten 1990). This observation has been confirmed and the data was retained to enable comparisons to be made between the present study and those from previous studies.

It is interesting to note that the release of all ions tested was still continuing for most materials between forty eight and seventy days, the rate being relatively higher at acidic pH levels.

4.4.2 Significance of the elements selected for analysis

Many *in vitro* and *in vivo* studies have examined the release of fluoride and other ions from glass-ionomers and the effects of this release on plaque and bacteria (Forss, Jokinen et al. 1991; Friedl, Schmalz et al. 1997). It has been assumed that fluoride is the active agent that is mainly responsible for the observed caries inhibition and remineralising properties of glass-ionomers. These results indicate that on a molecular basis, other ions are released in comparative concentration and the release of calcium and strontium also plays an important role on the remineralisation of adjacent dental hard tissues.

4.4.3 Comparison of profiles of ions released between product categories

Within the lining and luting materials tested, release rates for all elements tested were similar with the exception of Ketac Cem where there was a greater level of release of all ions in comparison with Ketac Bond at pH 3.5. This could be explained by the much higher powder to liquid ratio of Ketac Bond (3:1) to that of Ketac Cem (2:1).

As described above, the rate of release of all elements from Fuji IIF was substantially higher than from the more modern materials. That from Ketac Fil Plus was lower than for Fuji II and was similar to that from the more viscous, high strength glass-ionomers, Ketac Molar at all pH levels tested, and to that in Fuji II LC at higher pH levels. The high release from Fuji IIF could be due to a combination of formulation of the glass, the surface treatment of the powder and its resulting reactivity and a low powder to liquid ratio (1.8:1).

4.4.4 Comparison between release profiles at different pH levels

Whilst the rate of ionic release is known to be higher at acidic pH levels for most glass-ionomers tested, the high concentrations of Al released at acidic pH for most of the products was of concern. Whether this is due to dissolution of glass components or from diffusion of loosely bound products will be discussed later. These levels were matched by

Ca or Sr profiles, which again matched those from F, in molar terms, in many cases. The levels of mineral loss are even more surprising when it is considered that they are released against a gradient of calcium within the eluant solution which was designed to be just greater than within normal saliva. In many former studies, these have been released into DDW (Forsten 1990; Horsted Bindslev and Larsen 1990; Forsten 1991; Hatibovic-Kofman and Koch 1991; Hattab, el Mowafy et al. 1991; Horsted Bindslev and Larsen 1991; Forsten 1995; Francci, Deaton et al. 1999), where the level of release might be expected to be high. These data indicate that there are many ionic products being released other than F, and the role of these in caries inhibition and remineralisation need to be more fully analysed.

4.4.5 Consideration of the mechanism of release

The mechanism of ionic release from glass-ionomer is not fully understood. Analysis of the release profiles provides some evidence of mainly a diffusion process, though particularly at acidic pH levels and in eluants with low ionic content, e.g: DDW, a process of dissolution may precede diffusion. Other factors need to be considered, such as ionic load and type within the eluting medium, and whether there is sufficient volume of eluting medium to not become saturated with eluted products during the time of continuous exposure. Also to be considered are temperature and level of agitation of the eluting solutions.

In this study, the eluting solution contained a concentration of calcium and phosphate ion intended to be slightly in excess of that found in saliva. As described previously, this did not appear to inhibit relatively high profiles of cumulative and sustained release of Ca or Sr. All samples were agitated and maintained at constant temperature. The volumes of eluant should have been adequate to maintain a hypotonic eluant concentration for each ion during the short term exposures. Whether this was adequate for the longer term periods, when release rate had declined, is not known, particularly in low pH solutions. If not, the

results would be less than optimum and thus an underestimation of the real potential for their release.

4.4.6 A preliminary analysis for evidence of diffusion

Diffusion phenomena play a significant role in the caries process, as described by Featherstone et al. (Featherstone, McIntyre et al. 1987). That paper describes how diffusion is evidenced by a straight line response between accumulated depths of demineralisation against square root of time. The analysis of some of the present data in terms of cumulated amount of ionic material released against square root of time (**Figure 35, Figure 36, Figure 37**) showed some interesting results. In most cases analysed, the data closely followed a straight line of best fit, which might be considered as indicating mainly a diffusion mechanism of release. As might be expected, the rates of diffusion varied for each ion between glass-ionomers and at differing pH levels as indicated by the slopes of the lines. The only variations were within the first few sets of data, and these need more intense investigation. Whether these results exclude an element of dissolution at a regular rate is not known.

An interesting observation may be made from these results. The rate of diffusion of calcium ions from Ketac Bond appeared to be resistant to pH change. Otherwise a consistent hierarchy of ionic loss between different glass-ionomers was evident, with that for the modern glass-ionomers and resin modified glass-ionomer appearing less than for the luting cements. As might be expected, the Fuji IIF had the highest level of fluoride release of the glass-ionomers tested.

4.4.7 Significance of the results

There has developed a belief that the more F is released from a glass-ionomer, the more effective it is as a restorative material due to the anti caries effect. However, if there is a

significant loss of Al, and of Ca or Sr at the same time, this may not be so desirable. This would be particularly so if loss of ions resulted from dissolution of material which might contribute to structural integrity of the glass-ionomer. These data indicate the need for a very thorough investigation of this release process, and determination of its relative benefits.

Chapter 5: Initial studies to investigate the ionic transfer from Fuji IXGP into demineralised dentine *in vivo* and *in vitro* and into sound dentine

The three series of experiments in this chapter were designed to answer the following questions:

1. Under clinical conditions, do ions which assist the formation of apatite such as strontium and fluorine cross from glass-ionomer into carious dentine?
2. Can a valid *in vitro* model be set up to simulate the *in vivo* situation?
3. In the laboratory, do strontium and fluorine cross from glass-ionomer into sound dentine?

5.1 Fuji IXGP and demineralised dentine *in vivo*

5.1.1 Introduction

The success of the ART method of placing restorations in cavities following removal of all softened dentine to a point where the patient begins to sense pain, relies on the remineralisation of remaining soft dentine through contact with the glass ionomer restoration. The mechanism whereby the remineralisation occurs is currently under investigation. It was suggested that the ability of glass ionomer cements to release fluoride to adjacent tissues would likely be the main contributor to this remineralisation. However, earlier studies in this laboratory have suggested that there may be other factors contributing to the remineralisation of the carious dentine at the base of the cavity.

The objective of this experiment was to determine whether evidence of remineralisation could be achieved following an *in vivo* placement of ART restorations, and if so, to determine the nature of ionic transfers from glass-ionomer which may have contributed to remineralisation.

5.1.2 Materials and Methods

5.1.2.1 General organisation of the in vivo study

As this was designed as a clinical trial, it was necessary to find a source of teeth which were carious and needed to be extracted for the benefit of the patient. At the time, a colleague had been seconded to the Dental School of the Department of Medicine, Colonial War Memorial Hospital, Suva, Fiji. He was assisting in the introduction of a new curriculum and the development of a full Bachelor of Dental Surgery course of training for the University of the South Pacific. He was aware of a series of patients in the age range from 12 years to 16 years who had already had two or more of their first molars extracted because of rampant caries and it was apparent that the loss of the remaining carious first molars would, in fact, offer some level of balance in their occlusion. A proposal was placed before the Department of Health, Government of Fiji, requesting permission to approach young people, and their parents, who were due to have such serial extractions carried out, to ask if they would be willing to have the carious teeth due for extraction, restored initially using the A.R.T. technique. Permission was granted by the Government of Fiji, and Ethical approval was also granted by the Committee for the Ethics of Human Experimentation, The University of Adelaide, South Australia.

A clear description of the proposed action was provided in writing to each patient and their parents, and their consent was also obtained in writing. The designated staff member carried out the A.R.T. restorations, abiding strictly by the methods outlined by the WHO for this technique to be most effective (Frencken, Pilot et al. 1996). A total of 13 subjects volunteered, and the restorations were placed using Fuji IXGP (GC International Corp., Tokyo, Japan) as the restorative material. This is an encapsulated glass-ionomer which contains a strontium glass to enhance radiopacity rather than the conventional calcium glass. An incidental advantage of the presence of strontium is that it has been shown to be universally present in whole enamel (Curzon and Losee 1977). As an element, it has close

similarity to calcium in both chemical and physical properties, it has a similar ionic radius and valence to that of calcium ($\text{Sr}^{2+} = 1.13\text{\AA}$, $\text{Ca}^{2+} = 0.99\text{\AA}$), so it can replace calcium without disrupting the structure of hydroxyapatite (Curzon 1983). This suggests that calcium lost from dentine during development of the caries lesion should be able to be replaced with strontium from glass-ionomer in the healing process and that this replacement should be able to be traced using EPMA techniques.

5.1.2.2 Collection of the ART restored teeth

The protocol for the experiment involved extraction of the series of teeth over a period between one to three months following restoration placement. In all thirteen teeth were harvested over this period. Immediately following extraction the teeth were preserved in 2% glutaraldehyde until they could be prepared for EPMA analysis.

5.1.2.3 Preparation of the teeth for EPMA

Each tooth was sectioned mesio-distally through the centre of the glass-ionomer restoration, as described previously in Chapter 3, (**Figure 38**). To minimise shrinkage the specimens were then dehydrated using a series of solutions with decreasing concentrations of alcohol as previously described (Perdigao and Swift 1994). The specimens were embedded in epoxy resin (Adelaide Epoxy Supplies, Adelaide, Australia), plano-parallel specimens were prepared then polished progressively down to a 0.3 μm diamond grit (Struers, Copenhagen, Denmark), before coating with carbon (**Figure 39**).

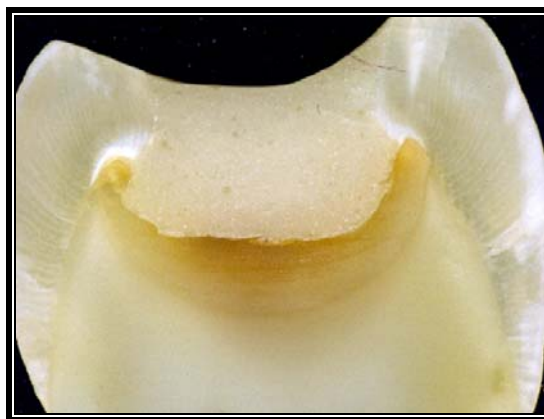


Figure 38: A sample immediately after sectioning, showing the extent of demineralised dentine left under the glass-ionomer restoration

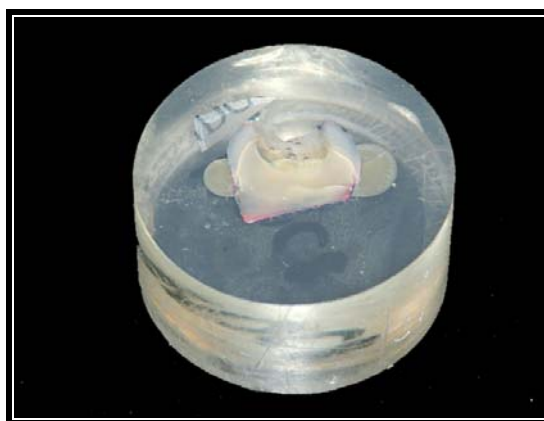


Figure 39: Sample ready for coating with carbon before EPMA and SEM

5.1.2.4 EPMA method

The electron probe microanalysis (EPMA) was carried out using a Cameca SX51 microanalyser (Cameca, Corbevoie, France) set at 15kV and 20 mA, with a beam diameter of 1000 Å, running in wavelength dispersive spectrometry (WDS) mode and a collection time of ten seconds at each point. Calibration for the EPMA used a minerals mount MINM25-53 (Astimex Scientific, Toronto, Canada), with apatite, fluorite and celestite used as standards to calibrate Ca and P, F and Sr respectively. The calculated minimum detection limits (MDL) are listed in **Table 4**. A programmed spot analysis for calcium, phosphorus, fluorine and strontium was performed along a line perpendicular to the glass-

ionomer and dentine interface at 5 μm intervals, reaching into sound dentine. Data was collected from several regions in each sample and a set of three lines was performed for each region (Ngo, Ruben et al. 1997). An average was calculated from the three lines to represent the mineral profile for that region of analysis.

	Calibration levels (weight %)	Minimum Detection Limit (weight %)
Ca	39.85	0.05
P	18.50	0.12
F	48.67	0.05
Sr	47.52	0.05

Table 4: Concentrations found in the standard used for calibration and Minimum Detection Limits for the elements of interest.

5.1.2.5 SEM analysis

A Philips XL30 field emission scanning electron microscope (Philips, Eindhoven, The Netherlands) set at 10kV with a spot size of 3 μm and operating in back scattered mode was used to highlight the overall mineral distribution in the samples. The SEM micrographs were used together with the mineral profiles derived from EPMA to determine the average depth of the lesions and the depth of penetration for Sr and F as shown in **Table 5**.

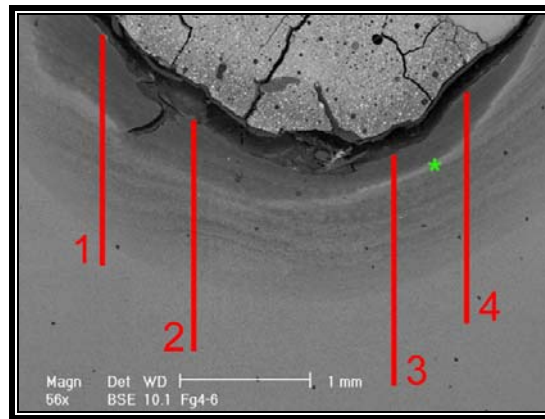


Figure 40: For this sample, EPMA was carried out in four separate regions, marked by the four red lines. The green star shows a region with high mineral content, Ca, P and Sr. This is the same sample shown in Figure 38.

5.1.3 Results

The results from the EPMA are presented as mineral profiles (**Figure 41**). This is the analysis of the sample previously shown in **Figure 38** and **Figure 40**. The horizontal axis represents distance from the interface into dentine expressed in μm , with the interface being on the left side of the chart. The concentrations of the elements are shown on the vertical axes, where the weight percentages for calcium and phosphorous are shown on the left vertical axis (0 - 40%) and those for fluorine and strontium are shown on the right vertical axis (0 -7%).

Figure 41 and **Figure 42** show typical profiles of Sr and F, found in a large and a small lesion in carious dentine. These profiles can be roughly divided in to three distinct zones, namely:

- A. Adjacent to the glass-ionomer restoration. This area is heavily demineralised with the levels of Ca and P being close to or below 10 weight% in comparison to normal dentine which is approximately 30 weight%
- B. The transition zone between zone A and zone C, C being sound dentine
- C. Sound dentine, with level of calcium approximately above 30 weight%

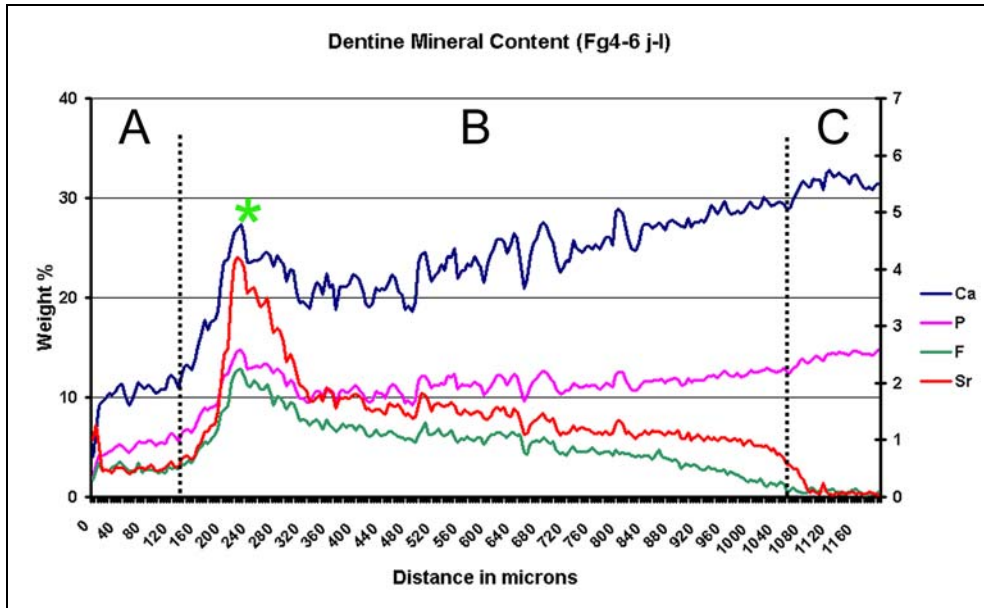


Figure 41: Typical mineral profiles found in carious dentine, in a large lesion, adjacent to the glass-ionomer restoration. Ca and P are charted on the left hand scale. F and Sr are charted on the right hand scale.

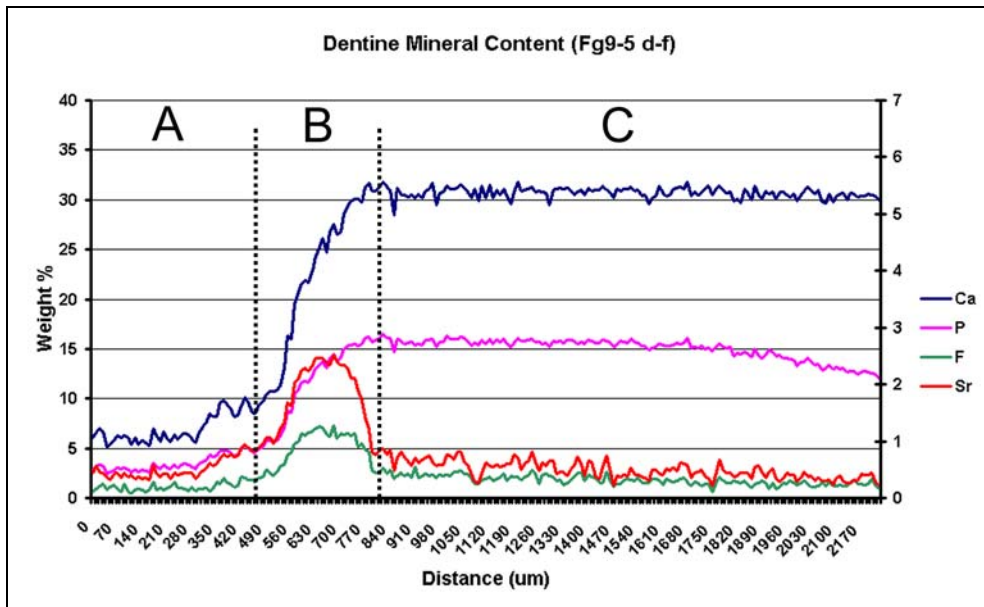


Figure 42: Typical mineral profiles found in a small carious lesion in dentine, adjacent to a glass-ionomer restoration.

Table 5 shows the average depth of carious dentine found in each of the thirteen samples and the depth of penetration of both Sr and F into both zone A and B. It is evident that the penetration of these two elements finishes where zone C starts. This observation is confirmed by the strong correlation coefficient between the depth of carious dentine and the depth of penetration of Sr ($r = .98$, significant at 0.01 level). When the depth of penetration of fluorine is compared with the depth of carious dentine, the correlation is again significant ($r = .95$, significant at 0.01 level).

Sample ID	Ave. depth of carious dentine in μm (SD)	Ave. depth of penetration of Sr in μm (SD)	Ave. depth of penetration of F in μm (SD)
1	1178 (101)	1160 (104)	1056 (164)
2	900 (218)	940 (298)	577 (125)
3	350 (71)	350 (71)	350 (71)
4	300 (141)	400 (141)	350 (212)
5	100 (0)	150 (0)	50 (0)
6	1735 (78)	1645 (120)	1515 (191)
7	1210 (241)	1380 (85)	1105 (148)
8	845 (92)	875 (35)	830 (56)
9	707 (192)	700 (201)	577(172)
10	790 (497)	917 (578)	723 (441)
11	550(14)	540 (28)	375 (70)
12	497 (199)	467 (179)	487 (179)
13	905 (205)	1105 (233)	1120 (212)
Mean	774(121)	818(121)	701(113)

Table 5: Average depth of carious dentine and average depth of penetration of Sr and F.

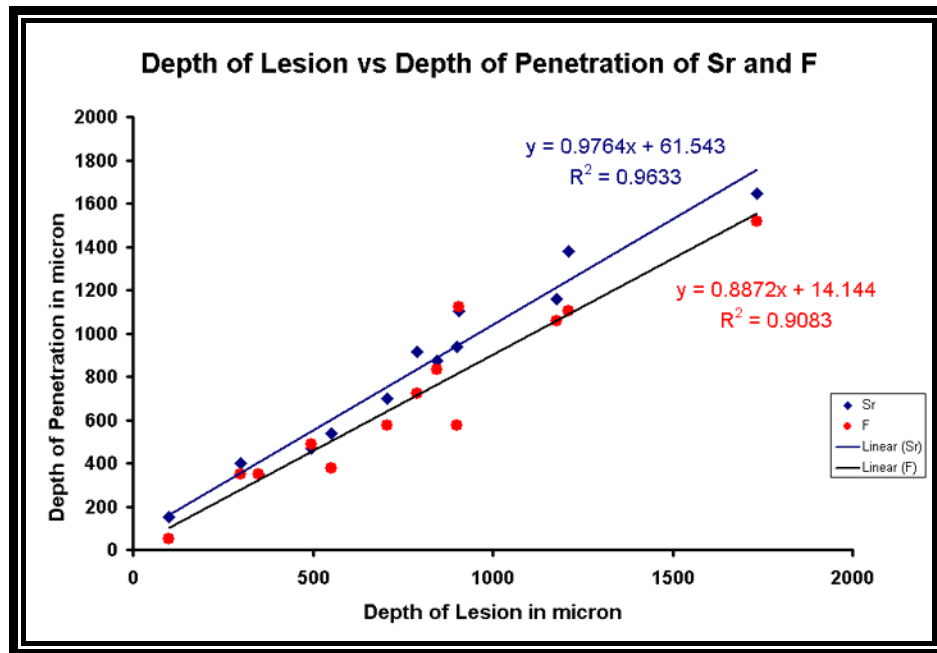


Figure 43: Depth of lesion and depth of penetration of Sr and F found in the thirteen samples.

Table 6 shows that there is a strong correlation between the level of the ΔSr and ΔF , especially in zone B.

	Zone A	Zone B	Zone C
Large lesion Figure 41	- 0.13	0.93*	0.28
Small lesion Figure 42	0.82*	0.97*	0.84*

Table 6: Correlation coefficient for the levels of strontium and fluorine in the three zones A, B and C. (* significant at 0.01 level)

All specimens were examined using SEM in back scattered electron (BSE) mode to highlight the overall mineral distribution of the sample and also to measure the depth of the demineralised area, zones A and B.

The green star in **Figure 40** corresponds to a thin bright band, which is due to a higher level of mineral as well as the presence of Sr which has a higher atomic number. This zone of elevated mineral content was quantitatively confirmed in **Figure 41**.

5.1.4 Interpretation

The objective in these analyses was to determine the level of ion exchange between glass-ionomer and partially demineralised dentine and to determine whether this exchange might increase the potential for remineralisation.

As stated previously, Fuji IXGP releases both fluorine and strontium. This means that there will be strontium ions available rather than calcium, so for the purposes of this experiment, any possible remineralisation will occur through deposition of strontium. In fact, this study showed that a substantial amount of both strontium and fluorine crossed the interface into the partially demineralised dentine adjacent to the restorative material. Any strontium and fluorine above background levels, which were found in these samples, must come from the restorative glass-ionomer because these elements are not normally found at high levels in dental tissues. This observation was confirmed by the low levels of strontium and fluorine recorded by EPMA in sound dentine (**Figure 41** and **Figure 42**).

It is important to consider that the whole remineralisation process might also involve Ca diffusing through from the dentine tubule fluids. Unfortunately it is not possible to measure the contribution of this source of Ca as its concentration could not be measured against unknown original concentrations. One of the limitations of an *in vivo* study of this nature is the lack of controls and the original calcium and phosphorous profiles are unknown.

The presence of strontium and fluorine in the remineralised dentine is most likely controlled by both diffusion and remineralisation. However, observation of the profiles of strontium and fluorine distribution in **Figure 41** and **Figure 42** allows the following general observations to be made:

1. The depth of penetration of the remineralising ions is related to the physical state of the demineralised dentine. The accumulation is greatest in zone B where the concentrations of the two major elements, calcium and phosphorus, vary between 10 and 30 weight % for calcium and 5 and 15 weight % for phosphorus
2. The accumulation of strontium and fluorine ceases in the region of the junction between demineralised (zone B) and sound dentine (zone C). The correlation coefficient between the depth of penetration and the depth of the lesion are highly significant, at 0.98 for strontium and 0.95 for fluorine
3. Both strontium and fluorine accumulated deep into the lesion. For strontium, the mean depth was 818 μ m and the maximum depth was 1645 μ m. The equivalent figures for fluorine were 701 μ m and 1515 μ m
4. There is a clear relationship between the concentration of strontium and fluorine in zone B, for both large ($r=0.93$) and small lesions ($r=0.97$)

It is known that the pH of the liquid component of a glass-ionomer is close to pH 1.0 and that, as the powder is added to the liquid, there will be an ion release from the surface of the powder particles that will include both fluorine and strontium. As the freshly mixed material is placed against a cavity wall there will be a release of ions from the enamel and dentine as well, leading to the exchange of ions which is recognised as the ion exchange adhesion. It has been demonstrated that the same ion exchange can occur in the presence of partially demineralised carious dentine. The ions released from both the cement and the tooth structure will combine to buffer the low pH until such time as it rises to a level where ion activity ceases. During this period of activity there will be both fluorine and strontium ions available to undertake apatitic activity in relation to areas in dentine where calcium ion levels are low with strontium ions replacing the missing calcium ions.

It is suggested that this occurs through a diffusion process driven partly by the concentration gradient, which exists between the glass-ionomer and the dentine with

respect to these two elements. As both strontium and fluorine contribute to apatite formation, they react with the demineralised dentine. If the process is purely controlled by diffusion then one would expect to see the level of strontium and fluorine to be highest at the interface and lowest deep into the sound dentine.

These observations offer support to the original hypothesis. There remains a need to design an *in vitro* model to study the effects of other possible variables such as time of exposure and prior levels of demineralisation.

Remineralisation of demineralised dentine has been demonstrated by various glass-ionomers *in vitro* (Creanor, Awawdeh et al. 1998; Ngo 2002; Ngo, Fraser et al. 2002) and hypermineralised dentine has been reported using an *in situ* model (ten Cate, Buijs et al. 1995). The results from this study demonstrate that at least partial remineralisation is possible in an *in vivo* model.

Findings from this clinical study support the laboratory evidence that glass-ionomer can contribute directly in the remineralisation of carious dentine. However, there are two important requirements for this to happen; firstly the restoration has to provide a total seal to the external environment (Mertz Fairhurst, Curtis et al. 1998) and secondly there is intimate contact between the glass-ionomer and the partly demineralised dentine.

The extent to which the remineralisation from glass-ionomer re-establishes the physical property of carious dentine that had undergone remineralisation could not be determined in this study.

5.2 Development and validation of an *in vitro* model

5.2.1 Introduction

As described in 5.1 above, it was realised that it was not possible to use a human *in vivo* method to analyse the ionic interactions between glass-ionomer and partially demineralised dentine in detail. For this reason, it was decided to develop an *in vitro* model of the ART

method of restoration placement. This method is described below, along with the results of a variety of tests designed to validate this method as closely simulating the *in vivo* process. The main experiments, which will be described in Chapter 6, were designed to assess the effects of two variables on the uptake of strontium and fluorine, the first variable being the remaining level of mineral and the second, the exposure time to glass-ionomer. The artificial lesions were designed with the first variable in mind, so the samples were divided into three groups based on how long the teeth were exposed to the demineralising solution. These periods were 7, 14 and 21 days.

The criteria used to assess the validity of this model are:

- A. The correlation of the mineral profiles found in the areas where the test and control areas would be. The control is only valid if there is a strong correlation between the two
- B. The profiles of strontium and fluorine collected from the *in vitro* model, have similar features with those found in the *in vivo* study

5.2.2 Materials and methods

5.2.2.1 General descriptions

The following is a summary of the steps taken in producing the artificial lesions and the preparation for EPMA. The methodologies described below are used in the experiments described in Chapters 5 and 6.

5.2.2.1.1 Preparation of artificial carious dentine lesions

Thirty five freshly extracted third molars with caries free surfaces were collected and stored in 0.5% chloramine solution at 4°C until used. Immediately before the experiment, these teeth were cleaned and immersed in de-ionised water in an ultrasonic bath for fifteen minutes before being air dried. A cavity of approximately 5 mm in diameter was prepared, using an air turbine and 100 µm grit diamond burs (Komet, Lemgo, Germany) to a depth

of approximately half way through the coronal dentine. The roots of the teeth were removed and the crown covered with acid resistant nail varnish except for the area of the cavity (**Figure 44**).

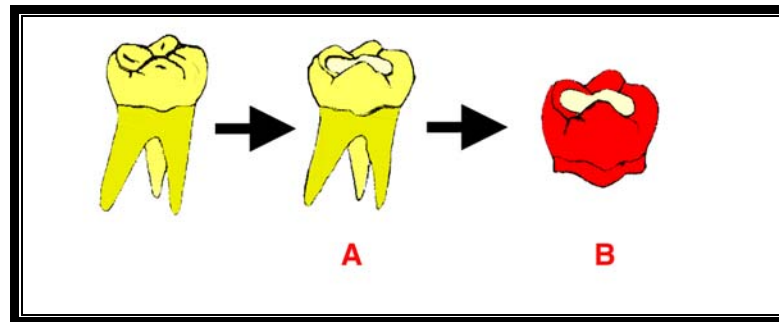


Figure 44: The first two steps in the preparation of the *in vitro* model

A: A cavity was prepared using a diamond bur

B: The crown was then covered with an acid resistant nail varnish

The specimens were immersed individually in 40 ml of artificial caries demineralising solution, as described by ten Cate et al (ten Cate and Duijsters 1982). This solution is composed of 50 mmol/L acetate, 2.2 mmol/L calcium and 2.2 mmol/L phosphate adjusted to pH 4.3 using 0.5M NaOH.

The solution and teeth were incubated at 37°C without agitation for prescribed time periods. Ten teeth were exposed for 7 days, 15 for 14 days and 10 for 21 days. The three time periods will produce lesions of different characteristics with different levels of mineral loss, depth of the lesions and permeability. The 14 days group was assigned a larger number of teeth as it was felt that the variation among the samples would be highest for this demineralising period.

These samples were tested to ensure a strong correlation of mineral profiles between the left and right sides of the cavity (test and control) as outlined in 5.2.1.

5.2.2.1.2 Placement of the restorations

Nail varnish was painted on half the floor of the cavity and was allowed to dry (**Figure 45**) before the entire cavity was gently scrubbed with Dentine Conditioner, 10% polyacrylic acid, (GC Corporation, Tokyo, Japan) for ten seconds. The cavity was washed with an air and water spray for twenty seconds then gently dried with air for five seconds. The restorative material was placed according to the manufacturers' instructions and allowed to set. The sample was placed in a sealed container with 40 ml of DDW and incubated at 37°C for the time periods prescribed in the protocol for the separate experiments as described in Chapter 6.

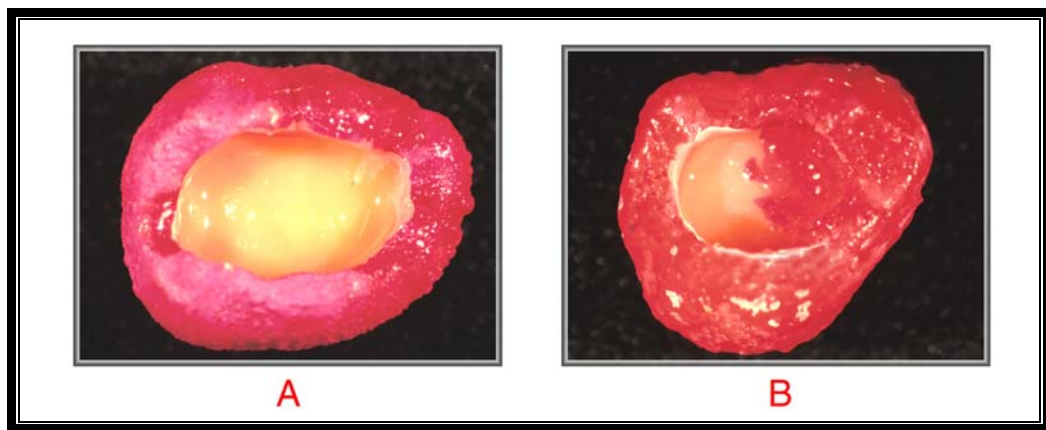


Figure 45: Molars with prepared cavity, ready for the placement of glass-ionomer:

A: Tooth with artificial caries, immediately after being removed from demineralised solution.

B: Half the cavity is covered with more nail varnish to create a control area. The tooth is now ready to receive the restoration.

5.2.2.1.3 Preparation of samples for EPMA analysis

The teeth were sectioned into halves, mesio-distally through the middle of the restorations, using an Isomet Slow Speed Saw (Buehler, USA), with Diamond Wafering Blade, No. 11-4244 (Buehler, USA) (**Figure 46**).



Figure 46: Isomet Slow Speed Saw

This is shown as step number 3 in **Figure 47**, the two halves were fixed overnight in a solution containing 2.5% glutaraldehyde with 4% paraformaldehyde and 4% glucose in PBS Buffer at pH 7.4. One half was prepared for EPMA analysis while the other was stored in a sealed container at 4°C, in case it was needed later; this is illustrated as step 4 in **Figure 47**.

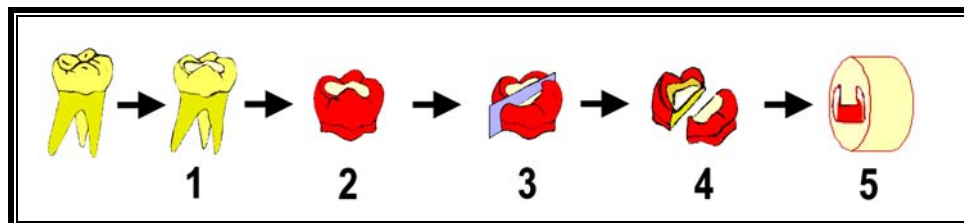


Figure 47: The five steps involved in preparing the sample for EPMA

The next step in the preparation for EPMA was to minimise shrinkage by dehydrating the samples using a series of solutions with decreasing concentrations of alcohol as previously described (Perdigao and Swift, 1994). The samples were then embedded in epoxy resin at a ratio of 100:25 for epoxy resin LC 191 and epoxy hardener HY 956 (Adelaide Epoxy Supplies, Adelaide, Australia) under vacuum. Plano-parallel specimens were necessary for EPMA so both sides of the mounting blocks were made parallel to each other using a

levelling device (**Figure 48**). The final polishing was done on an Abramin polishing machine (Struers, Copenhagen, Denmark) (**Figure 49**).

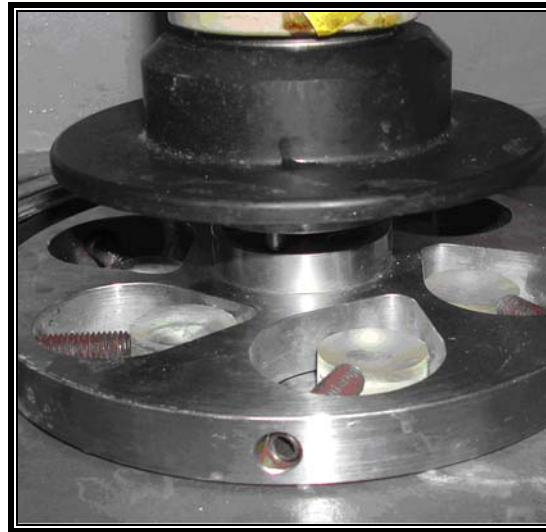


Figure 48: Samples in a special holder to ensure plano-parallelism



Figure 49: Abramin polishing machine (Struers, Copenhagen Denmark)

The test surface was then polished using polishing clothes (Struers, Copenhagen, Denmark) and diamond paste (Kemet, England), starting with 15 μm diamond paste at 150 rpm and lubricated with DP-Lubricant Green (Struers, Denmark) for 5 minutes at 200N. This was followed with 3 μm then finally 1 μm diamond pastes. Both cycles were set at 150

rpm, for three minutes, at 200 N, and lubricated with DP-Lubricant Green. The samples were cleaned with water, air dried and viewed under a microscope after every step to make sure the regions of interest were well polished.

The sample was then coated with carbon before EPMA analysis (**Figure 50**). As illustrated in **Figure 50B**, the demineralised dentine was directly exposed to the glass-ionomer on the test side. The control was achieved by isolating the demineralised dentine with a thick layer of red nail varnish.

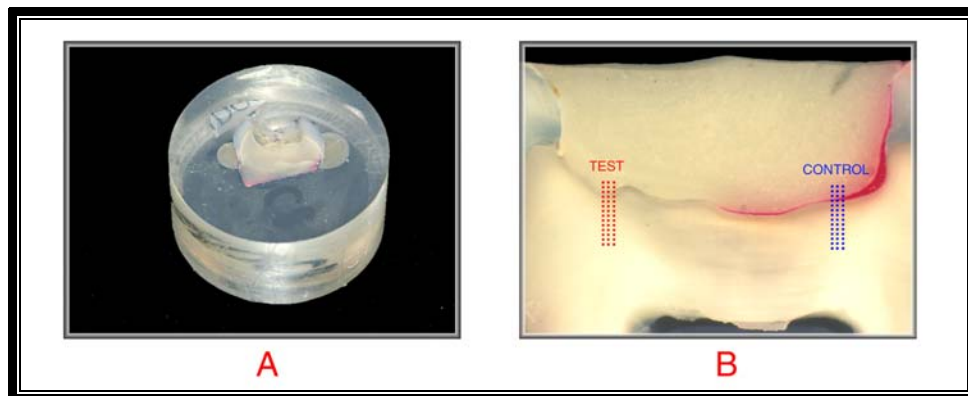


Figure 50: Example of a sample ready for EPMA

A: Sample ready for EPMA

B: The test and control areas where the mineral profiles were acquired

5.2.2.1.4 EPMA

The analysis method for EPMA was previously described in Chapter 3. In brief, a Cameca SX51 microanalyser (Cameca, Corbevoie, France) (**Figure 51**) was used with the beam set at 15kV and 20 mA and a beam diameter of 1000 Å, running in wavelength dispersive spectrometry (WDS) mode and a collection time of ten seconds at each point. Calibration for the EPMA used a minerals mount MINM25-53 (Astimex Scientific, Toronto, Canada), with apatite, fluorite and celestite used as standards to calibrate Ca and P, F and Sr respectively. The calculated minimum detection limits (MDL) are listed in **Table 7**.



Figure 51:EPMA machine, model SX51 (Cameca, Corbevoie, France)

	Calibration levels (weight %)	Minimum Detection Limit (weight %)
Ca	39.85	0.05
P	18.50	0.12
F	48.67	0.05
Sr	47.52	0.05

Table 7: Concentrations found in the standard used for calibration and Minimum Detection Limits for the elements of interest.

A programmed spot analysis for calcium, phosphorus, fluorine and strontium was performed along a line perpendicular to the glass-ionomer and dentine interface at 5 μ m intervals, reaching into sound dentine. Data was collected from two regions in each sample (test and control) and a set of three lines was performed for each region (**Figure 50**). An average was calculated from the three lines to represent the mineral profile for that region of analysis.

5.2.2.2 Experimental design

In this initial study, the mineral profiles were collected from the extreme right and left corners of the cavity, because in later experiments they represent the location of the test and control regions, as shown in part B of **Figure 50**. The analysis was done without the placement of a restoration so that the correlation of the consistency of the models could be evaluated.

As described in 5.2.1, the validity of the *in vitro* model was assessed according to the following criteria:

- A. The correlation of the mineral profiles found in the areas where the test and control would be
- B. The similarity of the profiles of strontium and fluorine found in the *in vitro* and *in vivo* studies

5.2.3 Results

5.2.3.1 Experiment A: Consistency of mineral profiles across the artificially produced carious lesions

In this section, the consistency of the mineral content of the test and control sides will be tested. For simplicity, only one representative chart is presented for each of the three types of sample: 7, 14 and 21 day lesions. The full set of charts can be found in Appendix C.

The individual mineral distribution profiles of Ca and P were simultaneously acquired and for each element, the following two main parameters were calculated:

- L = depth of the lesion in μm , this was determined from the distribution profile of calcium and phosphorous. The depth of the lesion was the distance from the surface of the cavity floor to the position where the mineral content is 95% of that of sound dentine. The mineral content of sound dentine was determined for each individual tooth

by using the mean of 20 points of EPMA analysis which were in sound dentine of that tooth.

- ΔZ = the surface area under the curve, representing the mineral loss of Ca and P (Arends, Christoffersen et al. 1989)

The distribution profile of calcium and phosphorous can be described by using the above two parameters with a suffix being the chemical symbol for that element. For example, LCa and ΔZCa representing depth of lesion and mineral lost calculated using the Ca curve (Figure 52).

The total mineral loss can be expressed as the sum of calcium and phosphorous, LCa+P and $\Delta ZCa+P$.

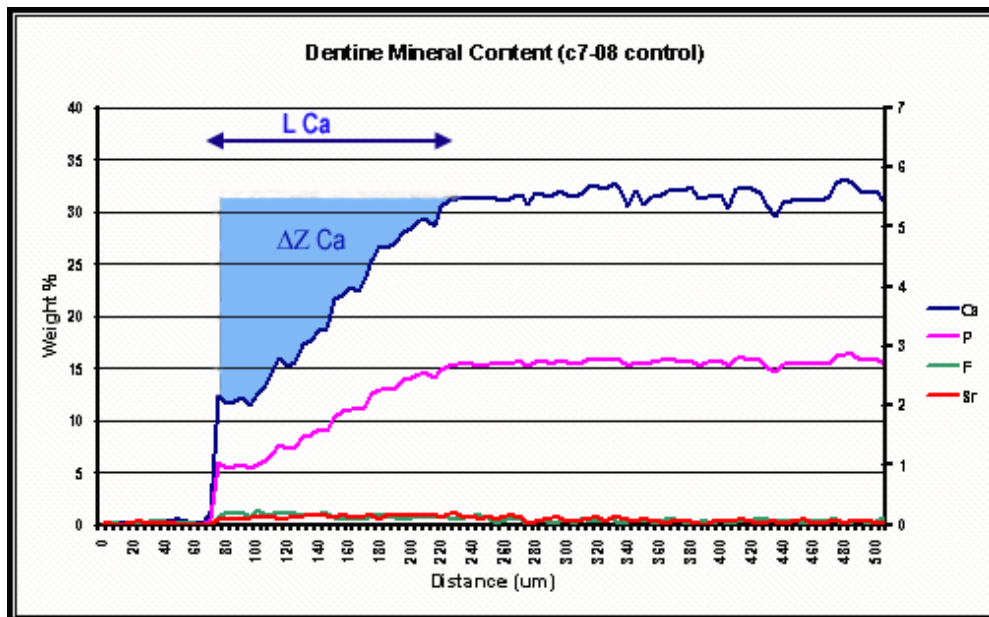


Figure 52: $\Delta Z Ca$, represented by the area shaded in blue, is a measure of Ca lost from dentine. LCa is the lesion depth as determined by the level of Ca

5.2.3.1.1 Group 1: 7 days of exposure to demineralising solution

A typical set of mineral profile for a 7 day lesion is shown below (Figure 53). LCa and $\Delta ZCa+P$ for every sample are listed in Table 8.

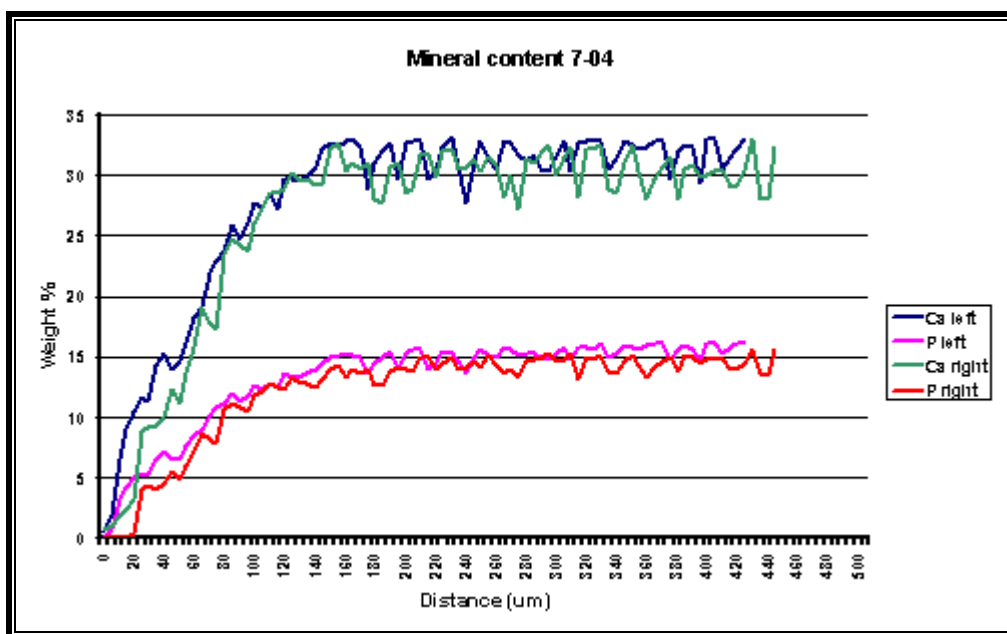


Figure 53: Mineral profile of a sample in the 7 day group, showing an example of good correlation between the left and right corners.

Sample id	L Ca left	ΔZ Ca+P left	L Ca right	ΔZ Ca+P right
7-01	260	5,439.80	325	5,038.80
7-02	135	1,823.74	170	2,949.51
7-03	155	1,303.13	130	784.73
7-04	145	2,409.34	125	2,476.38
7-05	300	1,939.94	135	1,018.43
7-06	230	2,069.84	130	1,134.21
7-07	245	4,802.01	220	3,707.97
7-08	230	4,058.31	115	1,755.83
7-09	240	4,630.76	230	4,275.16
7-10	180	969.92	185	1,567.75

Table 8: LCa and ΔZ Ca+P for all samples in the 7 day group.

5.2.3.1.2 Group 2: 14 days of exposure to demineralising solution

There were 15 samples in this group and a typical set of mineral profile for a 14 day lesion is shown below (**Figure 54**). LCa and $\Delta ZCa+P$. for every sample are listed in **Table 9**.

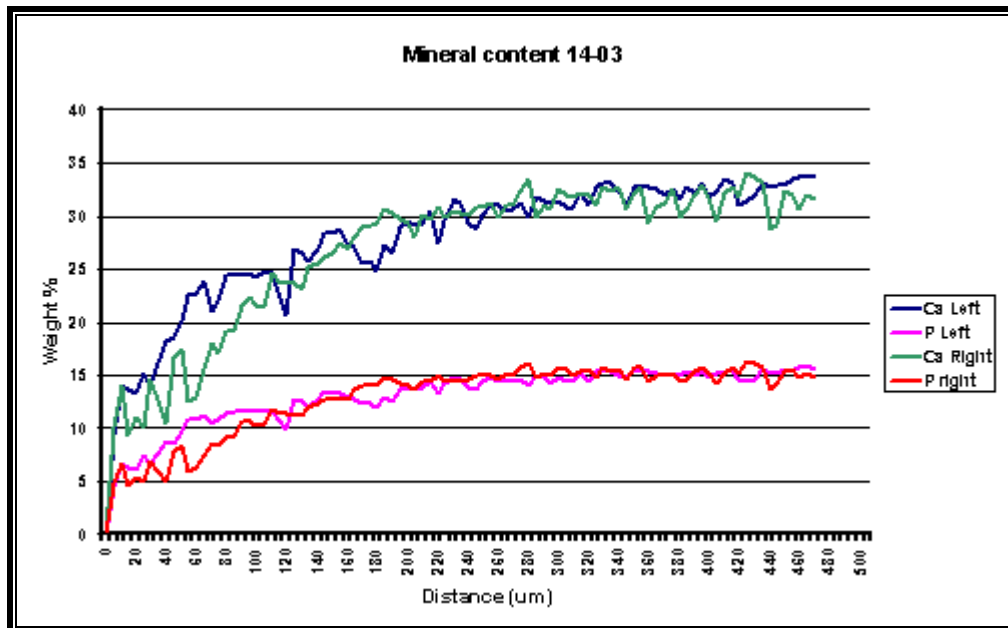


Figure 54: Mineral profile of a sample in the 14 day group, showing an example of good correlation between the left and right corners.

Sample id	L Ca left	ΔZ Ca+P left	L Ca right	ΔZ Ca+P right
14-01	285	4,450.43	350	5,607.19
14-02	150	1,992.32	160	1,174.69
14-03	330	3,196.20	275	3,176.35
14-04	200	2,192.39	160	1,875.40
14-05	295	4,658.25	325	5,148.06
14-06	295	4,594.50	400	6,250.49
14-07	80	602.18	145	648.66
14-08	170	2,453.07	330	5,477.62
14-09	75	638.72	215	1,604.72
14-10	120	905.07	205	1,842.02
14-11	300	3,126.77	225	2,923.17
14-12	180	3,000.43	230	3,575.95
14-13	195	2,116.44	145	2,257.92
14-14	130	1,659.25	130	1,977.72
14-15	155	1,385.47	145	1,092.30

Table 9: LCa and ΔZ Ca+P for all samples in the 14 day group

5.2.3.1.3 Group 3: 21 days of exposure to demineralising solution

There were 10 samples in this group and a set of good mineral profile for a 21 day lesion is shown in **Figure 55**. LCa and ΔZ Ca+P. for every sample can be found in **Table 10**.

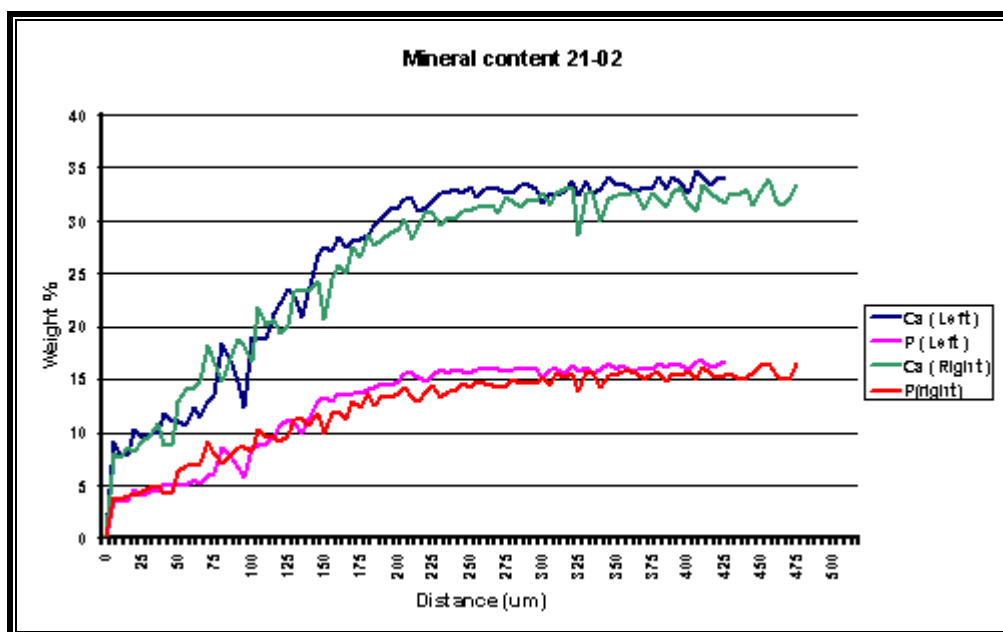


Figure 55: Mineral profile of a sample in the 21 day group, showing an example of good correlation between the left and right corners.

Sample id	L Ca left	ΔZ Ca+P left	L Ca right	ΔZ Ca+P right
21-01	195	3,337.01	320	6,312.63
21-02	345	4,595.11	300	4,331.84
21-03	355	4,652.98	270	4,414.74
21-04	295	4,513.14	265	4,353.14
21-05	120	3,956.75	350	6,541.97
21-06	215	2,294.51	190	2,255.01
21-07	325	4,404.23	265	3,916.85
21-08	240	3,255.10	390	5,645.53
21-09	190	3,410.57	225	1,769.50
21-10	275	4,846.69	400	8,068.26

Table 10: LCa and ΔZ Ca+P for all samples in the 21 day group

5.2.3.1.4 *Statistical analysis*

It is important that the *in vitro* model shows a high level of consistency between the left and right corners, as this will determine the level of confidence in interpreting the data of future experiments. All statistical analysis was carried out using SPSS (v.10.0.5) (SPSS Inc, Chicago, USA).

The above comparison between the left and right sides was carried out using reliability analysis (Shrout and Fleiss 1979; Litwin 1995) and the results were expressed through the following :

1. Mean and p value
2. Correlation Coefficient (Pearson's r)
3. Intraclass Correlation Coefficient (Cronbach Alpha) and its 95% CI
4. Paired t-test

The Intraclass Correlation Coefficient (ICC) was used to measure inter-rater reliability because the sample size is small (<15) or there are more than two tests (one test, one retest) to be correlated. In general, ICC is a coefficient which approaches 1 as the between-groups effect (the row effect) is very large relative to the within-groups effect (the column effect), whatever the rows and columns represent. In this way ICC is a measure of homogeneity: it approaches 1 when any given row tends to have the same values for all columns.

		Mean	P	Correlation Coefficient	ICC	95% CI for ICC
<i>L Ca</i>	L	212.0	0.15	0.33	0.49	-1.06-0.87
	R	176.5				
<i>ΔZ Ca</i>	L	1958.6	0.15	0.82	0.90	0.60-0.98
	R	1645.8				
<i>L P</i>	L	245.5	0.045	0.44	0.61	-0.59-0.90
	R	197.0				
<i>ΔZ P</i>	L	1018.7	0.11	0.81	0.89	0.56-0.97
	R	843.8				
<i>L Ca+P</i>	L	213.0	0.17	0.29	0.45	-1.22-0.86
	R	180.5				
<i>ΔZ Ca+P</i>	L	2944.7	0.15	0.82	0.90	0.58-0.97
	R	2470.9				

Table 11: Correlation between left and right sides of 7 day lesions (N=10)

		Mean	P	Correlation Coefficient	ICC	95% CI for ICC
<i>L Ca</i>	L	197.3	0.11	0.65	0.79	0.36-0.93
	R	229.3				
<i>ΔZ Ca</i>	L	1617.9	0.037	0.87	0.91	0.73-0.97
	R	1994.4				
<i>LP</i>	L	221.3	0.39	0.48	0.65	-0.04-0.88
	R	243.3				
<i>ΔZ P</i>	L	835.0	0.09	0.85	0.90	0.72-0.97
	R	980.9				
<i>L Ca+P</i>	L	213.0	0.33	0.54	0.70	0.11-0.90
	R	236.0				
<i>ΔZ Ca+P</i>	L	2464.8	0.057	0.86	0.90	0.72-0.97
	R	2975.5				

Table 12: Correlation between left and right sides of 14 day lesions (N=15)

		Mean	P	Correlation Coefficient	ICC	95% CI for ICC
<i>L Ca</i>	L	255.5	0.23	-0.11	-0.22	-3.95-0.69
	R	297.5				
<i>ΔZ Ca</i>	L	2616.5	0.18	0.48	0.51	-0.96-0.88
	R	3151.6				
<i>L P</i>	L	264.0	0.27	-0.04	-0.09	-3.39-0.73
	R	306.5				
<i>ΔZ P</i>	L	1319.2	0.15	0.30	0.40	-1.42-0.85
	R	1607.5				
<i>L Ca+P</i>	L	261.0	0.29	-0.13	-0.28	-4.19-0.68
	R	302.5				
<i>ΔZ Ca+P</i>	L	3926.6	0.17	0.42	0.47	-1.15-0.87
	R	4760.9				

Table 13: Correlation between left and right sides of 21 day lesions (N=10)

The paired t-test results for the 7, 14 and 21 day groups are listed in **Table 14**, **Table 15** and **Table 16**. There was no significant difference in LCa+P and ΔZCa+P between the left and right sides in all three categories of lesions.

	Left	Right
	LEFT MEAN (SD)	MEAN (SD)
<i>L Ca</i>	212.00 (55.04)	176.50 (66.17)
<i>ΔZ Ca</i>	1958.62 (1094.99)	1645.81 (990.95)
<i>L P *</i>	245.50 (59.93)	197.00 (63.95)
<i>ΔZ P</i>	1018.74 (545.79)	834.85 (492.63)
<i>L Ca+P</i>	213.00 (51.49)	180.50 (62.11)
<i>ΔZ Ca+P</i>	2944.68 (1621.75)	2470.88 (1478.57)

Table 14: Comparison between left and right sides of 7 day lesions

* p< 0.05

	Left	Right
	MEAN (SD)	MEAN (SD)
<i>L Ca</i>	197.33 (84.20)	229.33 (87.30)
<i>ΔZ Ca *</i>	1617.86 (918.66)	1994.44 (1243.51)
<i>L P</i>	221.33 (94.76)	243.33 (91.98)
<i>ΔZ P</i>	835.03 (456.46)	980.86 (588.35)
<i>L Ca+P</i>	213.00 (91.35)	236.00 (90.89)
<i>ΔZ Ca+P</i>	2464.77 (1363.27)	2975.48 (1834.66)

Table 15: Comparison between left and right sides of 14 day lesions

* p< 0.05

	Left	Right
	MEAN (SD)	MEAN (SD)
<i>L Ca</i>	255.50 (76.65)	297.50 (68.32)
<i>ΔZ Ca</i>	2616.50 (556.18)	3151.64 (1345.58)
<i>L P</i>	264.00 (94.39)	306.50 (62.32)
<i>ΔZ P</i>	1319.15 (313.49)	1607.48 (596.28)
<i>L Ca+P</i>	261.00 (87.68)	302.50 (66.26)
<i>ΔZ Ca+P</i>	3926.61 (824.80)	4760.95 (1935.40)

Table 16: Comparison between left and right sides of 21 day lesions

5.2.3.2 Experiment B: Similarity of the profiles of strontium and fluorine found in the *in vitro* and *in vivo* lesions

As a pilot experiment to evaluate this *in vitro* model before the main experiments, two 14 day samples were filled with Fuji IXGP and prepared according to the protocol described above. The mineral profile found in the control side where the artificially demineralised dentine was separated from the Fuji IXGP by a thick layer of nail varnish showed the absence of strontium and fluorine (**Figure 56**). In the test zone, there were significant amounts of strontium and fluorine. These elements crossed from the Fuji IXGP into the demineralised dentine (**Figure 57**). Furthermore, it was apparent that the pattern of penetration of strontium and fluorine into the artificially demineralised dentine was very similar to that found in the *in vivo* study, this was described in 5.1.3 and illustrated in **Figure 42**.

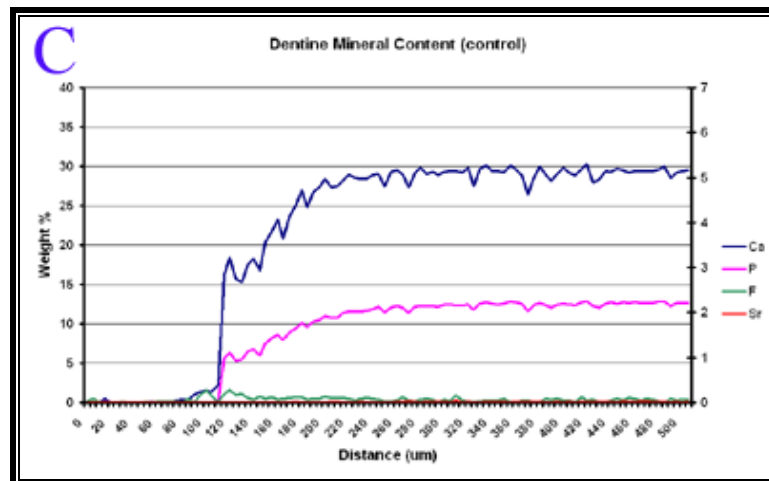


Figure 56: Mineral profiles found in the control region, showing no penetration of strontium and fluorine into the demineralised dentine.

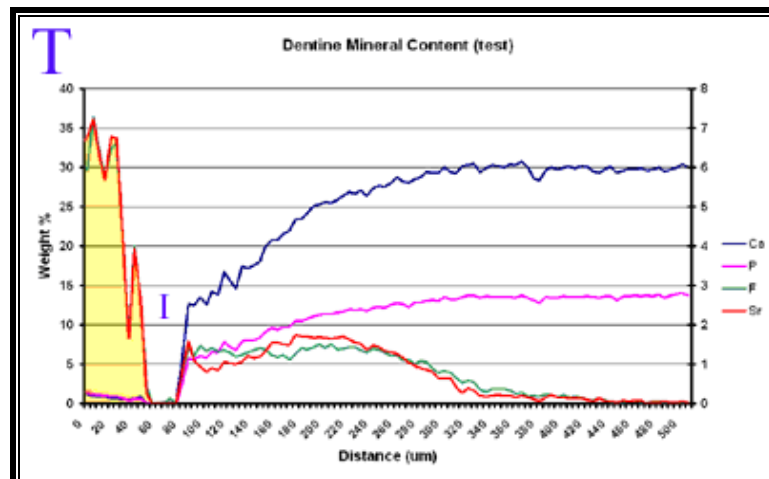


Figure 57: Mineral profiles found in the test region, showing the presence of strontium and fluorine. The pattern of penetration is similar to those found in the *in vivo* study. The area shaded yellow is within the glass-ionomer and I marks the interface of the restoration. The apparent gap is an artefact due to dehydration during sample preparation.

5.2.4 Interpretation

As stated in the introduction to Chapter 1, the major objective of this study was to determine if glass-ionomers contribute to the remineralisation of demineralised dentine and

if so what are the possible mechanisms? In order to start understanding this process, it is necessary to find answers to the following questions:

1. Which mineral was lost or gained?
2. How much mineral was lost or gained?
3. Where was the mineral lost or gained?

This can only be achieved with a series of experiments in the laboratory, where the variables can be controlled, the effect of the materials can be measured and most importantly the ionic exchange which was observed in the *in vivo* experiment, as described in Chapter 5, can be reproduced. The *in vitro* study provided these conditions.

5.2.4.1 Which mineral, how much and where?

It was suggested that with TMR it is possible to measure two main parameters: the lesion depth (Ld) and the mineral loss (ΔZ) (**Figure 10**) (Arends and ten Bosch 1992), these two parameters give answers to question two and three. However, only EPMA can provide answers to all three questions as it gives the profiles of the separate elements. Using EPMA it is possible to report the loss in calcium and phosphate separately as ΔZ_{Ca} and ΔZ_{P} and the combined loss as ΔZ_{Ca+P} which is the sum of ΔZ_{Ca} and ΔZ_{P} . In the later part of this thesis where the interaction between glass-ionomer and dentine is evaluated, it is expected that the net gain of strontium and fluorine can be measured. This are reported separately as ΔZ_{Sr} and ΔZ_{F} (**Figure 58**). Even though the detection limits of EPMA for both strontium and fluorine were calculated to be 0.05 weight% (**Table 7**), for the purpose of this study, the limit was set ten folds higher at 0.5 weight%. This level was used in calculating both ΔZ_{Sr} and ΔZ_{F} .

Using EPMA, the distribution of the different elements can also be displayed as elemental maps, and this will be discussed further in Chapter 6. The depth of the lesion will be

determined using LCa, expressed in μm , as the point where the calcium line reaches 95% of the value in sound dentine (**Figure 58**).

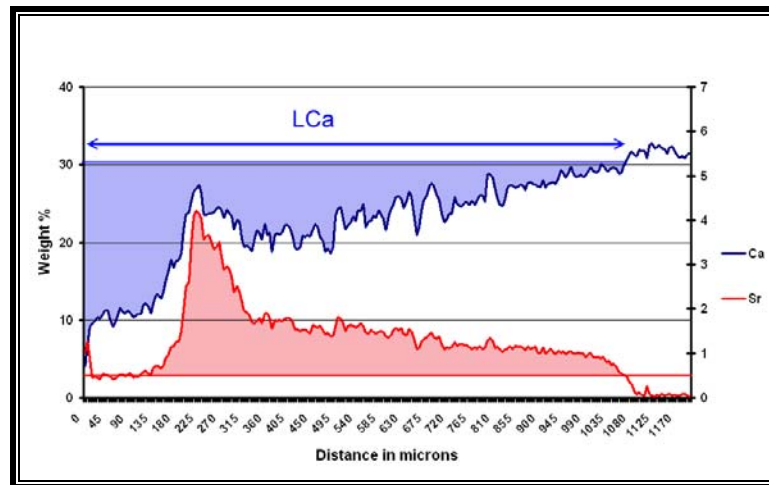


Figure 58: The parameters used to express the depth of the lesion (LCa), amount of calcium loss (ΔZ Ca: shaded blue) and amount of strontium gained (ΔZ Sr: shaded red).

5.2.4.2 How reproducible is the model?

One of the important variables which would have an influence on the level of strontium and fluorine penetration is the amount of mineral, namely calcium and phosphate, left in the demineralised dentine. The model was designed with the dentine being demineralised for three different periods: 7, 14 and 21, days to study the above variable.

The model was designed so that each sample carried its own control, as shown in **Figure 45**. The mineral profiles between the left and right sides, representing the test and control sides of the samples, show good reproducibility in relation to ΔZ Ca, ΔZ P and ΔZ Ca+P for all three groups. The ICC coefficients were highest for the 7 and 14 day groups and lowest for the 21 day. This was confirmed with the paired t test showing the only parameter with a significant difference between the two sides being ΔZ Ca in the 14 day group.

The LCa, LP and LCa+P showed a good but lower level of correlation. As the focus of attention is with the amount of strontium and fluorine gained, it was decided that the

parameter to be used in expressing the level of mineral loss would be ΔZ_{Ca+P} , which has the highest level of coefficient in all three groups.

5.2.4.3 Is the pattern of penetration of strontium and fluorine in the *in vitro* model consistent with that found in the *in vivo* study?

The mineral profiles of the two samples restored with Fuji IXGP showed very similar features with those found in the *in vivo* study. They demonstrated three distinct zones with the peak being in zone B and the penetration declines at the start of zone C. This was discussed in section 5.2.3.2 and illustrated in **Figure 57**.

Based on the above general observation, it was concluded that the *in vitro* model is valid for this study.

5.3 Baseline analysis of strontium and fluorine penetration from Fuji IXGP into sound dentine

5.3.1 Background

To determine whether there is a process of ion exchange between glass-ionomer and sound dentine, it was considered necessary to establish a baseline control, before carrying out tests for ion exchange profiles between glass-ionomer and artificially demineralised dentine.

5.3.2 Materials and methods

The protocols used in this experiment were described in Chapter 5 with the exception that the samples were not put through the demineralising process. Single cavities were cut into the crowns of five sound and freshly extracted molars. The cavities were treated with Dentine Conditioner (GC Corporation, Tokyo, Japan) for ten seconds, washed with a water spray for fifteen seconds, dried with a gentle stream of air for seconds then immediately

filled with Fuji IXGP, which was used in the *in vivo* study. This was allowed to set for three minutes and then was protected with Vaseline. The specimens were stored at 37°C in DDW for 14 days then sectioned through the cavity, fixed, dehydrated, resin embedded and analysed using EPMA according to standard protocols described previously in Chapter 5.

5.3.3 Results

The results from the five samples are presented below. The mineral profiles were only assessed visually as it is apparent that there was no significant strontium or fluorine penetration, with the limit set at 0.5 weight%, beyond the boundary of the interface between Fuji IXGP and sound dentine.

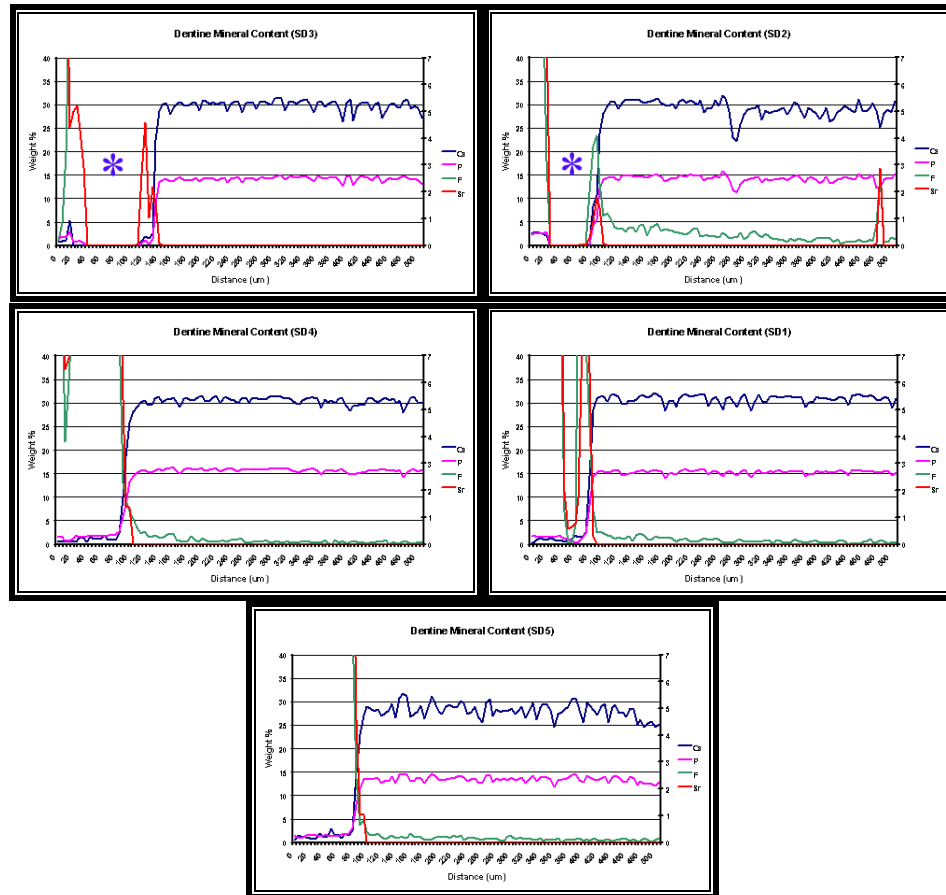


Figure 59: Ionic exchange pattern between Fuji IXGP and sound dentine. In the first two charts the * indicated an artefact.

In **Figure 59** the top two charts showed a gap, marked by a blue star. On the left is the glass-ionomer and on the right of the star is the sound dentine with the remnant of the glass-ionomer. This is an artefact due to the dehydration of the sample. This cohesive failure of the interface was previously described (Ngo, Mount et al. 1997).

5.3.4 Interpretation

The result shows that any strontium and fluorine which crossed the interface into sound dentine was very much restricted to the immediate area around the interface between Fuji IXGP and sound dentine. The deepest distance of penetration by fluorine only, was found

in sample SD2 (**Figure 59**) to be approximately 120 μm . It was observed that in three out of the five samples, fluorine penetrated deeper into the sound dentine than strontium. The pattern of penetration for both strontium and fluorine was consistent with a diffusion pattern with the highest concentration at the interface and it then tapered gradually. The pattern was quite different from what was observed in the *in vivo* study, involving demineralised dentine.

Chapter 6: A comprehensive analysis of the ionic exchange behaviour from different types of glass-ionomer and demineralised dentine

6.1 Introduction

Having demonstrated the validity of the *in vitro* model as a method of analysis of the ionic exchange between glass-ionomer and demineralised dentine, this chapter will focus on this process using a variety of different glass-ionomers under similar circumstances. The objective of this broad analysis was to investigate any major differences in ionic transfer between the different categories of glass-ionomer and demineralised dentine in laboratory settings.

The data presented in Chapter 4 was helpful in the selection of different glass-ionomers to be used in this study. It was clear that strontium provides particular advantages as it can substitute for calcium in the apatite and it is not present at substantial levels in either enamel or dentine, so together with fluorine, it can be traced into the demineralised dentine. It was shown earlier that Fuji IIF releases much higher levels of fluoride than the other materials. However, it was a calcium based glass ionomer, so the GC Corporation (Tokyo, Japan) were requested to provide Fuji VI for testing. This is a strontium based high fluoride releasing restorative glass-ionomer which is now commercially available as Fuji VII. The second material to be tested was Fuji IXGP because it was used in the previous *in vivo* study. It was decided to include a resin modified glass-ionomer with low powder to liquid ratio and GC Corporation provided an experimental material, Fuji Bond LL, which is both strontium containing and high fluoride releasing.

For each material, the effects of the following two main variables were studied:

- Degree of demineralisation of dentine
- Contact time with the glass-ionomers

A summary of the experimental design is presented in **Figure 60**.

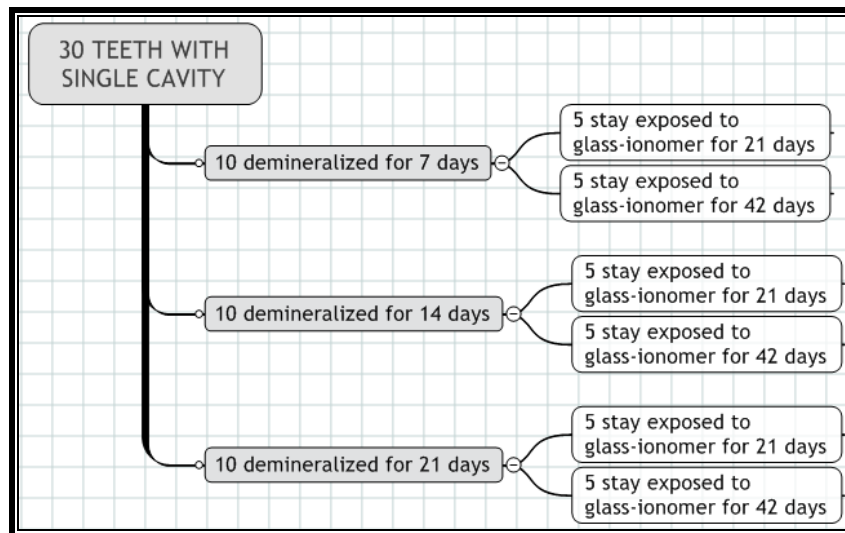


Figure 60: Overview of experimental design for each material.

6.2 High strength glass-ionomers: Fuji IXGP

6.2.1 Background

Fuji IXGP is a high strength restorative glass-ionomer, it has been closely associated with the ART and was used in the previous *in vivo* experiment. Based on the results in Chapter 4, it has a much lower level of fluoride and strontium release, in comparison with Fuji VI and Fuji Bond LL used in the next experiment. This may provide a chance to study any difference in the level of fluoride and strontium ion transfer.

6.2.2 Materials & Methods

6.2.2.1 Study design

Thirty freshly extracted third molars were stored in 0.5% chloramine solution at 4°C until used. A single cavity was cut in each and artificial lesions were prepared as previously described in section 5.2.2.1.1. The experimental design was as illustrated in **Figure 60**.

6.2.2.2 Placement of the restorations

Half of the cavity was covered with nail varnish (**Figure 45**). The margin of the cavity was refreshed using a diamond bur at high speed. The cavities were treated with Dentine

Conditioner (GC Corporation, Tokyo, Japan) for ten seconds, washed with a water spray for fifteen seconds, dried with a gentle stream of air for fifteen seconds then immediately filled with Fuji IXGP.

The material was allowed to set for three minutes then protected with Vaseline. The restored teeth were stored in DDW at 37°C. Five in each group were prepared for EPMA at 21 days while the other 5 were prepared after 42 days (**Figure 60**).

6.2.2.3 EPMA and statistical analysis

The samples were prepared for EPMA according to the protocol set out in section 5.2.2.1.3 and section 5.2.2.1.4. The statistical analysis was carried out using SPSS (v. 10.0.5) (SPSS Inc, Chicago, USA), paired t test and one-way ANOVA. Tukey posthoc tests were performed where appropriate.

For this experiment, it was decided to collect maps of elemental distribution using EPMA. To acquire the map, the EPMA machine scans the pre-programmed designated area of the specimen and the electron beam was held on the same setting as for the spot analysis. However the EPMA runs in energy dispersive spectrometry (EDS) mode and therefore the results are semiquantitative.

The map gives an idea of the relative distribution of a particular element in the different sites of the specimen, but it does not provide the actual weight% of the element in the specimen. When a set of maps of the different elements was obtained from the same specimen, the difference in the colour brightness between the maps represent the difference in the weight% of each element present in that particular specimen. The dimensions of a map were 512x128 μm .

6.2.3 Results

One representative chart is presented for each group. The full set of results is presented in Appendix D.

6.2.3.1 Representative EPMA profiles (Fuji IXGP)

6.2.3.1.1 7 day artificial lesion

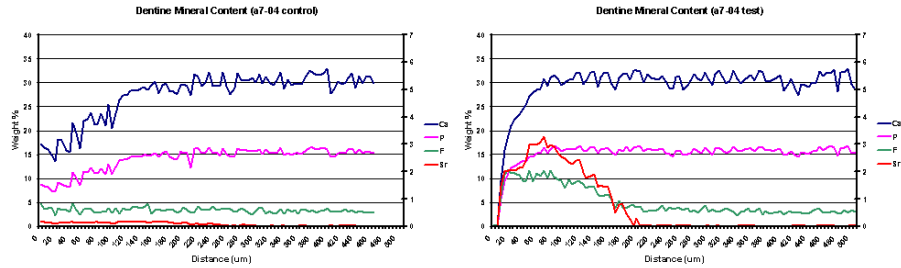


Figure 61: 7 day lesion treated with Fuji IXGP for 21 days.

Left chart: Control, Right chart: Test.

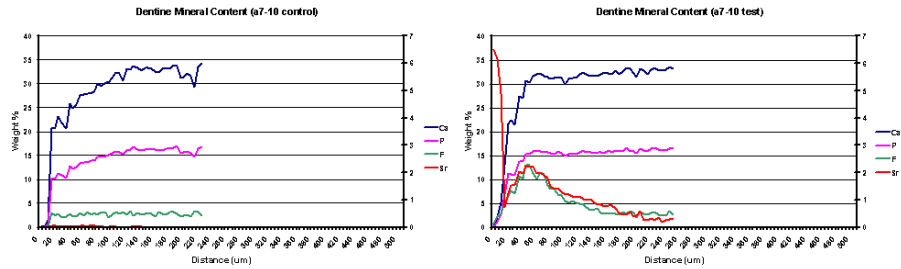


Figure 62: 7 day lesion treated with Fuji IXGP for 42 days

Left chart: Control, Right chart: Test

6.2.3.1.2 14 day artificial lesion

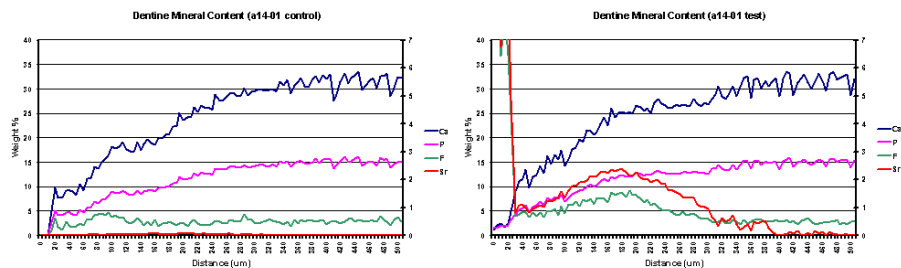


Figure 63: 14 day lesion treated with Fuji IXGP for 21 days

Left chart: Control, Right chart: Test.

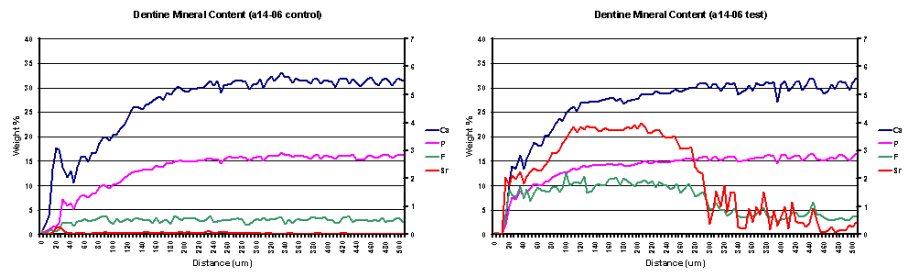


Figure 64: 14 day lesion treated with Fuji IXGP for 42 days

Left chart: Control, Right chart: Test.

6.2.3.1.3 21 day artificial lesion

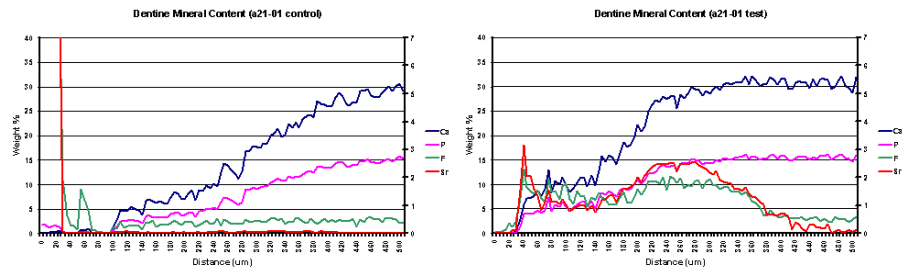


Figure 65: 21 day lesion treated with Fuji IXGP for 21 days

Left chart: Control, Right chart: Test.

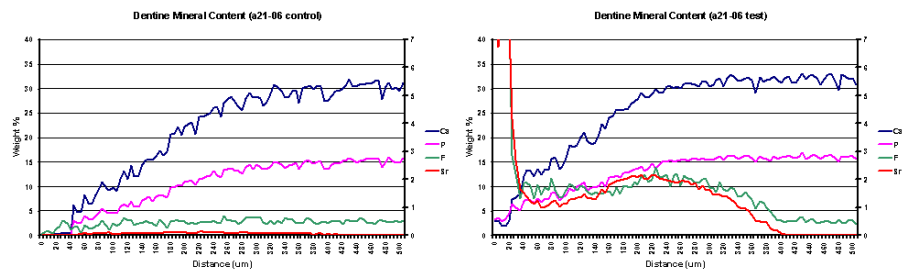


Figure 66: 21 day lesion treated with Fuji IXGP for 42 days

Left chart: Control, Right chart: Test.

6.2.3.2 EPMA elemental maps

The maps were prepared on the test side only to demonstrate the distribution of strontium and fluorine. The EPMA line analysis shown as the mineral profile chart was performed in the centre of the maps.

6.2.3.2.1 7 day artificial lesion treated for 21 days

There is a colour scale on the side of each map, with white being the maximum and black being the minimum. This range of colour scale is only relative.

The blue arrow on the chart indicated the LCa or the depth at which calcium returned to the level found in sound dentine. This corresponded with the blue arrow found on the calcium distribution map. As Fuji IXGP is a strontium based material containing very little calcium, the material is barely visible on the map.

The glass-ionomer could be seen very clearly on the maps for strontium and fluorine and these elements are concentrated in the glass particles which are visible in these two maps.

The red and green arrows on the chart indicated the depth of uptake of these elements into the demineralised dentine. This can also be observed on the maps of strontium and fluorine. As these elements do not exist in much quantity in normal dentine, the map shows dentine as almost black. In the areas where there is a build up of these two elements in the dentine, they are shown as blue.

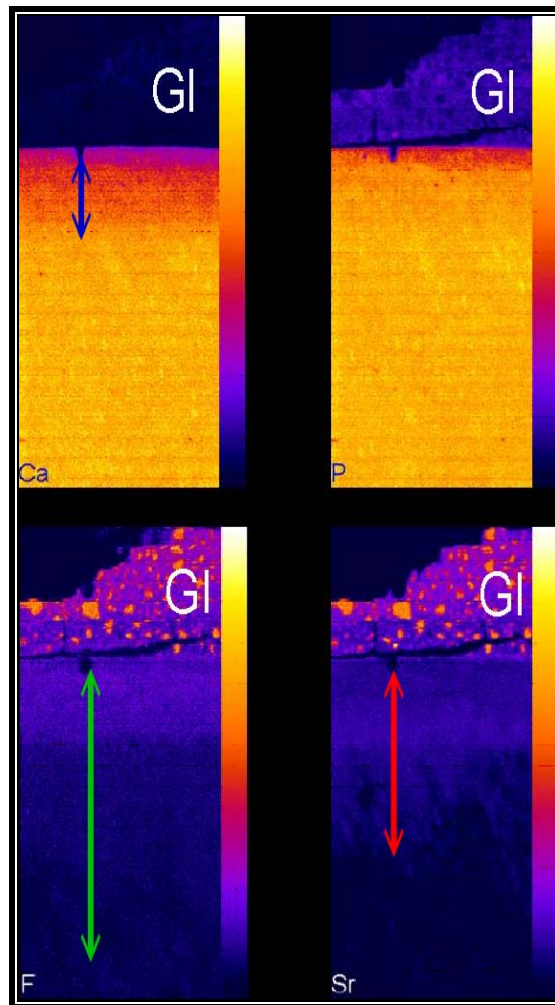
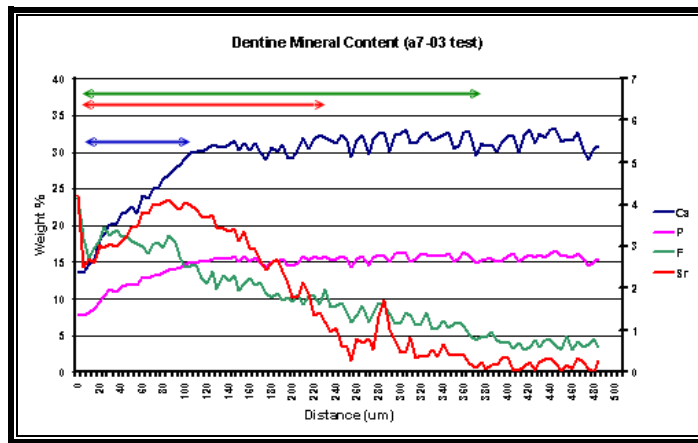


Figure 67: 7 day lesion exposed to Fuji IXGP for 21 days.

6.2.3.2.2 7 day artificial lesion treated for 42 days

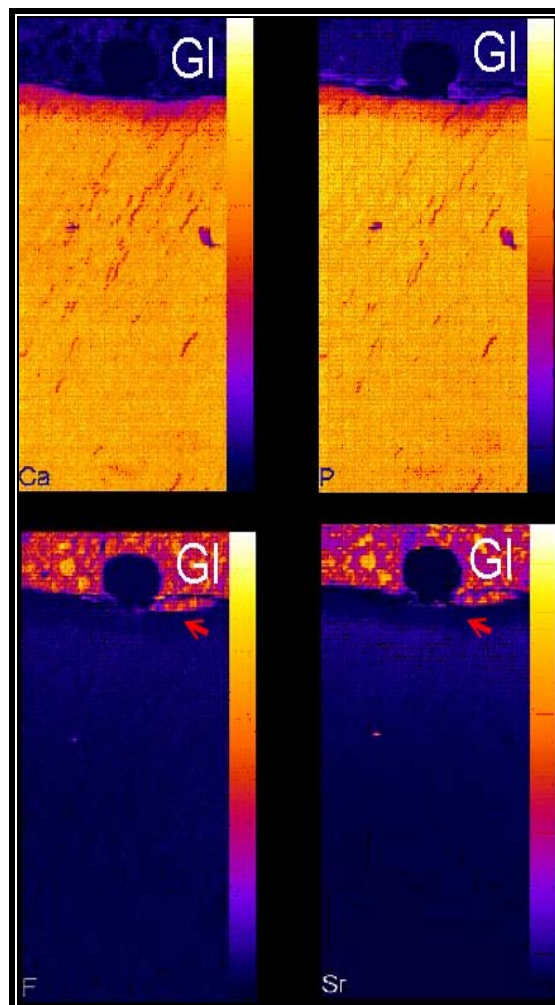
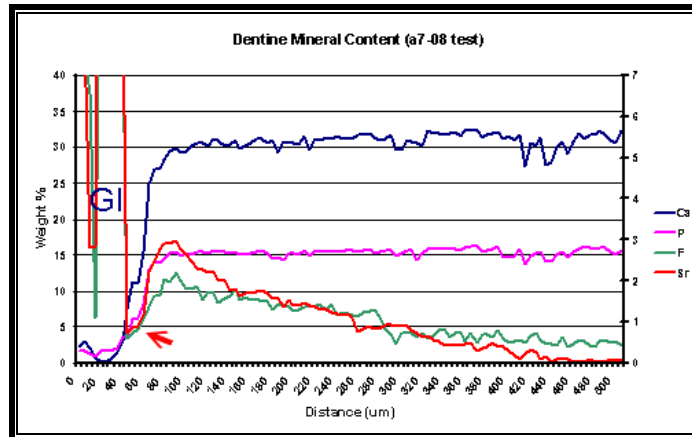


Figure 68: 7 day lesion exposed to Fuji IXGP for 42 days.

In this sample the glass-ionomer adhered well to the dentine. The arrow on the chart corresponded with a dip in the level of strontium and fluorine, which was reflected on the map as the dark band where the red arrow is.

6.2.3.2.3 14 day artificial lesion treated for 21 days

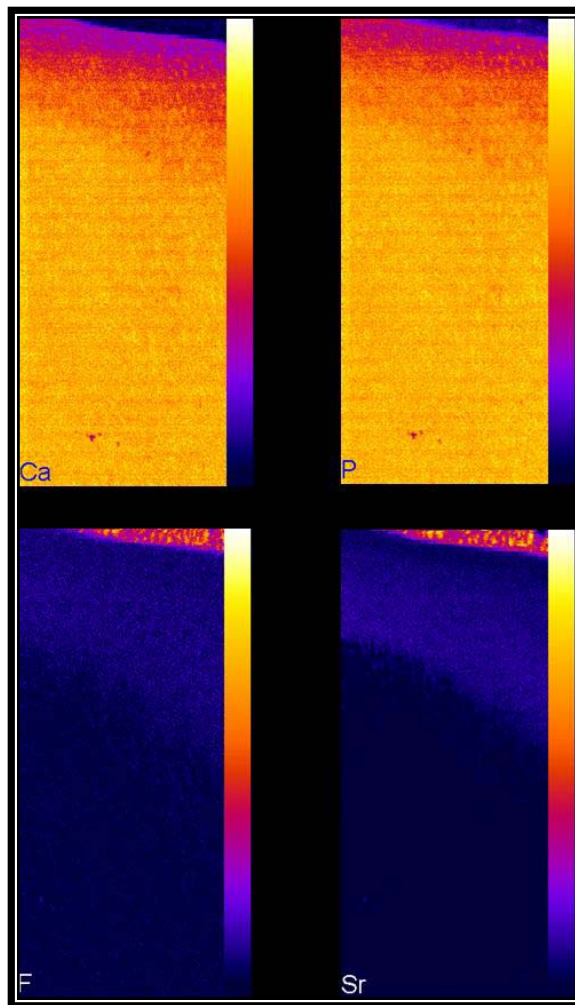
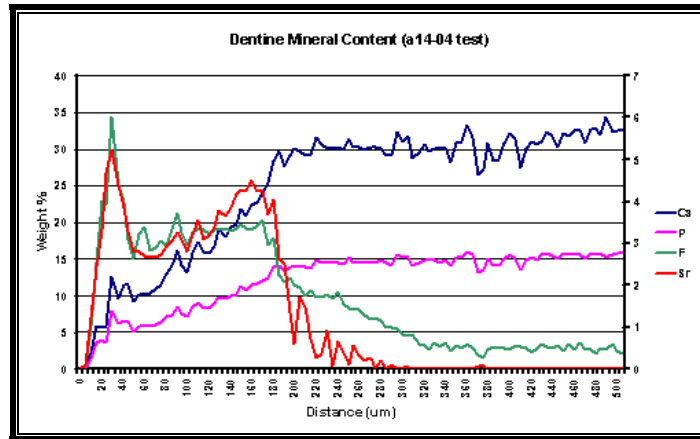


Figure 69: 14 day lesion exposed to Fuji IXGP for 21 days

The high level of strontium and fluorine build up from the interface is well illustrated by the even and darker blue bands on the strontium and fluorine maps.

6.2.3.2.4 14 day artificial lesion treated for 42 days

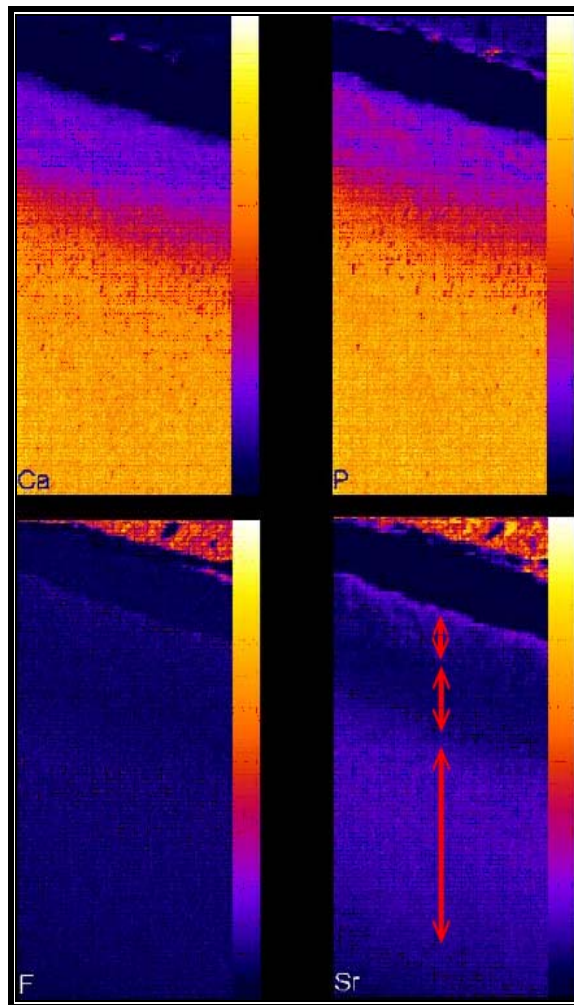
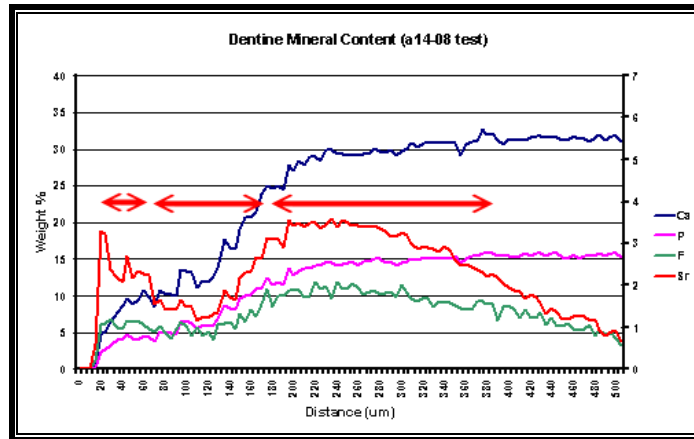


Figure 70: 14 day lesion exposed to Fuji IXGP for 42 days

The profile of strontium showed three distinct zones with a dip in the middle zone. This was confirmed on the map for strontium.

6.2.3.2.5 21 day artificial lesion treated for 21 days

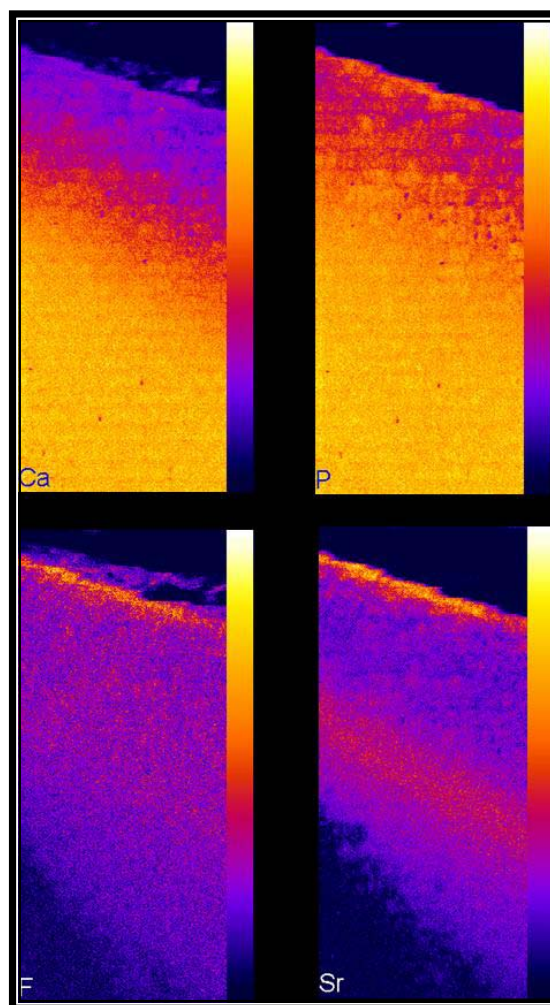
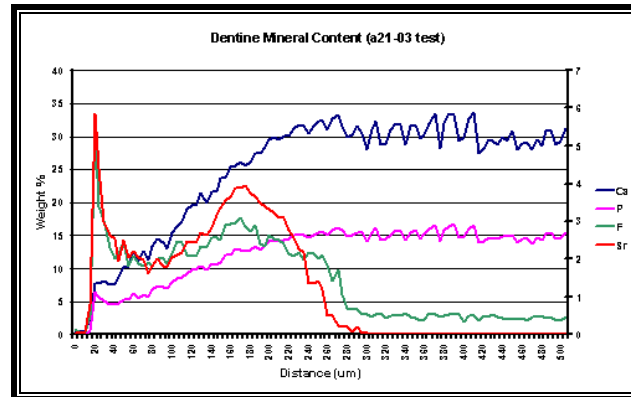


Figure 71: 21 day lesion exposed to Fuji IXGP for 21 days

Similar to the previous sample, the three zones were very clearly reproduced in the elemental maps.

6.2.3.2.6 21 day artificial lesion treated for 42 days

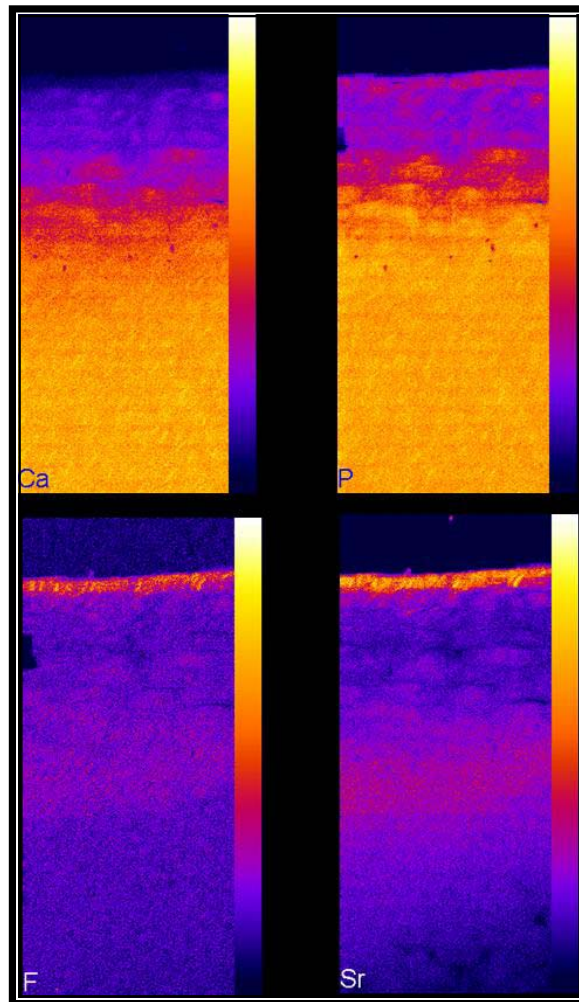
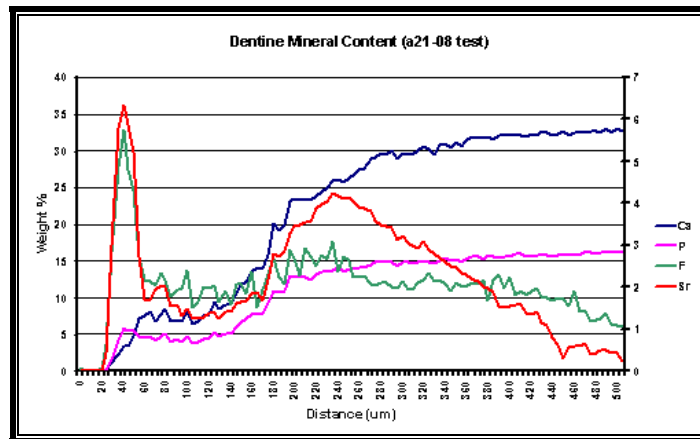


Figure 72: 21 day lesion exposed to Fuji IXGP for 42 days

6.2.3.3 Statistical analysis

Paired t-test was performed to check the control and test sides for consistency in all groups.

There was no significant difference between the two sides of the artificial lesions.

$\Delta ZCa+P$	7d/21d	7d/42d	14d/21d	14d/42d	21d/21d	21d/42d
Control	1219(827)	325(134)	4496(3396)	2530(2440)	5335(3090)	4368(1849)
Test	687(490)	312(194)	4964(942)	2431(1508)	4818(2201)	4088(1138)

Table 17: Mean $\Delta ZCa+P$ and intra group consistency of $\Delta ZCa+P$ for the different groups.

Paired t-test: Non Significant

6.2.3.3.1 7 day lesion treated with Fuji IXGP

	21 Days (n=5)	42 Days (n=5)
L F	302.00 (112.56)	196.00 (79.17)
$\Delta Z F$	237.56 (206.91)	169.28 (56.72)
L Sr	183.00 (76.37)	173.00 (75.71)
$\Delta Z Sr$	277.91 (208.06)	196.69 (76.16)

Table 18: 7 day lesion, comparison between treatment times with Fuji IXGP

* One-way ANOVA, Tukey posthoc test, Non Significant

6.2.3.3.2 14 day lesion treated with Fuji IXGP

	21 Days (n=5)	42 Days (n=5)
L F	378.00 (79.34)	406.00 (81.19)
$\Delta Z F$	420.65 (203.03)	426.12 (137.16)
L Sr	351.00 (113.49)	389.00 (100.09)
$\Delta Z Sr$	557.61 (195.43)	780.08 (194.84)

Table 19: 14 day lesion, comparison between treatment times with Fuji IXGP

* One-way ANOVA, Tukey posthoc test, Non Significant

6.2.3.3.3 21 day lesion treated with Fuji IXGP

	21 Days (n=5)	42 Days (n=5)
L F	401.00 (84.73)	374.00 (27.02)
ΔZ F	527.12 (141.56)	453.76 (176.20)
L Sr	354.00 (93.50)	393.00 (57.51)
ΔZ Sr	476.12 (68.78)	444.21 (165.80)

Table 20: 21 day lesion, comparison between treatment times with Fuji IXGP

* One-way ANOVA, Tukey posthoc test, Non Significant

6.3 High fluoride releasing GIC: Fuji VI

6.3.1 Background

It was noted in Chapter 4 the material which stood out by far with regards to fluoride release was Fuji IIF (**Figure 36**). For this experiment, it was substituted with Fuji VI for reasons discussed earlier. A version of this material is now commercially available as Fuji VII.

6.3.2 Materials and methods

Fuji VI was used as the test restorative material. The study design and methodology was similar to that described earlier in 6.2.2.

6.3.3 Results

One set of charts, control and test, which was representative for a group will be presented.

The full set of results can be found in Appendix D.

6.3.3.1 Representative EPMA profiles (Fuji VI)

6.3.3.1.1 7 day artificial lesion

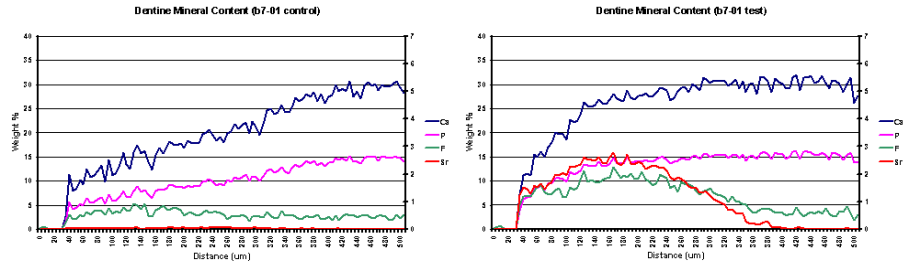


Figure 73: 7 day lesion treated with Fuji VI for 21 days. Left: Control, Right: Test.

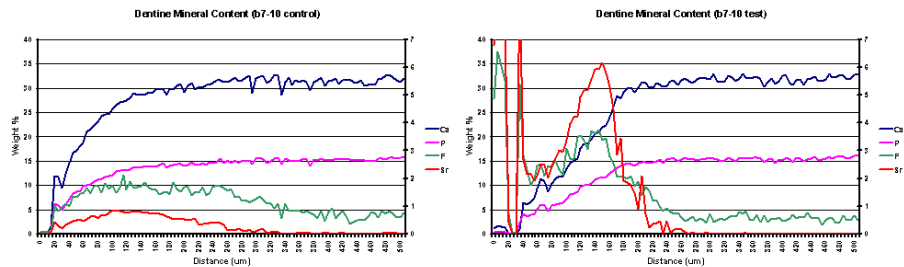


Figure 74: 7 day lesion treated with Fuji VI for 42 days. Left: Control, Right: Test.

6.3.3.1.2 14 day artificial lesion

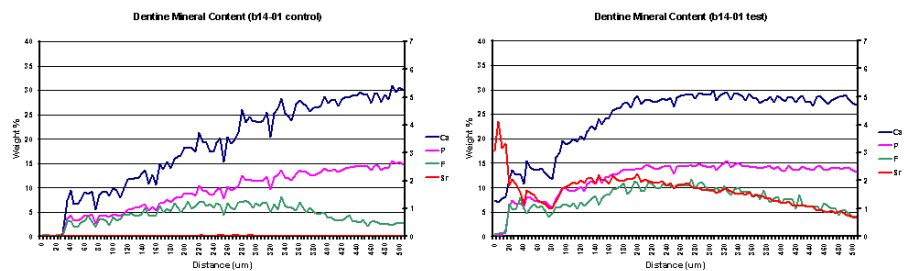


Figure 75: 14 day lesion treated with Fuji VI for 21 days. Left: Control, Right: Test.

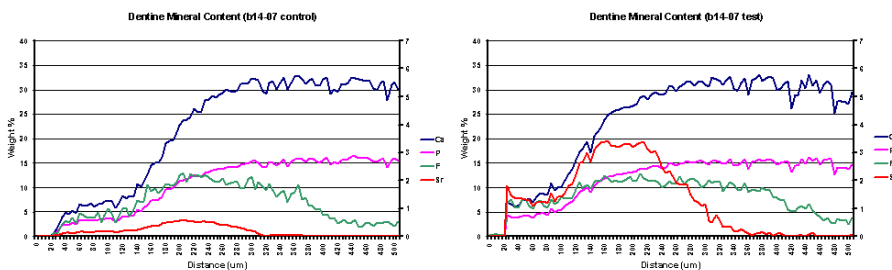


Figure 76: 14 day lesion treated with Fuji VI for 42 days. Left: Control, Right: Test.

6.3.3.1.3 21 day artificial lesion

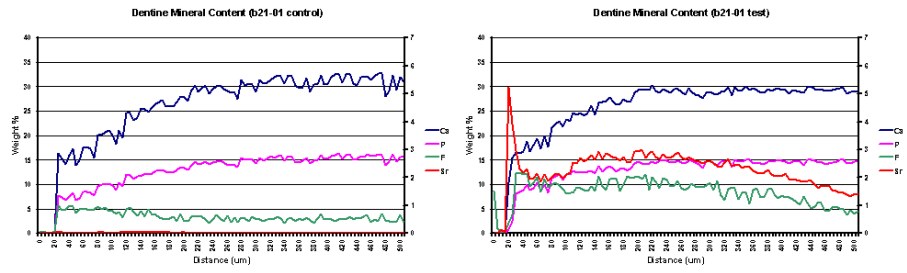


Figure 77: 21 day lesion treated with Fuji VI for 21 days. Left: Control, Right: Test.

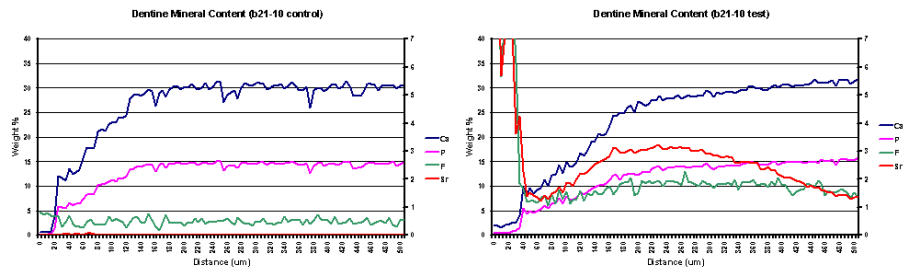


Figure 78: 21 day lesion treated with Fuji VI for 42 days. Left: Control, Right: Test.

6.3.3.2 EPMA elemental maps

The maps were collected as described previously in 6.2.3.2.

6.3.3.2.1 7 day artificial lesion treated for 21 days

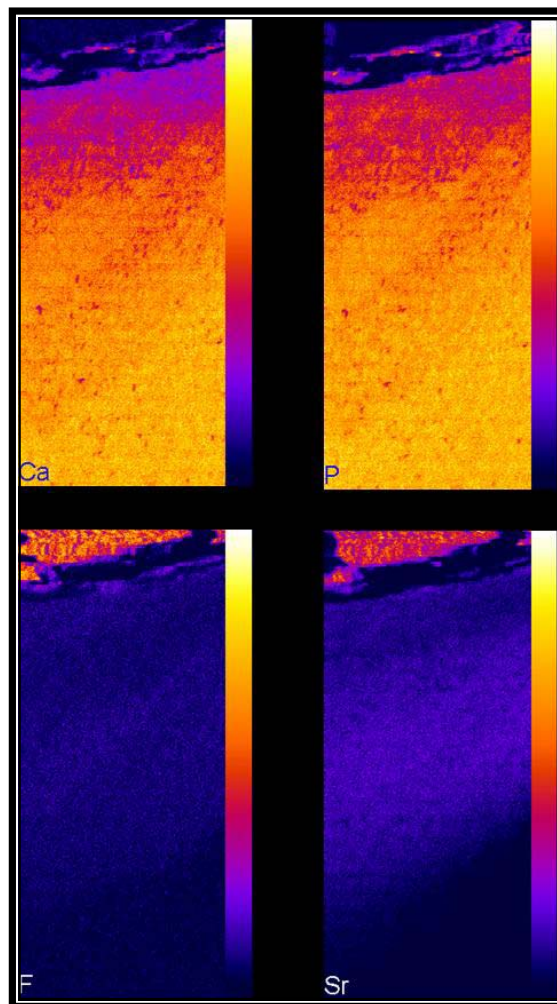
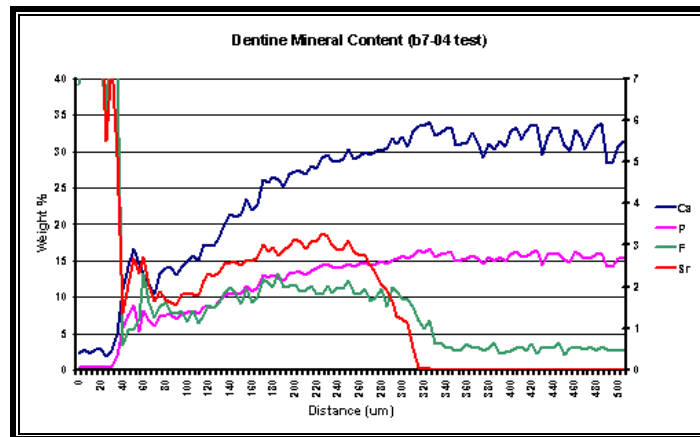


Figure 79: 7 day lesion exposed to Fuji VI for 21 days

6.3.3.2.2 7 day artificial lesion treated for 42 days

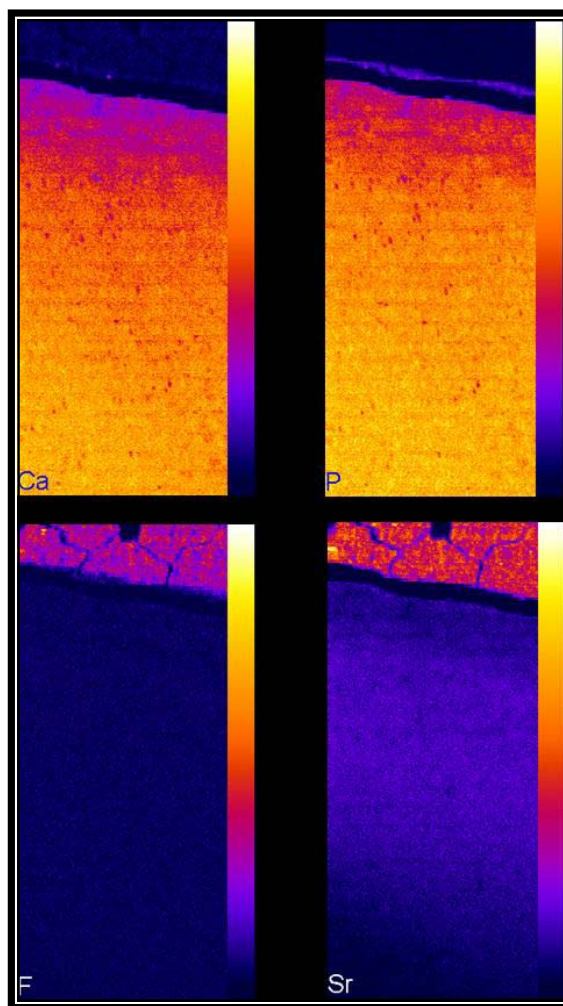
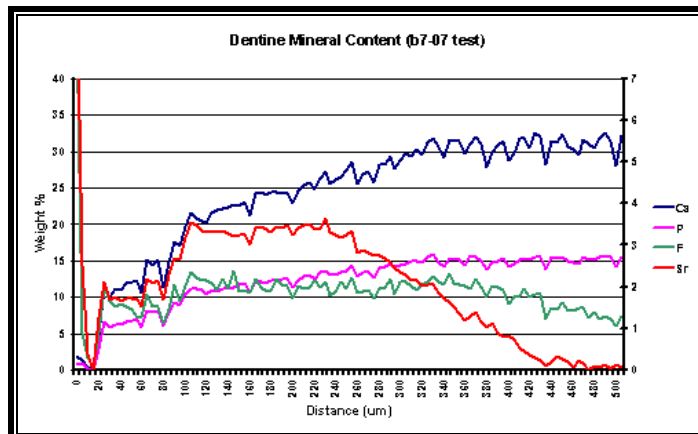


Figure 80: 7 day lesion exposed to Fuji VI for 42 days.

6.3.3.2.3 14 day artificial lesion treated for 21 days

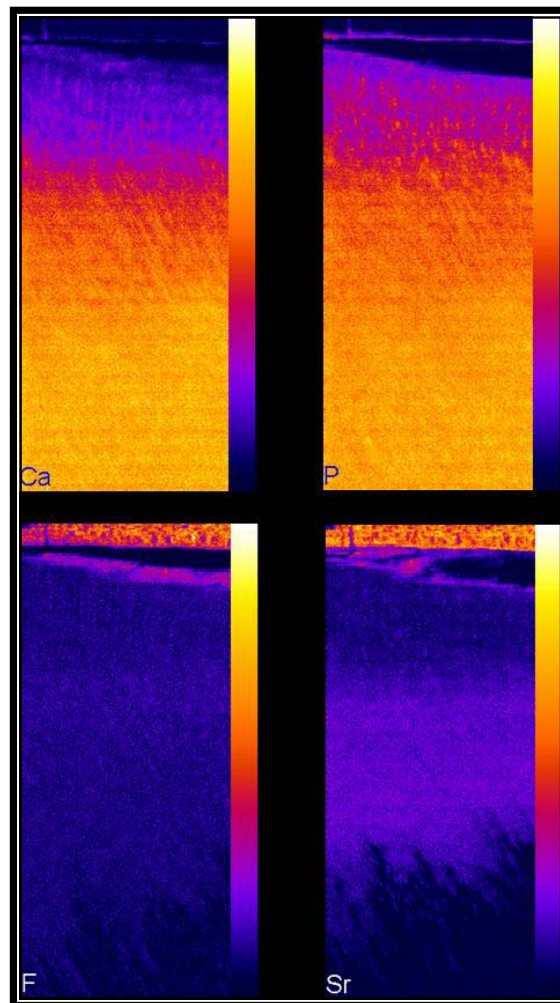
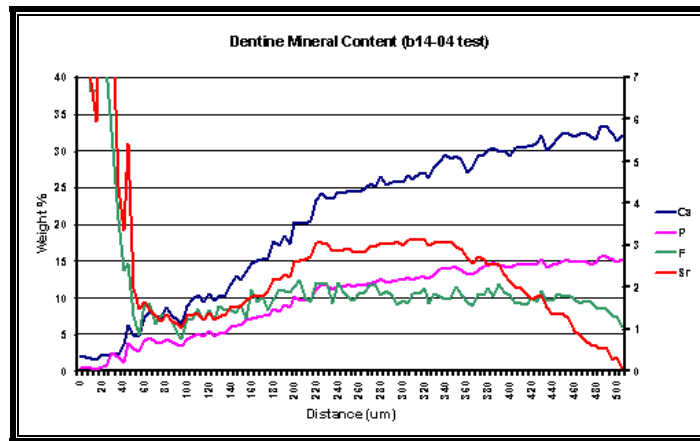


Figure 81: 14 day lesion exposed to Fuji VI for 21 days

6.3.3.2.4 14 day artificial lesion treated for 42 days

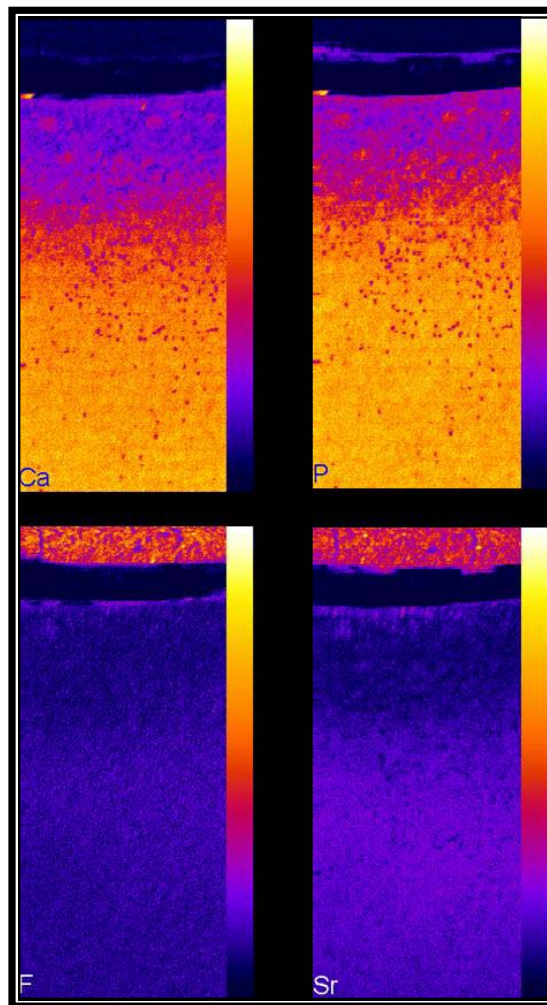
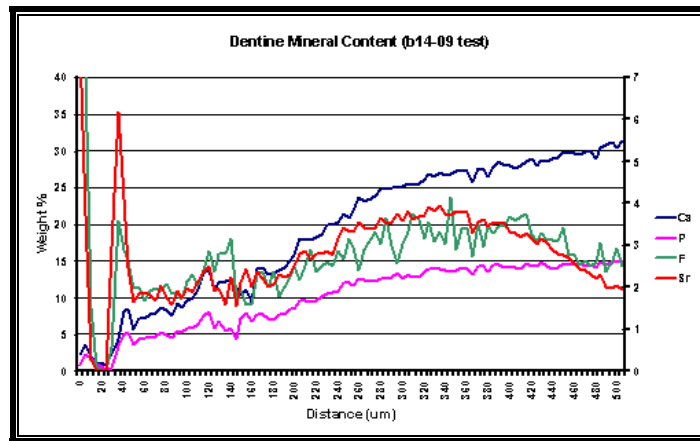


Figure 82: 14 day lesion exposed to Fuji VI for 42 days

6.3.3.2.5 21 day artificial lesion treated for 21 days

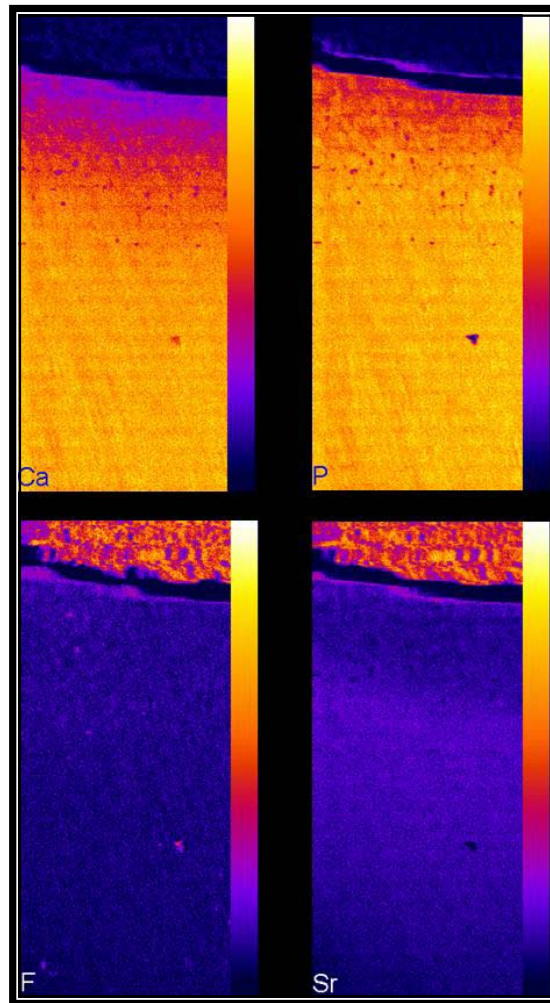
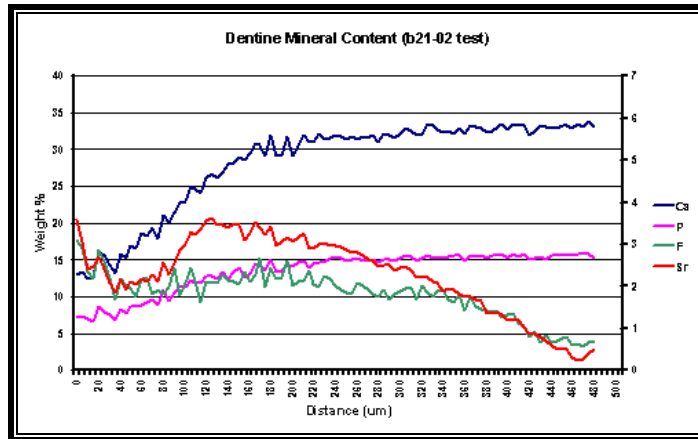


Figure 83: 21 day lesion exposed to Fuji VI for 21 days

6.3.3.2.6 21 day artificial lesion treated for 42 days

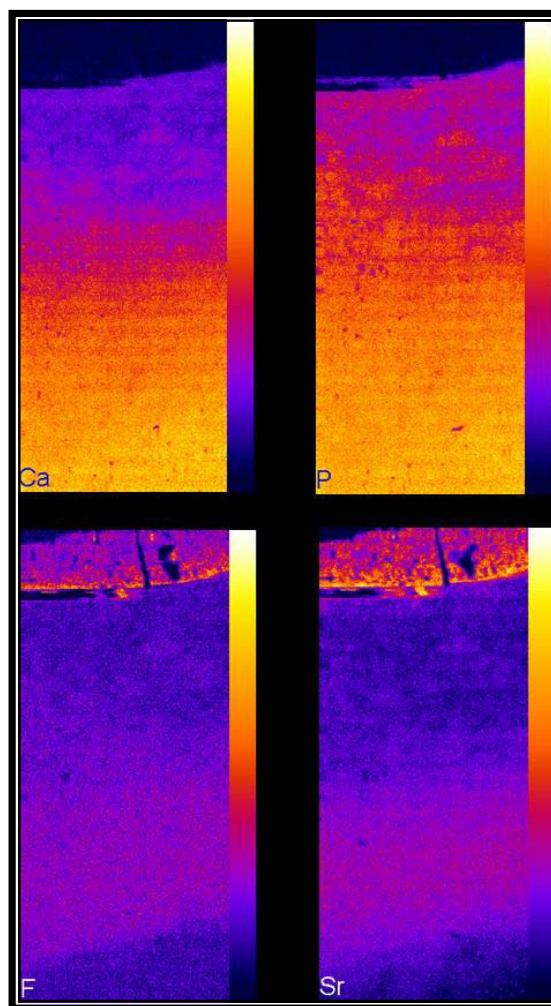
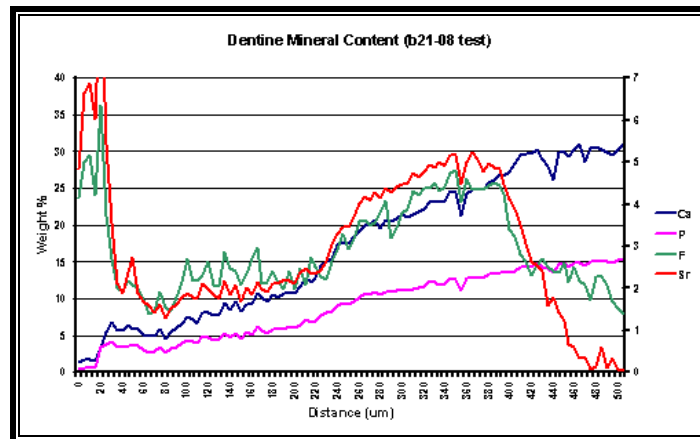


Figure 84: 21 day lesion exposed to Fuji VI for 42 days

6.3.3.3 Statistical analysis

Paired t-test was performed to compare the control and test sides for all groups. There was no significant difference between the two sides of the artificial lesions.

ΔZ_{Ca+P}	7d/21d	7d/42d	14d/21d	14d/42d	21d/21d	21d/42d
Control	3298(2406)	3172(1602)	4214(1813)	3540(1593)	2993(904)	5269(2654)
Test	2127(966)	5314(1905)	3572(1872)	4997(1454)	2091(806)	5125(2741)

Table 21: Intra group consistency between control and test of ΔZ_{Ca+P} for the different groups Paired t-test: Non Significant

6.3.3.3.1 7 day lesion treated with Fuji VI

	21 Days (n=5)	42 Days (n=5)
L F	383.00 (77.35)	413.00 (111.84)
ΔZ F	452.07 (202.68)	858.69 (422.30)
L Sr	271.00 (41.29)	323.00 (100.04)
ΔZ Sr	410.52 (73.11)*	819.73 (310.08)*

Table 22: 7 day lesion, comparison between treatment times with Fuji VI

* One-way ANOVA, Tukey posthoc test, $p < 0.05$

6.3.3.3.2 14 day lesion treated with Fuji VI

	21 Days (n=5)	42 Days (n=5)
L F	459.00 (53.55)	456.00 (14.75)
ΔZ F	387.34 (164.17)*	712.71 (199.95)*
L Sr	411.00 (94.17)	421.00 (72.06)
ΔZ Sr	559.63 (214.31)	774.94 (216.12)

Table 23: 14 day lesion, comparison between treatment times with Fuji VI

* One-way ANOVA, Tukey posthoc test, $p < 0.05$

6.3.3.3.3 21 day lesion treated with Fuji VI

	21 Days (n=5)	42 Days (n=5)
L F	395.00 (97.02)	470.00 (7.07)
ΔZ F	487.90 (135.85)	712.18 (285.34)
L Sr	349.00 (147.96)	342.50 (228.93)
ΔZ Sr	668.23 (313.80)	651.65 (469.80)

Table 24: 21 day lesion, comparison between treatment times with Fuji VI

* One-way ANOVA, Tukey posthoc test, Non Significant

6.4 RMGIC dentine adhesive FujiBond LL

6.4.1 Background

Up to now, only glass-ionomer has demonstrated an ion exchange adhesion to tooth structure. When composite resin is used in a similar situation the bond is micro-mechanical in nature. FujiBond is the only adhesive in which there is a combination of resin with glass-ionomer and this is expected to provide both a mechanical and a chemical bond to tooth structure.

This class of material has been included in this study in the form of FujiBond LL to determine the effect that the presence of resin may have on the ionic exchange process.

6.4.2 Materials and methods

The design of the study and statistical analysis were as previously described in 6.2.2. The focus will be on the placement of the restoration as this is different from the previous two materials.

Half of the cavity was covered with nail varnish (**Figure 45**). The margin of the cavity was refreshed using a diamond bur at high speed. The cavities were treated with Dentine Conditioner (GC Corporation, Tokyo, Japan) for ten seconds, washed with a water spray

for fifteen seconds, dried with a gentle stream of air for fifteen seconds. Fuji Bond LL was mixed according to the manufacturer's instruction, and then applied to the whole cavity using a disposable brush and light-cured for ten seconds (Polylux, Sirona, Germany). A second application was placed before a composite resin was incrementally built using Z100 (3M ESPE, St. Paul, USA). Minimal polishing was carried out. The restored teeth were stored in DDW at 37°C until prepared for EPMA as previously described.

6.4.3 Results

6.4.3.1 Representative EPMA profiles (Fuji Bond LL)

6.4.3.1.1 7 day artificial lesion

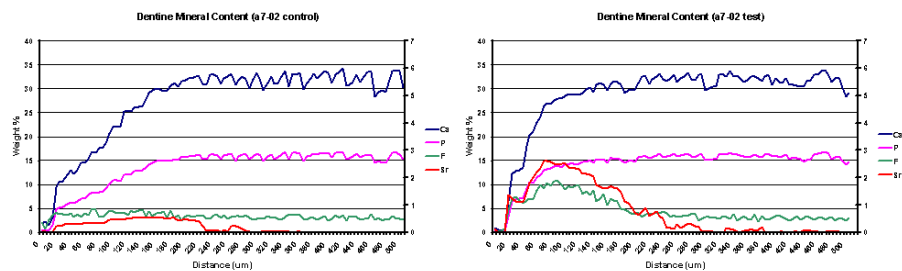


Figure 85: 7 day lesion exposed to Fuji Bond LL for 21 days.

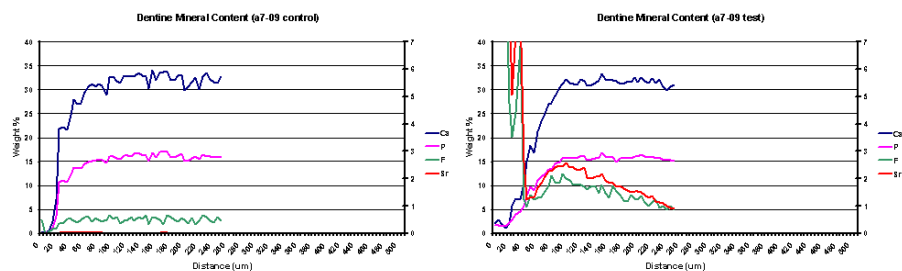


Figure 86: 7 day lesion exposed to Fuji Bond LL for 42 days.

Left: Control, Right: Test.

6.4.3.1.2 14 day artificial lesion

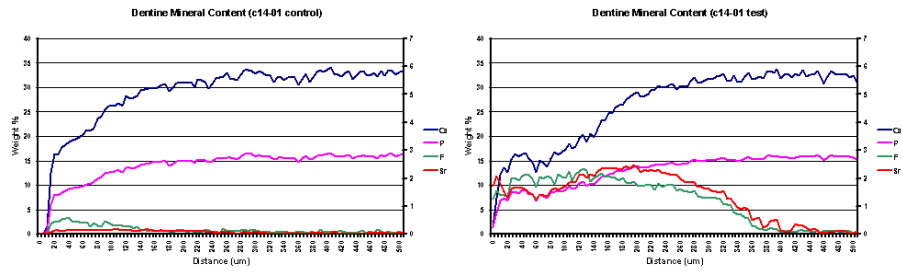


Figure 87: 14 day lesion exposed to Fuji Bond LL for 21 days.

Left: Control, Right: Test.

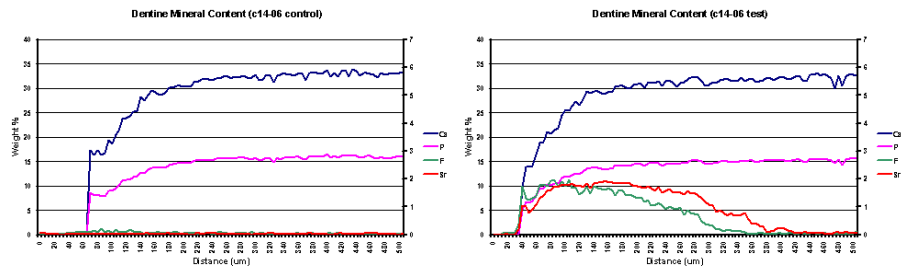


Figure 88: 14 day lesion exposed to Fuji Bond LL for 42 days.

Left: Control, Right: Test.

6.4.3.1.3 21 day artificial lesion

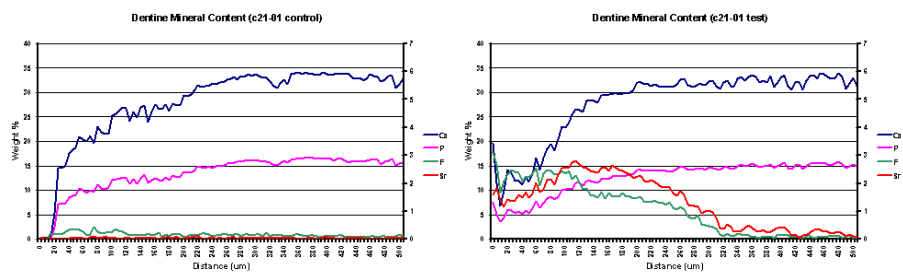


Figure 89: 21 day lesion exposed to Fuji Bond LL for 21 days.

Left: Control, Right: Test.

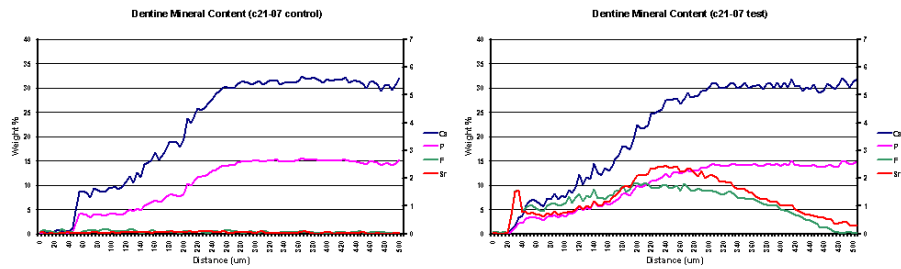


Figure 90: 21 day lesion exposed to Fuji Bond LL for 42 days.

Left: Control, Right: Test.

6.4.3.2 Statistical analysis

Paired t-tests were performed to compare the control and test sides for all groups. There was no significant difference between the two sides of the artificial lesions.

ΔZ_{Ca+P}	7d/21d	7d/42d	14d/21d	14d/42d	21d/21d	21d/42d
Control	2536(2349)	2019(950)	2162(630)	2957(913)	3265(1059)	3187(1442)
Test	2555(2049)	2282(1244)	2741(892)	2851(1217)	3301(1236)	4013(1798)

Table 25: Intra group consistency between control and test of ΔZ_{Ca+P} for the different groups

Paired t-test: Non Significant

6.4.3.2.1 7 day lesion treated with Fuji Bond LL

	21 Days (n=5)	42 Days (n=5)
L F	235.00 (119.53)	320.00 (147.65)
$\Delta Z F$	231.12 (113.73)	362.66 (217.21)
L Sr	224.00 (140.06)	338.00 (102.14)
$\Delta Z Sr$	317.31 (233.96)	576.39 (372.03)

Table 26: 7 day lesion, comparison between treatment times with Fuji Bond LL

One-way ANOVA, Tukey posthoc test, Non Significant

6.4.3.2.2 14 day lesion treated with Fuji Bond LL

	21 Days (n=5)	42 Days (n=5)
L F	277.00 (133.02)	310.00 (127.52)
$\Delta Z F$	235.14 (159.66)	307.99 (221.86)
L Sr	246.00 (139.79)	330.00 (121.60)
$\Delta Z Sr$	342.95 (197.30)	390.22 (296.00)

Table 27: 14 day lesion, comparison between treatment times with Fuji Bond LL

One-way ANOVA, Tukey posthoc test, Non Significant

6.4.3.2.3 21 day lesion treated with Fuji Bond LL

	21 Days (n=5)	42 Days (n=5)
L F	309.00 (107.61)	261.00 (111.43)
$\Delta Z F$	298.14 (149.99)	250.31 (156.48)
L Sr	335.00 (127.13)	259.00 (180.81)
$\Delta Z Sr$	386.70 (237.62)	334.16 (187.74)

Table 28: 21 day lesion, comparison between treatment times with Fuji Bond LL

One-way ANOVA, Tukey posthoc test, Non Significant

6.5 Statistical analysis of combined results for 21 day exposure

The comparison, in ΔZF and ΔZSr for Fuji IXGP, Fuji VI and Fuji Bond LL in the 7 day (**Table 29**), 14 day (**Table 30**) and 21 day (**Table 31**) groups, was carried out and presented below.

	ΔZF	ΔZSr
Fuji IXGP	237.56 (206.91)	277.91 (208.06)
Fuji VI	452.07 (202.68)	410.52 (73.11)
Fuji Bond LL	231.12 (113.73)	317.31 (233.96)

Table 29: The uptake of fluorine and strontium in 7 day group. One-way ANOVA: NS

	ΔZF	ΔZSr
Fuji IXGP	420.65 (203.03)	557.61 (195.43)
Fuji VI	387.34 (164.17)	559.63 (214.31)
Fuji Bond LL	235.14 (159.66)	342.95 (197.30)

Table 30: The uptake of fluorine and strontium in 14 day group. One-way ANOVA: NS

	ΔZF	ΔZSr
Fuji IXGP	527.12(141.56)	476.12 (68.78)
Fuji VI	487.90 (135.85)	668.23 (313.80)
Fuji Bond LL	298.14 (149.99)	386.70 (237.62)

Table 31: The uptake of fluorine and strontium in 21 day group. One-way ANOVA: NS

6.6 Statistical analysis of combined results for 42 day exposure

The comparison, in ΔZF and ΔZSr for Fuji IXGP, Fuji VI and Fuji Bond LL in the 7 day (**Table 32**), 14 day (**Table 33**) and 21 day (**Table 34**) groups, was carried out and presented below.

	ΔZF	ΔZSr
Fuji IXGP	169.28 (56.72)**	196.69 (76.16)*
Fuji VI	858.69 (422.30)** Θ	819.73 (310.08)*
Fuji Bond LL	362.66 (217.21) Θ	576.39 (372.03)

Table 32: The uptake of fluorine and strontium in 7 day group.

One-way ANOVA: * p=0.007, ** p=0.002, Θ p=0.048

	ΔZF	ΔZSr
Fuji IXGP	426.12 (137.16)	780.08 (194.84) Θ
Fuji VI	712.71 (199.95)	774.94 (216.12)*
Fuji Bond LL	307.99 (221.86)	390.22 (296.00)* Θ

Table 33: The uptake of fluorine and strontium in 14 day group.

One-way ANOVA: * p=0.02, Θ p=0.039

	ΔZF	ΔZSr
Fuji IXGP	453.76 (176.20)	444.21 (165.80)
Fuji VI	712.18 (285.34)*	651.65 (469.80)
Fuji Bond LL	250.31 (156.48)*	334.16 (187.74)

Table 34: The uptake of fluorine and strontium in 21 day group.

One-way ANOVA: * p=0.013

6.7 Interpretation

6.7.1 General observations

The paired t-test results indicated that there was no significant difference in the mean $\Delta ZCa+P$ from the control and test sides for all group of samples, **Table 17**, **Table 21** and

Table 25. This confirms the validity of the *in vitro* model and indicates that all three glass-ionomers tested did not change the calcium and phosphorus contents of the artificially demineralised dentine.

There was migration of fluorine and strontium from the three glass-ionomers to the artificially demineralised dentine, the differences in L and ΔZ for Sr and F between control and test were significant. It can be concluded that, for all samples, there was a significant build up of these two elements on the test side.

On the control side, the majority did not show any significant level of fluorine and strontium. It was assumed that any fluorine and strontium found on the control side was due to seepage of these elements, underneath the nail varnish. The following was observed on the control side for the three materials:

- Fuji IXGP, out of thirty samples, two showed a slightly elevated level of strontium and fluorine
- Fuji VI, only four samples showed a level of strontium exceeding 0.5 weight% and twenty two showed a low level of fluorine
- Fuji BondLL, three showed both fluorine and strontium above the 0.5 weight%. This was not present in the remaining twenty seven samples

One possible reason for the observed leakage under Fuji VI was the higher concentration of fluoride it contains. The seepage was restricted only to fluorine and strontium did not behave in a similar fashion. As mentioned earlier, Fuji VI was designed in similar fashion to Fuji IIF and at neutral pH it released fluorine at much higher relative level than the other ions (**Figure 26**). In the case of Fuji IXGP, fluorine and strontium were released at a similar rate (**Figure 30**).

6.7.2 Elemental distribution map

These maps give the overall distribution of a particular element. In this case, the samples were mapped for calcium, phosphorous, strontium and fluorine. There is a strong correlation between the features observed on the mineral profiles and the elemental maps. For example, in **Figure 67** the blue arrow depicted the depth of the artificial lesion as determined by loss of calcium, the red and green arrows showed the depth of penetration of both strontium and fluorine. These features can be easily seen on the corresponding elemental distribution maps.

In **Figure 70**, the different levels of strontium can be easily detected on the elemental map. On the chart, there is a clear pattern to the uptake of strontium. Starting at the interface, there is a narrow band where there is a high level of strontium, follows by a dip then a wide band of higher uptake. This is shown with the three arrows on the chart and the strontium distribution map.

The elemental distribution map can only be used to show a widespread view of the distribution of the different elements. They were acquired using EDS and the colour scale only represents relative concentration.

Chapter 7: Discussion

It is currently recognised that a minimally invasive approach to management of dental caries benefits the long term dental health of the patient (Tyas, Anusavice et al. 2000). This minimally invasive or minimally interventionist approach impacts on restorative procedures leading to a wide variety of modifications of the traditional techniques.

One such technique is the Atraumatic Restorative Technique and its application in both developing and developed countries. In developing countries, it has been used to stem the widespread extraction of carious teeth, in particular for children in remote areas where traditional dental equipment is not available (Frencken, Pilot et al. 1996). In developed countries, it is increasingly used to minimise the removal of dentine in deep cavities, thus reducing the potential for direct pulp exposure and the possible need for endodontic treatment.

The anecdotal and scientific reports that glass-ionomer is able to bring about the remineralisation of partly demineralised dentine are very significant in terms of the preferred approach to management of deep caries lesions. If the circumstances which result in remineralisation of demineralised dentine by glass-ionomer are more fully understood, and this remineralisation can be routinely achieved, it would greatly reduce the amount of pulp damage resulting from the restorative management of caries.

7.1 Restatement of objectives and overall design of the study

The major objective of this study was firstly, to attempt to demonstrate that glass-ionomer does enhance remineralisation of carious dentine *in vivo*, and then to investigate the ways in which this is achieved chemically. It was also hoped that those factors which greatly influence the remineralisation process within this system could be more fully understood.

These objectives have been partially met and also point to the direction in which further investigation should proceed. Also, the results have demonstrated the usefulness of the

analytical method of EPMA, in allowing a greater understanding of the precise chemical nature of the mineral profiles across areas of demineralised tooth structures.

However, because of the difficulties described previously in obtaining optimal conditions for *in vivo* testing of the remineralising effects of glass-ionomer on partially demineralised dentine, it was necessary to modify the original objectives of the study.

Whereas it was hoped to be able to routinely use an *in vivo* model, it became necessary ultimately to confine the project to the use of an *in vitro* model. Furthermore, it was realised that a number of aspects of the technological mechanisms for assessing the degree of de- and remineralisation needed validation. Also it was necessary to profile more fully the environmental interactions of the various glass-ionomers with their usual surroundings. The results of each of these aspects of the investigation are explored more fully below.

7.2 EPMA as a measurement method

The experiment in Chapter 3 was designed to compare the effectiveness of EPMA with TMR, which is a widely accepted tool in the study of remineralisation. As stated in Chapter 3, the results show a strong correlation between the mineral profiles acquired using EPMA and TMR.

The two parameters normally used to express re- and demineralisation in TMR studies, L_d and ΔZ , can also be measured with EPMA. The ΔZ data from TMR are expressed as vol%, while EPMA gives results in weight%. The conversion between the two sets of data is complicated by the fact that, under EPMA, the samples are exposed to high vacuum and the local density is unknown due to the varying degree of shrinkage of partly demineralised dentine.

TMR can only measure total mineral content of the sample, while EPMA has the advantage of being able to identify and quantify the elements present in a very small volume. This is important for this study because one of its objectives is to track the

migration of strontium and fluorine into the demineralised dentine, under different circumstances.

As described previously, the other major advantages of EPMA, in comparison with TMR, are:

- Simple sample preparation: EPMA works with bulk samples while TMR requires the preparation of thin plano-parallel samples, which required a high level of skill to produce consistent results.
- Quantitative data at microstructural level: EPMA analyses a small volume of material, in the range of a few μm^3 , while TMR is a projection technique which measures the sum of total mineral over the thickness of the section.

The disadvantages are:

- Dehydration of the samples: even though the samples were fixed and carefully dehydrated, the effect of shrinkage of demineralised dentine on EPMA results is important but unknown and should be considered when interpreting the results on L_d . Due to this factor, it was decided to focus on describing the mineral profiles of dentine found on the control and test sides of the *in vitro* model, as $\Delta Z_{\text{Ca+P}}$, ΔZ_{Sr} and ΔZ_{F} .
- Dependence on the homogeneity of the samples: dentine poses a problem because of the presence of dentinal tubules. It was shown that the diameters of tubules in demineralised dentine increases in size with the degree of dehydration (Arends and Ruben 1995). This problem was addressed by making EPMA analysis over multiple lines then plot their average values in the final charts.

With the use of appropriate computer software, EPMA can now report results in atomic%, which is useful in exploring the mechanism of the observed movement of the different elements. Unfortunately, this capability was not available when the bulk of analysis for this study was carried out. For future studies, it would also be important to find a way to

convert the ΔZ from volume% to weight%, so a direct comparison between TMR and EPMA can be explored.

In this study, the results from EPMA analysis could be reported in quantitative form, as profiles of the different elements across a surface, and in semi quantitative form as distribution maps of an element. The maps give a general view of the distribution of the various elements and there is good correlation between the two sets of data, as described in 6.2.3.2.

In conclusion, EPMA is a simple and accurate way to study the migration of strontium and fluorine into demineralised dentine. In other studies, it could also be used to map changes in calcium and phosphorus contents and in other component elements of glass-ionomer.

7.3 Selection of glass-ionomer to be tested

The selection of the three glass-ionomers to be tested in the *in vitro* model was based on the results from the experiments described in Chapter 4. Because strontium is interchangeable with calcium, and calcium and fluorine are used to measure the extent of any remineralisation, all glass-ionomers tested were based on strontium formulation. It was also decided to use glass-ionomers from the same manufacturer to minimise manufacturing variables because it was assumed that the glass powders would be treated similarly in the manufacturer's proprietary methods.

- Fuji IXGP was used to allow a direct comparison between the *in vivo* and *in vitro* experiments
- Fuji VI was selected because its fluoride releasing properties are similar to those of Fuji IIF which shows the highest release of fluoride of all materials tested. Fuji IIF was a calcium based glass-ionomer and is no longer available on the market. It was decided to include an experimental material which can be used as a lining under a restorative glass-ionomer

- Fuji BondLL is a resin modified glass-ionomer adhesive which can be used in conjunction with a restorative composite resin. This selection was made based on the relatively high level of release from Fuji II LC Improved, which also belongs to the resin modified glass-ionomer class of material

It has been assumed that fluoride release is the reason for the caries inhibition and remineralising properties associated with glass-ionomers. However, the results of this study show that a significant amount of aluminium and calcium or strontium are lost at the same time. This release does not come with loss of structural integrity of the glass-ionomers as these materials perform reasonably well under clinical conditions (Mount 1986; Ngo, Earl et al. 1986; Mount 1997). It can then be assumed that the mechanism of release is more complex than a straight diffusion of these ions out of the material.

There is a need of a thorough investigation on the potential role that calcium or strontium and aluminium, from glass-ionomers, play in the remineralising process. While the interaction of calcium and strontium with any fluorine ions would enhance remineralisation, aluminium, with its strong complexing properties with fluorine, can have a reverse effect (Curzon and Cutress 1983). Due to the configuration of the EPMA equipment at the time of the study, it was not possible to include aluminium in the study without sacrificing the sensitivity to both strontium and fluorine. This should be part of a future study as aluminium may have an impact on the remineralising process.

Overall, these experiments presented a comprehensive analysis of the nature and quantity of ion release under circumstances resembling those which can occur intra-orally. They also permitted a more rational selection of the glass-ionomers to be tested in later experiments.

7.4 *In vivo* study

Based on the results from the *in vivo* study, it is evident that under clinical conditions both strontium and fluorine migrate from Fuji IXGP into demineralised dentine. This migration seems to peak at the boundary between demineralised and sound dentine, in some specimens the depth of penetration exceeding 1 mm.

The main benefits from the results of this study are:

- Provided an example of mineral profiles under clinical conditions, which information was used in the validation of the *in vitro* model
- Demonstrated very clearly, that a significant level of transfer of strontium and fluorine can occur, which is known to indicate demineralisation

However, there are also the following limitations:

- There is a random mix of depth and degree of demineralisation of dentine
- The initial levels of calcium and phosphorus are unknown, so it is not possible to identify any contribution of pulpal fluid to the remineralisation process

It is important to expand this initial study using either a human or an animal model so that the biological effect on remineralisation can be assessed. One of the early sign of dental caries is increased synthesis of collagen, followed by its mineralisation, which is histologically manifested as reparative dentine formation (Larmas 2003) and this can not be simulated using an *in vitro* model.

7.5 Design and validation of the *in vitro* model

One of the limitations of this study is the inability to account for any contribution to the overall remineralisation process by the dentinal fluid. This is because the original concentrations of calcium and phosphate, left in the carious dentine at the base of the restorations, are unknown. The dentinal fluid contains a high levels of calcium and phosphate (Driessens 1982) so if these are delivered to the front of the lesion they would

also contribute to the overall remineralisation process. However, the most common defense reaction by the pulpo-dentinal organ is tubular sclerosis which results in their eventual occlusion (Massler 1967; Mjor 1983). It is unclear how much of the dentinal fluid actually reaches the demineralised site and this should be the focus for further investigations.

Ideally, the ionic interaction between glass-ionomer and carious dentine should be studied under clinical conditions. However, it was not possible to organise this within the time available for this study, so an *in vitro* model was designed to simulate the ART method of restoration placement.

The results of the experiments in Chapter 5 indicate that the *in vitro* model is suitable for the study of the migration of strontium and fluorine from the glass-ionomer restoration into demineralised dentine because of the following reasons:

- There is consistency of mineral profiles in the control and test areas and the model is reproducible for each of the 7, 14 and 21 day group, as described in 5.2.4.2.
- The profiles of strontium and fluorine collected from the *in vitro* model simulate those found in the *in vivo* study and in both cases the patterns are not consistent with a diffusion process, as described in 5.2.4.3.
- When Fuji IXGP was placed onto sound dentine, there is minimal uptake of both strontium and fluorine. This is restricted to the immediate area at the interface and follows a pattern of diffusion, as described in 5.3.4.

Nail varnish was used to separate and protect the control side of the cavity before the placement of the materials. It was not totally satisfactory as some seepage of fluoride was observed in some of the restorations placed with Fuji VI. It is possible to improve on this by cutting a narrow groove, with a number 1 round steel bur, to separate the test and control sides before applying the nail varnish.

This *in vitro* model allows the study of the effects of two separate variables on the migration of strontium and fluorine into artificially demineralised dentine. The first is the

remaining level of mineral in the dentine following 7, 14 and 21 days of demineralisation, and the second is the exposure time to the glass-ionomers, either 14 or 21 days. However, the effect of the dentinal fluid was not considered in this study and should be included in future studies to complete our understanding of the processes involved.

7.6 Ionic exchange behaviour of the three glass-ionomers and demineralised dentine

For Fuji IXGP, a restorative glass-ionomer with a high powder to liquid ratio, there is no difference in the uptake of both strontium and fluorine when the exposure time is doubled from 21 days to 42 days for the 7, 14 and 21 day lesions. This may be due to the fact that this type of material is designed to become stable very quickly after placement and as such it also loses its reactivity and the potential to further interact with the demineralised dentine.

A similar result is found with Fuji BondLL, even though this material has a low powder to liquid ratio. It is a resin modified glass-ionomer designed as an adhesive to be used in conjunction with a composite resin restorative material. As such, it is light cured immediately after placement and the chemical reaction would be terminated soon after.

For both materials, the longer exposure time of 42 days does not lead to a higher uptake of fluorine and strontium in the demineralised dentine. There is no statistically significant difference in L and ΔZ of strontium and fluorine between the two treatment times.

However, for Fuji VI, there are differences between the two exposure periods:

- In the 7 day group, the longer exposure period of 42 days, leads to a statistically significant higher level of ΔZ_{Sr} and there is also a higher ΔZ_F , but this is not statistically significant (**Table 22**)
- In the 14 day group, the longer exposure time of 42 days leads to a statistically significant higher ΔZ_F and a higher ΔZ_{Sr} which is not statistically significant

- The 21 day group does not show any difference between the two exposure periods

When the effect of material is considered, the following observations can be made:

- With the 21 day exposure, there is no statistically significant difference among the three materials
- However, with 42 day exposure there are differences in all three groups of lesion:
 - In the 7 day lesion which was treated for 42 days, Fuji VI performs much better than Fuji IXGP with both ΔSr and ΔF being more than 400% higher. When comparing with Fuji BondLL, ΔF is over 200% higher with Fuji VI (**Table 32**).
 - In the 14 day lesion, there is no difference between Fuji IXGP and Fuji VI. However, ΔSr for both materials are 200% higher than Fuji BondLL.
 - In the 21 day lesion, there is a difference in ΔF with Fuji VI outperforms Fuji BondLL by close to 300%. Even though there is also a large difference in ΔSr between these two materials, this is not statistically significant.

The better results produced by Fuji VI can be partly explained by the higher release of both fluorine and strontium. The material is designed to have higher reactivity with a longer period of maturation so it can react to demineralised dentine for a longer period.

7.7 Overall summary and conclusion

The results provide a comprehensive analysis of the interaction of glass-ionomers with the various environments with which they are likely to come in contact, in particular with demineralised dentine. This was only possible with the use of the EPMA approach to determine changing mineral profiles with the demineralised dentine.

They demonstrate that remineralisation does take place in terms of strontium replacing lost calcium and that the conditions are created for a more extensive replacement of lost calcium in demineralised dentine through the increased potential for calcium and

phosphate from dentinal tubular fluid to reform lost apatite, assisted by the enhanced levels of fluoride.

To further our understanding of the mechanism involved in the remineralisation of carious dentine, it is suggested that further investigation should include:

- Closer analysis of short term changes in demineralised dentine immediately following glass-ionomer placement
- Studies on the micro-structural and physical changes of the remineralised dentine
- Closer look at the effect of other components of glass-ionomers, such as aluminium and silicate ions on the remineralisation process
- Investigations on the reliability of the remineralisation process, including possible enhancing and inhibiting factors
- Addition of a simulated dentine tubular fluid to the *in vitro* model

In conclusion, the results of this study support the hypothesis that the close adaptation of glass-ionomer cement to demineralised dentine will lead to the uptake of apatite forming ions into dentine and lead to its remineralisation. The combination of Fuji VI with a treatment time of 42 days has the best potential for remineralisation. It involves the diffusion then precipitation of strontium and fluorine in both natural and artificial demineralised dentine. However, further study is required before the mechanism involved can be fully explained.

Bibliography

- Almqvist H, Wefel JS, *et al.* *In vitro* root caries progression measured by 125I absorptiometry: comparison with chemical analysis. *J Dent Res* 1998; 67: 1217-20.
- Anderson MH, Loesch WJ, *et al.* Bacteriologic study of a basic fuchsin caries-disclosing dye. *J Prosthet Dent* 1985; 54: 51-55.
- Angmar Mansson B, Carlstrom P, *et al.* Studies on the ultrastructure of dental enamel. IV. The mineralization of normal human enamel. *J Ultrastruct Res* 1963; 8: 12-23.
- Arends J, Christoffersen J. Nature and role of loosely bound fluoride in dental caries. *J Dent Res* 1990; 69: 634-6.
- Arends J, Christoffersen J, *et al.* Remineralization of bovine dentine *in vitro*. The influence of the F content in solution on mineral distribution. *Caries Res* 1989; 23: 309-14.
- Arends J, Davidson CL. HPO₄ content enamel. *Calcif Tissue Res* 1975; 18: 65-79.
- Arends J, Ruben J. Effect of air-drying on demineralized and on sound coronal human dentine: a study on density and on lesion shrinkage. *Caries Res* 1995; 29: 14-9.
- Arends J, Schuthof J, *et al.* Lesion depth and microhardness indentations on artificial white spot lesions. *Caries Res* 1980; 14: 190-5.
- Arends J, Ten Bosch JJ. *In vivo* de- and remineralization of dental enamel. Factors relating to demineralization and remineralization of the teeth. Leach SA, ed. Oxford, IRL Press. 1985, pp1-11.
- Arends J, ten Bosch JJ. Demineralization and remineralization evaluation techniques. *J Dent Res* 1992; 71: 924-928.
- Armstrong WG. Modifications of the properties and composition of the dentin matrix caused by dental caries. *Adv Oral Biol* 1964; 1: 309-332.
- Armstrong WG. A method for the simultaneous separation and assays of peptides and attached carbohydrate and fluorescent components. *Automat Anal Chem* 1968; 1: 295-9.

- Bakhos Y, Brudevold F, *et al.* In-vivo estimation of the permeability of surface human enamel. *Arch Oral Biol* 1977; 22: 599-603.
- Bao MU, Vernois V, *et al.* Study of physiopathological phenomena in dental enamel by neutron activation analysis. *Biol Trace Elem Res* 1990; 26: 169-76.
- Benelli EM, Serra MC, *et al.* In situ anticariogenic potential of glass-ionomer cement. *Caries Res* 1993; 27: 280-284.
- Bergman G. Microscopic demonstration of liquid flow through human dental enamel. *Arch Oral Biol* 1963; 8: 317-27.
- Bibby BG, Fu J. Effects of fluorides on *in vitro* acid production by dental plaque. *J Dent Res* 1986; 65: 686.
- Bibby BG, van Kesteren M. The effect of fluoride on mouth bacteria. *J Dent Res* 1940; 19: 391.
- Bjorndal L, Larsen MJ, *et al.* A clinical and microbiological study of deep carious lesions during stepwise excavation using long treatment intervals. *Caries Res* 1997; 31: 411-417.
- Bjorndal L, Thylstrup A. A structural analysis of approximal enamel caries lesions and subjacent dentin reactions. *Eur J Oral Sci* 1995; 103: 25-31.
- Bjorndal L, Thylstrup A. A practice-based study on stepwise excavation of deep carious lesions in permanent teeth: a 1-year follow up study. *Community Dent Oral Epidemiol* 1998; 26: 122-128.
- Bodecker CF. Histologic evidence of the benefits of temporary fillings and successful pulp capping of deciduous teeth. *J Am Dent Assoc* 1938; 25: 777-786.
- Boskey AL. The role of Ca-phospholipid-phosphate complexes in tissue mineralization. *Metabol Bone Dis* 1978; 1: 137.
- Boue D, Armau E, *et al.* A bacteriological study of rampant caries in children. *J Dent Res* 1987; 66: 23-8.

- Bowden GHW. Effects of fluoride on the microbial ecology of dental plaque. *J Dent Res* 1990; 69: 653.
- Boyan-Salyers BD. Proteolipid and calcification of cartilage. *Trans Orthopaed Res Soc* 1980; 5: 9.
- Brudevold F, Steadman LT, *et al.* Inorganic and organic components of tooth structure. *Ann N Y Acad Sci* 1960; 85: 110-32.
- Cranfield M, Kuhn AT, *et al.* Factors relating to the rate of fluoride ion release from glass-ionomer cement. *J Dent* 1982; 10: 333-341.
- Creanor SL, Awawdeh LA, *et al.* The effect of a resin-modified glass ionomer restorative material on artificially demineralised dentine caries *in vitro*. *J Dent* 1998; 26: 527-31.
- Crisp S, Wilson AD. Reactions in Glass Ionomer Cement: I. Decomposition of the powder. *J Dent Res* 1974; 53: 1408-1413.
- Curzon ME. Strontium. In: *Trace elements and dental disease*. Curzon ME and Cutress TW, eds. Boston, John Wright PSG Inc; 1983: pp 283-304.
- Curzon ME, Cutress TW. *Trace elements and dental disease*. Curzon ME and Cutress TW, eds. Boston, John Wright PSG Inc; 1983.
- Curzon ME, Losee FL. Strontium content of enamel and dental caries. *Caries Res* 1977; 11: 321-326.
- Daculsi G, LeGeros RZ, *et al.* Possible physico-chemical processes in human dentin caries. *J Dent Res* 1987; 66: 1356-9.
- Darling AI, Mortimer KV, *et al.* Molecular sieve behaviour of normal and carious human dental enamel. *Arch Oral Biol* 1961; 5: 251-73.
- de Josselin de Jong E, ten Bosch JJ, *et al.* Optimised microcomputer-guided quantitative microradiography on dental mineralised tissue slices. *Phys Med Biol* 1987; 32: 887-99.

- de Josselin de Jong E, van der Linden AH, *et al.* Determination of mineral changes in human dental enamel by longitudinal microradiography and scanning optical monitoring and their correlation with chemical analysis. *Caries Res* 1988; 22: 153-9.
- de Josselin de Jong E, van der Linden AH, *et al.* Longitudinal microradiography: a non-destructive automated quantitative method to follow mineral changes in mineralised tissue slices. *Phys Med Biol* 1987; 32: 1209-20.
- De Moor RJG, Verbeek RM, *et al.* Fluoride release profiles of restorative glass-ionomer formulations. *Dent Mater* 1996; 12: 88-95.
- De Schepper EJ, Berry EA, *et al.* Fluoride release from light cure liners. *Am J Dent* 1990; 3: 397-400.
- Dezand T, Johansson B. Experimental secondary caries around restorations in roots. *Caries Res* 1984; 18: 548-554.
- Diaz-Arnold AM, Holmes DC, *et al.* Short term fluoride release/uptake of glass ionomer restoratives. *Dent Mater* 1995; 11: 96-101.
- Dijkman AG, Schuthof J, *et al.* *In vivo* remineralization of plaque-induced initial enamel lesions--a microradiographic investigation. *Caries Res* 1986; 20: 202-8.
- Dimuzio MT, Veis A. Phosphoryns-major non-collagenous proteins of rat incisor dentin. *Calcif Tissue Res* 1978; 25: 169.
- Dreizen S, Spirakis CN, *et al.* *In vitro* studies of the chromogenic reactions between selected carbohydrate derivatives and the amino acids common to human enamel and dentine. *Arch Oral Biol* 1964; 9: 733-7.
- Driessens, FCM. Mineral aspects of dentistry. In: *Monographs in oral science*. H. M. Myers, ed. Basel, Karger; 1982; pp 10.
- Dung T, Liu A. Molecular pathogenesis of root dentin caries. *Oral Dis* 1999; 5: 92-99.
- Eidelman E, Finn SB, *et al.* Remineralization of carious dentin treated with calcium hydroxide. *J Dent Child* 1965; 32: 218-25.

- El-Mallakh BF, Sarkar NK. Fluoride release from glass-ionomer cements in de-ionized water and artificial saliva. *Dent Mater* 1990; 6: 118-122.
- Engel W. Zum biochemischen ablauf der schmelzverfaerbung beim karieprozess unter dem einfluss verschiedener fluorkonzentrationen. *Bull Group Int Rech Sci Stomatol* 1971; 14: 243-58.
- Erickson RL. Surface interactions of dentin adhesive materials. *Oper Dent Suppl* 1992; 5: 81-94.
- Featherstone JD. Consensus conference on intra-oral models: evaluation techniques. *J Dent Res* 1992; 71: 955-956.
- Featherstone JD. Fluoride, remineralization and root caries. *Am J Dent* 1994; 7: 271-4.
- Featherstone JD, McIntyre JM, et al. *Physico-chemical aspects of root caries progression*. Rochester, NY, Eastman Dental Centre; 1987: pp 127-137.
- Featherstone JD, Nelson DG. The effect of fluoride, zinc, strontium, magnesium and iron on the structural disorder in synthetic carbonated apatites. *Aus J Chem* 1980; 33: 2363-2368.
- Featherstone JD, Shields CP, et al. Acid reactivity of carbonated apatites with strontium and fluoride substitutions. *J Dent Res* 1983; 62: 1049-1053.
- Featherstone JD, ten Cate JM, et al. Comparison of artificial caries-like lesions by quantitative microradiography and microhardness profiles. *Caries Res* 1983; 17: 385-91.
- Forss H. The release of fluoride and other elements from light-cured glass ionomers in neutral and acidic conditions. *J Dent Res* 1993; 72: 1257-62.
- Forss H, Jokinen J, et al. Fluoride and *mutans streptococci* in plaque grown on glass-ionomer and composite. *Caries Res* 1991; 25: 454-458.
- Forss H, Seppa L. Prevention of enamel demineralization adjacent to glass-ionomer filling materials. *Scand J Dent Res* 1990; 98: 173-175.

- Forsten L. Short and long term fluoride release from glass ionomers and other fluoride containing filling materials *in vitro*. *Scand J Dent Res* 1990; 98: 179-185.
- Forsten L. Fluoride release and uptake by glass-ionomers. *Scand J Dent Res* 1991; 99: 241-245.
- Forsten L. Resin modified glass ionomer cements: fluoride release and uptake. *Acta Odontol Scand* 1995; 53: 222.
- Forsten L. Fluoride release and uptake by glass-ionomers and related materials and its clinical effect. *Biomaterials* 1998; 19: 503-8.
- Francci C, Deaton TG, *et al*. Fluoride release from restorative materials and its effects on dentin demineralization. *J Dent Res* 1999; 78: 1647-54.
- Frank RM, Voegel JC. Ultrastructure of the human odontoblast process and its mineralization during dental caries. *Caries Res* 1980; 14: 367-380.
- Frencken JE, Pilot T, *et al*. Atraumatic Restorative Treatment (ART): Rationale, Technique, and Development. *J Public Health Dent* 1996; 56: 135-140.
- Friedl KH, Schmalz G, *et al*. Resin-modified glass ionomer cements: fluoride release and influence on *Streptococcus mutans* growth. *Eur J Oral Sci* 1997; 105: 81-5.
- Fusayama T. Ideal cavity preparation for adhesive composites. *Asian J Aesthet Dent* 1993; 1: 55-62.
- Fusayama T, Okuse K, *et al*. Relationship between hardness, discoloration and microbial invasion in carious dentin. *J Dent Res* 1966; 45: 1033-46.
- Fusayama T, Terashima S. Differentiation of two layers of carious dentin by staining. *Bull Tokyo Med Dent Univ* 1972; 19: 83.
- Geiger SB, Weiner S. Fluoridated carbonatoapatite in the intermediate layer between glass ionomer and dentin. *Dent Mater* 1993; 9: 33-6.
- Gelhard TB, Arends J. Remineralisatie van glazuur in een '*in vivo*' model. *Ned Tijdschr Tandheelkd* 1983; 90: 286-91.

- Glimcher MJ. Composition, structure and organization of bone and other mineralized tissues and mechanism of calcification. In: *Handbooks of physiology-endocrinology VII*. Baltimore, Williams & Wilkins; 1976: pp 25.
- Grayson W, Marshall SJ, *et al*. The dentin substrate: structure and properties related to bonding. *J Dent Res* 1997; 25: 441-458.
- Groeneveld A, Arends J. Influence of pH and demineralization time on mineral content, thickness of surface layer and depth of artificial caries lesions. *Caries Res* 1975; 9: 36-44.
- Hallgren A, Oliveby A, *et al*. Salivary fluoride concentrations in children with glass-ionomer cemented orthodontic appliances. *Caries Res* 1990; 24: 239-241.
- Hamilton IR. Biochemical effects of fluoride on oral bacteria. *J Dent Res* 1990; 69: 660.
- Hatibovic-Kofman S, Koch G. Fluoride release from glass-ionomer cement *in vivo* and *in vitro*. *Swed Dent J* 1990; 15: 253-258.
- Hattab FN, el Mowafy OM, *et al*. An *in vivo* study on the release of fluoride from glass-ionomer cement. *Quintessence Int* 1991; 22: 221-224.
- Hauschka PV. *Osteocalcin in developing bone systems, in Vitamin K metabolism and Vitamin K dependent proteins*. Madison, University Park Press; 1979.
- Hayacibara MF, Rosa OPS, *et al*. Effects of Fluoride and Aluminum from Ionomeric Materials on *S. mutans* Biofilm. 2003; 82: 267-271.
- Herkstroter FM, Noordmans J, *et al*. Wavelength-independent microradiography used for quantification of mineral changes in thin enamel and dentin samples with natural surfaces, pseudo-thick tooth sections, and whole teeth. *J Dent Res* 1990; 69: 1824-7.
- Hicks MJ, Flaitz CM, *et al*. Secondary cavities formation *in vitro* lesions around glass-ionomer restorations in human teeth. *Quintessence Int* 1986; 17: 527-532.
- Hilton TJ, Summit JB. Pulpal considerations. In: *Operative Dentistry*. Summitt JB and Robbins JW, eds. Chicago, Quintessence; 2000.

- Hohling HJ, Neubauer G, *et al.* Electron microscopical and laser diffraction studies of nucleation and growth of crystals in the organic matrix of dentine. *Z Zellforsch* 1971; 117: 381.
- Horsted Bindslev P, Larsen MJ. Release of fluoride from conventional and metal-reinforced glass-ionomer cements. *Scand J Dent Res* 1990; 98: 451-5.
- Horsted Bindslev P, Larsen MJ. Release of fluoride from light cured lining materials. *Scand J Dent Res* 1991; 99: 86-8.
- Inaba D, Ruben J, *et al.* Effect of sodium hypochlorite treatment on remineralization of human root dentine *in vitro*. *Caries Res* 1996; 30: 218-24.
- Johnson NW, Taylor BR, *et al.* The response of deciduous dentine to caries studied by correlated light and electron microscopy. *Caries Res* 1969; 3: 348-368.
- Kashani H, Birkhed D, *et al.* Effect of toothpicks with and without fluoride on de- and remineralization of enamel and dentine *in situ*. *Caries Res* 1998; 34: 422.
- Kent BE, Lewis BG, *et al.* Glass ionomer cement formulations: I. The preparation of novel fluoroaluminosilicate glasses high in fluorine. *J Dent Res* 1979; 58: 1607-19.
- Kidd E. How clean must a cavity be before restoration? *Caries Res* 2004; 38: 305-313.
- Kidd E, Joyston-Bechal S, *et al.* The use of a caries detector dye during cavity preparation: a microbiological assessment. *Br Dent J* 1993; 174: 245-248.
- Kidd EAM, Joyston-Bechal S, *et al.* Staining of residual caries under freshly packed amalgam restorations exposed to tea and chlorhexidine *in vitro*. *Int Dent J* 1990; 40: 219-24.
- Kleter GA. Discoloration of dental carious lesions (a review). *Arch Oral Biol* 1998; 43: 629-32.
- Kleter GA, Damen JJ, *et al.* The influence of the organic matrix on demineralization of bovine root dentin *in vitro*. *J Dent Res* 1994; 73: 1523-9.

- Klont B, ten Cate JM. Release of organic matrix components from bovine incisor roots during *in vitro* lesion formation. *J Dent Res* 1990; 69: 896-900.
- Klont B, ten Cate JM. Remineralization of bovine incisor root lesions *in vitro*: the role of the collagenous matrix. *Caries Res* 1991; 25: 39-45.
- Klont B, ten Cate JM. Susceptibility of the collagenous matrix from bovine incisor roots to proteolysis after *in vitro* lesion formation. *Caries Res* 1991; 25: 46-50.
- Koch G, Hatibovic-Kofman S. Glass-ionomer cements as a fluoride release system *in vivo*. *Scand J Dent Res* 1990; 14: 267-273.
- Koulourides T. Dynamics of tooth surface-oral fluid equilibrium. *Adv Oral Biol* 1966; 2: 149-71.
- Koulourides T, Keller SE, *et al*. Enhancement of fluoride effectiveness by experimental cariogenic priming of human enamel. *Caries Res* 1980; 14: 32-9.
- Kuboki Y, Ohgushi K, *et al*. Collagen biochemistry of the two layers of carious dentin. *J Dent Res* 1977; 56: 1233-7.
- Lager A, Thornqvist E, *et al*. Cultivable bacteria in dentine after caries excavation using rose-bur or carisolv. *Caries Res* 2003; 37: 206-211.
- Larmas M. Dental Caries Seen from the Pulpal Side: a Non-traditional Approach. *J Dent Res* 2003; 82: 253-256.
- Larsen MJ, Bruun C. Caries chemistry and fluoride mechanisms of action. In: *Textbook of Clinical Cariology*. Thylstrup A and Fejerskov O, eds. Copenhagen, Munksgaard: 1996; 231-257.
- Lee WLS, Shalita AR, *et al*. Comparative studies of porphyrin production in *Propionibacterium acnes* and *Propionibacterium granulosum*. *J Bacteriol* 1978; 133: 811-5.
- LeGeros RZ. Calcium phosphates in oral biology and medicine. In: *Monographs in oral science*. Myer HM, eds. Basel, Karger. 1991; pp 1-201.

LeGeros RZ, Ming S, *et al.* Chemical stability of carbonate and fluoride containing apatites. *Caries Res* 1983; 17: 419-29.

Leskell E, Ridell K, *et al.* Pulp exposure after stepwise versus direct complete excavation of deep carious lesions in young posterior permanent teeth. *Endod Dent Traumatol* 1996; 12: 192-196.

Little MF, Steadman LT. Chemical and physical properties of altered and sound enamel. IV: Trace element composition. *Arch Oral Biol* 1966; 11: 273-8.

Litwin, M. S. How to measure survey reliability and validity. Los Angeles, Sage Publications 1995.

Magnusson BO, Sundell SO. Stepwise excavation of deep carious lesions in primary molars. *J Int Assoc Dent Child* 1977; 8: 36-40.

Malone WF, Bell C, *et al.* Physicochemical characteristics of active and arrested carious lesions of dentin. *J Dent Res* 1966; 45: 16-26.

Marquis RE. Antimicrobial actions of fluoride for oral bacteria. *Can J Microbiol* 1995; 41: 955.

Massler M. Pulpal reactions to dental caries. *Int Dent J* 1967; 17: 441-460.

Melberg R, Castrovince LA, *et al.* *In vitro* remineralization by monofluorophosphate dentifrice as determined with a thin section sandwich method. *J Dent Res* 1986; 65: 1087.

Mertz Fairhurst EJ, Curtis JW, *et al.* Ultraconservative and cariostatic sealed restorations: results at year 10. *J Am Dent Assoc* 1998; 129: 55-66.

Meryon S, Smith AJ. A comparison of fluoride release from three glass-ionomer cements and a polycarboxylate cement. *Int Endod J* 1984; 17: 16-24.

Mjor IA. Dentin and the pulp. In: *Reaction patterns in human teeth*. Mjor IA, ed. Boca Raton, CRC Press; 1983: pp 63-156.

Momoi Y, Mc Cabe JF. Fluoride release from light activated glass-ionomer restorative cements. *Dent Mater* 1993; 9: 151-154.

- Mount GJ. Longevity of glass ionomer cements. *J Prosthet Dent* 1986; 55: 682-5.
- Mount GJ. Clinical considerations in the prevention and restoration of root surface caries. *Am J Dent* 1988; 1: 163-8.
- Mount GJ. Longevity in glass-ionomer restorations: review of a successful technique. *Quintessence Int* 1997; 28: 643-50.
- Nakajima M, Sano H, *et al.* Tensile bond strength and SEM evaluation of caries-affected dentin using dentin adhesives. *J Dent Res* 1995; 74: 1679-88.
- Nawrot CF, Campbell DJ, *et al.* Dental phosphoprotein induced formation of hydroxyapatite during *in vitro* synthesis of amorphous calcium phosphate. *Biochem J* 1976; 5: 3445.
- Ngo H. Biological potential of glass-ionomer. In: *An atlas of glass ionomer cements*. Mount GJ, ed. London, Martin Dunitz; 2002: pp 43-55.
- Ngo H, Earl A, *et al.* Glass-ionomer cements: a 12-month evaluation. *J Prosthet Dent* 1986; 55: 203-5.
- Ngo H, Fraser M, *et al.* Remineralisation of artificial carious dentine exposed to two glass ionomers. *J Dent Res* 2002; 81: 386.
- Ngo H, Mount GJ, *et al.* A study of glass-ionomer cement and its interface with enamel and dentin using a low-temperature, high-resolution scanning electron microscopic technique. *Quintessence Int* 1997; 28: 63-9.
- Ngo H, Ruben J, *et al.* Electron probe microanalysis and transverse microradiography studies of artificial lesions in enamel and dentin: a comparative study. *Adv Dent Res* 1997; 11: 426-32.
- Nikiforuk G. *Understanding Dental Caries/Etiology and Mechanisms, Basic and Clinical Aspects*. Basel, Karger; 1985.
- Ogaard B, ten Bosch J, *et al.* Quantitative longitudinal study of the remineralization of induced lesions in vital teeth. *Caries Res* 1989; 23: 436.

- Oppermann RV, Rolla G. Effect of some polyvalent cations on the acidogenicity of dental plaque *in vivo*. *Caries Res* 1980; 14: 422-427.
- Perdigao J, Swift EJ. Analysis of dental adhesive systems using scanning electron microscopy. *Int Dent J* 1994; 44: 349-59.
- Poole DFG, Tailby PW, *et al*. The movement of water and other molecules through human enamel. *Arch Oral Biol* 1963; 8: 771-2.
- Povis DR, Pioneer HJ, *et al*. Long term monitoring of microleakage of dental cements by radiochemical diffusion. *J Prosthet Dent* 1988; 59: 651-657.
- Reiss A. Ueber oxydasen der Karies-Erreger und ihren einfluss auf die harten zahnsbstanzen. *Zahnaerztl Rundschau* 1938; 47: 2033-41.
- Retief DH, Bradley EL, *et al*. Enamel and cementum fluoride uptake from a glass-ionomer cement. *Caries Res* 1984; 18: 250-257.
- Rezk Lega F, Ogaard B, *et al*. Availability of fluoride from glass-ionomer luting cements in human saliva. *Scand J Dent Res* 1991; 99: 60-63.
- Ribeiro C, Baratieri LN, *et al*. A clinical, radiographic and scanning electron microscope evaluation of adhesive restorations on carious dentin in primary teeth. *Quintessence Int* 1999; 30: 591-599.
- Robinson R. The possible significance of hexosephosphate esters in ossification. *Biochem J* 1923; 17: 286.
- Saito S, Tosaki S, *et al*. Characteristics of Glass-Ionomer Cements. In: *Advances in Glass-Ionomer Cements*. Davidson CL and Mjor IA, eds. Carol Stream, Quintessence Books; 1999: pp 15-50.
- Sakkab NY, Cilley WA, *et al*. Fluoride in deciduous teeth from an anti-caries clinical study. *J Dent Res* 1984; 63: 1201-1205.
- Seppa L, Salmenkivi S, *et al*. Enamel and plaque fluoride following glass-ionomer application *in vivo*. *Caries Res* 1992; 26: 340-344.

- Seppa L, Torppa-Saarinen E, *et al.* Effect of different glass ionomers on the acid production and electrolyte metabolism of *Streptococcus mutans*. *Caries Res* 1992; 26: 434-438.
- Shah HN, Bonnett R, *et al.* The porphyrin pigmentation of subspecies of bacteroides melaninogenicus. *Biochim J* 1979; 180: 45-50.
- Shrout PE, Fleiss JL. Intraclass correlations: Uses in assessing rater reliability. *Psychological Bulletin* 1979; 86: 420-428.
- Silverstone LM, Hicks MJ. The structure and ultrastructure of the carious lesion in human dentin. *Gerodontics* 1985; 1: 185-195.
- Skartveit L, Tveit AB, *et al.* *In vivo* fluoride uptake in enamel and dentin from fluoride-containing materials. *J Dent Child* 1980; 57: 97-100.
- Sognaes RF, Shaw JH, *et al.* Radiotracer studies on bone, cementum, dentin and enamel of rhesus monkeys. *Am J Physiol* 1955; 180: 409-420.
- Stanley HR, Pemeira JC, *et al.* The detection and prevalence of reactive and physiologic sclerotic dentin, reparative dentin and dead tracts beneath various types of dentinal lesions according to tooth surface and age. *J Path* 1983; 12: 257-289.
- Strang R, Damato FA, *et al.* Comparison of *in vitro* demineralization of enamel sections and slabs. *Caries Res* 1988; 22: 348-349.
- Sullivan RJ, Charig A, *et al.* *In vivo* detection of calcium from dicalcium phosphate dihydrate dentifrices in demineralized human enamel and plaque. *Adv Dent Res* 1997; 11: 380-7.
- Suzuki Y, Tosaki S, *et al.* Physical properties of glass-ionomer for restorative filling. *J Dent Res* 1995; 74: 561.
- Swartz MC, Phillips RW, *et al.* Long term F release from glass-ionomer cements. *J Dent Res* 1984; 63: 158-160.

Swift EJ. *In vitro* caries inhibitory properties of a silver cermet. *J Dent Res* 1989; 68: 1088-1093.

Takahashi K, Emilson CG, *et al.* Fluoride release *in vitro* from various glass-ionomer cements. *Dent Mater* 1993; 9: 350-354.

Tam LE, Chan GP, *et al.* *In vitro* caries inhibition effects by conventional and resin-modified glass-ionomer restorations. *Oper Dent* 1997; 22: 4-14.

Tam LE, McComb D, *et al.* Physical properties of proprietary light-cured lining materials. *Oper Dent* 1991; 16: 210-217.

ten Bosch JJ, Angmar Mansson B. A review of quantitative methods for studies of mineral content of intra-oral caries lesions. *J Dent Res* 1991; 70: 2-14.

ten Cate JM, Buijs MJ, *et al.* The effects of GIC restoration on enamel and dentin demineralization and remineralization. *Adv Dent Res* 1995; 9: 384-388.

ten Cate JM, Damen JJ, *et al.* Inhibition of dentin demineralization by fluoride *in vitro*. *Caries Res* 1998; 32: 141-7.

ten Cate JM, Duijsters PP. Alternating demineralization and remineralization of artificial enamel lesions. *Caries Res* 1982; 16: 201-10.

ten Cate JM, Exterkate RA. Use of the single section technique in caries research. *Caries Res* 1986; 20: 525-528.

ten Cate JM, Featherstone JD. Mechanistic aspects of the interactions between fluoride and dental enamel. *Crit Rev Oral Biol Med* 1991; 2: 283-96.

ten Cate JM, van Duinen RN. Hypermineralization of dentinal lesions adjacent to glass-ionomer cement restorations. *J Dent Res* 1995; 74: 1266-71.

Thewlis J. The structure of teeth as shown by X-ray examination. *Medical Research Council Special Report No:238*. London 1940.

Thorton JB, Retief DH, *et al.* Fluoride release from and tensile bond strength of Ketac-Fil and Ketac-Silver to enamel and dentin. *Dent Mater* 1986; 2: 241-245.

- Thylstrup A, Qvist V. Principal enamel and dentine reactions during caries progression. In: *Dentine and dentine reactions in the oral cavity*. Thylstrup A, Leach SA and Qvist V, eds. Oxford, IRL Press; 1987: pp 3-16.
- Torell P. Determination of iron in dental enamel. *Odont Tidskr* 1957; 65: 20-3.
- Torell P. The substance of arrested caries in relation to intact enamel. *Odont Tidskr* 1957; 65: 28-35.
- Trautz OR. Crystalline organization of dental mineral. In: *Structural and chemical organization of teeth*. Miles AEW, ed. Washington, Academic Press; 1967: 165-197.
- Tsanidis V, Koulourides T. An *in vitro* model for assessment of fluoride uptake from glass-ionomer cements by dentin and its effect on acid resistance. *J Dent Res* 1992; 71: 7-12.
- Tveit AB. Fluoride uptake by enamel surfaces, root surfaces and cavity walls following application of a fluoride varnish *in vitro*. *Caries Res* 1980; 14: 315-323.
- Tveit AB, Totdal B, Klinge B, Selvig KA. Fluoride uptake by dentin surfaces following topical application of TiF₄, NaF and Fluoride Varnishes *in vivo*. *Caries Res* 1985; 19: 240-247.
- Tyas MJ, Anusavice KJ, *et al*. Minimal intervention dentistry--a review. FDI Commission Project 1-97. *Int Dent J* 2000; 50: 1-12.
- Van Dyke TF, Levine MJ, *et al*. Isolation of low molecular weight glycoprotein inhibitor of calcium phosphate precipitation from the extra-parotid saliva of macaque monkeys. *Arch Oral Biol* 1979; 24: 85.
- van Reenen JF. The yellow brown pigmentation of dental caries. A survey of the literature. *J Dent Assoc S Afr* 1955; 10: 262-267.
- Walls AWG. Glass polyalkenoate (glass ionomer) cements: A review. *J Dent* 1986; 14: 231-246.
- Weatherell JA, Robinson C. The inorganic composition of teeth. In: *Biological mineralization*. Zipkin I, ed. New York, Wiley; 1973: pp 43-74.

- Wefel JS, Clarkson BH, *et al.* Natural root caries: a histologic and microradiographic evaluation. *J Oral Pathol* 1985; 14: 615-623.
- Wefel JS, Maharry GJ, *et al.* Development of an intra-oral single section remineralization model. *J Dent Res* 1987; 66: 1485-1489.
- Wesenberg G, Hals E. The *in vitro* effect of a glass ionomer cement on dentine and enamel walls. An electron probe and microradiographic study. *J Oral Rehabil* 1980; 7: 35-42.
- White DJ. Reactivity of fluoride dentifrices with artificial caries. I. Effects on early lesions: F uptake, surface hardening and remineralization. *Caries Res* 1987; 21: 126-40.
- White DJ. Use of synthetic polymer gels for artificial carious lesion preparation. *Caries Res* 1987; 21: 228-42.
- White DJ. Reactivity of fluoride dentifrices with artificial caries. II. Effects on subsurface lesions: F uptake, F distribution, surface hardening and remineralization. *Caries Res* 1988; 22: 27-36.
- White DJ. The application of *in vitro* models to research on demineralization and remineralization of the teeth. *Adv Dent Res* 1995; 9: 175-93.
- White DJ, Bowman WD, *et al.* 19F MAS-NMR and solution chemical characterization of the reactions of fluoride with hydroxyapatite and powdered enamel. *Acta Odontol Scand* 1988; 46: 375-89.
- White DJ, Nancollas GH. Physical and chemical considerations of the role of firmly and loosely bound fluoride in caries prevention. *J Dent Res* 1990; 69: 634-6.
- Wilson AD. The chemistry of dental cements. *Chem Soc Rev* 1978; 77: 265-96.
- Wilson AD, Crisp S, *et al.* Aluminosilicate glasses for polyelectrolyte cements. *Ind Eng Chem Prod Res Dev* 1980; 19: 263-270.
- Wilson AD, Groffman DM, *et al.* The release of fluoride and other chemical species from a glass-ionomer cement. *Biomaterials* 1985; 6: 431-3.

Wilson AD, Kent BE. A new translucent cement for dentistry. The glass ionomer cement. *Br Dent J* 1972; 132: 133-5.

Wilson AD, Mc Lean JW. *Glass-Ionomer Cement*. Chicago, Quintessence; 1988.

Yap AU, Khor E, *et al*. Fluoride release and antibacterial properties of new-generation tooth-colored restoratives. *Oper Dent* 1999; 24: 297-305.

Yen PKJ, Bogoroch R, *et al*. Topographic sampling method for quantitative radiotracer evaluation in bones and teeth. *J Dent Res* 1958; 37: 458-66.

Zero DT, Rahbek I, *et al*. Comparison of the iodide permeability test, the surface microhardness test, and mineral dissolution of bovine enamel following acid challenge. *Caries Res* 1990; 24: 181-8.

Zuidegeest TG, Herkstroter FM, *et al*. Mineral density and mineral loss after demineralization at various locations in human root dentine. A longitudinal microradiographic study. *Caries Res* 1990; 24: 159-63.

Appendix A: Additional results for Chapter 4

Ketac Cem: Incremental Release

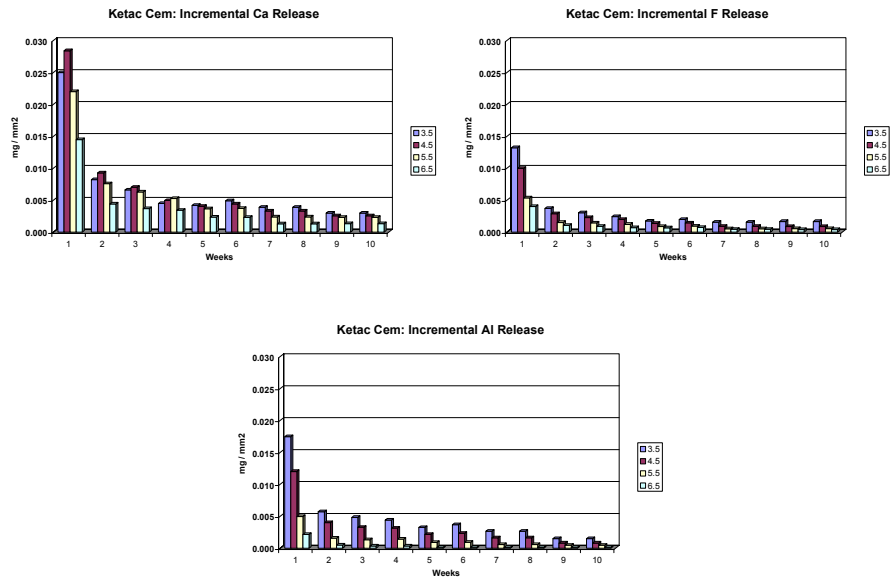


Figure 91: Ketac Cem, relative incremental release of Ca, F and Al at different pH

Ketac Bond: Incremental Release

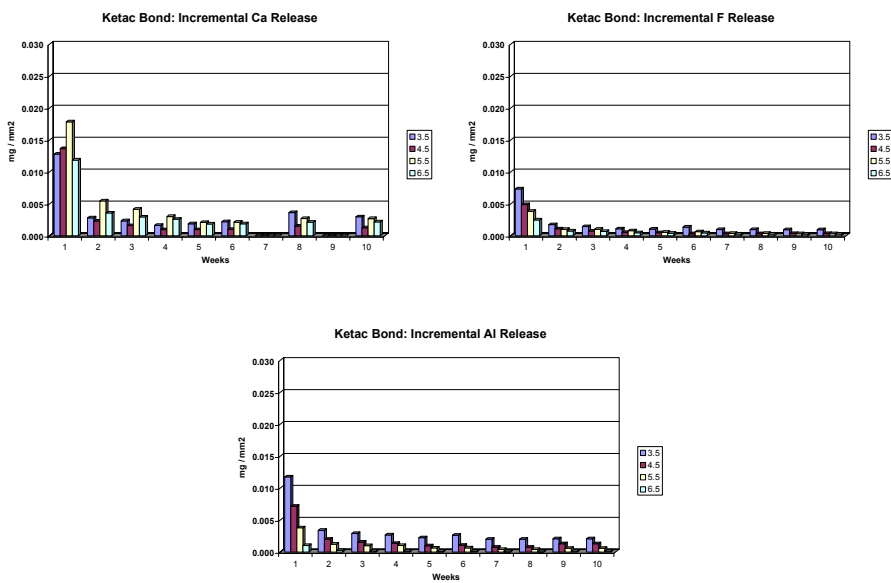


Figure 92: Ketac Bond, relative incremental release of Ca, F and Al at different pH

Fuji II: Incremental Release

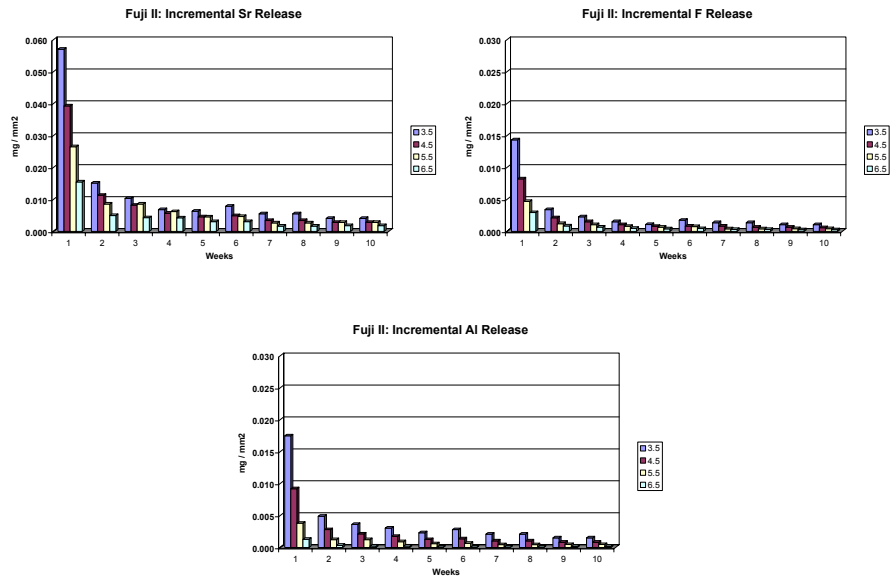


Figure 93: Fuji II, relative incremental release of Sr, F and Al at different pH

Fuji II F: Incremental Release

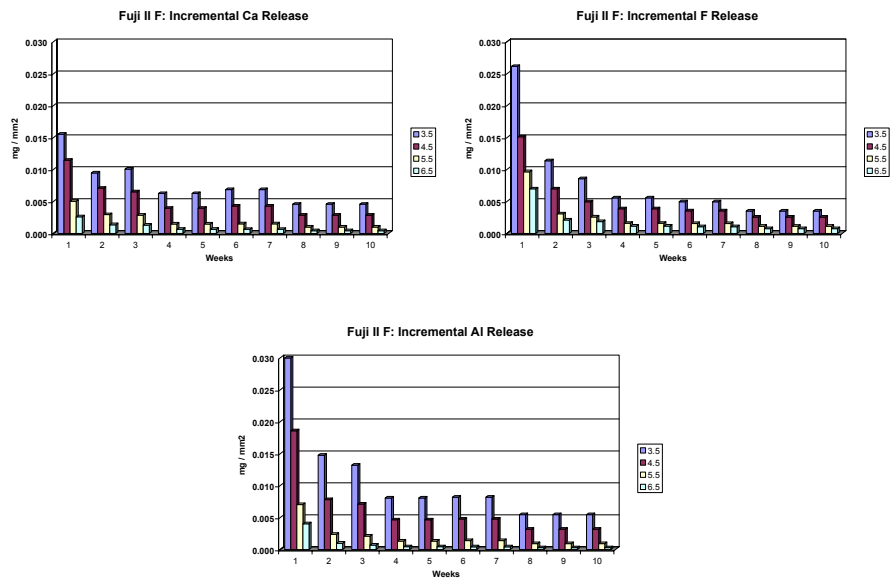


Figure 94: Fuji II F, relative incremental release of Ca, F and Al at different pH

Fuji II LC Improved: Incremental Release

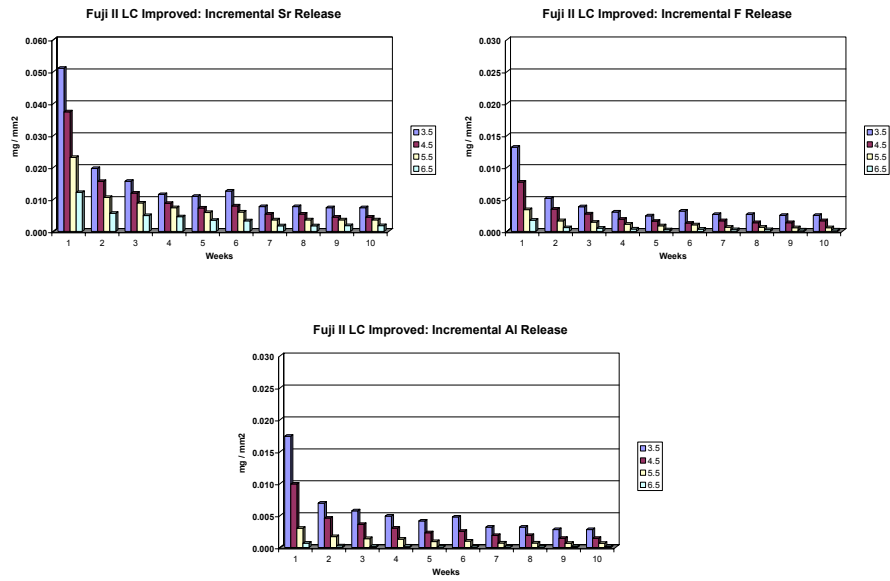


Figure 95: FujiII LCImproved, incremental release of Sr, F and Al at different pH

Ketac Fil Plus: Incremental Release

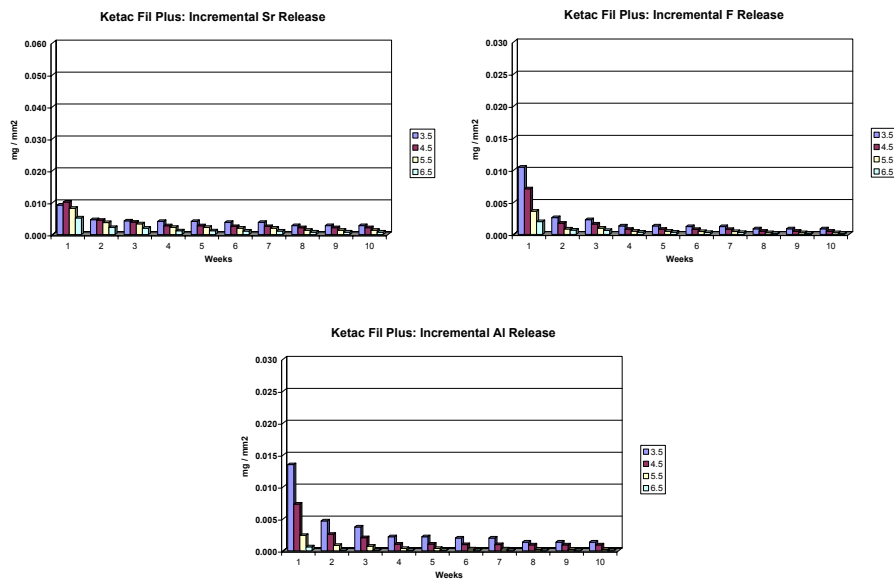


Figure 96: Ketac Fil Plus, incremental release of Sr, F and Al at different pH

Ketac Molar: Incremental Release

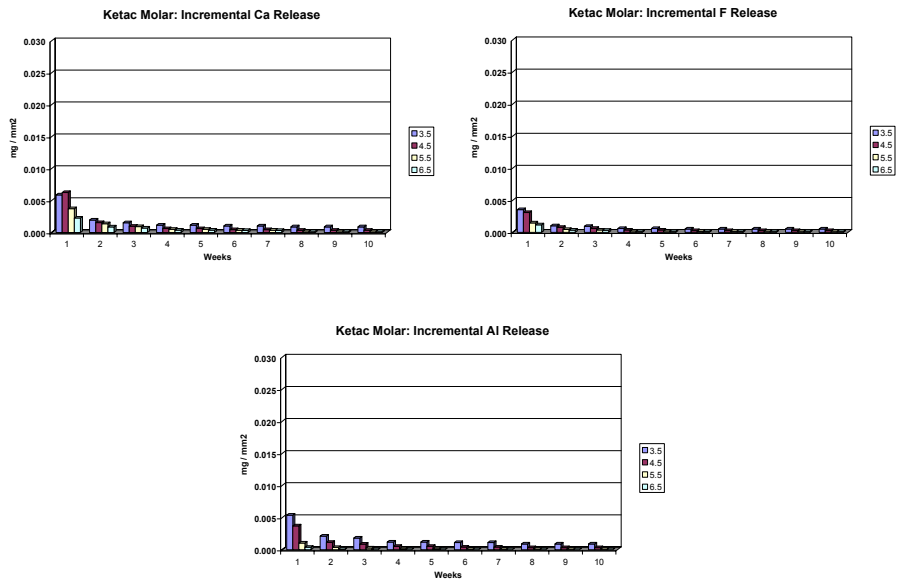


Figure 97: Ketac Molar, incremental release of Ca, F and Al at different pH

Fuji IXGP: Incremental Release

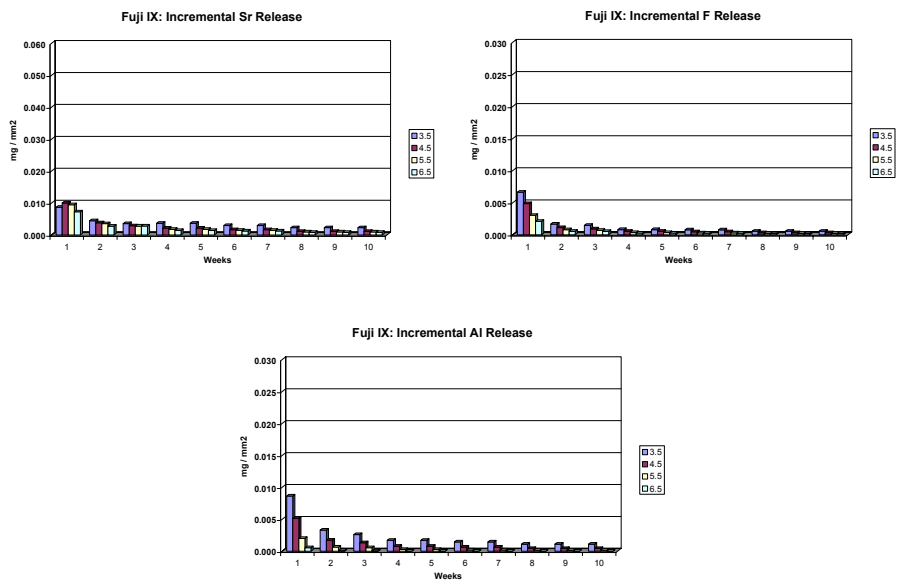


Figure 98: Fuji IXGP, incremental release of Sr, F and Al at different pH

APPENDIX B: Additional results for Chapter 5.1

This section contains the full results for Chapter 5. Each of the thirteen samples will have a SEM micrograph showing the region of interest and the mineral profiles collected from different areas of the lesions. Samples 12 and 13 did not have much demineralised dentine left under the glass-ionomer.

Sample 1: Coded as FG46

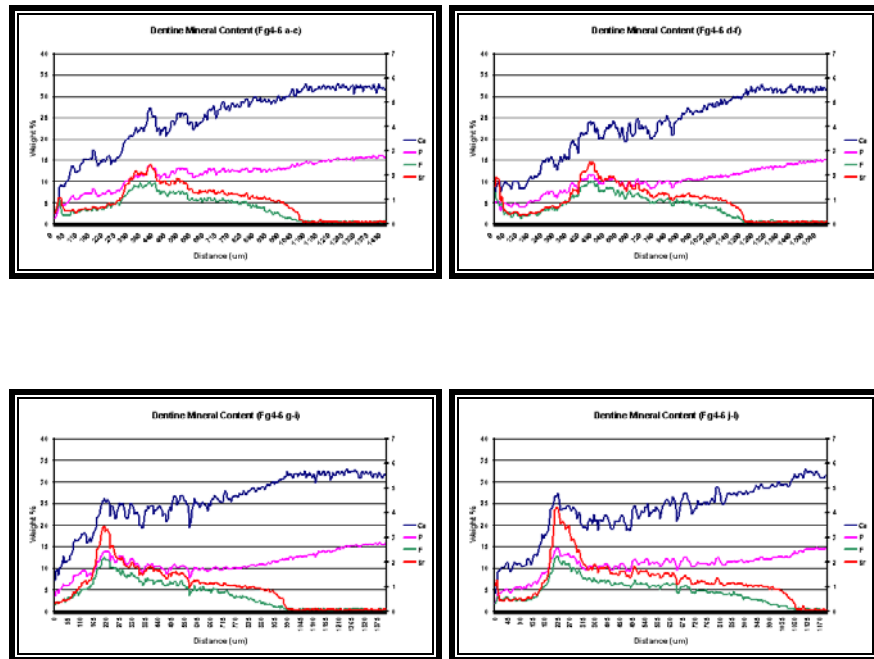
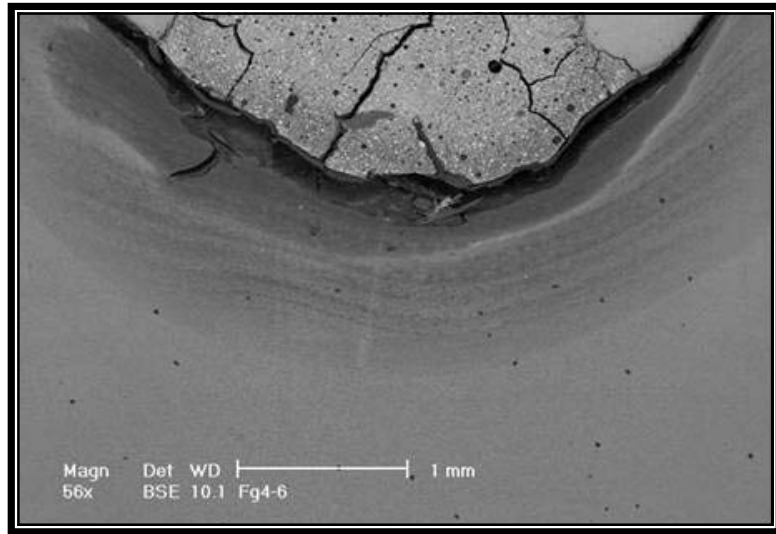


Figure 99: Mineral profiles of four regions in sample FG46

Sample 2: Coded as FG95

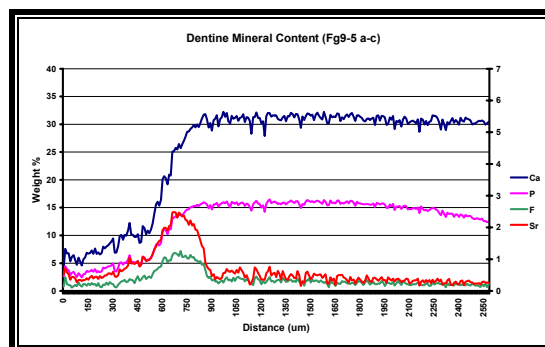
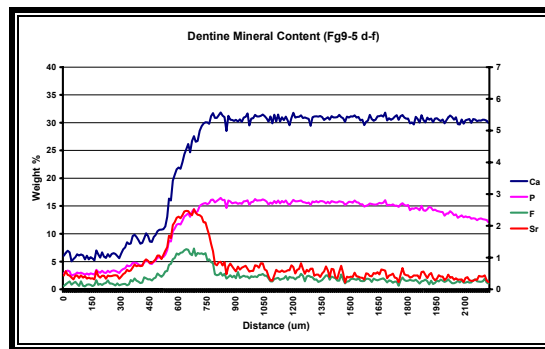
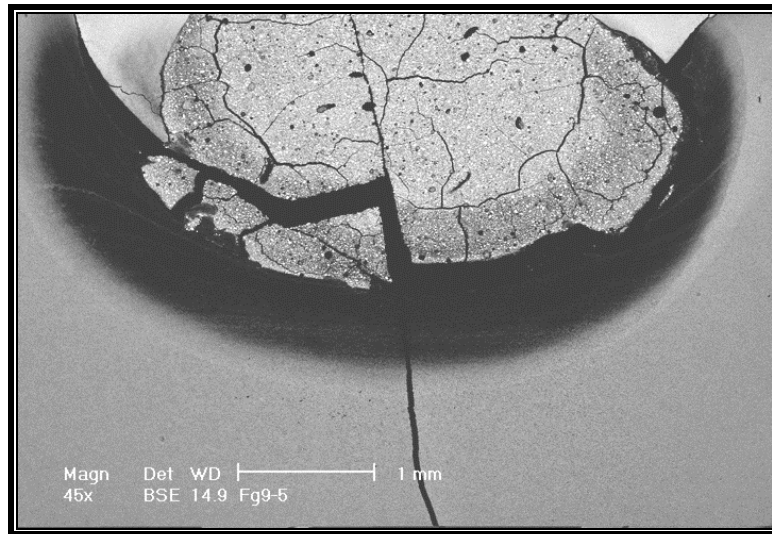


Figure 100: Mineral profiles of two regions in sample FG95

Sample 3: Coded as FG22

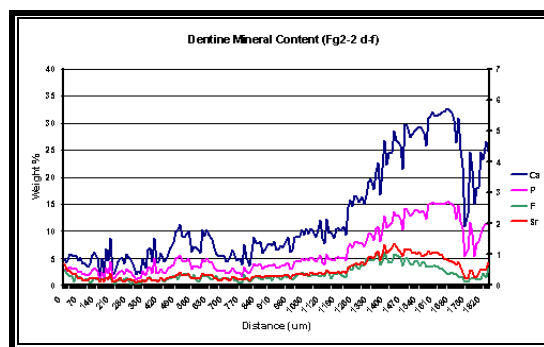
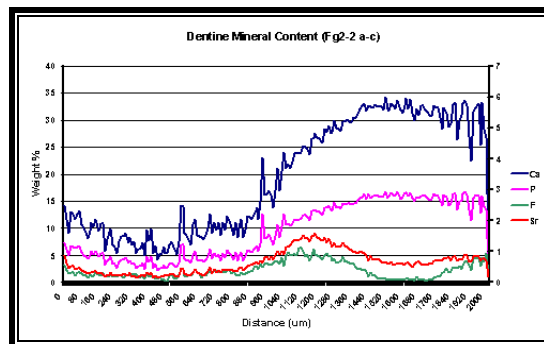
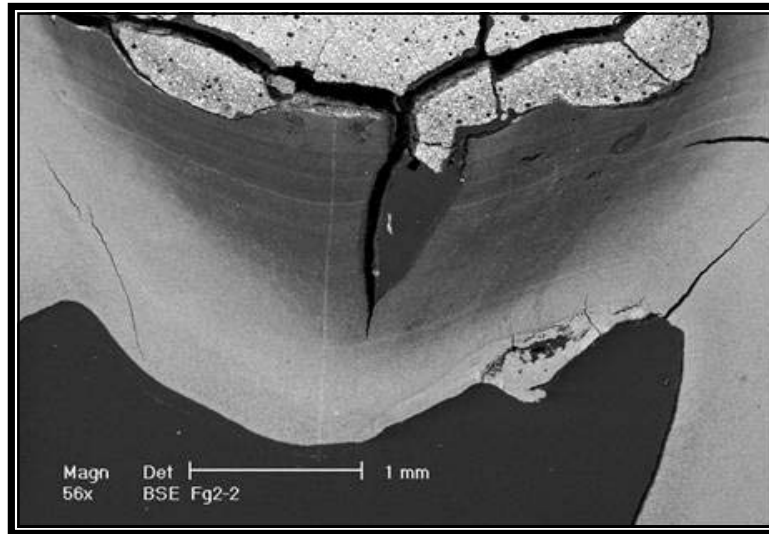


Figure 101: Mineral profiles in two regions of FG22

Sample 4: Coded as FG32

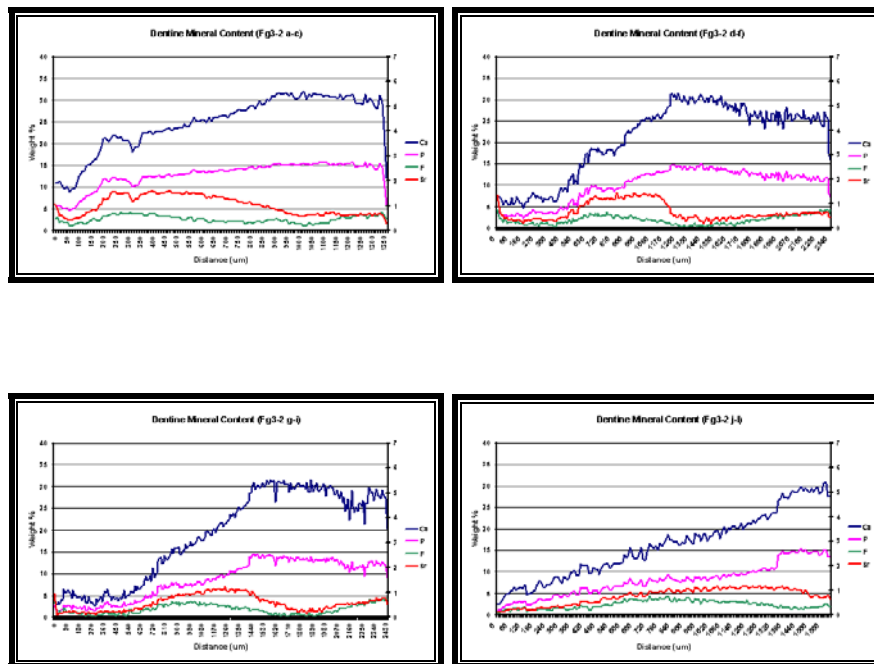
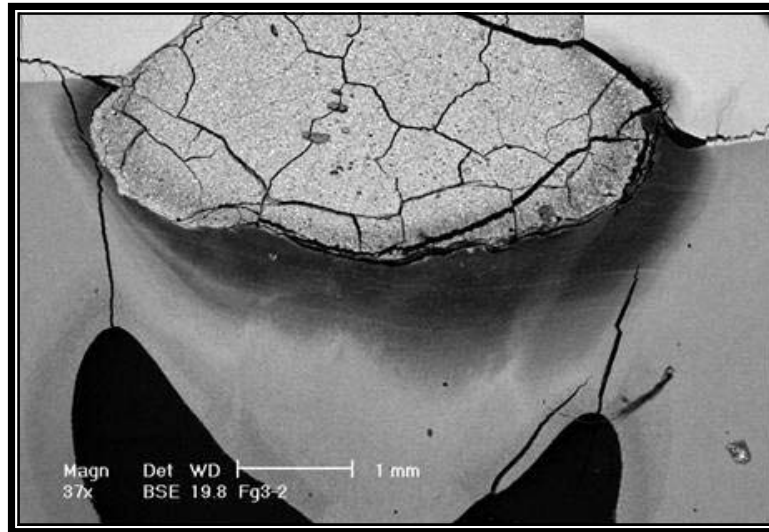


Figure 102: Mineral profiles of four regions in sample FG32

Sample 5: Coded as FG54

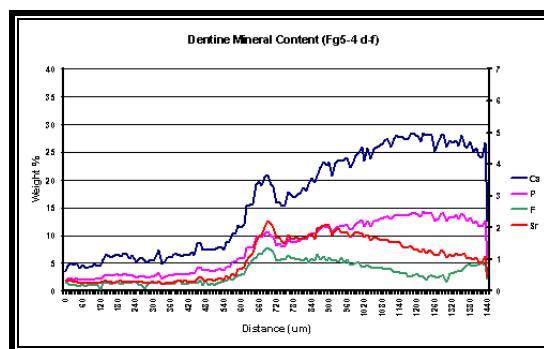
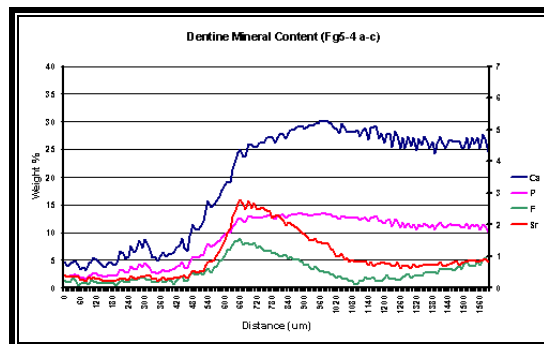
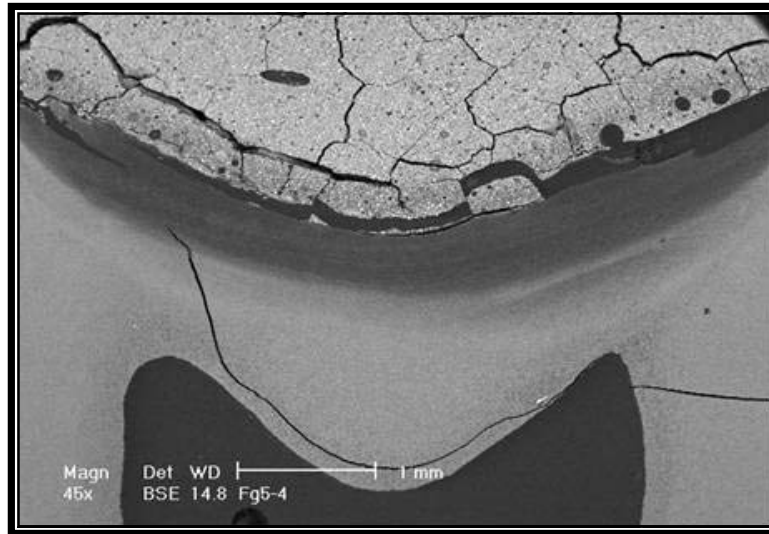


Figure 103: Mineral profiles in two regions of FG54

Sample 6: Coded as FG61

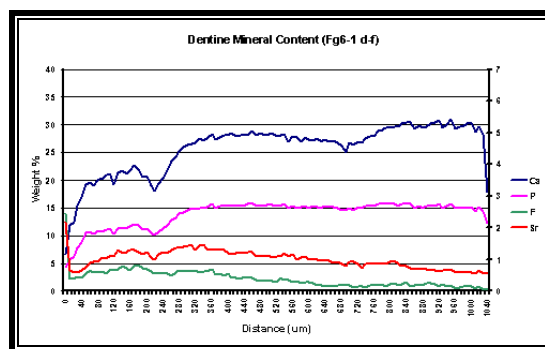
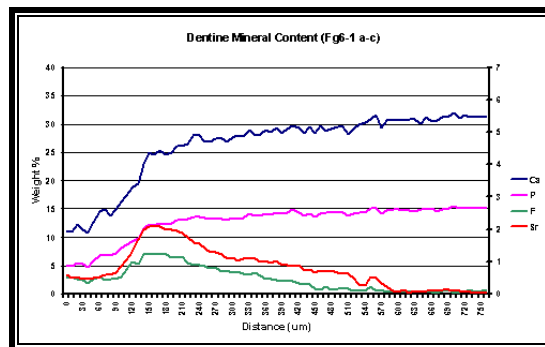
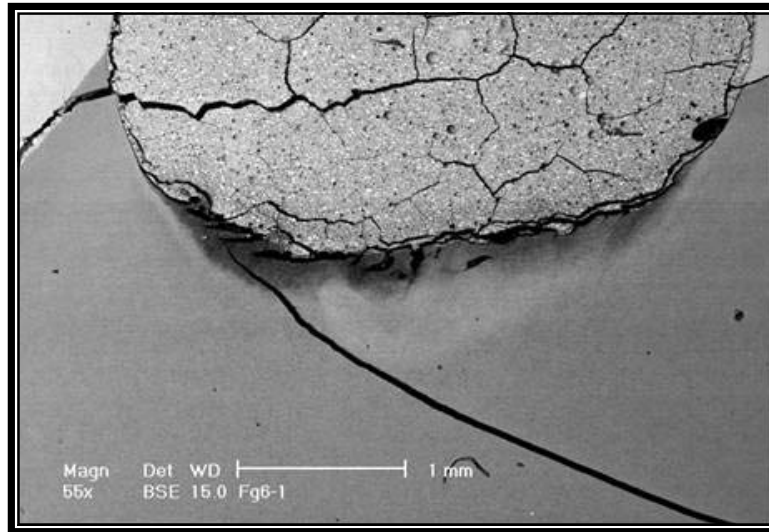


Figure 104: Mineral profiles in two regions of FG61

Sample 7: Coded as FG72

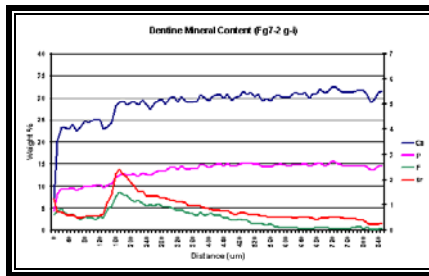
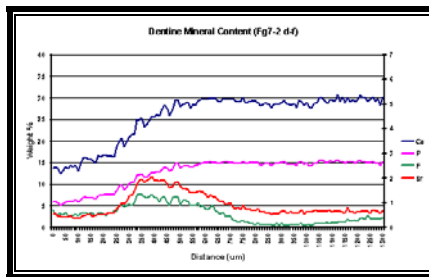
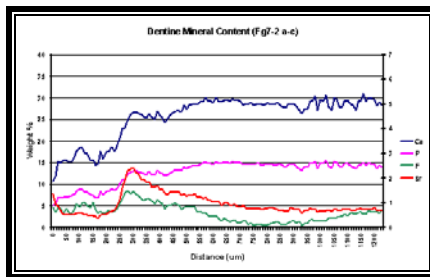
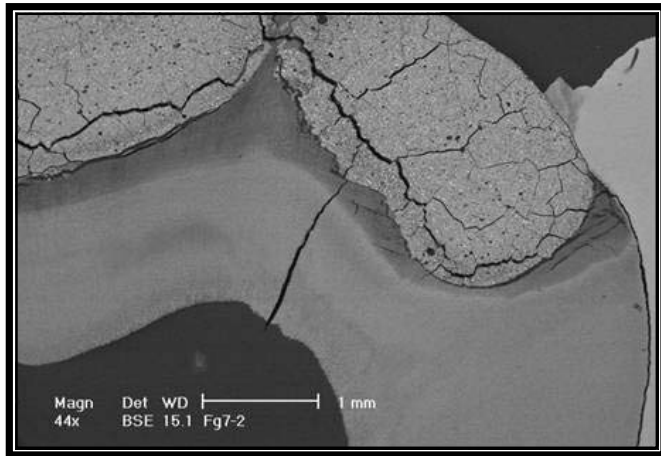
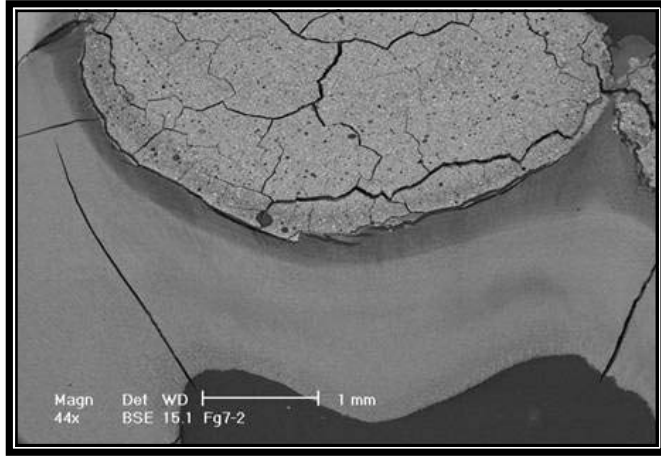


Figure 105: Mineral profiles in three regions of FG72

Sample 8: Coded as FG1001

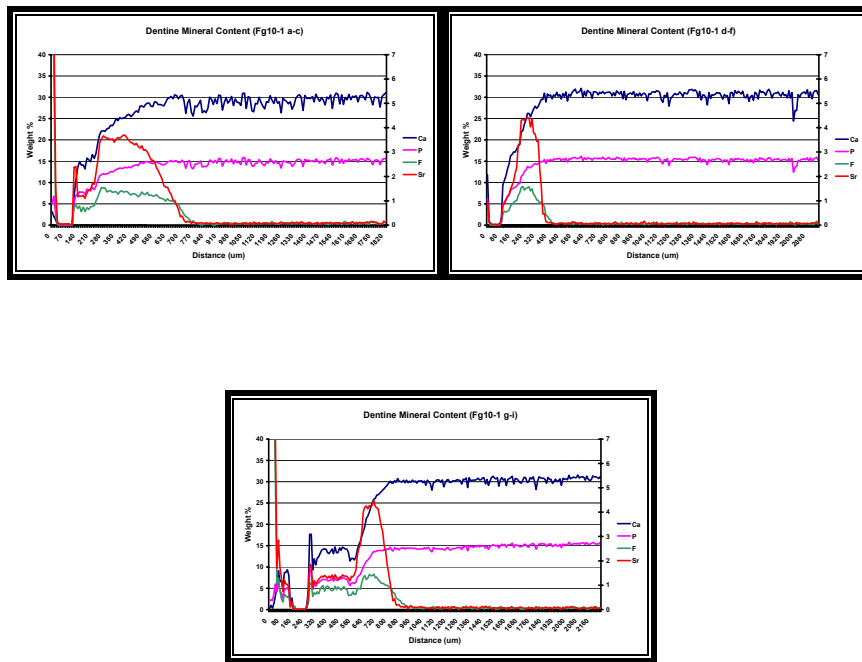
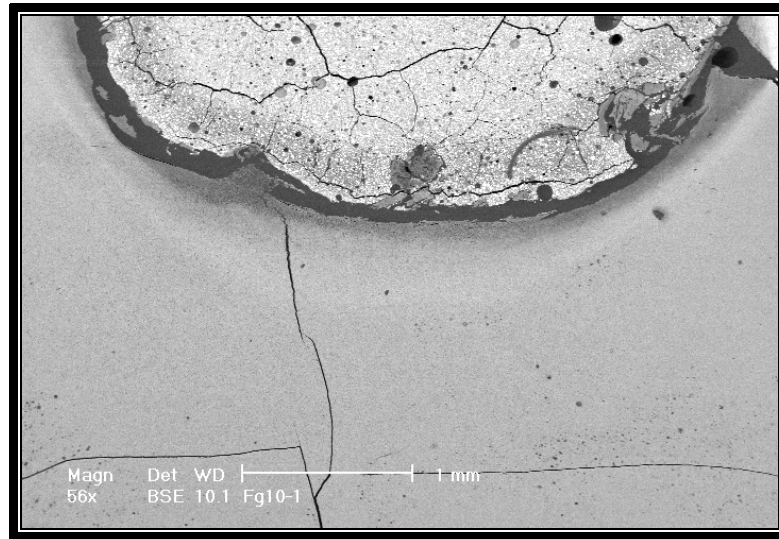


Figure 106: Mineral profiles in three regions of FG72

Sample 9: Coded as FG1203

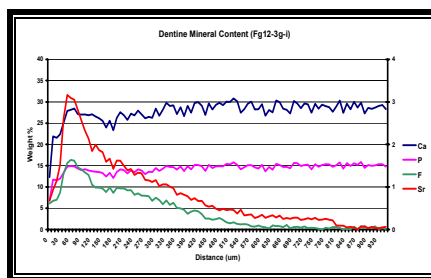
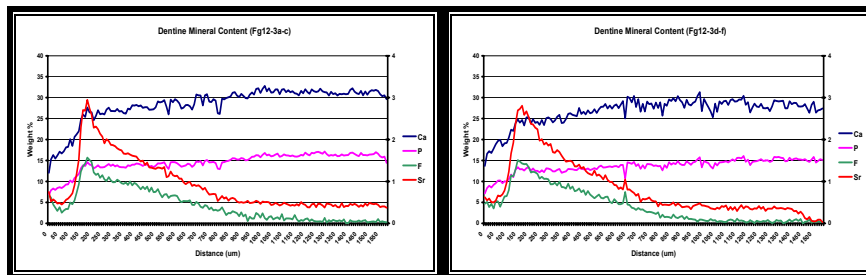
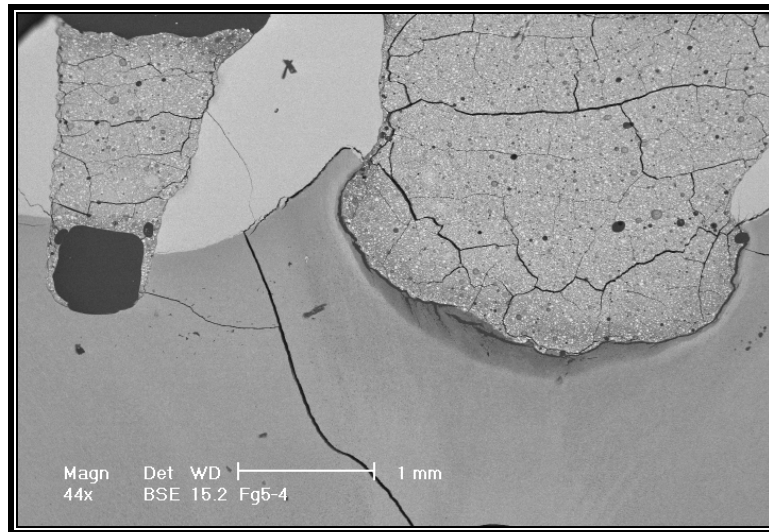


Figure 107: Mineral profiles in three regions of FG54

Sample 10: Coded as FG135

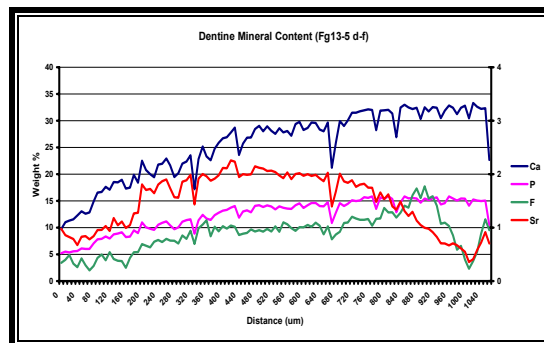
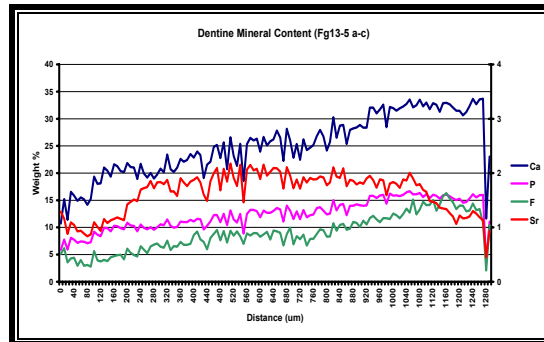
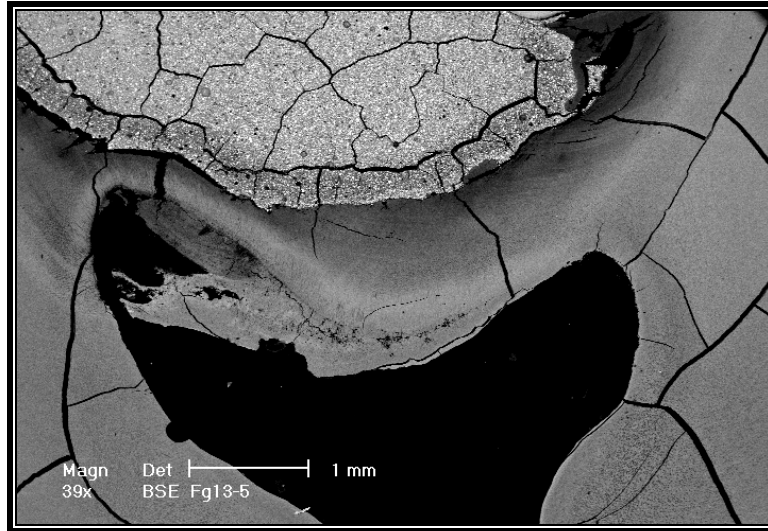


Figure 108: Mineral profiles in two regions of FG135

Sample 11: Coded as FG1502

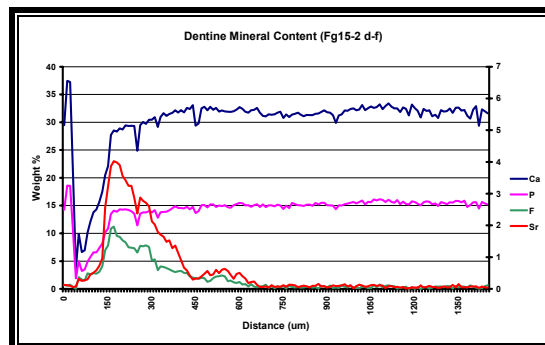
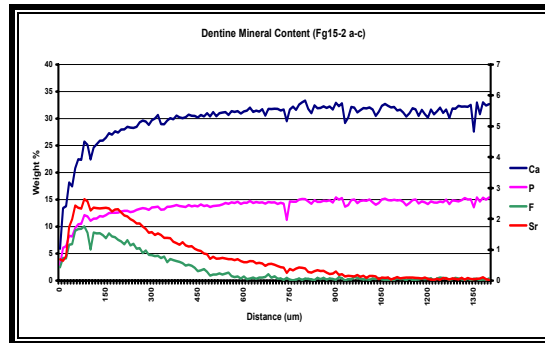
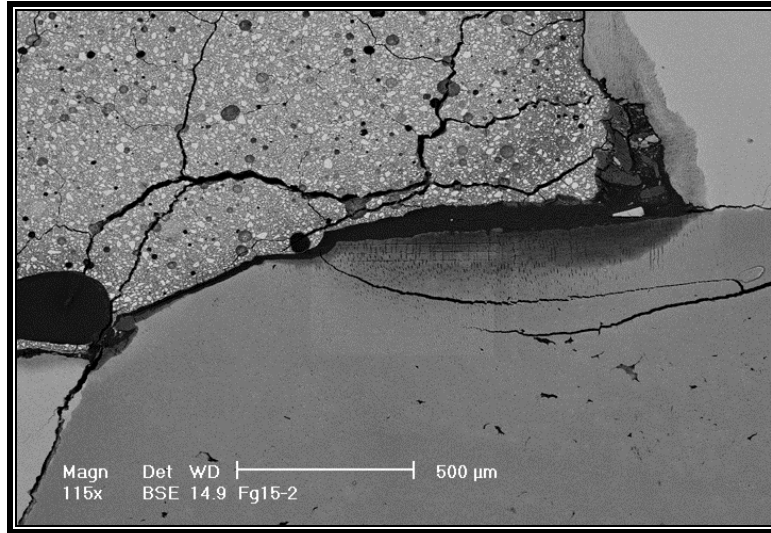


Figure 109: Sample FG1502

Sample 12: Coded as FG1103

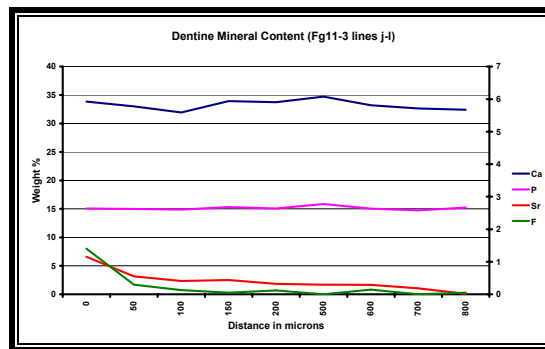
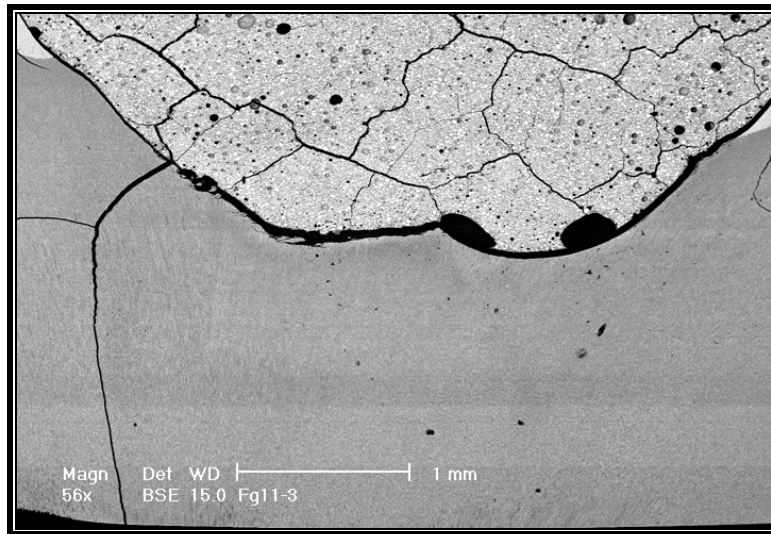


Figure 110: Sample FG1103

Sample 13: Coded as FG1402

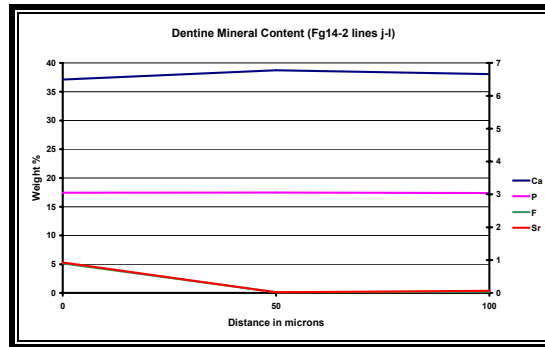
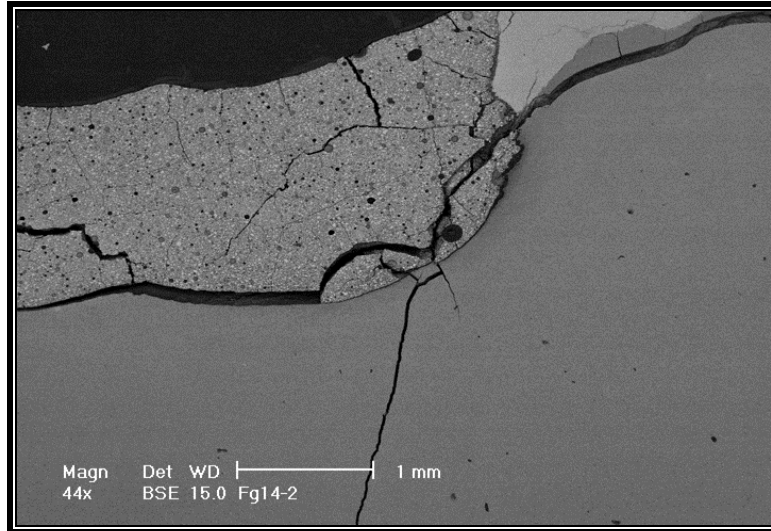
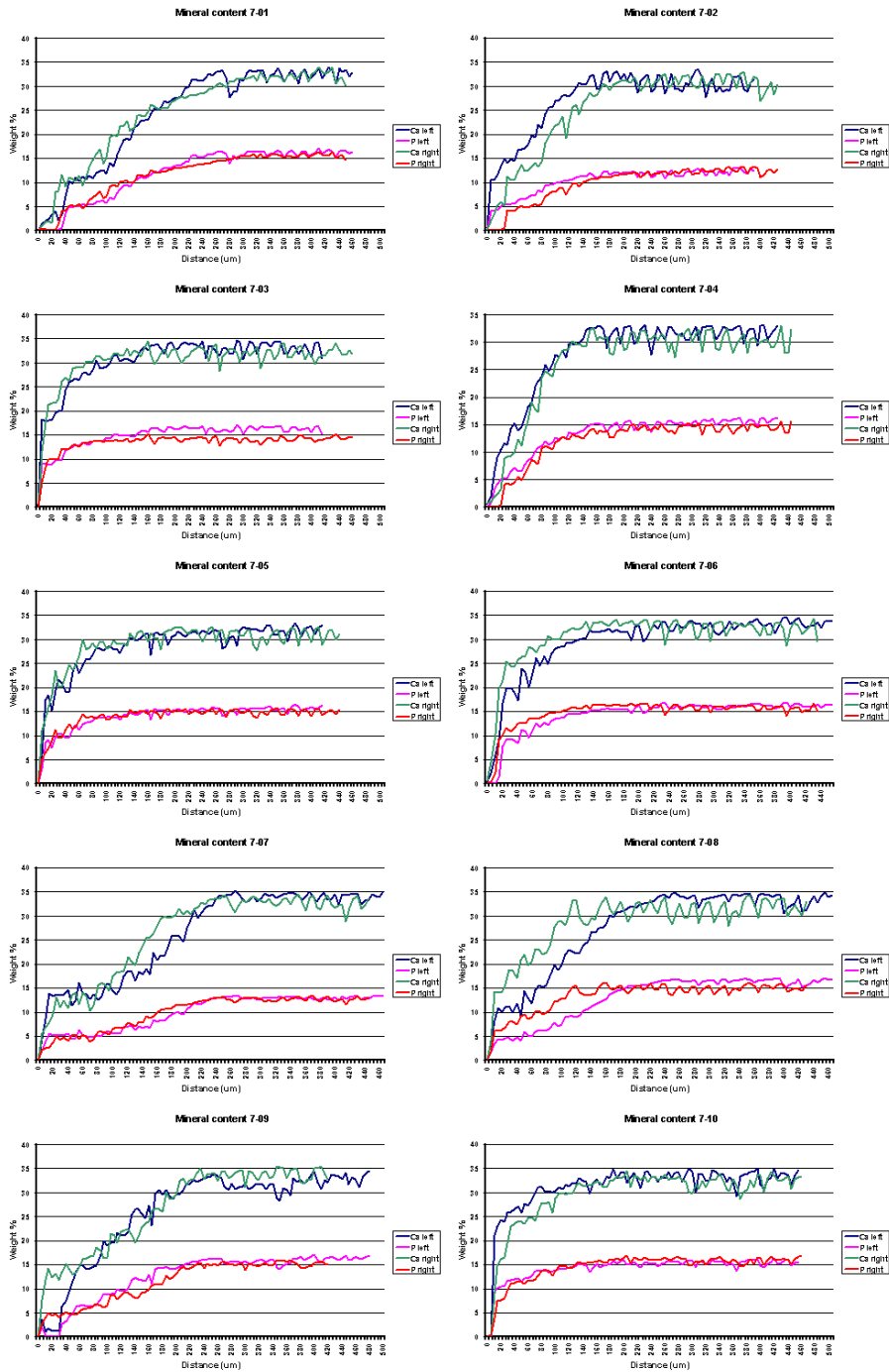


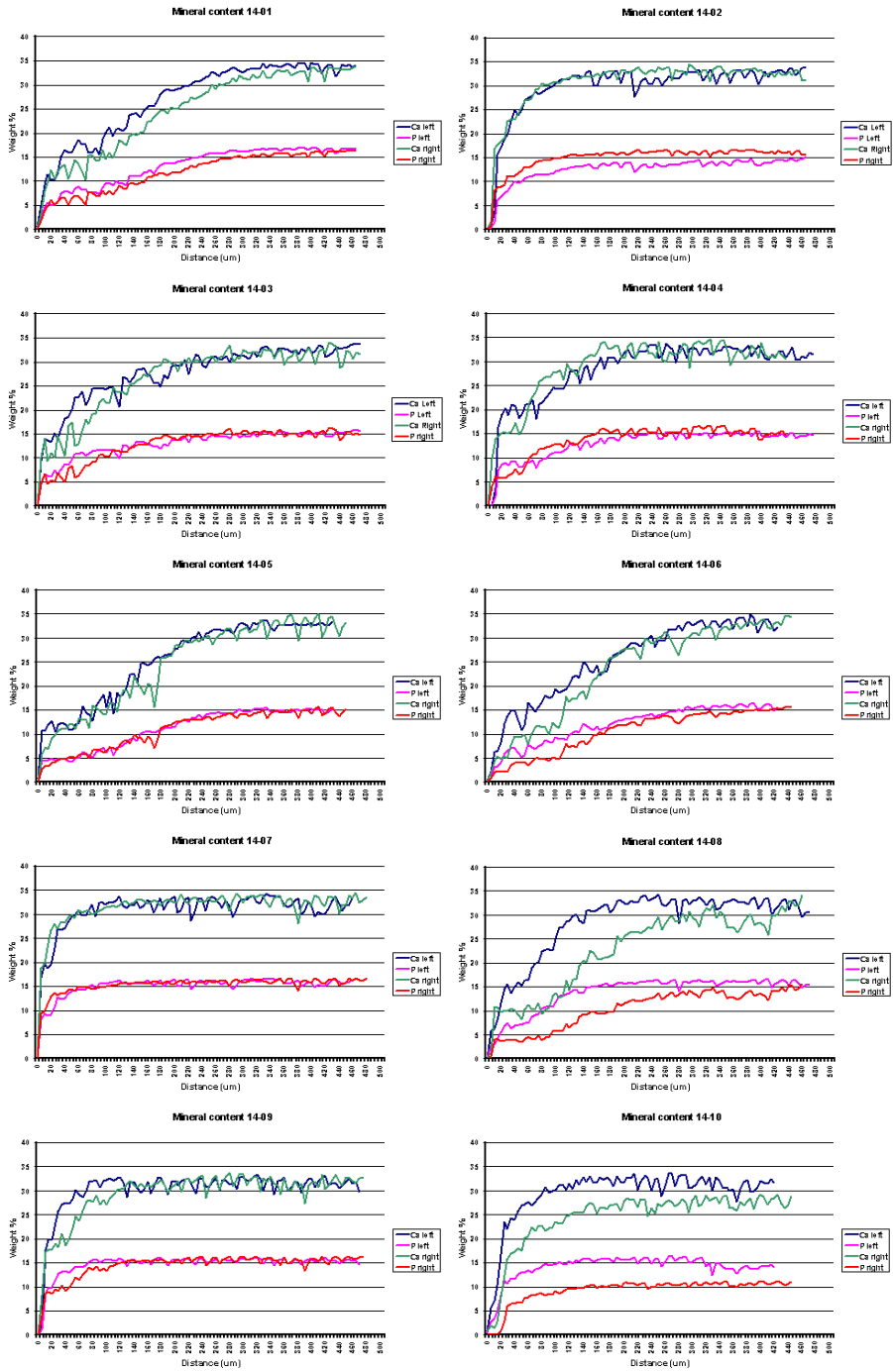
Figure 111: Sample FG1402

Appendix C: Additional results for Chapter 5.2

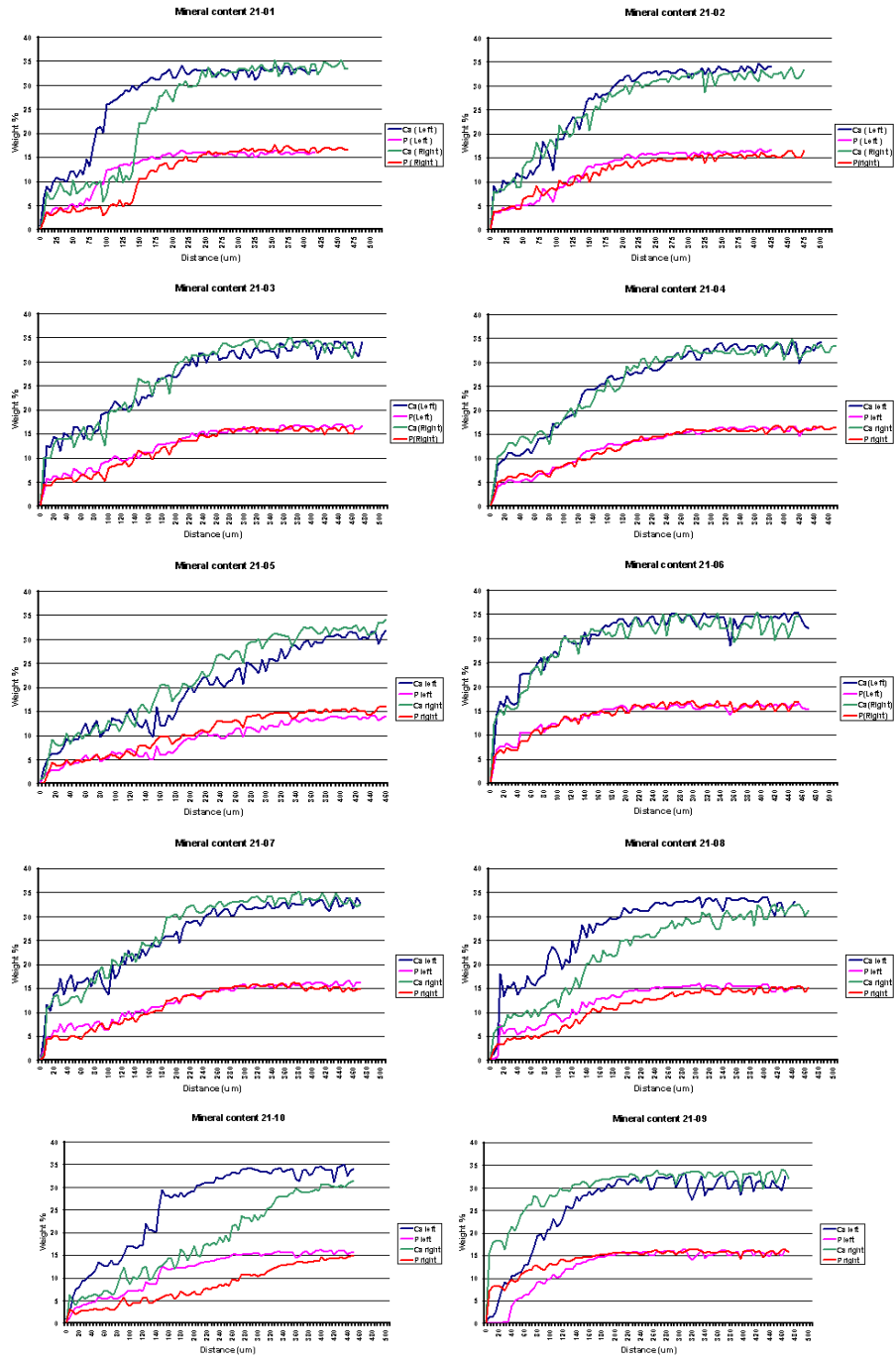
Correlation between left and right sides of 7 day lesions



Correlation between left and right sides of 14 day lesions



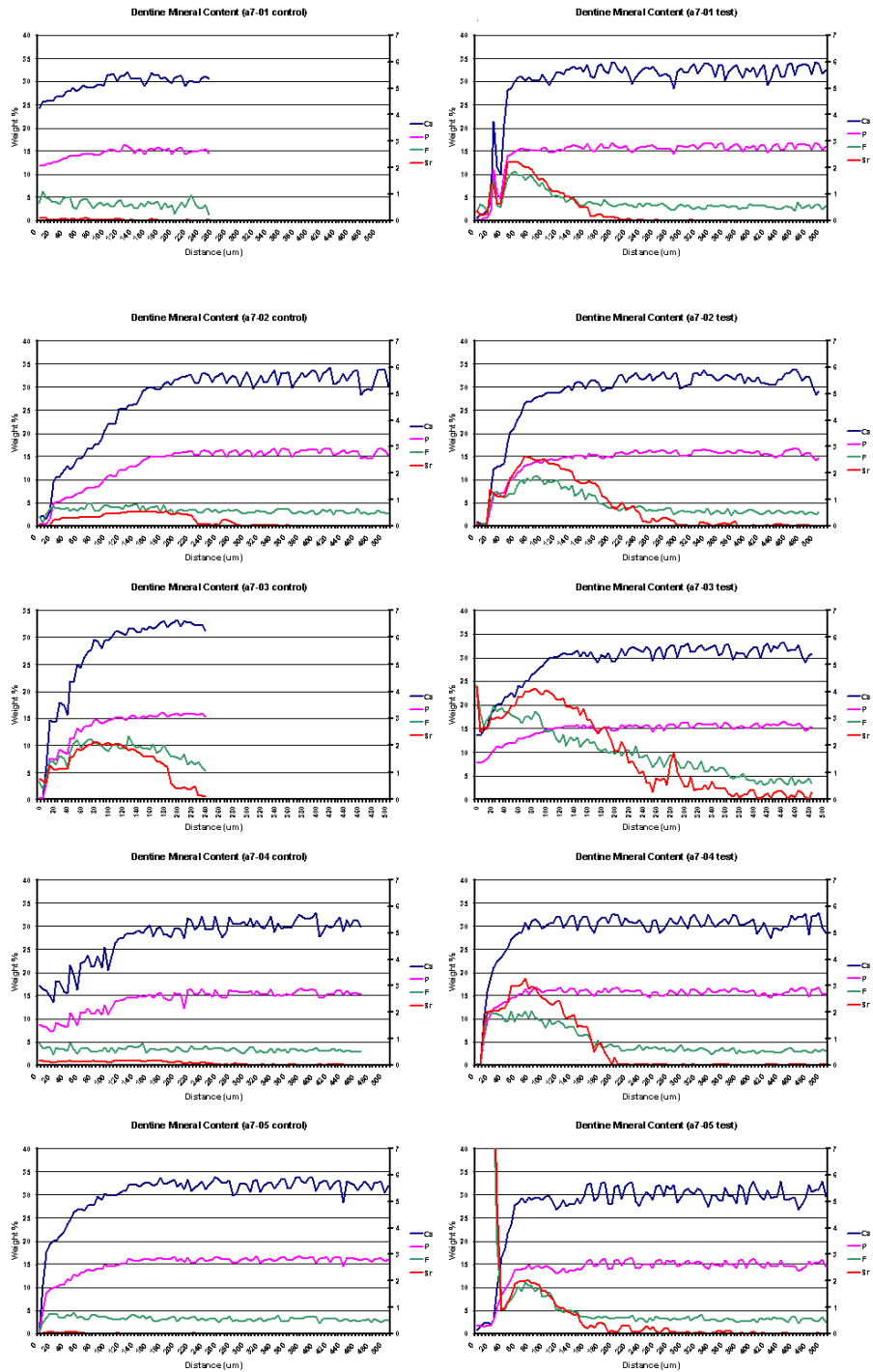
Correlation between left and right sides of 21 day lesions



Appendix D: Additional results for Chapter 6.2

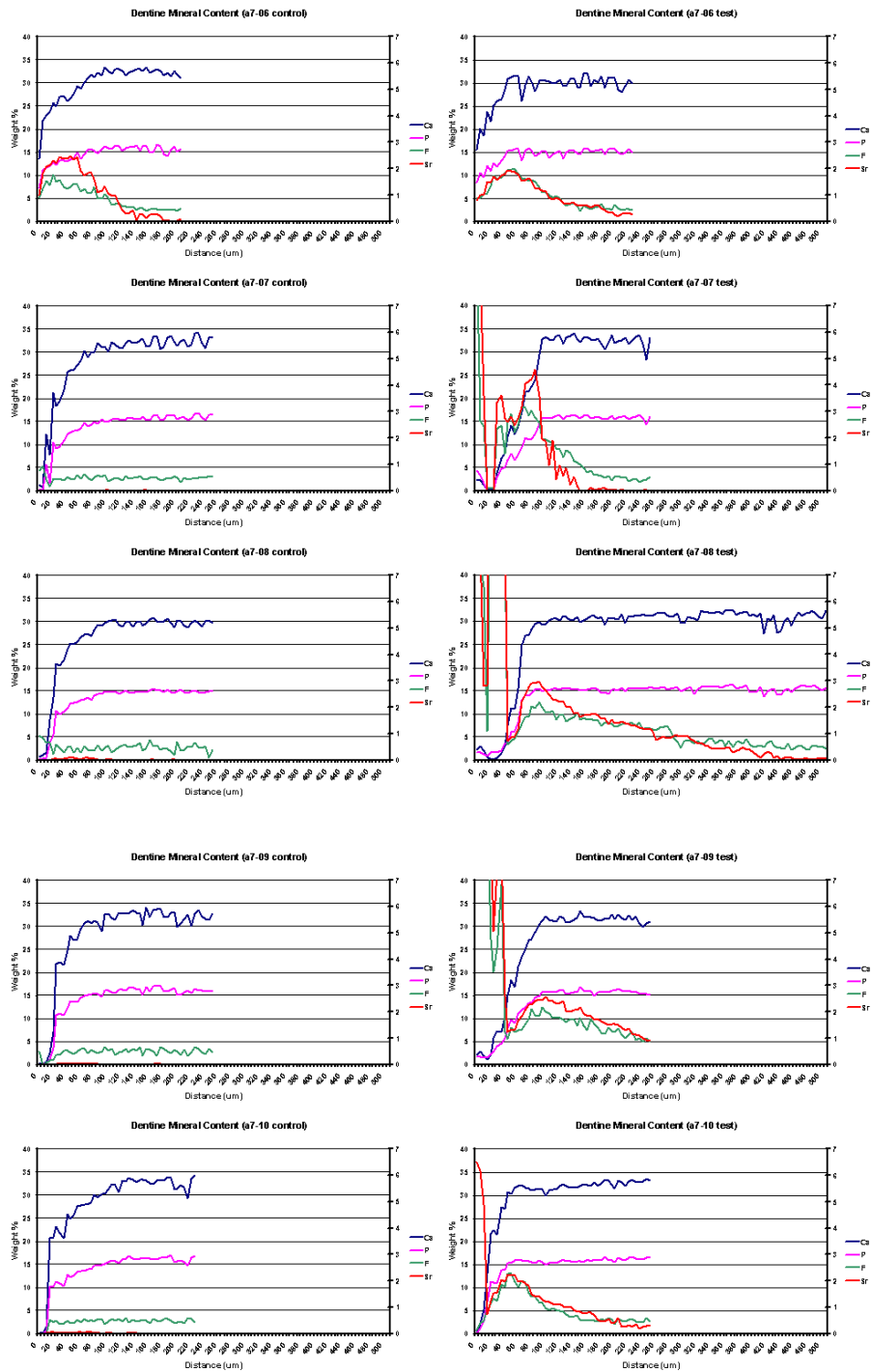
High strength glass-ionomer: Fuji IXGP

7 day artificial lesion treated for 21 days



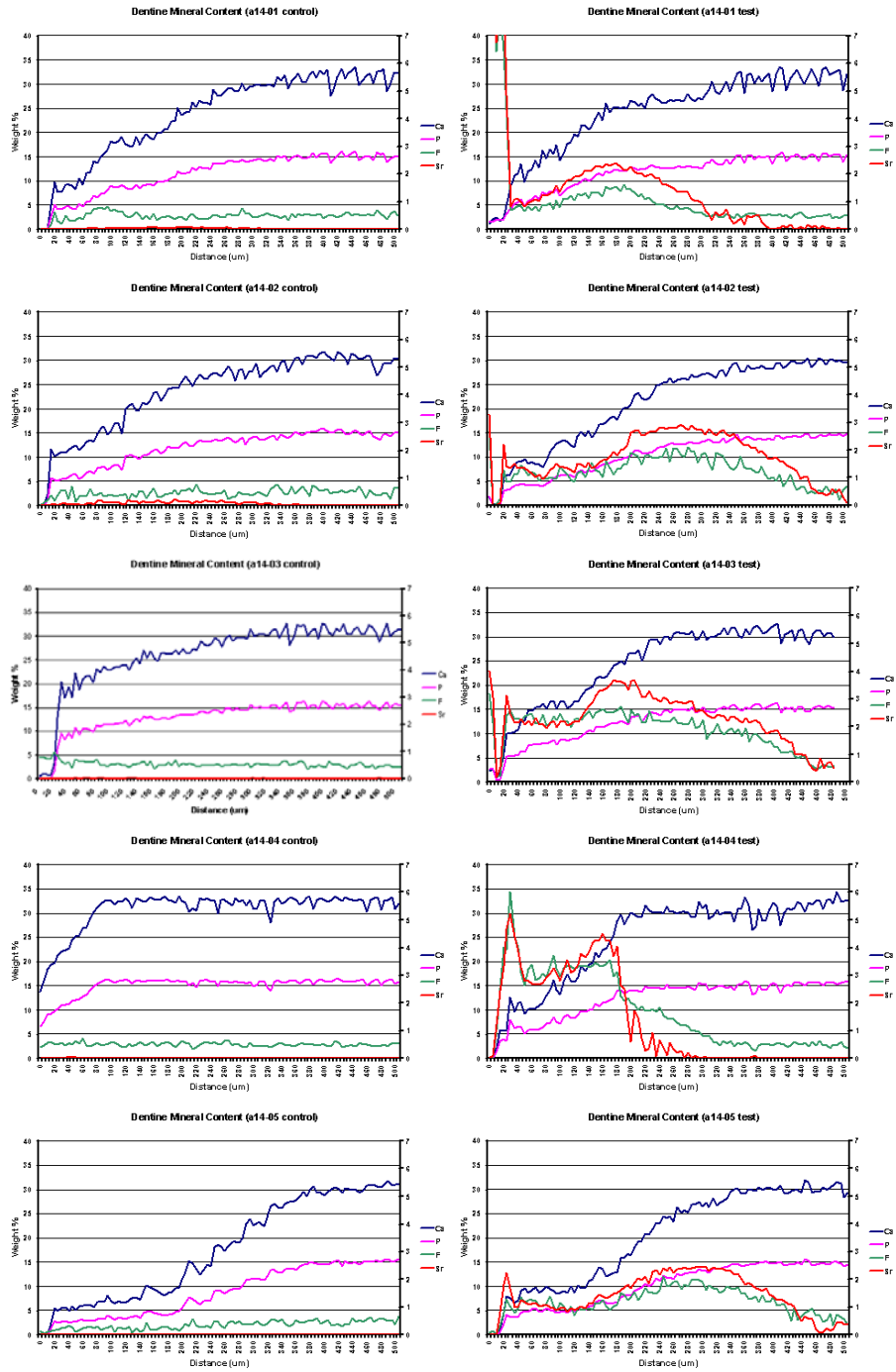
High strength glass-ionomer: Fuji IXGP

7 day artificial lesion treated for 42 days



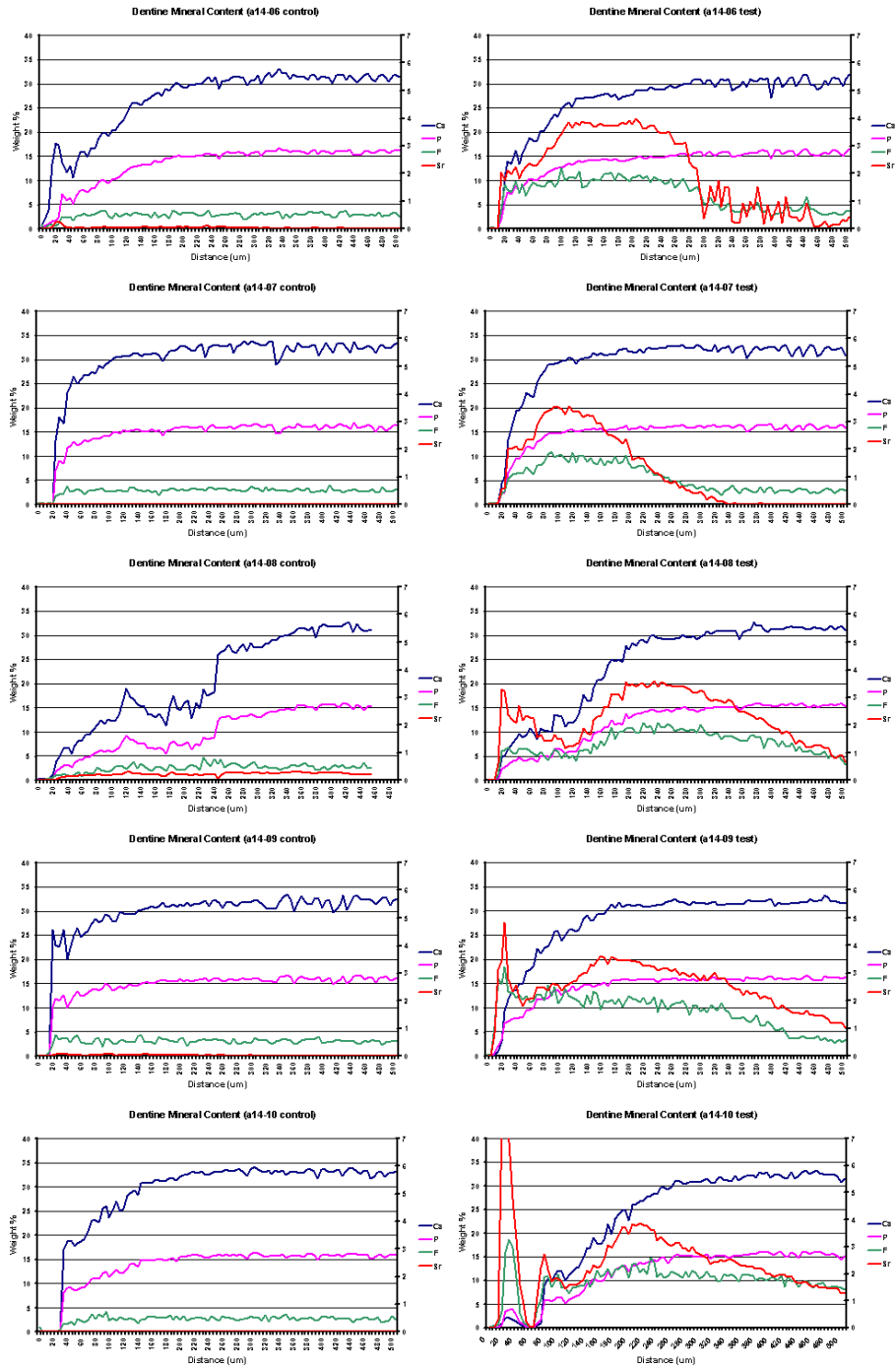
High strength glass-ionomer: Fuji IXGP

14 day artificial lesion treated for 21 days



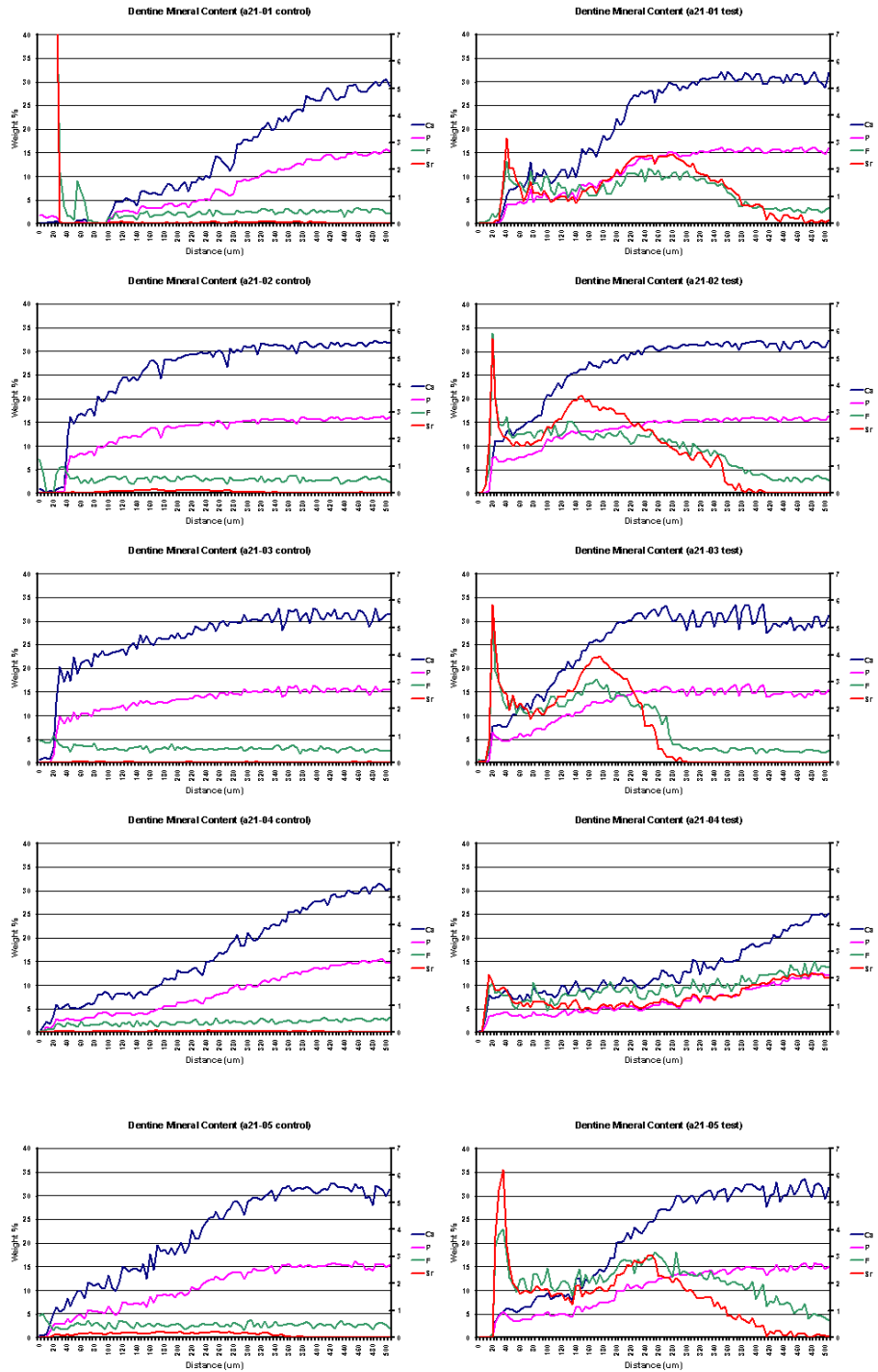
High strength glass-ionomer: Fuji IXGP

14 day artificial lesion treated for 42 days



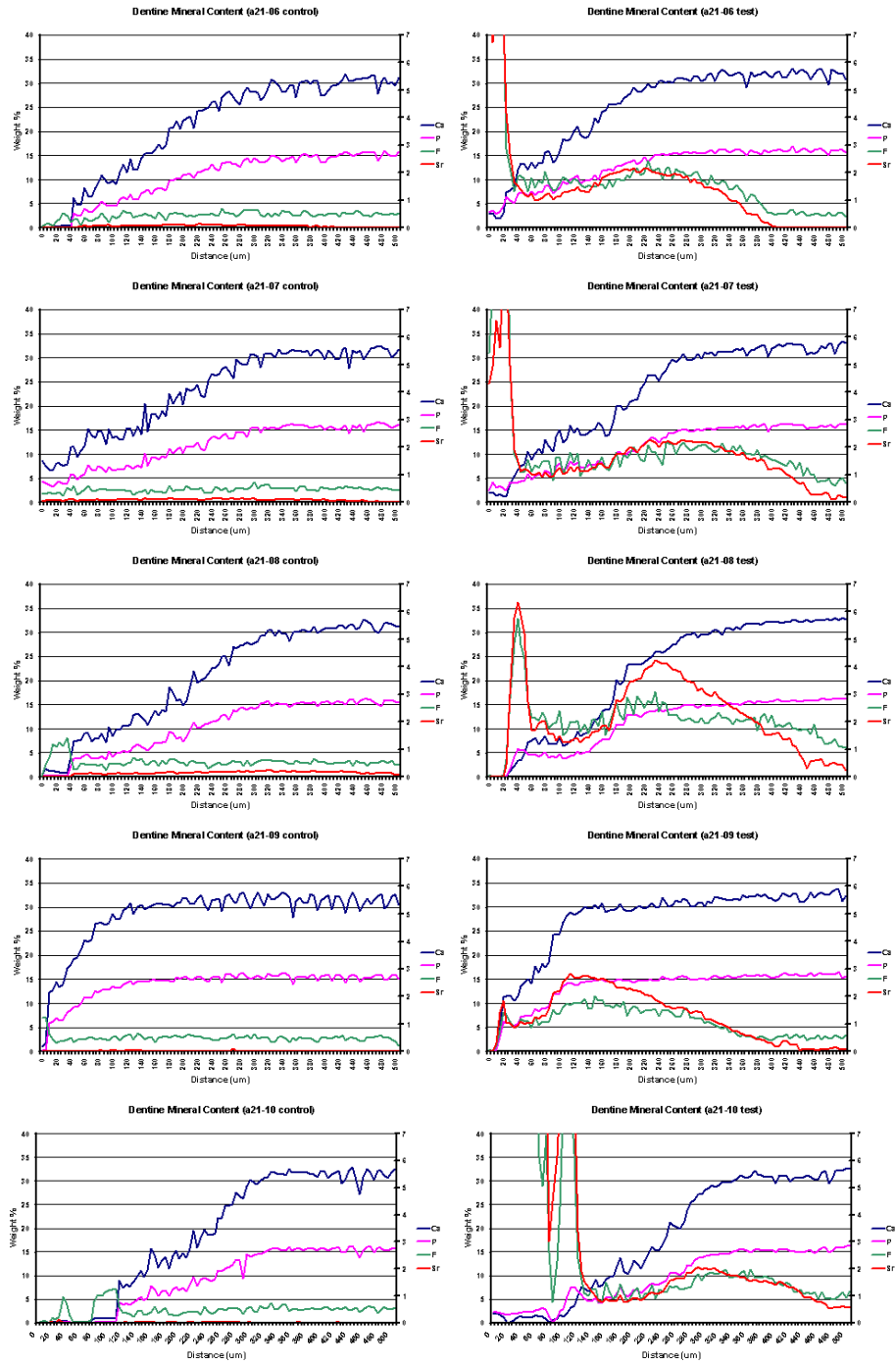
High strength glass-ionomer: Fuji IXGP

21 day artificial lesion treated for 21 days



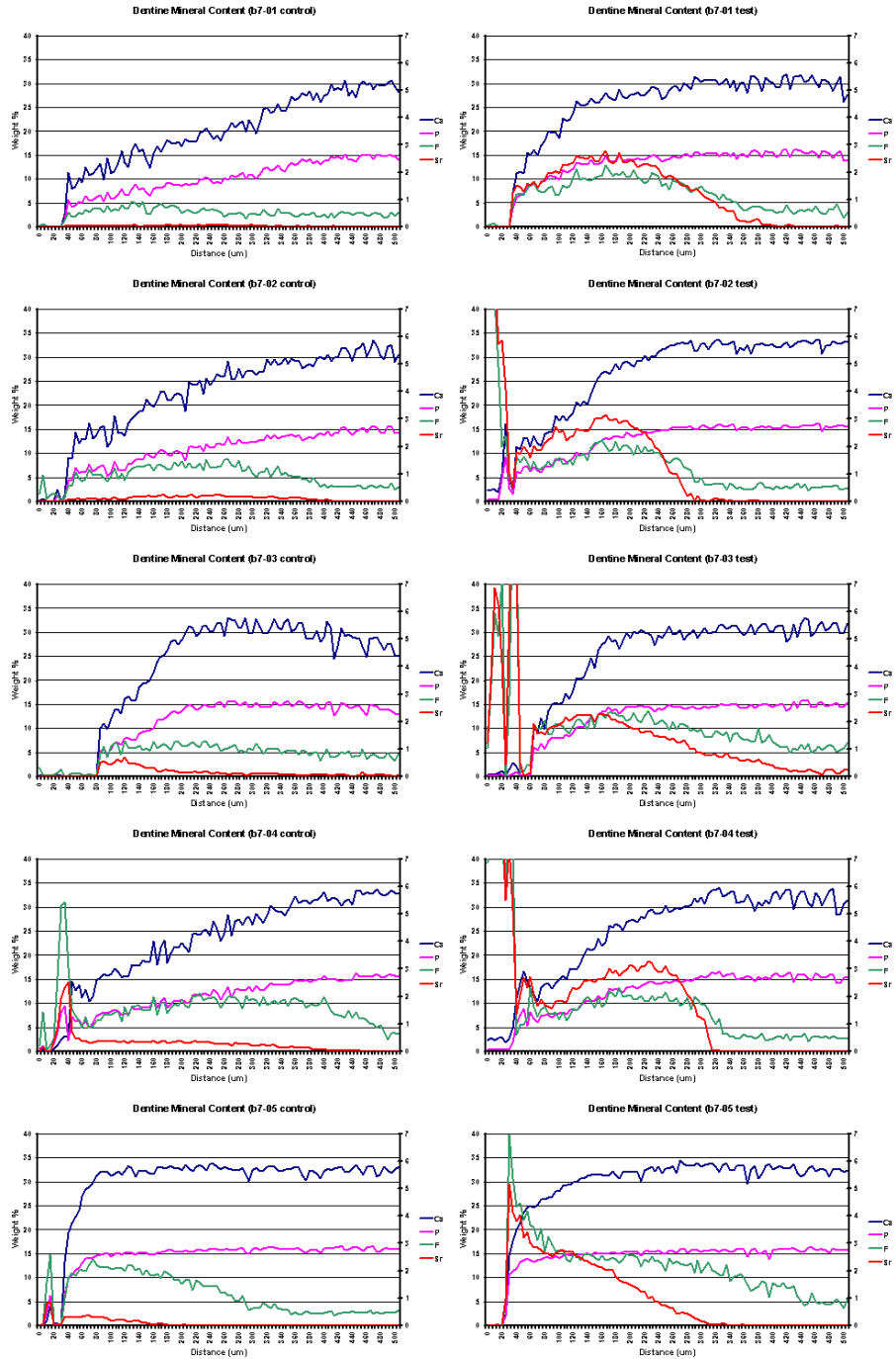
High strength glass-ionomer: Fuji IXGP

21 day artificial lesion treated for 42 days



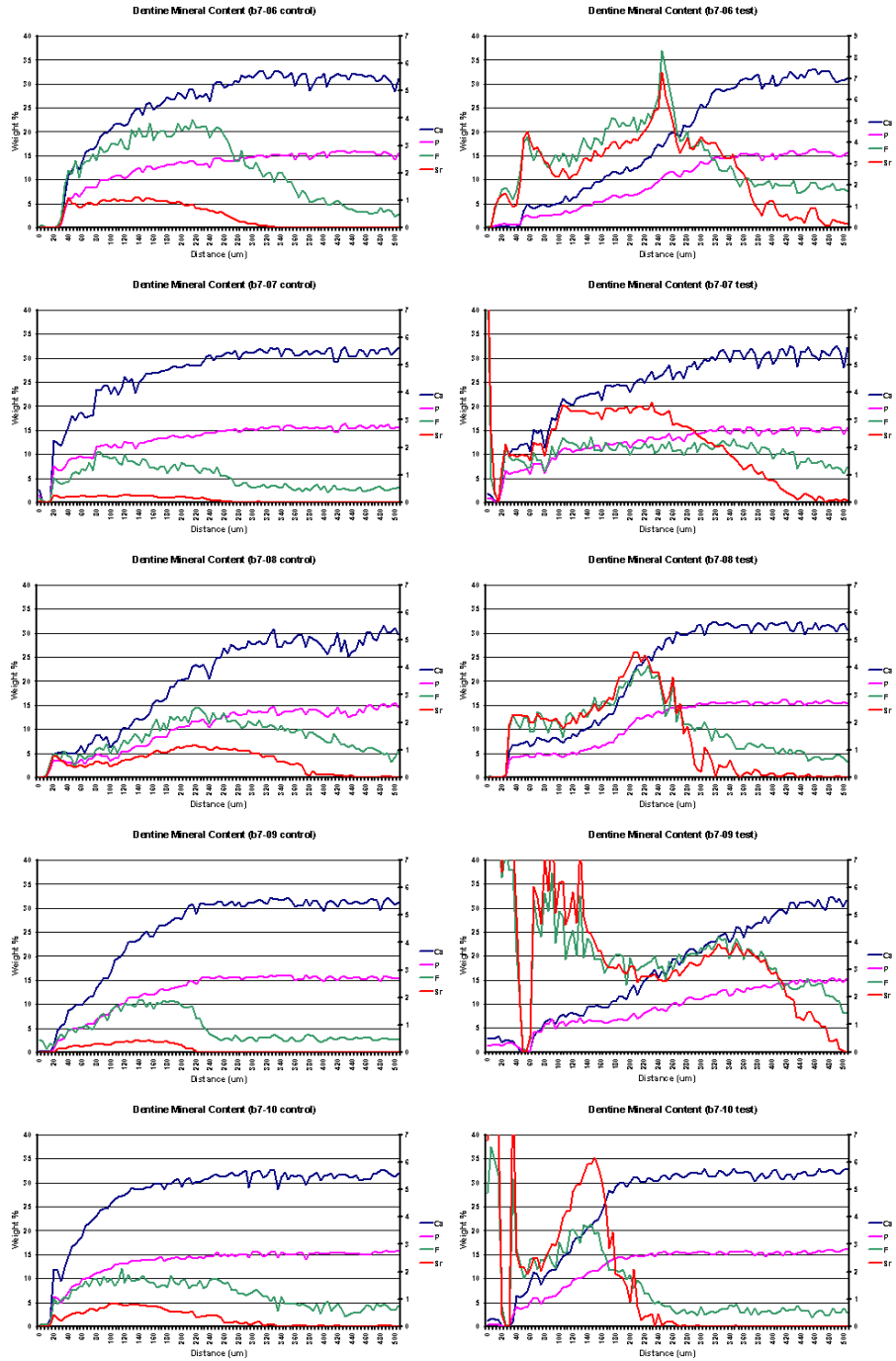
High fluoride releasing glass-ionomer: Fuji VI

7 day artificial lesion treated for 21 days



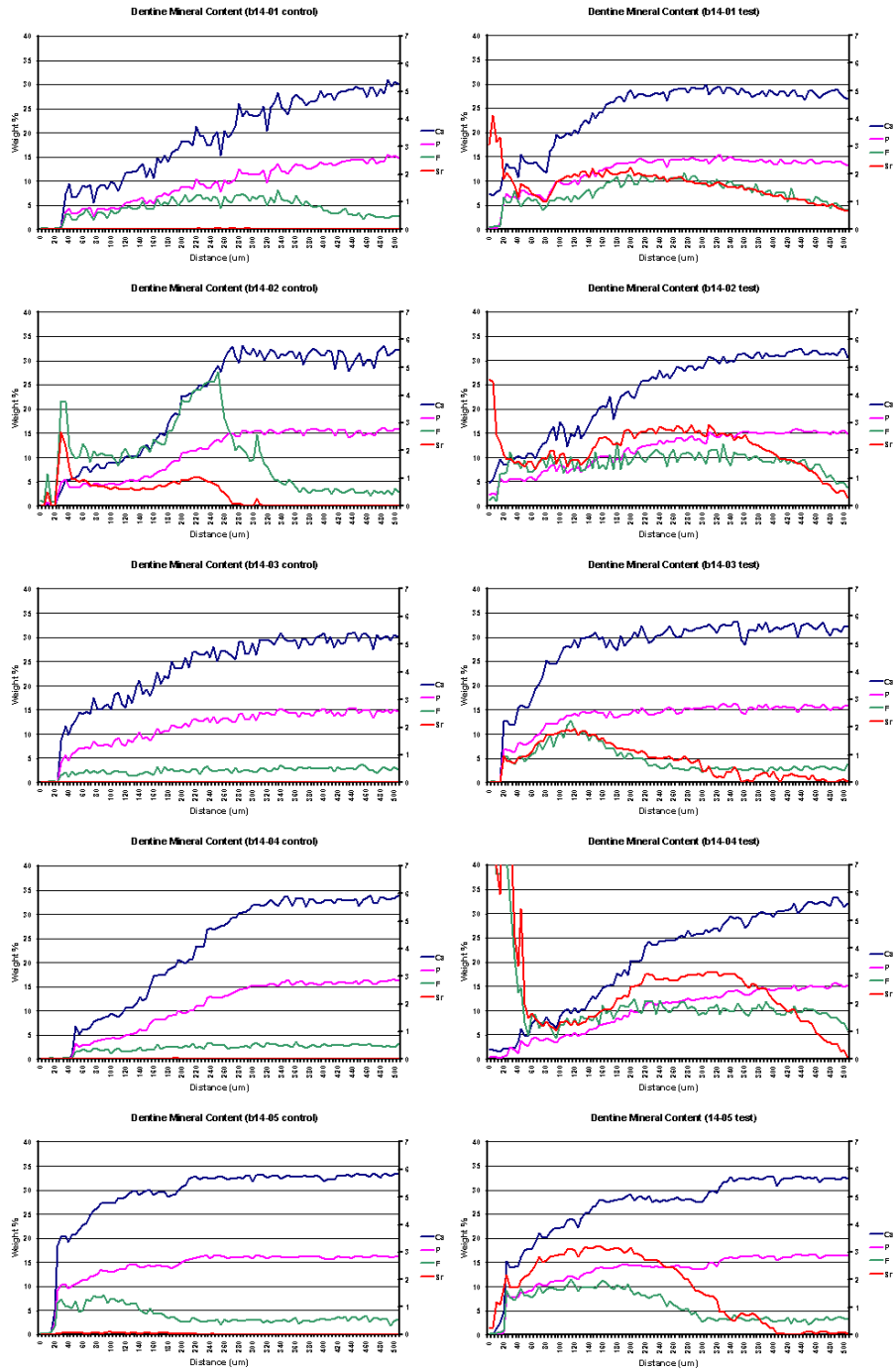
High fluoride releasing glass-ionomer: Fuji VI

7 day artificial lesion treated for 42 days



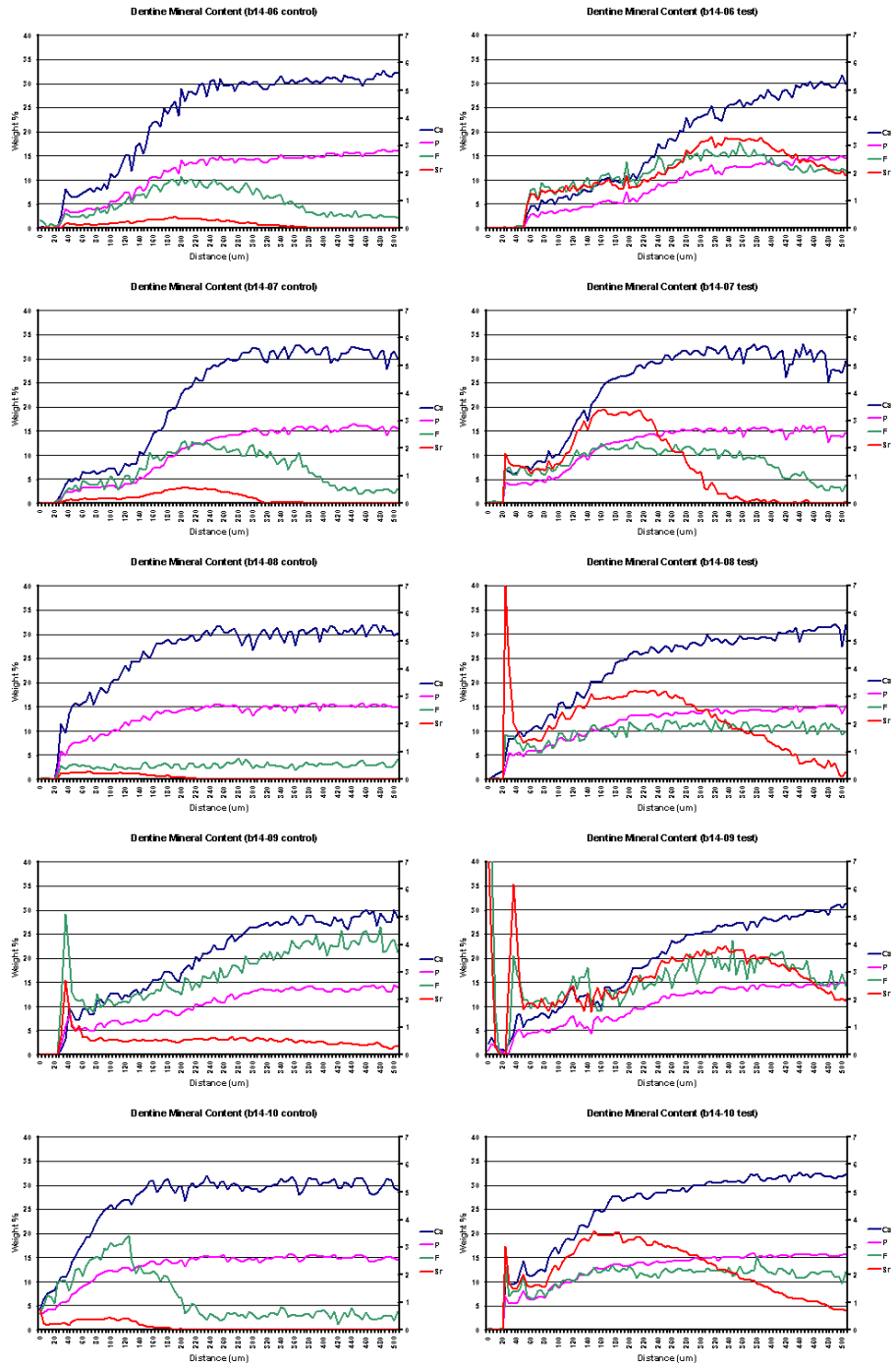
High fluoride releasing glass-ionomer: Fuji VI

14 day artificial lesion treated for 21 days



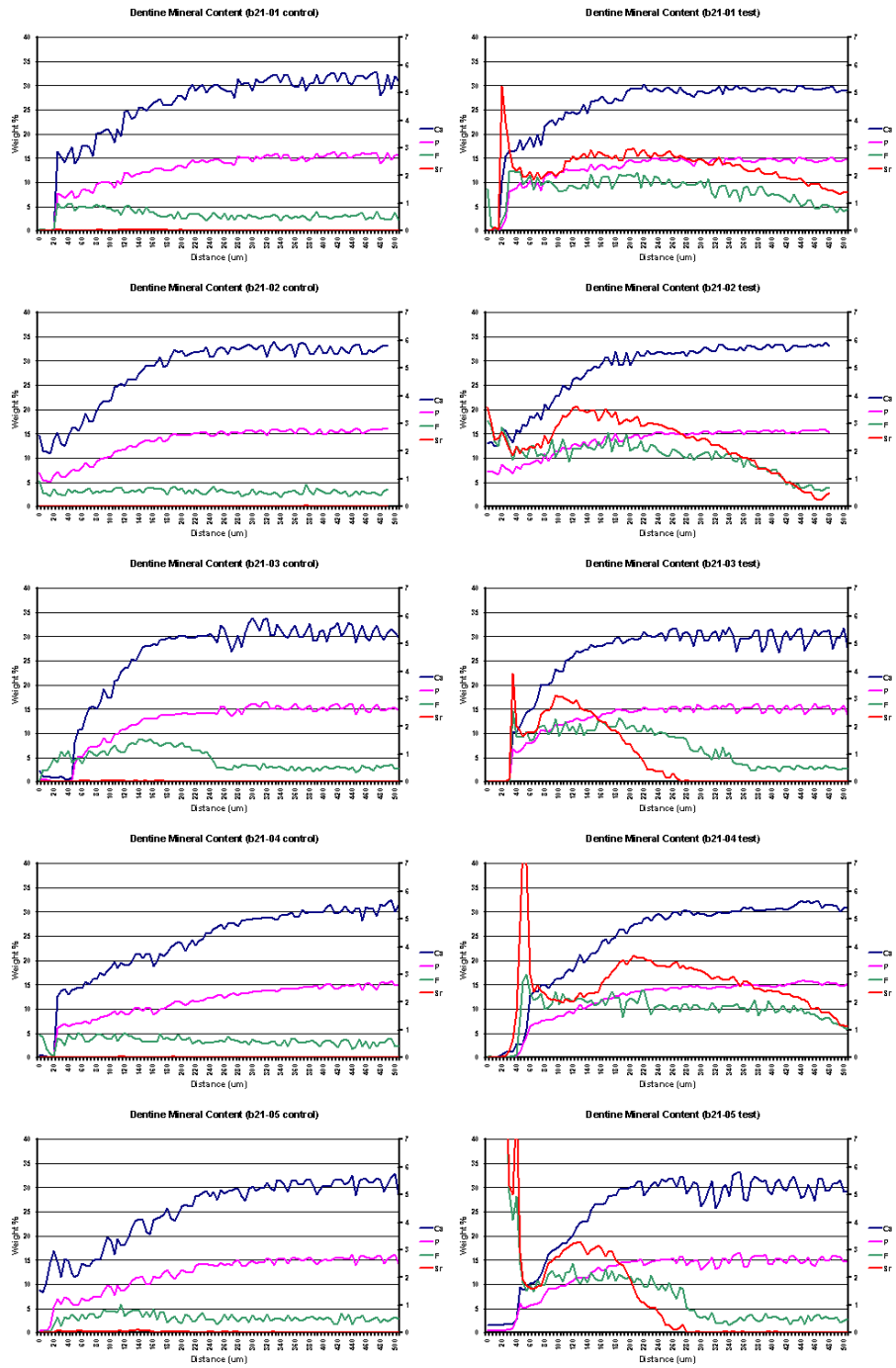
High fluoride releasing glass-ionomer: Fuji VI

14 day artificial lesion treated for 42 days



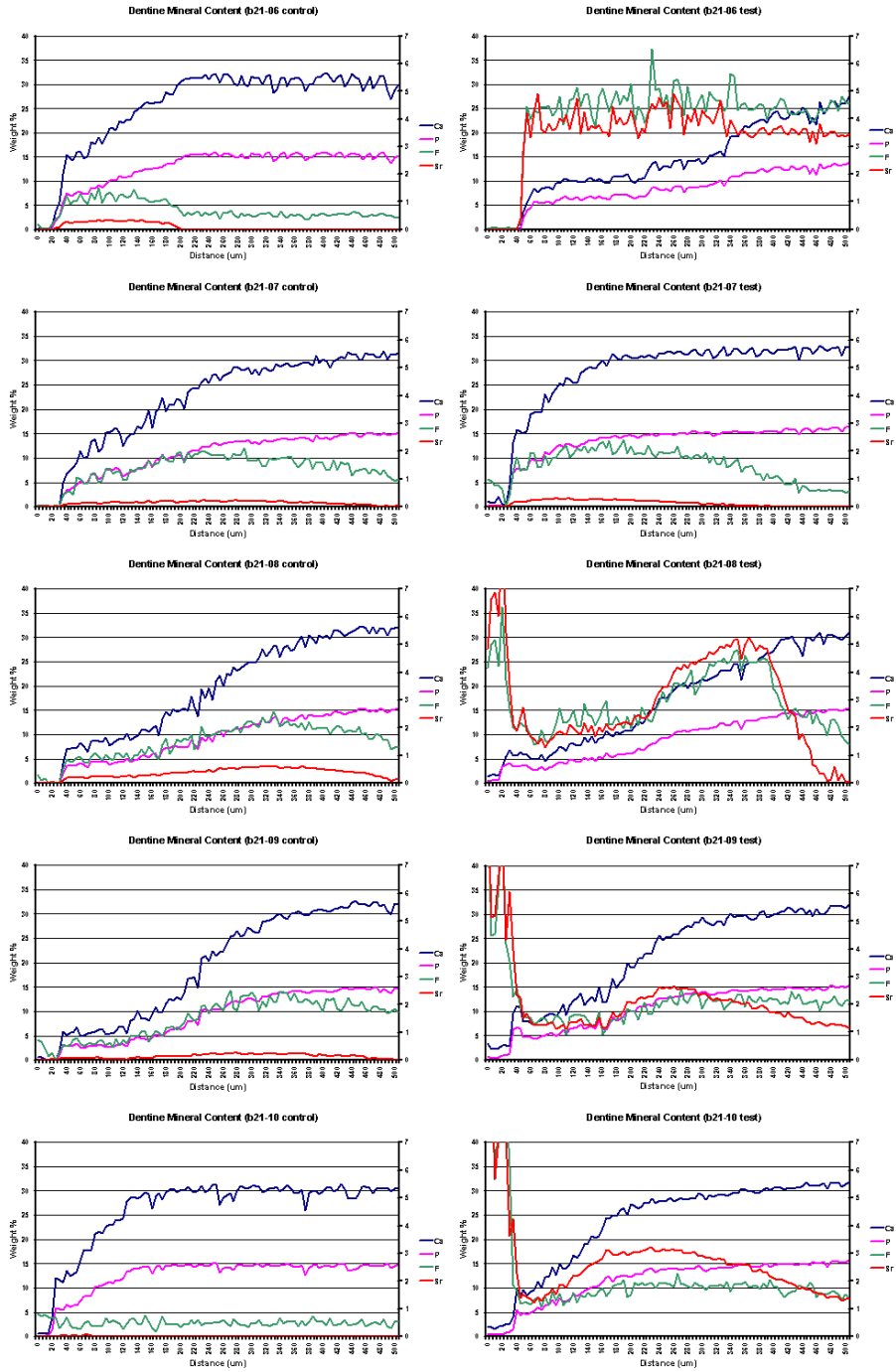
High fluoride releasing glass-ionomer: Fuji VI

21 day artificial lesion treated for 21 days



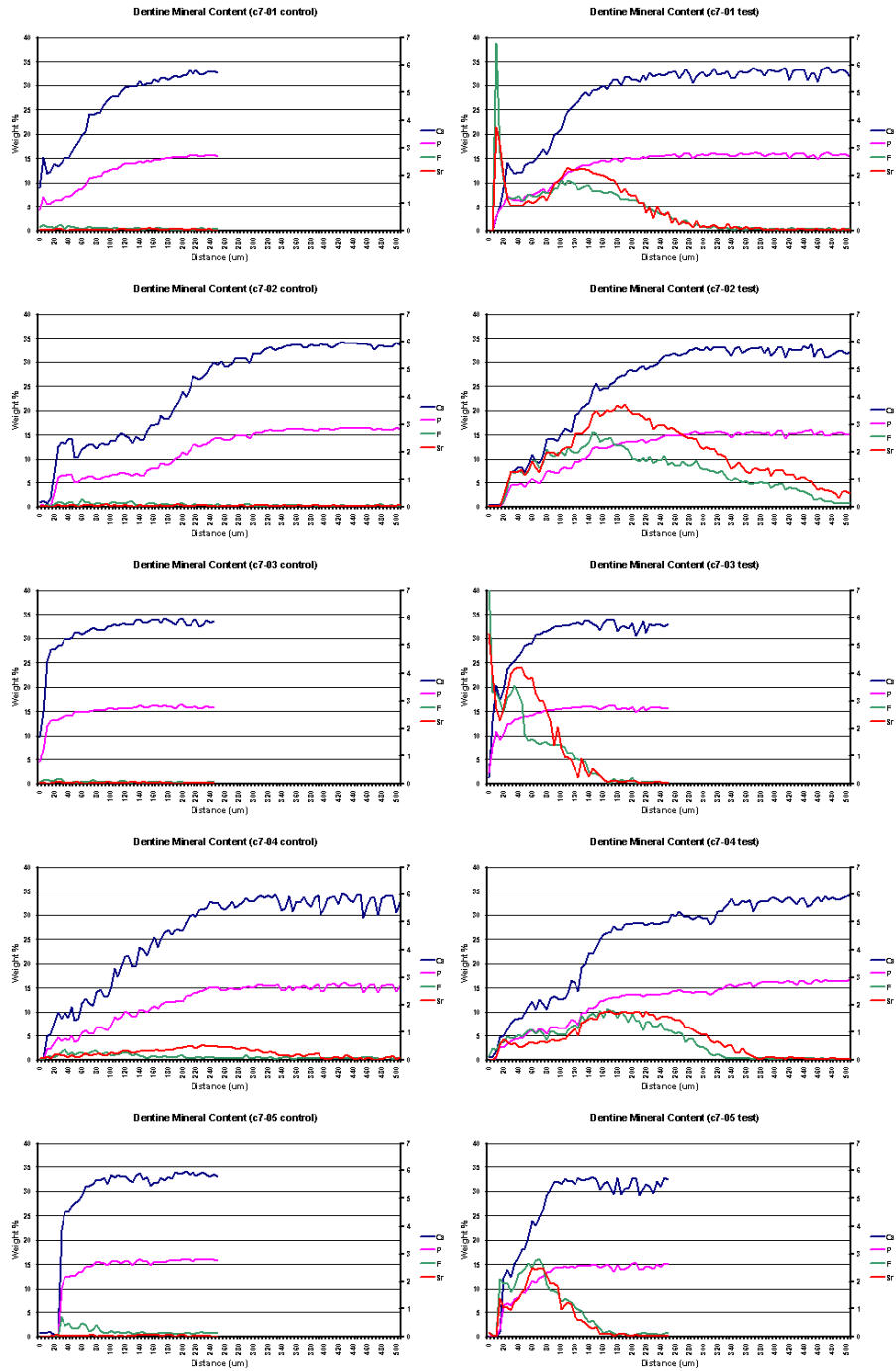
High fluoride releasing glass-ionomer: Fuji VI

21 day artificial lesion treated for 42 days



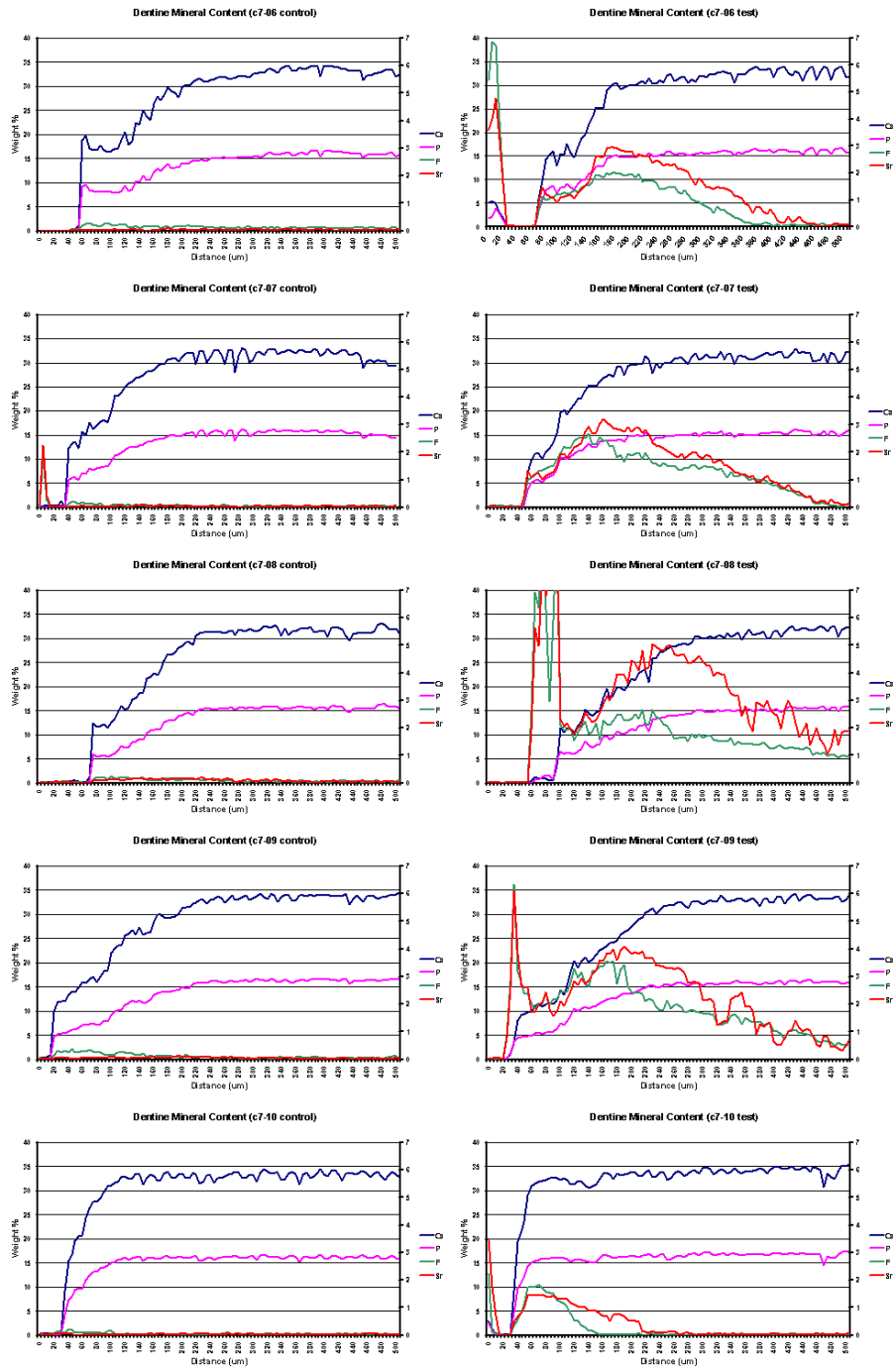
Resin Modified Glass Ionomer adhesive: FujiBondLL

7 day artificial lesion treated for 21 days



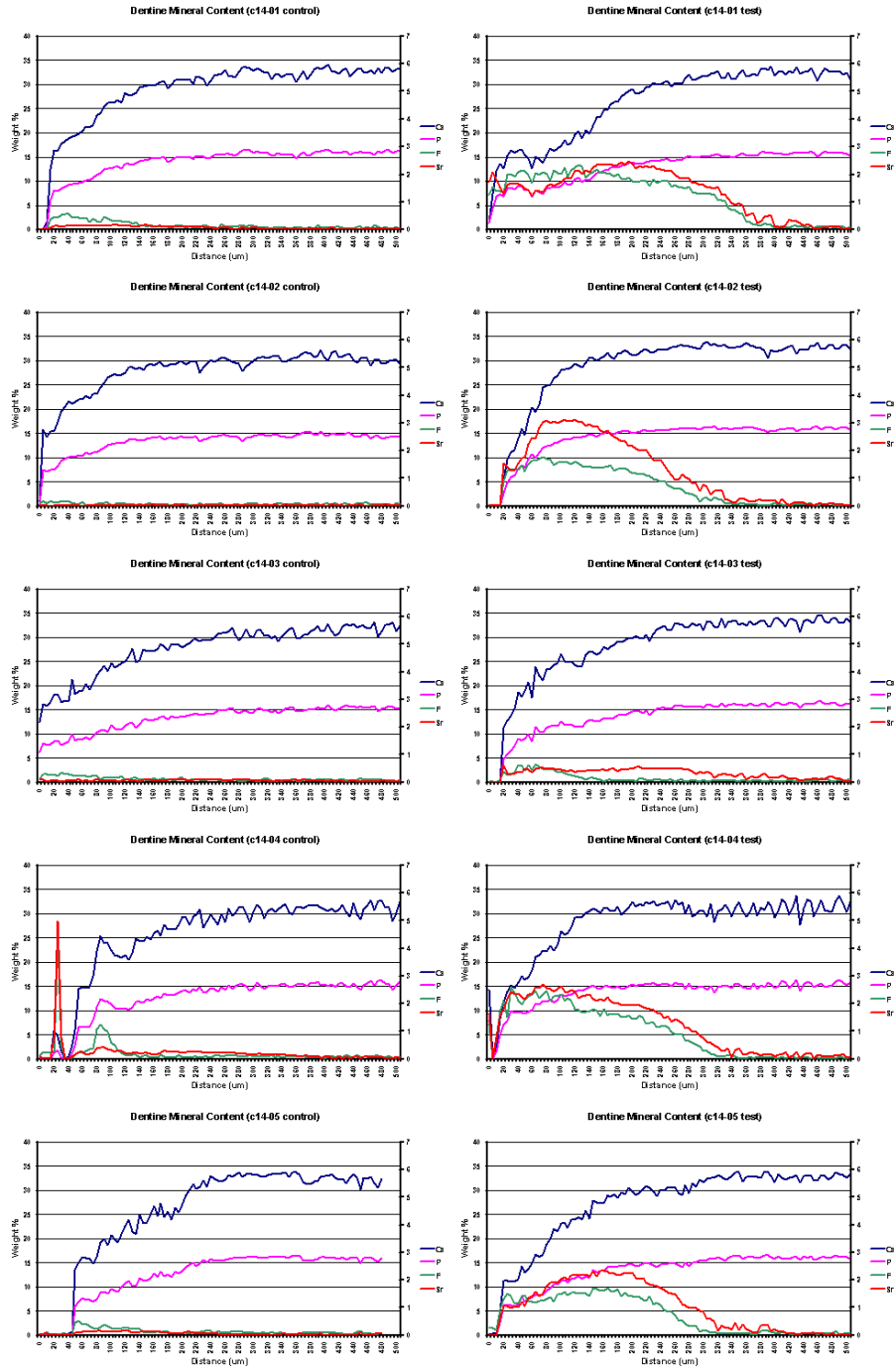
Resin Modified Glass Ionomer adhesive: FujiBondLL

7 day artificial lesion treated for 42 days



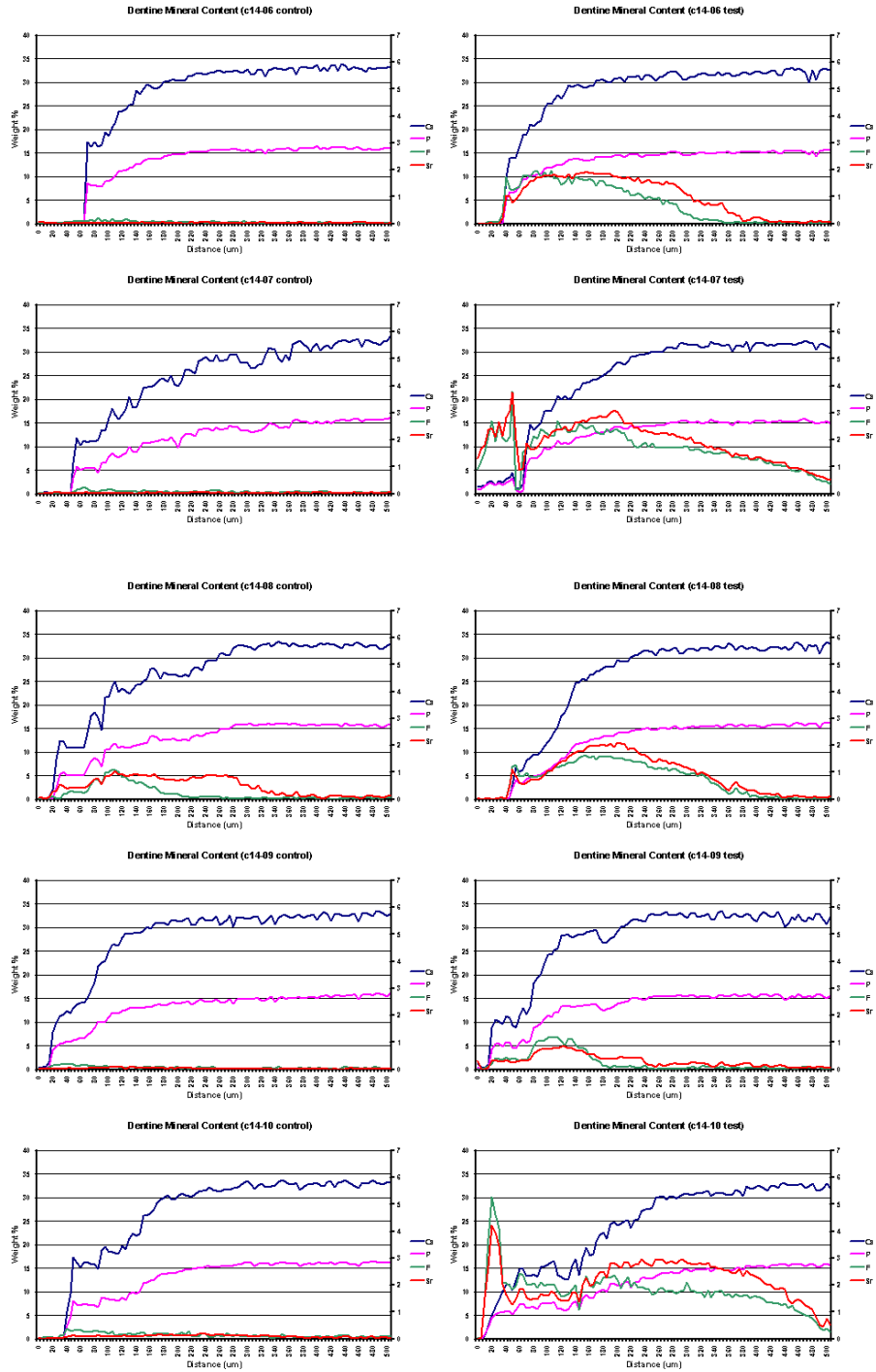
Resin Modified Glass Ionomer adhesive: FujiBondLL

14 day artificial lesion treated for 21 days



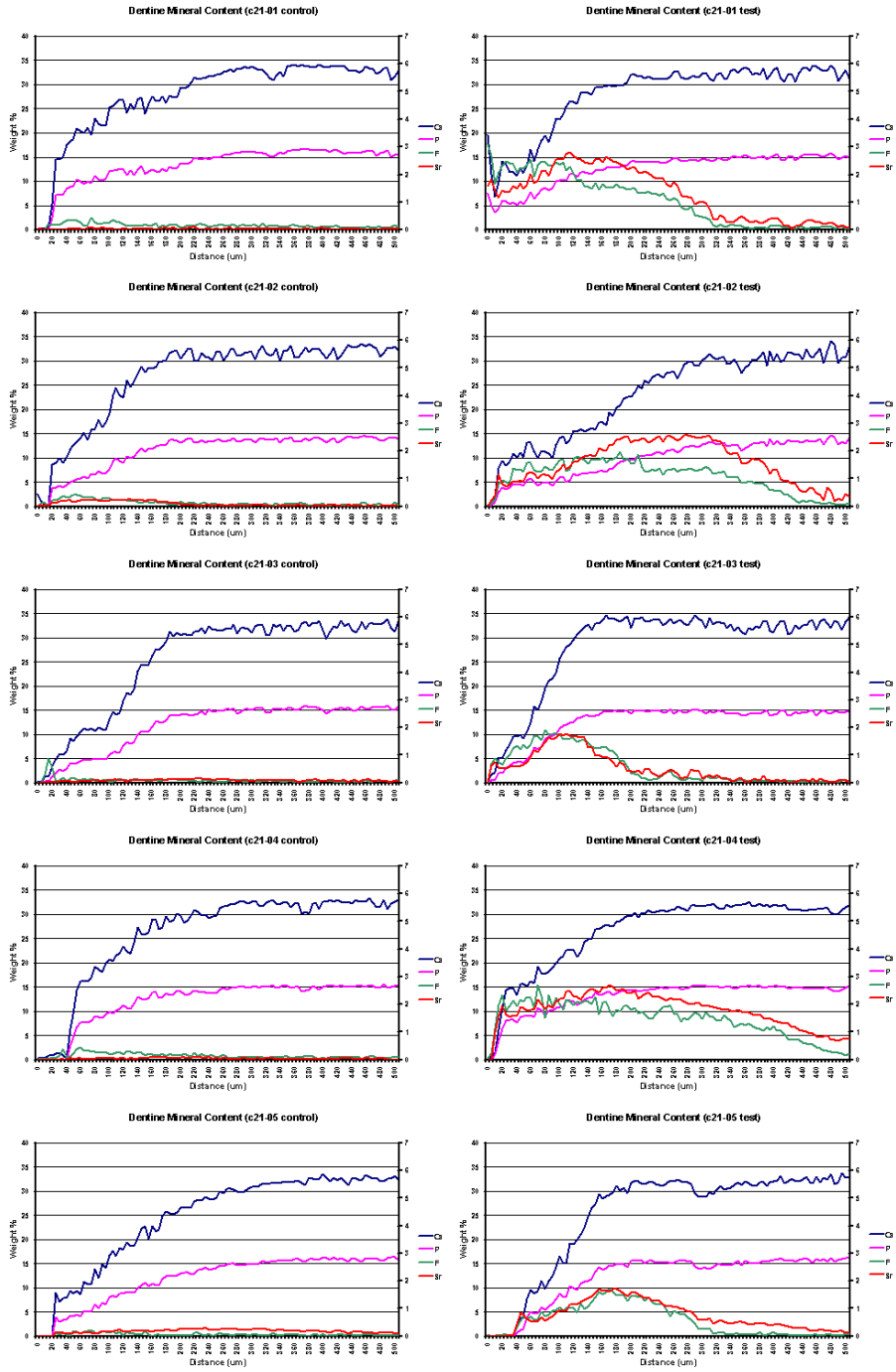
Resin Modified Glass Ionomer adhesive: FujiBondLL

14 day artificial lesion treated for 42 days



Resin Modified Glass Ionomer adhesive: FujiBondLL

21 day artificial lesion treated for 21 days



Resin Modified Glass Ionomer adhesive: FujiBondLL

21 day artificial lesion treated for 42 days

